Single-cell analysis of the antagonism between resistance and tolerance during the adaptive response to hydrogen peroxide in budding yeast

Basile Jacquel

UNIVERSITÉ DE STRASBOURG

ÉCOLE DOCTORALE ED414

CNRS UMR 7104 – Inserm U 964

Thèse présentée par Basile JACQUEL

Pour obtenir le grade de : **Docteur de l'université de Strasbourg**

Discipline/ Spécialité : Sciences de la vie

Single-cell analysis of the antagonism between resistance and tolerance during the adaptive response to hydrogen peroxide in budding yeast

Dr Gilles CHARVIN	DIRECTEUR DE THESE	DR, IGBMC
Pr Peter SWAIN	RAPPORTEUR EXTERNE	PR, University of Edinburgh
Pr Bruce MORGAN	RAPPORTEUR EXTERNE	PR, Universität des Saarlandes
Pr Nathalie BALABAN	EXAMINATRICE	PR, The Racah Institute of Physics
Dr Michel TOLEDANO	EXAMINATEUR	DR, CEA Saclay
Dr Bill KEYES	EXAMINATEUR	DR, IGBMC

Abbreviations

ATP	Adenosine Triphosphate
bZIP	basic leucine zipper
cAMP	cyclic adenosine monophosphate
Cp	peroxidic cysteine
Cr	resolving cysteine
DNA	Deoxyribonucleic acid
dNDP	deoxyribonucleosides di-phosphate
DS	Diauxic shift
DTT	dithiothreitol
E. coli	*Escherichia coli*
G6PDH	glucose-6-phosphate dehydrogenase
GAPDH	Glyceraldehyde 3-phosphate dehydrogenase
GAS	General adaptation Syndrome
GFP	Green Fluorescent Protein
Gpx	Glutathione peroxidase
GSH	Glutathion
GSR	General Stress Response
GTP	Guanosine triphosphate
HAP	Heme Activator Protein
HMW	Height Molecular Weight
HOG	high-osmolarity glycerol pathway
LMW	Low Molecular Weight
MAPK	mitogen-activated protein kinase
mPrx	mitochondrial Prx
mRNA	messenger ribonucleic acid
NADPH	Nicotinamide adenine dinucleotide phosphate
NLS	Nuclear Localization Signal
nPrx	nuclear Prx
PDMS	Polydimethylsiloxane
PKA	Protein Kinase A
PPP	Pentose phosphate pathway
Prx	peroxiredoxin
PSG	Proteasome Storage Granules
ROS	Reactive oxygen species
RR	Ribonucleotide Reductase
rRNA	ribosomal ribonucleic acid
S. cerevisiae	*Saccharomyces cerevisiae*
SNF1	Sucrose Non-Fermenting 1
STRE	Stress Response Element
TF	transcription factor
TORC1	Target Of Rapamycin Complex 1
TPI	Triose-phosphate isomerase
Trx	thioredoxin
WT	Wild type

Table of Contents

General Introduction

In the general introduction, I will introduce the main historical and current concepts that shape the understanding of the plastic behaviours of living organisms in response to changing environments.

First, I will describe the **paradigm of homeostasis** in living organisms and how the maintenance of **constant internal physicochemical conditions drives physiological adaptation to stress**. Then, I will introduce **negative feedback loops**, the main mechanism by which cells achieve restoring homeostasis in changing environments.

I will then introduce homeostasis from an evolutionary perspective, based on the concepts of **fitness** and **stress resistance** (the propensity to adapt to stressors). Finally, this will lead us to the notion of **stress tolerance** (the propensity to survive stressors) as another key determinant of fitness.

I will finally expose the motivations and general questions that drive the work presented in this thesis manuscript.

1. The *sine qua non* conditions of life

1.1. The historical concept of “milieu interieur”

In the middle of the 19th century, while the structural bases of organisms were still largely unknown, Claude Bernard, a French physiologist, already stated that accomplishment of biological functions may be driven by their highly specific internal physico-chemical properties:

“*Les phénomènes extérieurs que nous apercevons dans cet être vivant sont au fond très complexes, ils sont la résultante d’une foule de propriétés intimes d’éléments organiques dont les manifestations sont liées aux conditions physico-chimiques de milieux internes dans lesquels ils sont plongés.”* (C. Bernard, Introduction à l'étude de la médecine expérimentale).

He came out with the notion of **‘milieu interieur’: living organisms must be secluded from their surrounding environment,** maintaining specific physico-chemical conditions within their body. This ‘milieu interieur’ must be seen as the sum of *sine qua non* internal conditions required for the ‘*free life’* of living organisms.

Indeed, in 1853, Claude Bernard had observed in the historical experiment of the “washed liver” that the liver was producing sugar and could regulate the glucose concentration in the blood independently of the diet of the animal. Some years later, in 1859, he observed that organisms were producing heat and regulating their internal temperature (Corvol, 2013). Those experiments demonstrated for the first time that

the ‘milieu interieur’ of organisms was actively regulated in order to maintain constant physico-chemical properties that are required for the organism’s life.

1.2. The dilemma between the need of constancy and the openness to the external environment

Living systems need to maintain a constant internal environment (the “milieu interieur”) but it is also necessary for their viability to be in constant interaction with their fluctuating environment. It is therefore interesting to explore the intrinsic relation that living systems share with their environment and what makes them particular in a physical perspective.

In 1944 in “*What’s life?”* Edwin Schrödinger (Schrodinger, 1944) asked this fascinating question:

‘How does the living organism avoid decay?’

Following the second law of thermodynamics, physical systems have an inherent tendency to increase their entropy over time, therefore losing their internal order and tending toward a thermodynamic rest state. However, living systems can maintain their organized structure over time, apparently challenging the laws of physics. Indeed, the second law of thermodynamics applies to isolated physical systems that necessarily tend toward a disordered state of maximal entropy and then remain at thermodynamic rest. On the contrary, open systems can maintain their internal order if energy continuously flows into them. The decrease of their internal entropy is compensated

through the consumption and the dissipation of energy in their environment (Schneider and Kay, 1995).

Of course, if energy dissipation is a prerequisite to maintain the organized structure of living systems, it is obviously not sufficient. For example, tornadoes are efficient dissipative structures that do not create order. On the contrary, in biological systems, the consumption of energy must enable the accomplishment of highly complex biological functions such as growth and proliferation, ultimately creating, maintaining, and reinforcing their highly organized structure.

From a thermodynamics point of view, living organisms can therefore be seen as open out-of-equilibrium machines that continuously dissipate energy coming from their surrounding environment to accomplish biological functions and avoid reaching a disordered rest state and die**. Organism-environment interactions are at the onset of the self-sustainability of living organisms** since they are critical to constantly fuel the biological functions of the organisms. However, external perturbations may in turn induce deviations in the internal physico-chemical variables of living organisms.

Organisms thus need to conciliate the stability of their 'milieu interieur' with the necessity to interact with their external environment.

2. The homeostatic framework and stress adaptation

2.1. The historical concept of homeostasis

The study of how organisms cope with external stressors has been formalized with the work of Walter Cannon, who developed the concept of "homeostasis".

In 1932, the idea of “milieu interieur” of Claude Bernard was generalized by Walter Cannon in “In the wisdom of the body” (Cannon, 1932) with the concept of homeostasis (literally ‘staying the same’). Homeostasis corresponds to the ability of an organism to maintain the internal environment of the body within limits that allow it to perform biological functions and therefore to survive. The inability of an organism to maintain its internal conditions can lead to deleterious effects.

Through multiple experiences, Cannon studied and described how external perturbations may induce physiological defects within organisms. Confronted to external perturbations, living organisms must compensate and adapt their behaviour to cope with external stressors. This set of adjustments can be defined as the stress response of organisms.

The ability of an organism to restore its biological functions, i.e. to adapt to a stressor is, in this view, directly depending on the maintenance of internal homeostasis in the presence of a stressor (Fig 1).

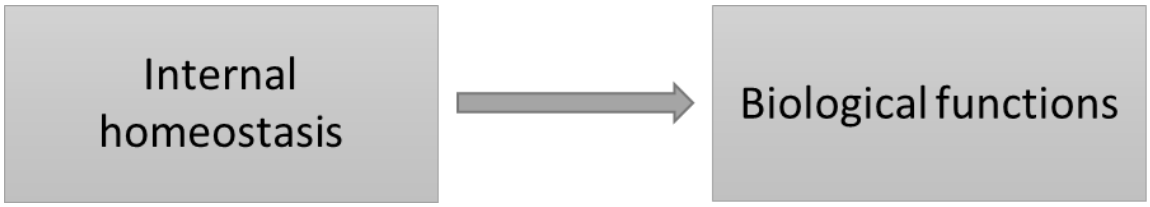

Figure 1: **The relation between internal homeostasis and the accomplishment of biological functions.** *This scheme represents a core relation of living systems functioning.*

The work of Cannon marked the beginnings of the study of stress-response mechanisms in living organisms.

2.2. Heterostasis: homeostasis in changing environments

In order to maintain internal homeostasis, any environmental change must be actively compensated by the organism in order to maintain its internal constants. I will introduce the general adaptation syndrome as a useful framework to extend homeostasis to the cases of environmental changes and tackle the consequences of homeostasis loss.

In 1956, by exposing rats to different stressors, Hans Selye observed that they were all exhibiting stereotypical changes of behaviour following the stress exposure (Selye, 1956). He called this acute period under stress the alarm phase and interpreted it as a hallmark of the adaptive processes triggered by organisms when submitted to a stressful environment. He observed that this phase was accompanied by signs of homeostasis disturbances such as tachycardia, hypothermia, and hypothermia. Importantly, since those changes were independent of the stressor, Hans Selye interpreted them as part of the stress response of the organism and not as a defect due to the stressor. He therefore proposed that during the alarm phase, both the stressor and the adaptive mechanisms used by the organism to defend itself establish a new equilibrium inside the organism, called heterostasis (literally 'other fixity'). This state contrasts with homeostasis that represents '*a normal steady-state by means of endogenous variables*' (Selye, 1975).

Following the alarm phase, he noticed that the organisms entered in a second phase, called the adaptive phase, where they were restoring their internal homeostasis. This was accompanied by the rescue of a 'normal' behaviour in the organism. However, a prolonged incapacity to restore homeostasis may lead to a third phase, called the

phase exhaustion and *in fine* to death. Hans Selye named those three phases the General Adaptation Syndrome (GAS) (Selye, 1956).

Selye's model **thus associates physiological adaptation to the rescue of homeostasis within organisms**. At the contrary, the permanent loss of homeostasis in organisms must finally death. However, the transition of organisms into a heterostatic state implies that **they may remain alive, at least transiently (before the phase of exhaustion), in an 'out-of-equilibrium' state.** Selye linked this state of heterostasis to the activation of a stereotypical stress response of organisms. The GAS represents the classical scheme of the orchestration of stress response in organisms.

3. An integrative view of stress response in microorganisms: feedback controls drive internal homeostasis and physiological adaptation

3.1. Microorganisms are unicellular homeostatic machines

Having introduce those historical concepts, I will now turn to microorganisms to further develop the discussion. Indeed, microorganisms represent an idyllic framework to study and understand the physiological response of organisms to stress. Due to their high rate of proliferation and duplication (~dozens of minutes), one can follow on relatively short timescales how their physiological behaviour is affected by a stressor.

Moreover, microorganisms are unicellular homeostatic machines, that integrates whole set of sense-and-signal mechanisms enabling them to respond efficiently to environmental changes. Indeed, unicellular organisms are directly exposed to their

environment and therefore critically require sensing, interpreting, and responding to any environmental fluctuations that may impair their homeostasis (Hohmann, 2002; Schimel et al., 2007).

3.2. Negative feedback controls guarantee homeostasis maintenance

Typical regulatory motifs involved in homeostasis maintenance are feedback controls. They are mechanisms by which a system can probe its own status and, using this information, reacts accordingly (Thomas, 1990). Negative feedback have a crucial importance in living organisms due to their ability to maintain variables stable over time and avoid them reaching extreme non-wanted values (Umbarger, 1956). *In fine*, negative feedback controls can balance external fluctuations that may disturb homeostasis (Gómez-Schiavon and El-samad, 2020) (see Fig 2).

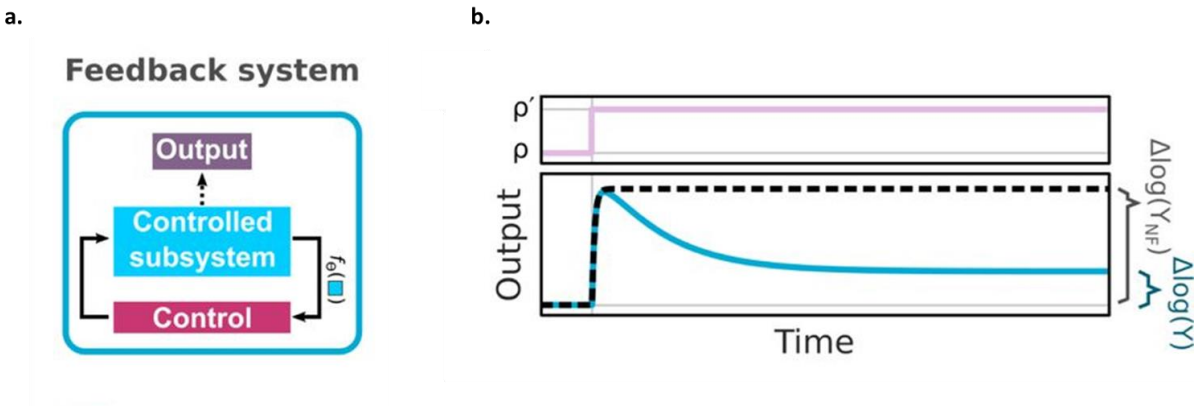

Figure 2 (adapted from Gómez-Schiavon and El-samad, 2020): **Negative feedback systems** (a) *Scheme of the feedback loop. The control unity sense the state of the system to be controlled and adjust its state at a set-point value.* (b) *Example of a variable submitted to a disturbance (rho in red) with a feedback control (blue curve), or without (dash black line).*

In 1956, a pioneered work discovered one of the first (if not the first) negative feedback control in biology. Authors reported that the presence of isoleucine in the medium of cells was negatively affecting the synthesis of isoleucine from threonine (Umbarger, 1956).

A critical step toward the understanding of how such feedbacks are orchestrated in biology has been made by Jacques Monod. By studying the adaptation of bacteria to sugar exhaustion (the diauxic shift), he understood that the sequential exhaustion of sugar and the recovery of growth after sugar exhaustion was depending on the control of gene expression at the transcriptional level (operon model).

From the 70's, René Thomas then formalized and generalized the functioning and the multiple roles of feedback loop mechanisms involved in regulatory networks of living organisms (Thomas, 1990).

Transcription regulation systems now appear as major schemes underpinning negative feedback controls in biology and are largely involved in the orchestration of stress response (Delaunay et al., 2000a; Hohmann, 2002; Muzzey et al., 2009; Sanchez and Lindquist, 1990).

Globally, they are composed of transcription factors (TF) and their target genes. Upon stimulation, a TF will sense the signal and adjust the expression of its target genes accordingly (Alon, 2007). Proteins represent the effector of the system since they achieve most of biological functions within cells.

Here, I will describe the osmoadaptation regulon in *S. cerevisiae* as a historical example of transcriptional negative feedback control involved in stress response.

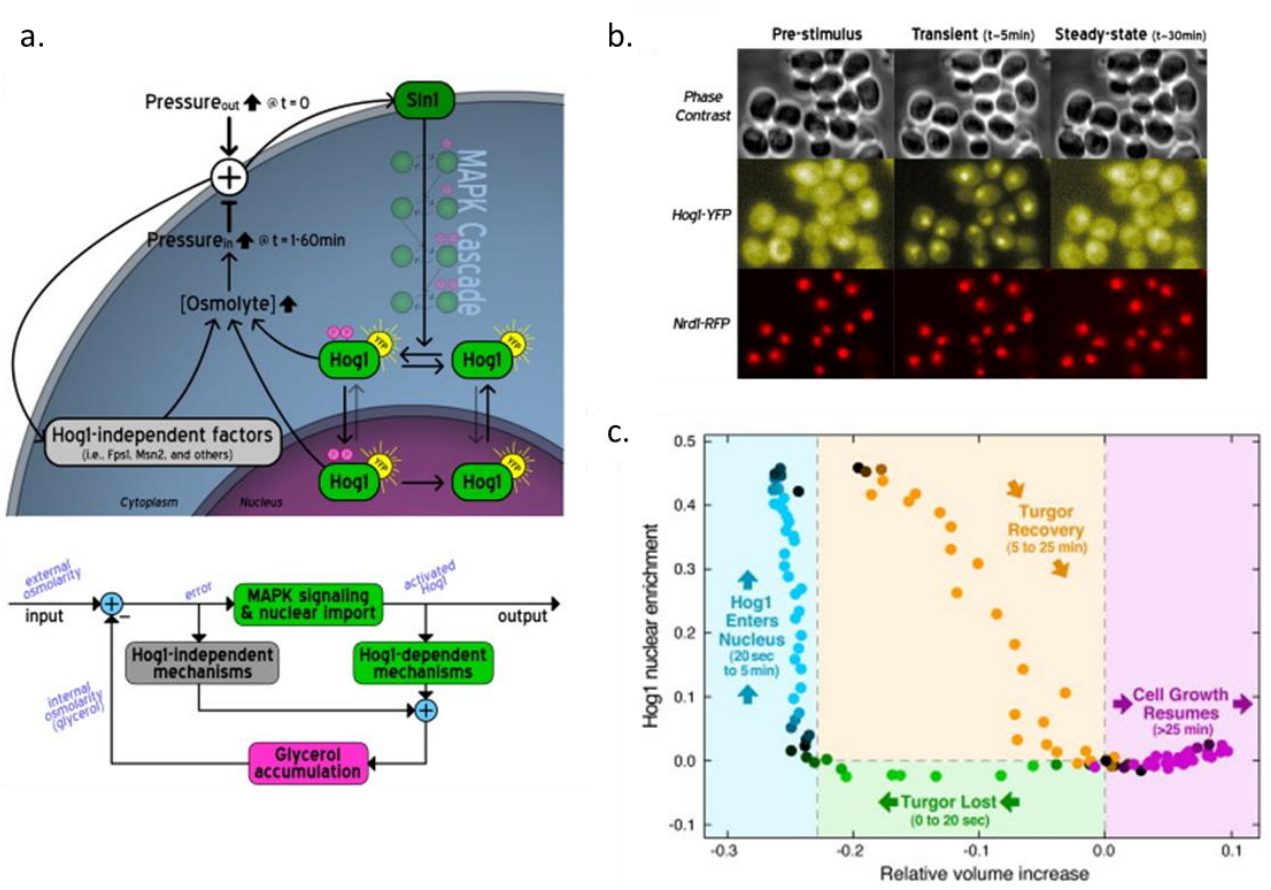

Figure 3 (adapted from Muzzey et al.): **The osmoregulon in budding yeast** (a) *Biological scheme of the MAPK-Hog1 osmo-regulon and the Network diagram. Input and Output of the systems are represented.* (b) *Hog1 nuclear relocalization upon activation of the MAPK pathway.* (c) *Sequence of events driving osmo-adaptation and physiological adaptation from the initial disturbance in turgor pressure.*

The ability of cells to maintain their turgor pressure constant and to adapt to osmotic changes are critical for cell viability. The sensing of the turgor pressure is achieved at the plasma membrane by different receptors (mainly Sln1 but also Sho1) that rapidly stimulate intracellular pathways involved in osmo-regulation (Hohmann, 2002). The main unit of the osmo-regulon is composed of the mitogen-activated protein kinase (MAPK) and is activated by Sln1 (Hohmann, 2002) (Fig 3a). The output of the MAPK is the phosphorylation of the high-osmolarity glycerol pathway (HOG) that will activate

the transcription of a battery of genes upon nuclear relocalization (Fig 3b). Upon nuclear relocalization, Hog1 activates the production of glycerol that is thought to largely drive osmo-adaptation (Hohmann, 2002; Muzzey et al., 2009). Overall, the osmo-regulon is therefore composed of a sensor (at the membrane), a control center (the MAPK-Hog pathways) and an effector, glycerol, that finely regulate turgor pressure (Alon, 2007). Together, it forms an efficient negative feedback control that regulate turgor pressure by transcriptionally regulating glycerol synthesis (Fig 3a, see the regulatory network).

Importantly, both the adaptation of cell volume (a parameter largely dependent on osmotic pressure) and the recovery of growth under osmotic stress are linked with the adaptation of the turgor pressure (the homeostatic parameter initially disturbed by the stressor) (Granados et al., 2017; Muzzey et al., 2009) (Fig 3c). In addition, the ability of cells to survive to different osmotic-stress patterns has been shown to be dependent upon the ability of the regulon to restore turgor pressure homeostasis (Granados et al., 2017).

Altogether, the context of the osmo-regulon illustrates well how negative feedback controls are central actors of both homeostasis maintenance and physiological adaptation. This validates at the cellular and molecular scales the tight relation between homeostasis and biological functions proposed by Walter Cannon ~100 years ago (see Fig 1).

4. Physiological adaptation, stress resistance and stress tolerance

4.1. Fitness optimization and stress resistance

NB: In this section, I do not have the pretention to introduce the concepts discussed in a formal manner or to tackle their complexity. I only aim at questioning the ambivalent physiological properties that may constrain and shape plastic responses of organisms to environmental changes.

In a general manner, the fitness function, F, corresponds to the integration of the growth of a microorganism over time:

$$F = \int \mu(t)$$

with μ(t) the growth rate of the microorganism.

From an evolutionary perspective, fitness represents the quantity maximized through Darwinian's evolution. In this view, **the homeostatic state of an organism represents the ensemble of physicochemical conditions, in a given environment, that maximizes its fitness.**
By restoring homeostasis, negative feedback controls are thus thought to participate and be required for physiological adaption. **The ability to recover growth and adapt under stress is called stress resistance** (Brauner et al., 2016).

This framework is likely to explain the propensity of organisms to recover homeostasis and proliferation through the action of feedback control systems. However, another physiological property must be considered when evaluating the behaviour of microorganisms in response to stress response.

Indeed, the ability of cells to remain alive under stress should also be considered. To include the 'weight' of the mortality, we can refine the Fitness function as:

$$F = \int \mu(t) - \alpha(t)$$

with μ(t) the growth rate and α(t) the death rate.

In particular, when growth is precluded, the ability of cells to remain alive is a critical determinant of cellular fitness. In the case where μ=0, the ability of organisms to remain alive, even without growing, avoid the Fitness function reaching negative value and thus the progressive decline of the population.

In an environment that would remain infinitely stable, remaining alive without growing would not make a critical difference for microorganism's fitness. **However, in the case environmental conditions may become more favourable, having avoid the complete death of the population may critically change the future fate of the population.**

4.2. Stress tolerance: a life 'out-of-homeostasis' exists

Indeed, it has been shown in various contexts that microorganisms could transiently survive harsh stressors that was precluding their adaption, a mechanism known as stress tolerance (or stress persistence in the case of a sub-population that exhibits an increased stress tolerance) (Brauner et al., 2016). Stress persistence have been first observed in the response of staphylococcus to penicillin (Bigger, 1944). Since this pioneered observation, bacterial and fungi persistence have been widely described (Amato et al., 2013; Balaban et al., 2004; Berman and Krysan, 2020; Harms et al., 2016; Radzikowski et al., 2016).

In particular, antibiotic stress tolerance/persistence has often been reported in comparison to other environmental stressors. This discrepancy may be explained by the important efforts that has been made in this field to define stress resistance and stress tolerance as distinct physiological properties (Balaban et al., 2019; Berman and Krysan, 2020; Brauner et al., 2016; Cohen et al., 2013). It is likely that stress tolerance drives survival in many other stress contexts.

In *E. coli*, it has been shown that antibiotic stress persistence could be linked to the entry of cells into a reversible non-growing state prior stress exposure (Balaban et al., 2004) (Fig 4). Alternatively, stress persistence can rather be induced by the stressor itself (induced persistence) (Brauner et al., 2016). However, in both situations, a common observation is the association of stress persistence with a reduced metabolism (Amato et al., 2013; Fisher et al., 2017; Radzikowski et al., 2016) and a vegetative non-growing state (Balaban et al., 2004b; Brauner et al., 2016; Harms et al., 2016). Additionally, if the maintenance of homeostasis has been shown to be a critical determinant of antibiotic stress resistance (Blair et al., 2015; Brauner et al., 2016), stress tolerance seems to be dependent upon different general stress response mechanisms (Brauner et al., 2016; Harms et al., 2016; Maisonneuve and Gerdes, 2014).

Overall, stress resistance and stress tolerance therefore appears as distinct stress response properties that depends on different molecular processes and both participate in optimizing fitness under stress.

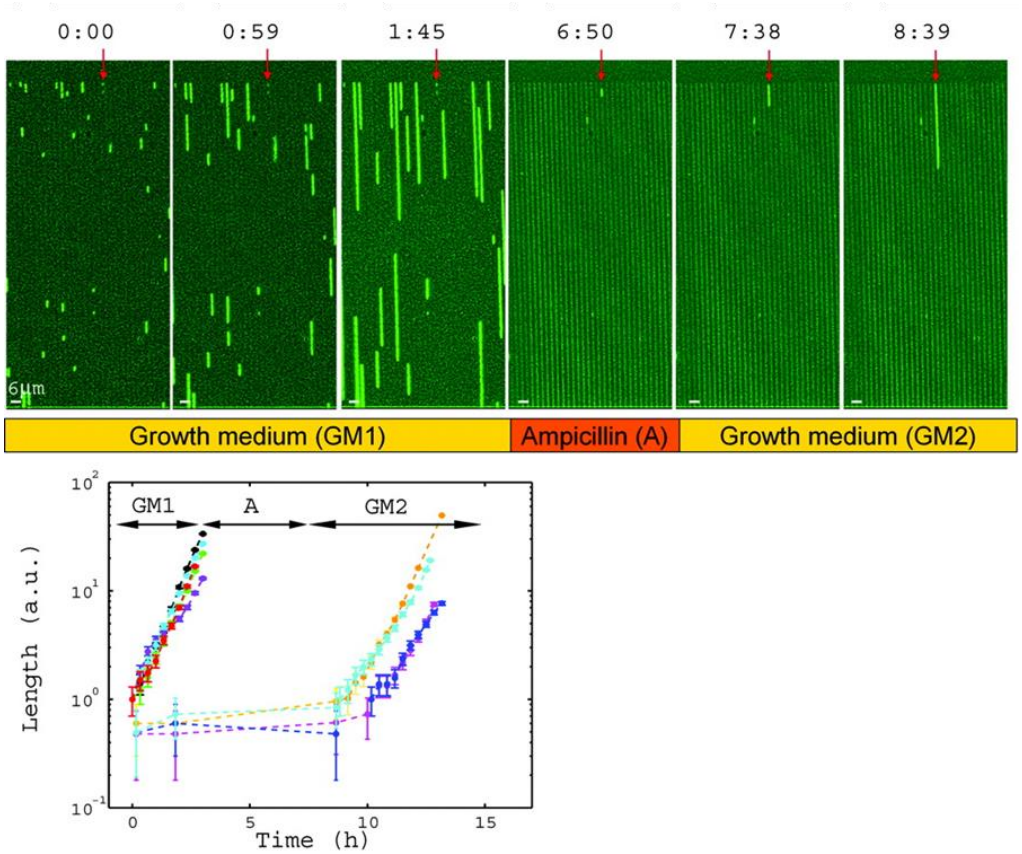

Figure 4 (from Balaban et al., 2004): *Growth of hipA7 bacteria in a microfluidic device (living cells in green) before, during and after an ampicillin treatment. The plot represents the 'length' of the green segments as a quantification of the growth of cells over time. After the stress, some cells survived by a mechanism of persistence: they did not elicit any proliferation under stress.*

PhD motivations and general questions

Microorganisms are constantly exposed to environmental changes and developed plastic response to cope with them and maintain their homeostasis.
Stress response behaviours, as any other biological processes, have been selected for and shaped by Darwinian's evolution to maximize organism's fitness. Stress tolerance, i.e. the ability to survive stress, and stress resistance, i.e. the ability to recover growth under stress and adapt, represent two critical properties that may greatly influence microorganisms' fitness under stressors.

Indeed, if stress tolerance may represent a valuable strategy to maximize survival in a stressful environment and avoid the complete extinction of a microbial colony, resistance represents a better alternative to maximize colony fitness by rescuing proliferation under the stressor. Remaining in a vegetative state while homeostasis and growth can be rescued would impair fitness non-necessary. Consequently, in response to natural stressors found in their ecological niche, evolution may have therefore tightly regulated the decision-making process of cells, favouring tolerance or adaptation depending on the inherent ability of cells to restore their homeostasis through feedback control mechanisms.

During those 4 years of *PhD*, I mainly explored the plastic stress responses and the physiological adaptation of the budding yeast *S. cerevisiae* to oxidative stress. In response to the ubiquitous oxidative stress hydrogen peroxide, we explored whether and how stress resistance and stress tolerance were encoded within the stress

responses of *S. cerevisiae*. In particular, we thought to decipher the role of the H_2O_2 scavenging homeostatic system for both stress resistance and stress tolerance. We hypothesized that in response to an environmental stressor into which yeast cells had evolved, both defense strategies may cover complementary functions. Finally, we explored whether stress tolerance and resistance were depending upon antagonistic cell states or if they could at the contrary simultaneously coexist. We envisioned that the orchestration of oxidative stress tolerance and resistance may represent a general scheme governing the environmental stress responses of microorganisms.

During this PhD, I also worked on a collaborative side project with another *PhD student* in the lab, Théo Aspert.

We aimed at exploring the whole transition of a single microorganism into a reversible vegetative state, called quiescence. This transition naturally occurs during the life cycle of the budding yeast, that first includes a transition from a fermentative phase to diauxie, then to a respirative phase before finally entering into quiescence. Most importantly, this complex sequence of events and its dynamics result from the exponential growth of the colony and cannot be recapitulated with synthetical stress patterns. We therefore aimed at developing a microfluidic-based methodology that would enable to observe the whole natural transition occurring from fermentation to quiescence in a fermenter at the single cell level. Such a methodology could be applied to any complex microbial environments.

Chapter 1: A trade-off between stress resistance and tolerance underlines the adaptive response to hydrogen peroxide

INTRODUCTION

1. Redox processes: physiological functions and harmful effects

Reactive oxygen species (ROS) include several molecules that have a strong propensity to react with other cellular compounds within cells due to their high redox potential. They are mainly **produced during the oxidative phosphorylation** within mitochondria, but other endogenous sources are present such as the NADPH oxidase in mammalian cells and the peroxisome. Exogenous sources of ROS also exist including xenobiotics, metals, and ionizing radiations.

When the intracellular level of reactive oxygen species is elevated, they can react in a non-controlled manner with several compounds within cells and cause damage to lipids, proteins, and DNA (Schieber and Chandel, 2014). However, despite their potential harmful effects, ROS have also been associated to **various signalling pathways and biological functions within cells** (D'Autréaux and Toledano, 2007).

ROS are therefore responsible for antagonistic effects, being detrimental when present in large quantities (**oxidative stress**) but critically required for multiple

biological processes (**redox biology**) (Schieber and Chandel, 2014; Sies and Jones, 2020).

2. The oxidative-specific stress response in *S. cerevisiae*

2.1 The H_2O_2 stimulon

To avoid the deleterious effects of ROS and to regulate their redox homeostasis, living organisms evolved toward efficient homeostatic feedback systems able to rapidly control ROS concentration by adjusting the concentration of scavenging molecules (D'Autréaux and Toledano, 2007).

While cells can be exposed to various oxidative compounds (such as diamide, menadione, ter-butyl hydroperoxide and cumene hydroperoxide), a study showed that among 456 single mutants that had been found to be sensitive to at least 1 oxidant (over 5 tested) only 12 mutants were sensitive to at least 4 oxidants out of the 5 tested (Thorpe et al., 2004). This study thus highlights **the specificity and the non-redundancy of the stress response to the different oxidative compounds.**

H_2O_2 is the most ubiquitous source of oxidative stress and has a central role in redox biology (Sies and Jones, 2020). Since sensing mechanisms and stress responses associated to those different oxidative compounds can largely differ (Delaunay et al., 2002; Ralser et al., 2007), I will focus our description on the mechanisms of sensing and response to H_2O_2.

2.1.1 The transcription factor Yap1

To scavenge H_2O_2, cells have to sense it and coordinate the expression of antioxidant regulatory processes. In the budding yeast *S. cerevisiae*, the exposure to H_2O_2 leads to the expression of at least 115 proteins and the down regulation of 52 others. This regulon is called the **H_2O_2 stimulon** (Godon et al., 1998). A further study reported up to 579 genes upregulated in response to H_2O_2 (Gasch et al., 2000). The activation of such an important number of genes rise the question of how cells coordinate the sensing and orchestrate the response to H_2O_2.

It has been shown that the response to H_2O_2 is in part controlled by the transcription factors Yap1 and Skn7 (Morgan et al., 1997). **Yap1 is a transcription factor with a basic leucine zipper DNA-binding domain** (bZIP). Once inside the nucleus, the bZIP preferentially binds a specific DNA motif (TGACTAA) and activate the transcription of targeted genes (Fernandes et al., 1997).

Yap1 controls the expression of at least 32 proteins and is only partially overlapping with the Skn7 factor (for 15 proteins) (Lee et al., 1999a). In agreement with that, the deletions of *YAP1* or *SKN7* lead to a loss of viability under H_2O_2. However, the deletion of *YAP1* exhibits a much stronger phenotype under H_2O_2 than a *skn7*Δ. Moreover, the double mutant *yap1*Δ *skn7*Δ elicits a phenotype similar to the one observed in the *yap1*Δ mutant (Lee et al., 1999a).

Together, those observations suggest that Yap1 is a pivotal determinant of the transcriptional H_2O_2 stress response.

2.1.2 Yap1 coordinates the sensing of H_2O_2 with downstream transcriptional expression

Now coming to the sensing mechanism, it has been further shown that Yap1 could be oxidized, thus enabling it to act as a sensor of the internal redox state of cells, in addition of its role of transcription factor (Delaunay et al., EMBO J, 2000). Importantly, in its oxidized form (Yap1ox), Yap1 forms a disulfide bond that masks an export signal sequence normally favouring its cytoplasmic localization (Kuge et al., 1997). Upon oxidation, Yap1 thus relocates from the cytoplasm to the nucleus due to the inability of the Crm1 nuclear exporter to bind Yap1ox (Yan et al., 1998). Importantly, this **redox-dependent nuclear localization enables the coordination of Yap1 function with the presence of H_2O_2 within cells.**

It has been further demonstrated that the oxidation of Yap1 was indirect. By being directly oxidized by H_2O_2, the glutathione peroxidase, Gpx3/Orp1, senses the stressor and further transduces the oxidation to Yap1 (Delaunay et al., *Cell*, 2002). Overall, the activation of Yap1 by H_2O_2 involves the multistep formation of 15 different disulfide bonds (S Okazaki, Mol Cell, 2007).

2.1.3 The specificity of the Yap1 regulon

Yap1 relocation is not observed in response to other environmental stressors (osmotic stress or starvation). As a consequence, it has been showed that the single activation of Yap1 carried enough information for a cell to distinguish an oxidative stress from another external stressor with an important predictability (Granados et al., 2018). This further confirms that Yap1 dependent response offers a specific response to H2O2 due to its ability to sense the oxidative state of cells.

Moreover, Yap1 can be reduced by proteins of its own regulon (mainly thioredoxins), enabling a negative feedback to regulate its activation and avoid any aberrant overexpression of the regulon (Delaunay et al., EMBO J, 2000).

Together, those elements demonstrate **that the Yap1 regulon represents an oxidative stress-dependent negative feedback system that ensures a broad transcriptional response following stress exposure** (Fig 5).

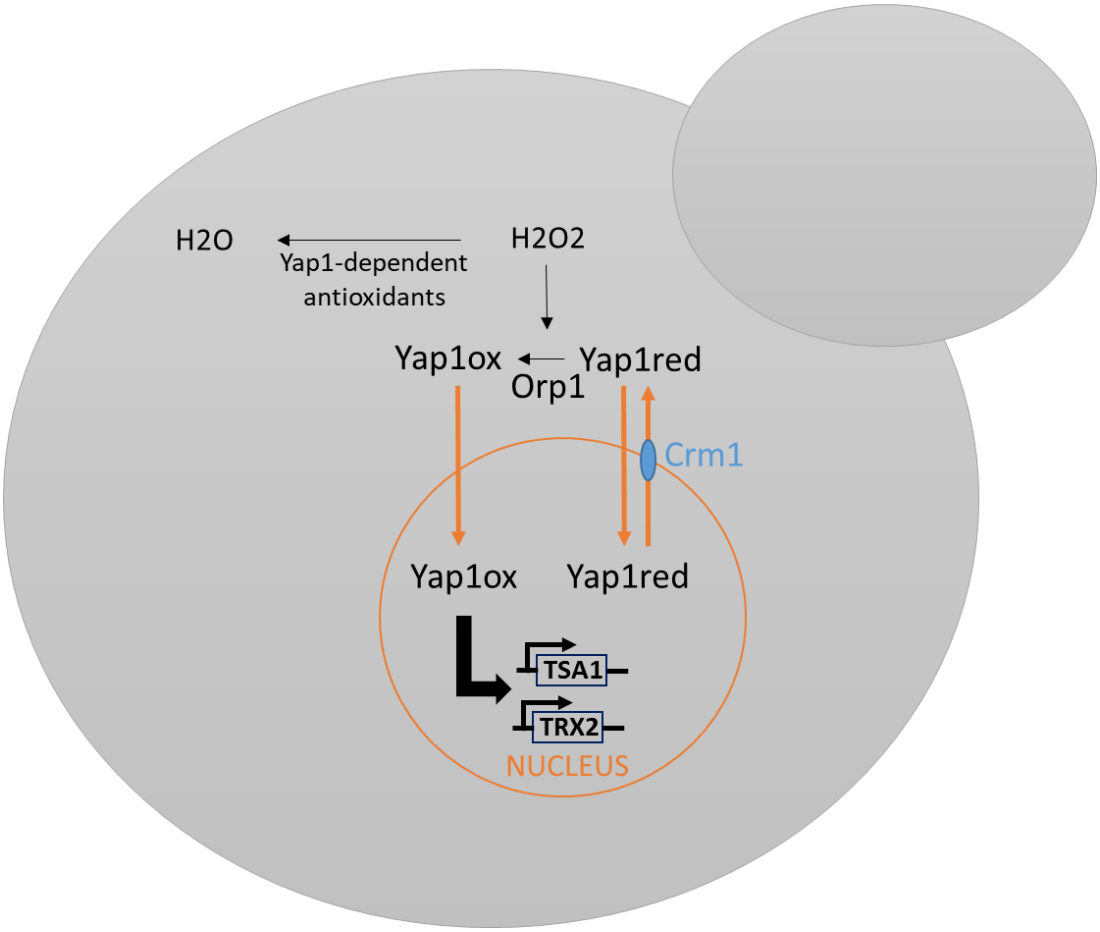

Figure 5: Simplified scheme of the Yap1 regulon. *Upon H_2O_2 exposure, Yap1 is oxidized through a Gpx3/Orp1-dependent redox relay. Its oxidation inhibits its nuclear export*

by Crm1 and thus causes its accumulation into the nucleus. In the nucleus, Yap1 binds to DNA and leads to the activation of specific genes implicated in the response and adaption to H_2O_2. The Yap1-dependent expression of antioxidants dampen the internal H_2O_2 concentration, thus leading to a negative feedback loop.

2.2. The cellular antioxidant machinery in *S. cerevisiae*

Among the antioxidants activated upon H_2O_2, different classes of enzymes such as catalases and peroxidases have been identified (Godon et al., 1998; Lee et al., 1999a). Those antioxidant enzymes have evolved toward a high reactivity toward H_2O_2, thus enabling its detoxification (D. Keilin et al., 1958, Biochim et Biophy Acta, Harris JR. et al., 1968; Mills GC. J Biol Chem, 1957). If both classes of enzymes ultimately transform H_2O_2 into H_2O, they work following distinct mechanisms.

In the following part, I will briefly introduce the biochemical mechanisms involved in the scavenging of H_2O_2 by the different antioxidant enzymes and introduce the constituents of the antioxidant machinery in *S. cerevisiae*.

The functional role of those enzymes will then be discussed. Indeed, several discrepancies exist between the biochemical functions and the effective functional role reported for those enzymes in the literature. Both aspects are therefore separated for the sake of clarity.

2.2.1. Catalase

Catalases catalyse the dismutation of H_2O_2 into H_2O following the reaction:

$$2\ H_2O_2 \rightarrow 2\ H_2O + O_2$$

The dismutation reaction is a two-step process that involves the fer atom of the catalase. This atom will first form an intermediate oxidant:

H_2O_2 + Fe(III)-Catalase → H_2O + O=Fe(IV)-Catalase

H_2O_2 + O=Fe(IV)-Catalase → H_2O + O_2 + Fe(III)-Catalase

By cutting the O-O bond of the H_2O_2 molecule, the Fe(III) group will form a transient and highly reactive Fe(V) complex that will then react with another H_2O_2 molecule. At the end of the reaction, the catalase thus recovers its initial form.

The budding yeast has one cytoplasmic catalase T (encoded by *CTT1*) and one peroxisomal catalase A (encoded by *CTA1*).

2.2.2. Thiol-peroxidases

Peroxidases catalyse the reduction of peroxides following the reaction:

ROOR' + 2e- + 2H+ → ROH + R'OH

In living organisms, the highly reactive thiol groups of cysteines often initiate the reaction with H_2O_2. The peroxidases that use cysteine as a catalytic element are called thiol peroxidases (L Flohé et al., Antioxid. Redox. Signal., 2011). Most of peroxidases have a high affinity for H_2O_2, but some peroxidases are specialized in lipid peroxide or also other peroxides (Fomenko et al., 2011; Lee et al., 1999b).

After reacting with H_2O_2 (or another peroxide), the thiol group of the peroxidase is in a sulfenyl form, that further react to form a disulfide bond with another thiol group. Unlike catalases, **the reduction of peroxidases requires other molecules that will specifically reduce their disulfide bond** (L Flohé et al., Antioxid. Redox. Signal., 2011). Two major classes of thiol peroxidases are distinguished in living organisms, the **peroxiredoxin** (Prx) and the **glutathion peroxidase** (Gpx), depending on the reduction pathway they use (see next section). Once in their oxidized form (disulfide bond), thiol peroxidases are indeed recycled by an electron donor, respectively by thioredoxin or glutathion for peroxiredoxins or glutathion peroxidases (Fourquet et al., 2008).

Peroxiredoxins have a conserved catalytic mechanism that involves a specific cysteine residue, the peroxidic cysteine (Cp), that have an important reactivity to H_2O_2. Once oxidized, the Cp residue attacks another cysteine, called the resolving cysteine (Cr) to form a disulfide bond (Hall et al., 2009) (Fig 6). Depending on whether or not the Cr residue comes from another Prx molecule, we distinguished 1-Cys and 2-Cys peroxiredoxins (Hall et al., 2009).

a

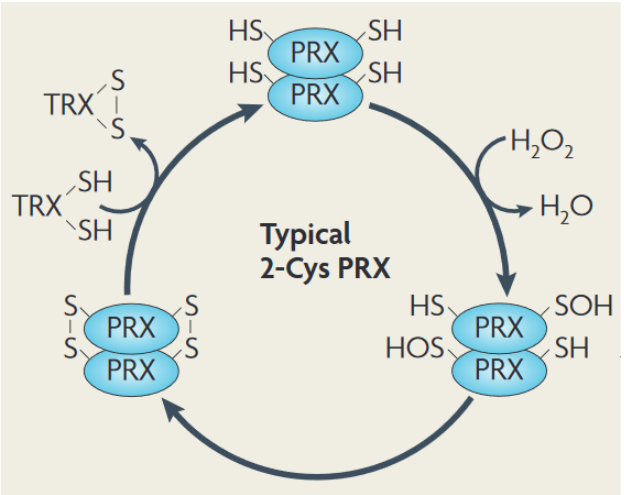

b

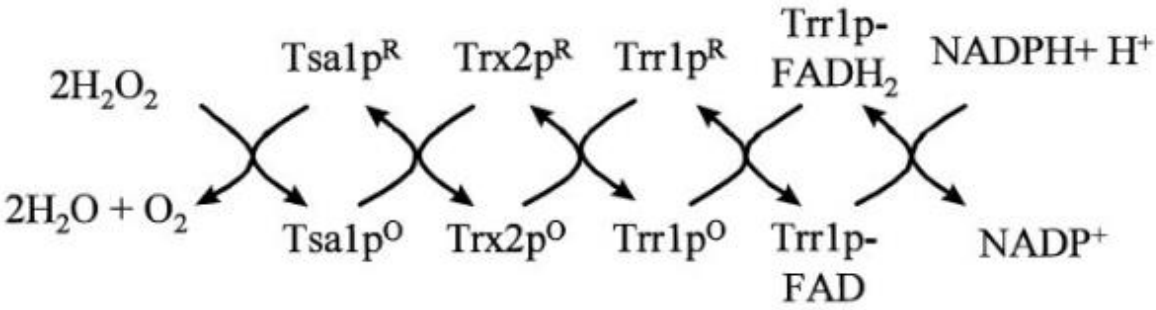

Figure 6 (adapted from D'Autréaux and Toledano, 2007): **The Prx cycle and the thioredoxin recycling process** (a) *Catalytic cycle of the typical 2-Cys Prx. The first step corresponds to the reaction of one Prx with H_2O_2. The resulting Tsa1-SOH reacts with another Prx molecule, leading to the formation of a dimer linked by a disulfide bond. Once formed, the disulfide bond can be reduced and recycled by thioredoxins* (b) *Scheme of the recycling of the main peroxiredoxin, Tsa1, by the thioredoxin pathway in the budding yeast S. cerevisiae. When Tsa1 reacts with H_2O_2, its cysteine is oxidized and then reduced by the main thioredoxin Trx2. Ultimately, NADPH sustains peroxiredoxins and thioredoxins in their reduced form (together with the thioredoxin reductase Trr1).*

The budding yeast has 3 CysGpx (Gpx1/2/3, Y Inoue et al., J Biol Chem, 1999 and AM Avery, J Biol Chem, 2001) and 5 Prx (CH Wong et al., J Biol Chem 2004). Among those Prx, there are 2 typical 2-cys cytoplasmic Prx (Tsa1/2) and an atypical cytoplasmic 2-cys Prx (Ahp1). The two remaining ones are a nuclear Prx (nPrx) and a mitochondrial Prx (mPrx) (Fourquet et al., 2008). In addition, Gpx2, one of the three homologs of glutathion peroxidase in yeast, is indeed an atypical 2-cys Peroxiredoxin that directly uses thioredoxin as an electron donor (T Tanaka et al., J Biol Chem, 2005).

2.2.3. The NADPH-dependent thioredoxin and glutathion pathways

Thioredoxins are enzymes that catalyse the reduction of disulfide bonds (-SS-) that results from the reaction of oxidized protein thiols (-SOH groups). Their catalytic activity holds on 2 cysteine residues that can be oxidized to form a disulfide bond (see Fig II.2b). They are involved in the reduction of several proteins within cells. Their role in H_2O_2 detoxification is linked to their ability to recycle the thioredoxin-dependent peroxidases, the Prx.

Once oxidized, thioredoxins can then be reduced by another enzyme, the thioredoxin reductase, that uses the reductive power of NADPH to sustain thioredoxin in their reduced form. Globally, thioredoxins and thioredoxin reductases sustain the peroxidase activity of peroxiredoxins thanks to the reductive power of NADPH (Hall et al., 2009) (Fig 6b).

Following a similar scheme, the tripeptide glutathione can reduce disulfide bonds in cells. In particular, it can reduce glutathion-dependent peroxidases by “capturing” the oxidation, being itself oxidized in the reaction (from a GSH reduced form to an oxidized GSSG form). Due to its abundancy within cells, it represents an important “buffer of oxidation” (Penninckx, 2002). It is synthesized from cysteine in a two-step processes, first requiring the γ-glutamyl-cysteine synthase and the glutathion synthase (Penninckx, 2002). Once oxidized, it can be reduced by the glutathion reductase thanks to the reductive power of NADPH. Due to the prominent role of the Pentose phosphate pathway (PPP) in NADPH production, the first enzyme and limiting step of the PPP, Zwf1, is often considered as an actor of both thioredoxin and glutathion cycles. In a following part, the pivotal role of the PPP to sustain those two cycles will be developed (see Ch1.3.).

Thioredoxin and glutathion pathways thus appear as two “parallel” pathways that enable the recycling of oxidized thiol-peroxidases in cells. Through this activity, they actively participate in H_2O_2 degradation within cells.

2.2.4. Sulfiredoxin

If thioredoxins can reduce peroxiredoxins from their disulfide form, peroxiredoxins can instead be further oxidized to a sulfinic acid form. This form is not reducible by thioredoxins. However, another enzyme has been discovered in the budding yeast, the sulfiredoxin Srx1, that exhibited an ATP-dependent reductive activity towards

peroxiredoxins in their sulfinic form (Biteau et al., 2003) (Fig 7). This function thus enables, together with thioredoxins, an efficient recycling of oxidized peroxiredoxins.

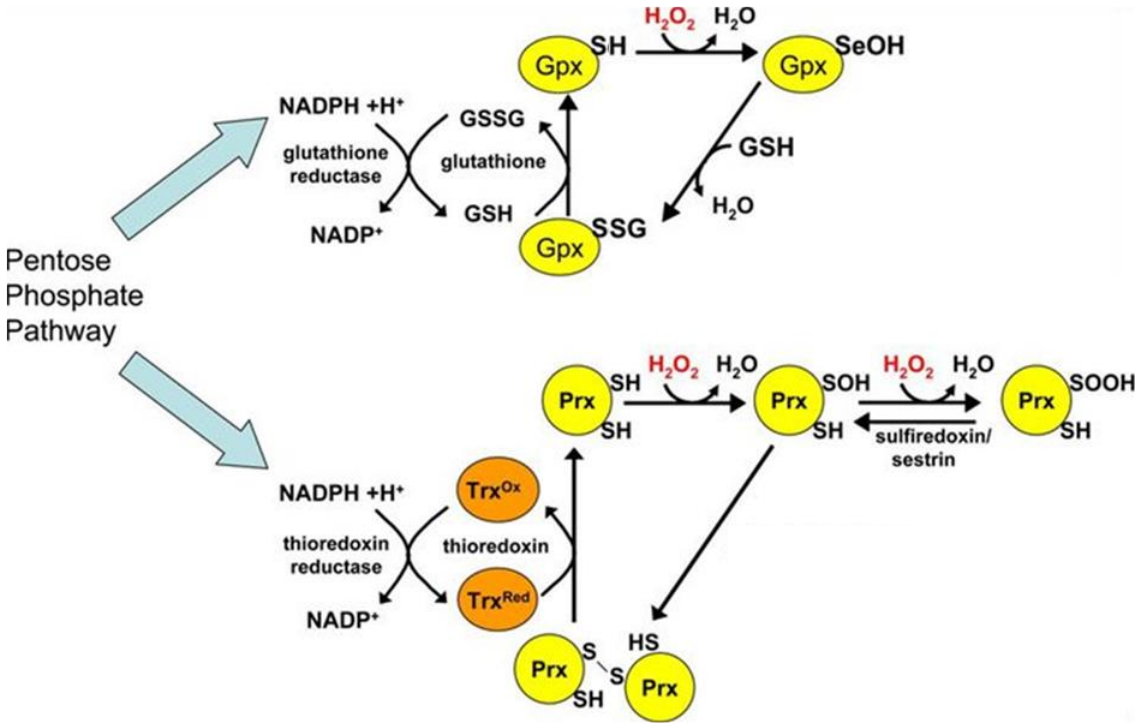

Figure 7 (adapted from …): **Scheme of the catalytic cycle of thiol peroxidases and their recycling by thioredoxin or glutathion cycles**.

2.2.5. Cytochrome c peroxidase

In addition, there is another class of peroxidase, called the cytochrome c peroxidase, that also scavenges H_2O_2. It has the particularity to work independently of thioredoxin and glutathion systems and therefore does not require the reductive power of NADPH. The reduction of H_2O_2 is initiated by the Fe atom of the cytochrome c, as in catalases, following the reaction:

2 ferrocytochrome *c* + H_2O_2 → 2 ferricytochrome *c* + 2 H_2O

2.3. H_2O_2 scavenging and physiological response to oxidative stress

The antioxidant described above have all the abilities to scavenge H_2O_2 based on their biochemical properties. However, in a physiological context, how the global redox homeostasis of cells is achieved and what is the role of each antioxidant in H_2O_2 scavenging is less clear.

Moreover, whether the scavenging capacity of the antioxidant explains its function for adaptation and survival under H_2O_2 challenges is also elusive. Indeed, if the physiological behaviour of strains deleted for most of the antioxidants of *S. cerevisiae* has been widely studied, several discrepancies still exist. In fact, the link between the physiological role of antioxidants for H_2O_2 stress adaptation and survival and the H_2O_2 scavenging function assigned to them remains unclear. In addition, some antioxidants, in particular the main peroxiredoxin Tsa1, possess other biological functions, independently of their role in H_2O_2 scavenging. It is therefore not always trivial to bridge the gap between the known molecular functions of a given antioxidant and its physiological role when exposed to a H_2O_2 stress.

In this section, I will briefly describe the biochemical properties of antioxidants, then introduce the current approaches enabling to probe the internal redox state of cells and then discuss the role of antioxidants in the response to oxidative stress challenges.

2.3.1 *In vitro* H_2O_2 scavenging properties of antioxidants and *in vivo* significance

As a first approach to the scavenging function of antioxidants, the biochemical properties of enzymes can help to understanding their functional specificity.

In an *in vitro* context, where the substrate (H_2O_2) of the antioxidant is at saturation, the H_2O_2 scavenging capacity (the rate at which an enzyme reacts with its substrate) of catalases and Selenium-Gpx (not present in yeast) is largely superior to the detoxification capacity of CysGpx and Prx (Fourquet et al., 2008). In this situation, the efficiency of the enzyme can be assessed by the kinetic efficiency (k_{cat}/K_M, k_{cat} measuring the rate of the reaction at substrate saturation and K_M the affinity of the enzyme for its substrate). k_{cat}/K_M thus measures the efficiency of an enzyme to convert its substrate into a given product when the substrate is at saturation (see Table 1).

However, those measures are unlikely to represent the *in vivo* efficiency of those proteins since H_2O_2 is often far from saturating the substrate. The *in vivo* activity of antioxidants towards H_2O_2 is best represented by the second order constant reaction ($[H_2O_2]$*[enzymes]) (Fourquet et al., 2008). In addition, the rate of reduction of the peroxidase must be considered since it can critically limit the ability of peroxidase to reduce H_2O_2.

However, even if such measures give a theoretical idea of the detoxification potential for each enzyme, their effective cellular detoxification cannot be directly assessed from those *in vitro* parameters. First, the enzyme concentration is not stable over time due to the activation dynamics of the H_2O_2 stimulon. For example, both peroxidases and catalases are massively expressed in response to hydrogen peroxide (Lee et al., 1999a; Martins and English, 2014). Such variation of concentrations (up to a 15-fold increase for Ctt1 (Martins and English, 2014)) may drastically change the relative role

of enzymes in H_2O_2 detoxification. Moreover, when cells are exposed to a given external H_2O_2 concentration, the resulting internal H_2O_2 concentration is difficult to measure since it results both from the rate of diffusion across the cellular membrane and the dynamics of internal detoxification.

Overall, it is nonetheless interesting to notice that based on their biochemical characteristics, Prx are highly efficient enzymes under low fluxes of H_2O_2. However, their reduction by thioredoxin (Khademian and Imlay) limits their function under high fluxes of H_2O_2 compared to catalases (Fourquet et al., 2008). On the contrary, catalases appear to be much more efficient under high H_2O_2 fluxes.

In the following sections, I will consider the maintenance of redox homeostasis under non-oxidative conditions, what I will call the **"basal redox state of cells"**, and the scavenging capacity of antioxidants under H_2O_2 challenges. Decoupling both aspects (the role of antioxidants in the maintenance of redox homeostasis and their role under stress) may help to understand their physiological role *in vivo*.

TABLE 1. KINETIC PARAMETERS OF SELECTED PEROXIREDOXINS (PRX), SELENOTHIOL GLUTATHION PEROXIDASES (SEGPX), AND HEME CATALASES (HECAT)

		Oxidizing substrate	k'_A (M/s)	k'_B (M/s)	k_{cat} (per s)	K_m (ROOH) (μM)	K_m (Red) (μM)	References
Prx	PRX2 *H. sapiens*	H_2O_2	1.3×10^{7a}	9.0×10^{5b}	2[c]	<20[h]	2.7[d]	12, 79
	PRX1 *H. sapiens*	H_2O_2	$>2.2 \times 10^{5b}$	8.0×10^{5b}	4.4[c]	<20[h]	5.5[d]	12
	PRX3 *H. musculus*	H_2O_2	$>2.4 \times 10^{5b}$	1.1×10^{6b}	4.8[c]	<20[h]	4.3[d]	12
	AhpC *S. typhimurium*	H_2O_2	3.7×10^{7b}	8.9×10^{6b}	52.4	1.4	5.9[e]	76, 81
		t-BOOH	2.3×10^{5b}	1.3×10^{7b}	54.7	238	4.1[e]	
		CH	4.9×10^{5b}	1.3×10^{7b}	52.0	107	4.0[e]	
	Tpx *E. coli*	H_2O_2	4.4×10^{4b}	3.0×10^{6b}	76	1,730	22.5[f]	3
		CH	7.7×10^{6b}		70.1	9.1	22.5[f]	
	Tsa1 *S. cerevisiae*	H_2O_2	2.5×10^{7a}		0.31	12	—	67, 71
		t-BOOH			0.29	7.9	—	
		CH			0.26	17.1	—	
	Tsa2 *S. cerevisiae*	H_2O_2	1.3×10^{7a}		0.39	13.8	—	67, 71
		t-BOOH			0.29	5.1	—	
		CH			0.28	4.5	—	
SeGPx	GPX1 *H. sapiens*	H_2O_2	4.1×10^{7g}	2.3×10^{5g}				91
		t-BOOH	4.2×10^{6g}	2.3×10^{5g}				
	GPX3 *H. sapiens*	H_2O_2	4.0×10^{7g}	7.9×10^{4g}				91
		t-BOOH	2.3×10^{6g}	7.9×10^{4g}				
	GPX4 *Pig heart*	PCH	1.5×10^{7g}	5.7×10^{4g}				
HeCat	Catalase *Horse erythrocytes*	H_2O_2	0.6×10^7	1.8×10^7				15
	Catalase *Horse liver*	H_2O_2	1.7×10^7	2.9×10^7				15
	Catalase *M. lysodeikticus*	H_2O_2	1.1×10^7	1.7×10^7				15

Table 1 (from Fourquet et al., 2008): Kinetic parameters of major antioxidants: *k_A and k_B represent the second-order rate constants for the first (oxidizing) step and the second (reductive) step of the reaction. K_{cat} is the rate of the reaction at substrate saturation and K_M, the affinity of the enzyme for its substrate.*

2.3.2 Probing the internal redox states of cells experimentally

Before discussing the role of antioxidants in H_2O_2 scavenging and the adaptation to H_2O_2 in greater details, I will first introduce the different redox sensors available to experimentally probe the redox state of cells. Indeed, measuring the redox homeostasis of cells is not an easy task and several approaches, all having advantages and inconvenient.

The characteristics of the methods described in this section are summarized in the Table 1.

a. H_2O_2 scavenging assays

To assess the ability of cells to scavenge H_2O_2, it has been proposed to measure the decrease of the external H_2O_2 concentration over time in a liquid culture containing cells. H_2O_2 is often measured with a simple colorimetric assay.

If they offer the possibility to measure the external decrease of the H_2O_2 concentration, they do not directly access to the internal redox state of cells. Indeed, there is no real evidence that the rate at which a strain scavenges H_2O_2 is always directly linked to its internal redox equilibrium. The internal redox equilibrium is the balance between the scavenging rate and the internal production of ROS/H_2O_2 and the internalization of external sources of oxidative stress. A difference in the scavenging rate of a strain can for example be balanced/compensated by changes in the internal production of ROS and thus finally results in an unchanged internal redox equilibrium.

However, in the context of an important oxidative stress, it appears reasonable to assume that the H_2O_2 scavenging rate is a good proxy of the ability of cells to maintain their redox equilibrium.

The main limitation of scavenging assays is their poor temporal resolution. The measured scavenging rates typically result from the time integration of the curve of decay of external [H_2O_2] (Hanzén et al., 2016; Roger et al., 2020; Seaver and Imlay, 2001). They can therefore not capture temporal changes in the scavenging rate of

cells. Consequently, they cannot depict the complex dynamics of the oxidative stress response usually observed in cells (see Ch2.5.).

b. Protein oxidation as a proxy of the internal redox equilibrium

I described previously that upon oxidative stress, several proteins were oxidized inside cells. In particular, peroxiredoxins, thioredoxins and other enzymes involved in H_2O_2 scavenging have a high reactivity toward H_2O_2 and are thus rapidly oxidized in case of redox imbalance. Most importantly, cysteines can remain in their oxidized forms for hours without being reduced or degraded *in vivo* (mostly in the form of a disulfide bond). Assessing the ratio of oxidized/reduced proteins can thus give prominent information about the redox state of cells.

Western blot can specifically target the oxidized form of a protein. Such assays have been widely used and enable a dynamical assessment of the redox state following H_2O_2 exposure (see Fig 8b.) (Biteau et al., 2003; Bodvard et al., 2017; Delaunay et al., 2000a, 2002; Domènech et al., 2018; Okazaki et al., 2007).

a

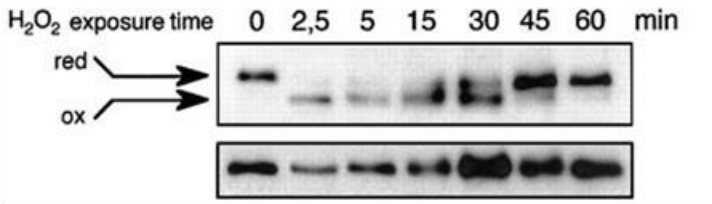

b

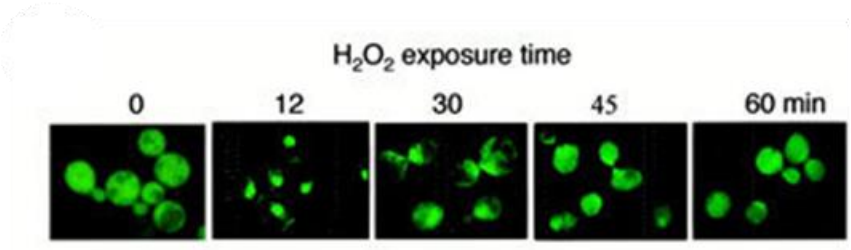

Figure 8 (adapted from Delaunay et al., 2000): Yap1 oxidaition and localization under H_2O_2. (a) *Western blot targeting yMyc-Yap1. Time course before and 2.5, 5, 15, 30, 45 and 60 min after treatment with 400 µM H_2O_2.* (b) *Time course of Yap1-GFP after a 300µM H_2O_2 treatment.*

In addition, the rise of quantitative mass spectrometry now offers the possibility to screen the oxidation status of the whole proteome. Using the mass spectrometry-based OxICAT approach (Leichert et al., 2008) that allows to screen the redox state of proteins in a broad manner, a study recently delineated the yeast redoxome by identifying the oxidation state of 4300 cysteine residues among 2200 different proteins (Topf et al., 2018).

Such methodology gives a molecular map of the oxidation state of cells, thus going beyond the scope of probing the global redox state of cells.

However, mass spectrometry still suffers from a low accessibility and a high cost that preclude its use for routine experiments. If western blot is a much a more accessible technique, it suffers from being semi-quantitative and remains low throughput.

Another limitation of those protein-based approaches is their inability to quantify information at the single-cell level. The clonal heterogeneities observed in a microbial population can therefore not be accessed.

c. Yap1 localization as a redox sensor

A promising alternative to biochemical approaches (western blot and mass spectrometry described above) is to use GFP-based approaches to probe the redox state of cells.

In the budding yeast, since Yap1 relocates in the nucleus upon oxidative stress (see 2.2) (Delaunay et al., 2000b), the nuclear/cytoplasmic Yap1 localization directly depends on the redox state of cells. Tagged with a fluorescent reporter, the Yap1 localization can be used as an internal fluorescent redox sensor (Delaunay et al., 2000b) (see Fig 8b). Importantly, the nuclear/cytoplasmic ratio is independent on the maturation time of the fluorophore and is therefore a highly dynamical readout of the redox state. In addition, such approach has the great advantage to offer a single-cell resolution, thus revealing the cell-to-cell heterogeneities in a microbial population.

However, a limitation of this approach is the rapid saturation of the Yap1 nuclear enrichment in response to relatively small doses of H_2O_2. It has been reported that the signal was saturating for an external dose of H_2O_2 of ~0.2 mM, so below the dose at which growth is inhibited under H_2O_2 (Goulev et al., 2017).

Moreover, as this Yap1 sensor is based on an endogenous protein, it is also dependent on several intracellular processes. For example, any change in the nuclear import/export processes may change the nuclear/cytoplasmic ratio of the sensor, independently of the redox state of the cell. Lastly, the signal to noise ratio of the Yap1 fluorescent signal is relatively low and requires an important light exposure that can be detrimental over long term experiments for cell toxicity.

d. Yap1-dependent transcription as a redox sensor

An alternative to the direct measure of the Yap1 localization is the quantification of the Yap1-dependent transcriptional activity. Indeed, since antioxidant genes are under the control of Yap1, their expression is finely coordinated to the redox state of cells:

any redox change sensed by Yap1 leads to its translocation into the nucleus and the expression of its target genes.

GFP-based measurements of endogenous proteins have the great advantage to assess internal redox state at the single-cell level with a single fluorophore and common excitation/emission wavelengths. Moreover, in comparison to the Yap1 nuclear signal quantification, the signal obtained from such GFP-based transcriptional reporters are much more trivial to quantify: the averaged fluorescence within the cell represents a robust and non-noisy signal.

However, looking at the transcriptional-based reporters also have drawbacks. The sensor depends on the transcriptional/translational activity of cells and can thus be modulated by the status of the transcriptional/translational machinery of cells. In addition, both the maturation time of the GFP and the long half-life of the GFP protein (~ the doubling time of cells, that corresponds to 90 min in budding yeast cells) contribute to limit the temporal resolution of the signal. To reduce the half-life of the protein and recovers a better dynamics, a degron sequence can be added to the GFP protein to favour its degradation by the proteasome (Goulev et al., 2017). By using the TRX2pr-GFP-deg signal, a burst-like expression in response to oxidative stresses has been reported (Goulev et al., 2017) (Fig 9), testifying its ability to access to the temporal redox changes following H_2O_2 exposure.

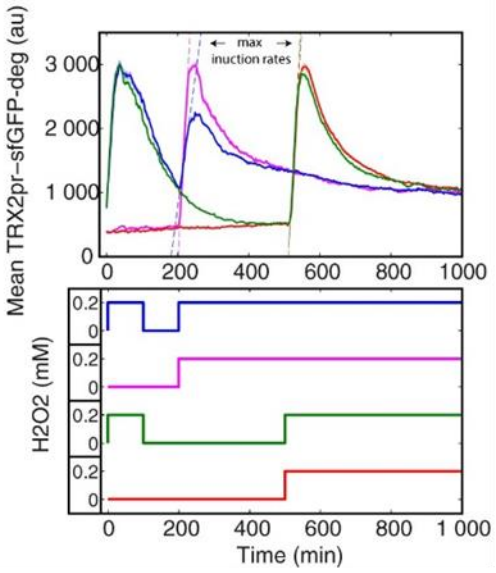

Figure 9. (adapted from Goulev et al., 2017): **Mean TRX2pr-GFP-deg fluorescence signal in S. cerevisiae yeast cells in response to various H_2O_2 stress patterns (from 0 to 0.2 mM H_2O_2)**. *The sensor enables to capture the initial redox imbalance following H_2O_2 exposure and the recovery of the redox homeostasis.*

e. Genetically encoded ratiometric redox sensors

Genetically encoded redox sensors offer another alternative to dynamically assess the internal redox state in living cells. Those probes are fluorescent-based ratiometric sensors coupled to an intracellular H_2O_2-sensing enzyme. The fluorescent excitation spectrum of the fluorophore is classically modified by the oxidative state of the coupled H_2O_2-sensor, therefore assessing the redox state of the cellular compartment in which the sensor is localized (Fig 10). The first probe using such strategy, HyPer, took advantage of the OxyR H_2O_2-sensing enzyme of E. Coli. YFP proteins were inserted into the OxyR regulatory domain to build a genetically encoded fluorescent H_2O_2-sensor (Belousov et al., 2006) (Fig 10a). Several other sensors were developed, based on different fluorophores and different endogenous H_2O_2 sensors (Bilan and Belousov, 2016; Gutscher et al., 2009) and enable to probe redox changes in response to mild or severe external oxidative stresses. Another sensor based on a redox relay with Tsa2, the roGFP2-Tsa2ΔC$_R$, also offers the possibility to assess the basal redox level of cells and redox changes in a physiological range (in order to make

the distinction between external stressors that are in the µM range) (Morgan et al., 2016). A version of this H_2O_2-sensor is also compatible to specifically access to the redox state within the mitochondria matrix (Morgan et al., 2016)m. The redox state of cells can therefore be probed in specific organelles and any change associated with sub-cellular redox defects can be quantified. Recently, the probe HyPer7 has been developed following the same concept than the Hyper probe. It has the advantage to be pH-stable, ultrasensitive and with an important dynamical range (Pak et al., 2020). The major inconvenience of ratiometric redox sensors is the necessity to excite cells at non-standard wavelengths that not commonly found in all microscopy set-ups. Moreover, despite their capacity to probe the redox state of single-cells, no study has reported single-cell imaging in yeast cells yet.

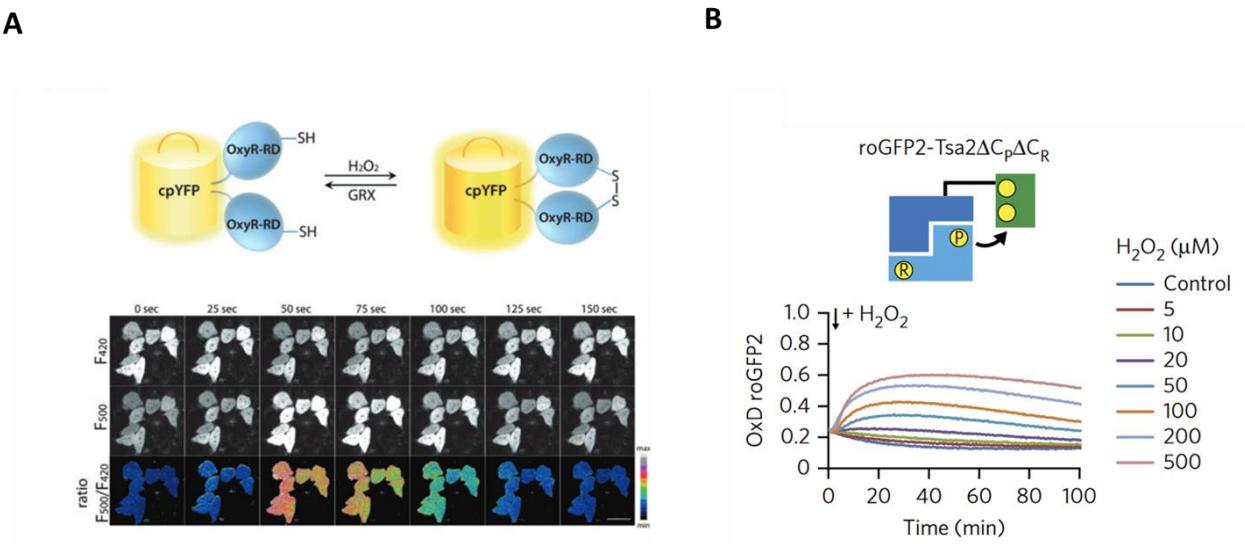

Figure 10 (adapted from Bilan et al., 2016 and Morgan et al., 2016): **HyPer and Tsa2rhoGFP redox sensors** (a) *Scheme of the HyPer sensor. The sensor can be reduced by glutaredoxins and oxidized by H_2O_2. Upon H_2O_2 exposure, the signal ratio of the cpYFP signal changes due to the oxidation of OxyR moieties.* (b) *Model of the roGFp2-tsa2 ΔcPΔcR probe. Tsa2 is shown in blue and roGFp2 in green. Cysteines are shown in yellow. Upon H_2O_2 exposure, the OxDroGFP2 ratio changes in a dose dependent manner.*

Different technical approaches are thus available to probe directly, or indirectly, the redox state of cells and the scavenging of H_2O_2 *in vivo*. They offer different advantages but also all have drawbacks, the choice of a given approach is largely dependent on the desired application (see Table 2 for a summary).

Method	Advantages	Inconvenient
H_2O_2 scavenging assay	-Easy to do -High throughput	-Indirect sensor of the internal redox state - No single-cell resolution -Low temporal resolution
Western blot targeting oxidized proteins	-Internal redox sensor	-Low troughput technique -Semi-quantitative -No single-cell resolution
Mass spectrometry	-Broad spectrum of protein oxidation status	-Low availability and not suitable for routine analyses -No single-cell resolution
Yap1 localization	-High temporal resolution -Single-cell resolution	-Dependent on endogenous processes -Saturation for low [H_2O_2] -Low signal to noise ratio
Transcriptional based reporters	-High signal to noise ratio -Common wavelength -Single-cell resolution -Relatively high temporal resolution	-Dependent on the transcriptional status of cells -Dynamics is limited by GFP maturation
Engineered redox sensors	-Sub-cellular resolution -High temporal resolution	-Use at the single-cell level not standardized in yeast cells -Ratiometric measurement (non-standard wavelength)

Table 2: Summary of the main techniques to investigate the redox state of cells and H_2O_2 scavenging.

2.4. The physiological role of antioxidants in H_2O_2 stress adaptation and survival

In this section, I will describe the different biological functions of antioxidants, associated or not to H_2O_2 scavenging. In addition, I will introduce the physiological defects associated with their deletion, both in non-oxidizing conditions and when submitted to a H_2O_2 stressor. For each antioxidant, I will discuss whether the physiological defect associated with the deletion of an antioxidant can be linked to a particular function of the enzyme, in particular H_2O_2 scavenging. The overlapping functions and the complementarity of the different antioxidants will also be commented.

2.4.1. Physiological functions of the NADPH-independent antioxidants: catalases and cytochrome-c peroxidase

Under non-oxidative conditions, the role of catalases to maintain the redox state of cells seems largely dispensable. A strain deleted for both *CTT1* and *CTA1*, the two catalases of *S. cerevisiae*, can grow in both a fermentative and a respirative media (Moradas-Ferreira and Costa, 2000).

However, using a scavenging assay, the catalase T has been identified as a major H_2O_2 scavenger in *E. coli* when cells were submitted to H_2O_2 (Seaver and Imlay, 2001). In addition, it has been shown in *E. Coli* that the cytochrome c peroxidase was

another prominent actor of H_2O_2 detoxification (Khademian and Imlay). In budding yeast, the role of the cytochrome c peroxidase for H_2O_2 detoxification has also been shown recently (Bodvard et al., 2017) with a similar assay.

Those observations are in agreement with the biochemical characteristics of antioxidants previously described (Ch1.2.3.1.): catalases are thought to become much more efficient than Prx under high H_2O_2 fluxes (Fourquet et al., 2008).

Since catalases were shown to display H_2O_2 scavenging capabilities, studies have characterized their role in the oxidative stress response and the phenotypic impairment associated with their deletion under H_2O_2.

Under oxidative stress, the Ctt1 protein level is increased up to 15 fold (Martins and English, 2014), suggesting its requirement to cope with H_2O_2. **It has also been reported that a mutant strain deleted for *CTT1* was much more sensitive to H_2O_2 than a WT strain.** However, a strain deleted for *CTA1* exhibited a WT phenotype (Martins and English, 2014; Nishimoto et al., 2016). In addition, the deletion of *CTT1* has been reported to increase the sensitivity of *S. cerevisiae* to ionizing radiations (Nishimoto et al., 2014). The catalase T (encoded by *CTT1*) thus appears as the major catalase of *S. cerevisiae* and is required to survive to various oxidative challenges.

However, it has been further observed that the double mutant *ctt1*Δ*cta1*Δ was only sensitive to H_2O_2 when the glutathion pathway was deleted (Grant et al., 1998). In line with that, another study observed that catalases were only required to survive oxidative stress during stationary phase while their role was dispensable during the exponential growth phase (Izawa et al., 1996). Accordingly, our lab recently showed that a strain deleted for both *CTT1* and *CTA1* could adapt and grow under oxidative stress, as a WT strain (Goulev et al., 2017).

Notably, the two papers that reported the role of *CTT1* in S. cerevisiae (Martins and English, 2014; Nishimoto et al., 2016) worked at high concentrations of H_2O_2 (2 and 4 mM) while in Goulev et al., authors worked with concentrations one order of magnitude below (0.4 mM). **This may suggest a prominent role of catalases only under high fluxes of H_2O_2** (Fourquet et al., 2008). In Goulev et al., authors also reported that a mutant deleted for *CCP1*, the cytochrome-c peroxidase, exhibited a lag in the growth recovery profile under 0.4 mM H_2O_2 (Goulev et al., 2017).

However, a more systematic study, challenging the role of catalases under various H_2O_2 concentrations, would be necessary to confirm the exact role of catalases in H_2O_2 adaptation and survival and whether their scavenging functions can be compensated by other antioxidants. Since no other biological functions have been reported to depend on catalases, it is widely assumed that they are required for their H_2O_2 scavenging.

2.4.2. Physiological functions of the glutathion-peroxidase and the glutathione pathway

The synthesis of glutathione (mostly by *GSH1*) is critically required for growth in *S. cerevisiae*, presumably due to its various functions for reductive processes within cells (Toledano et al., 2013). In line with that, the reductive compound dithiothreitol (DTT) can rescue a normal growth of a *gsh1*Δ mutant strain (Grant et al., 1996). Moreover, it has been shown that the deletion of the glutathion synthase, *GSH1*, was impairing growth under aerobic conditions (Lee et al., 2001), suggesting that the ROS induced by mitochondria respiration were sufficient to impair the basal redox state of cells deleted for *GSH1*. Moreover, it has been shown that the *gsh1*Δ mutant had a severe

mitochondrial genome instability and thus a high propensity to form 'petite' cells (Ayer et al., 2010). On the contrary, mutants deleted for other genes of the GSH pathway (*grx1*Δ*grx2*Δ or *glr1*Δ*)* elicit no particular phenotypes in non-oxidative conditions (Toledano et al., 2013). **Overall, glutathione seems to be involved in critical processes for the basal function of cells,** but in an **independent manner of the whole GSH cycle** (Toledano et al., 2013) .

In addition, the role of glutathion peroxidases (Gpx), in H_2O_2 stress response and adaptation is minor. The only Gpx-deleted mutant that exhibits an oxidative stress sensitivity is *gpx3/orp1*Δ (Y Inoue et al., J Biol Chem, 1999 and AM Avery, J Biol Chem, 2001), but this is likely due to its critical function in the activation of the Yap1 regulon (Delaunay et al., *Cell*, 2002) rather than because of its H_2O_2 scavenging activity.

Together, those data strongly suggest that the critical role of the **glutathion system is not required for H_2O_2 scavenging *per se.***

However, in a recent article, it has been shown that lysine harvesting enabled cells to reroute NADPH for glutathion synthesis, increasing the glutathion concentration up to 7.85 times within cells. This resulted in an increased NADPH-dependent reductive power and an increased survival under H_2O_2 challenges (Olin-Sandoval et al., 2019), This suggests that an increase in the intracellular concentration of glutathion accounts for the ability of cells to cope with H_2O_2. Moreover, authors showed that the increased survival to H_2O_2 was accompanied by an increased NADPH/NADP+ ratio under H_2O_2. Those data therefore furnish evidence that boosting the glutathion system can drive increased H_2O_2 survival through the maintenance of the redox state in cells.

Additionally, glutathion plays critical roles in proteostasis. The reductive capacity of glutathion is required for the reduction of protein's disulfide bonds, especially in the endoplasmic reticulum where glutathion can compete for the Ero1-dependent oxidation of protein's thiols (JW Cuozzo et al., *Nat Cell Biol* 1999 and reviewed in S Chakravarthi et al., *EMBO rep*., 2006). Moreover, under oxidative stress, glutathion can prevent the irreversible oxidation of proteins by H_2O_2 by reversibly 'capping' them through S-glutathionylation (Reichmann et al., 2018; Xiong et al., 2011). This protective mechanism is a typical example of how antioxidants can participate in the oxidative stress response without directly detoxifying the stressor. Overall, similarly than under basal conditions, **glutathione seems to play different functions under oxidative stress, but in an independent manner of the whole GSH cycle.**

2.4.3. Physiological functions of peroxiredoxins and the thioredoxin cycle

a. Redox homeostasis and peroxidase activity

Prx and the associated Prx cycle are thought to be prominent actors of the redox homeostasis in particular in non-oxidative conditions.

In Morgan et al., 2016, authors showed using a roGFP2-Tsa2ΔC$_R$ sensor that both the cytoplasmic and mitochondrial H_2O_2 levels were increased in a *tsa1*Δ*tsa2*Δ mutant strain, suggesting a major role of Prx in maintaining the basal redox state of cells.

Based on the same roGFP2-Tsa2ΔC$_R$ sensor, it has been further shown that the reduction of NADPH production in a *zwf1*Δ mutant (*ZWF1* encodes for the first enzyme of the Pentose Phosphate Pathway, glucose-6-phosphate dehydrogenase, or G6PDH, see Ch2.4.) greatly impaired the basal redox state of budding yeast cells (Pastor-

Flores et al., 2017). In addition to that, it has also been reported that a mutant deleted for *TRR1,* as well as one deleted for both thioredoxins *TRX1/2* exhibit an increased basal redox state in non-oxidative conditions (Kritsiligkou et al., 2018).

Overall, those data pinpoint the **crucial function of Prx to maintain the basal redox state of cells as well as the role of the whole NADPH-dependent Prx cycle** since multiple deletions within it also affects the basal redox state of cells in non-oxidative conditions (we include, by mentioning the Prx cycle, the reduction of Trx by Trx reductase).

In response to H_2O_2, the Prx Tsa1 and Ahp1 are described to be stress-inducible and abundant, suggesting their role in H_2O_2 detoxification. Tsa1 is considered as the main peroxiredoxin in *S. cerevisiae* due to its characteristics and functions: it has a greater reactivity with H_2O_2 than Ahp1 or Tsa2, and it is massively induced under H_2O_2, suggesting its role in the oxidative stress response (Fourquet et al., 2008). In agreement with this, it has been shown that, among mutant strains deleted for a single Prx, only the *tsa1Δ* strain exhibited an increased sensitivity to H_2O_2 (Jeong et al., 1999; Lee et al., 1999b). Ahp1 has been mainly linked to the degradation of lipid peroxides (Jeong et al., 1999; Lee et al., 1999b). In Lee et al., authors showed that the *tsa1*Δ strain could not grow under doses superior (or equal) to 3 mM, while a WT strain could grow under doses superior to 3.5 mM (Fig 11a). Similarly, a mutant deleted for thioredoxins (*trx1/2*Δ) has been shown to elicit a high sensitivity to H_2O_2 (Garrido and Grant, 2002; Kuge and Jones, 1994), demonstrating the role of the whole thioredoxin cycle in H_2O_2 stress response. In line with that, our lab showed that the deletion of the main peroxiredoxin (*tsa1*Δ) or both thioredoxins (*trx1/2*Δ) was greatly affecting the ability of the strain to grow under oxidative stress (Goulev et al., 2017).

However, a study showed that a budding yeast strain deleted for the 3 CysGpx and for the 5 Prx (thus deleted for all thiol peroxidases) could still grow under 0.25 mM H_2O_2 (Fig 11b) and could transiently survive under important concentrations of H_2O_2, in a manner close to be similar to a WT strain (1 or 2 mM, see Fig 11c) (Fomenko et al., PNAS, 2011). Most interestingly, authors showed that **the ability to grow under stress was much more affected by the deletion of thiol peroxidases than the ability to transiently survive under high doses of stress** (Figure 11b and c). This suggests a prominent role of Prx for growth under stress (resistance) rather than for oxidative stress survival (tolerance).

Overall, Prx seems to have a major role in the response and the adaption to H_2O_2, in particular the main Prx **Tsa1 that is critically required to grow under H_2O_2.**

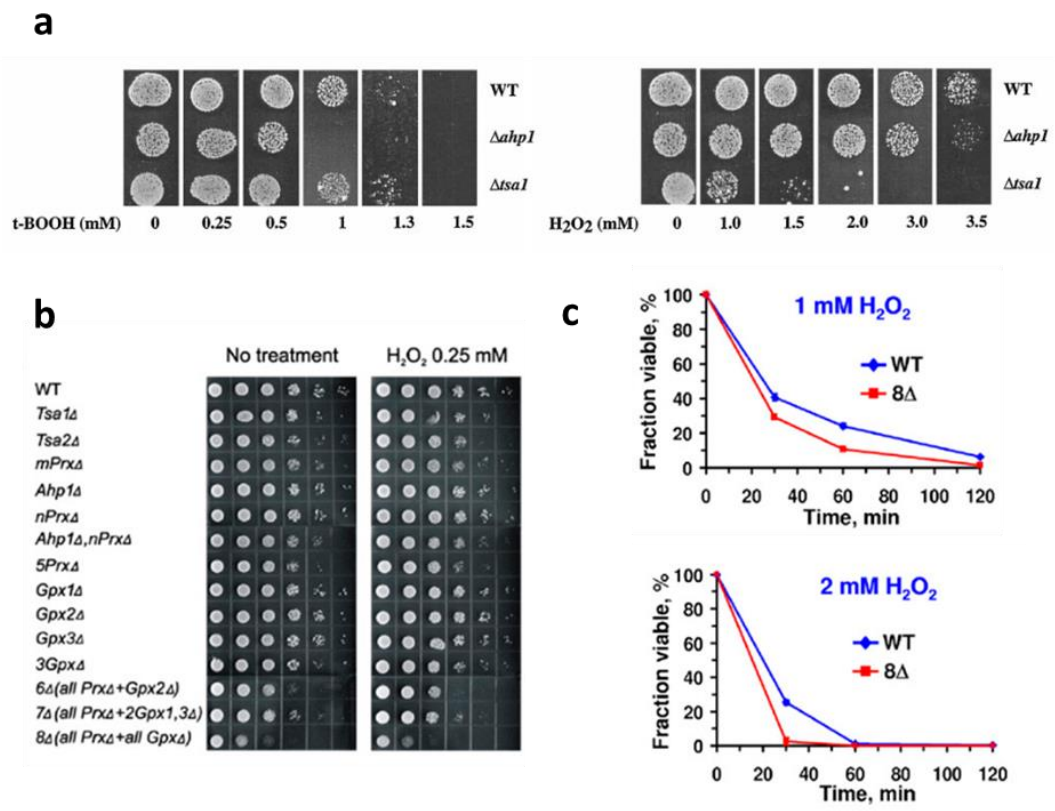

Figure 11 (adapted from Lee et al., 1999b and Fomenko et al., 2011): **Physiological defects associated with Prx deletion** *(a) The deletion for TSA1 or for AHP1 leads to a differential growth defect under H_2O_2 or under lipid peroxide (t-BOOH), respectively. (b) Growth under H_2O_2 for S. cerevisiae mutant strains deleted for one or several thiol peroxidases.* (c) *Post-stress survival fraction of a WT strain or a strain deleted for the 8 thiol-peroxidases after being exposed to severe doses of H_2O_2. (b) and (c) respectively evaluate the resistance and the tolerance of the strains under/after an H_2O_2 stress.*

However, **the link between the Prx scavenging activity and the sensitivity to H_2O_2 of a mutant deleted for Prx is less clear**. Using a scavenging assay, it has been observed that the main peroxiredoxin Tsa1 was not participating in H_2O_2 scavenging when cells were exposed to different H_2O_2 concentrations (ranging from ~100 to 1000 µM) (Fig 12) (Hanzén et al., 2016; Roger et al., 2020). This study therefore questions the link between the H_2O_2 scavenging property of the enzyme and its requirement to grow under stress.

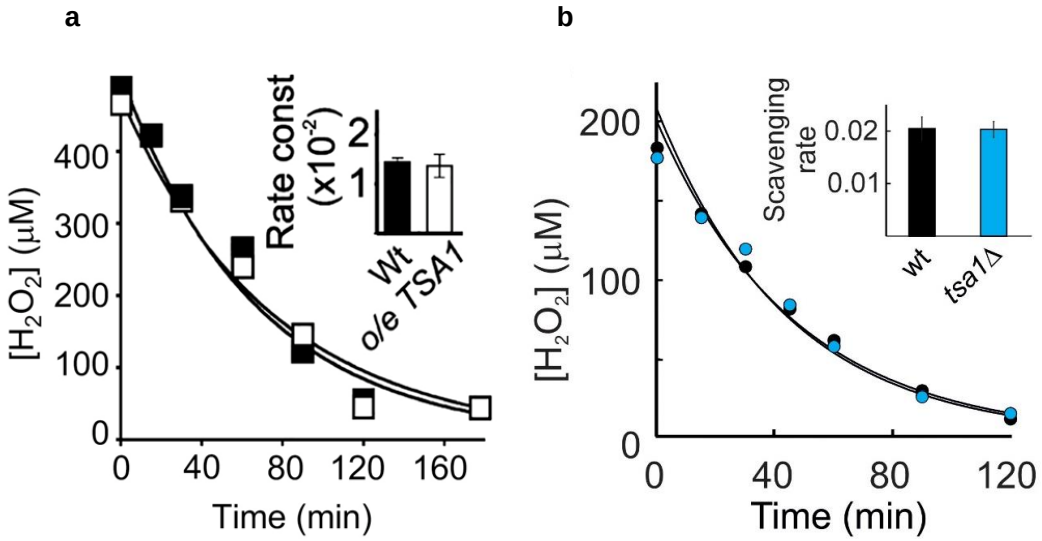

Figure 12 (adapted from Hanzén et al., 2016 and Roger et al., 2020): **Role of Prx in**

H_2O_2 scavenging *(a) and (b): H_2O_2 scavenging assays. The external H_2O_2 concentration is measured over time in budding yeast cells cultures after adding H_2O_2 (500 or 200 µM respectively). Neither the over expression nor the deletion of Tsa1 changed the H_2O_2 scavenging rate compared to a WT strain.*

b. Tsa1 underlies multiple functions that are independent of its peroxidase activity

Since Tsa1 is required for many other functions independent of its peroxidase activity, it has been proposed that its other functions may explain, at least partially, the H_2O_2 sensitivity of the *tsa1*Δ mutant.

Those different functions mainly include the regulation of **redox signaling**, a **chaperon role**, a role in **genome stability** and a **protective role for the ribosomal machinery** (Bodvard et al., 2017; Hanzén et al., 2016; Iraqui et al., 2009; Molin et al., 2011; Morgan and Veal, 2007; Rand and Grant, 2006a; Roger et al., 2020; Tang et al., 2009; Weids and Grant, 2014).

Among those functions, it is still debated whether the sensitivity of the *tsa1*Δ strain is linked or not to its peroxidase activity and to what extent the role of the chaperone and signaling functions are participating in the oxidative stress defense (Hanzen et al., Cell, 2016, AJ Weids, *JCS*, 2014, JD Rand et al., *MBOC*, 2005, Molin et al., *Mol Cell*, 2011, Bodvard et al., *Nat. Comm*., 2017, F. Rodger et al., *eLife*, 2020). It seems at least clear that the genome instability associated with *TSA1* deletion is independent from the role of Tsa1 under oxidative stress since it has mainly be linked to the shortening of the budding yeast lifespan (Iraqui et al., 2009; Tang et al., 2009).

c. The signaling function: Prx is an H_2O_2 floodgate

Another function that is dependent upon the peroxiredoxins is the transduction and the propagation of a redox dependent signal into cells.

In comparison to the 2-Cys Prx of bacteria, the **eukaryotic 2-Cys Prx are much more prone to be inactivated by oxidation** into a sulfinic form (Fig 13a) (Wood et al., 2003). Their propensity to be rapidly oxidized has been proposed to act as a floodgate. Under low doses of H_2O_2, Prxs maintain redox homeostasis while their **oxidation/inactivation under high doses of H_2O_2 may limit their scavenging function and open a floodgate, increasing H_2O_2-mediated redox signalling** (Fig 13b) (Georgiou and Masip, 2003; Wood et al., 2003).

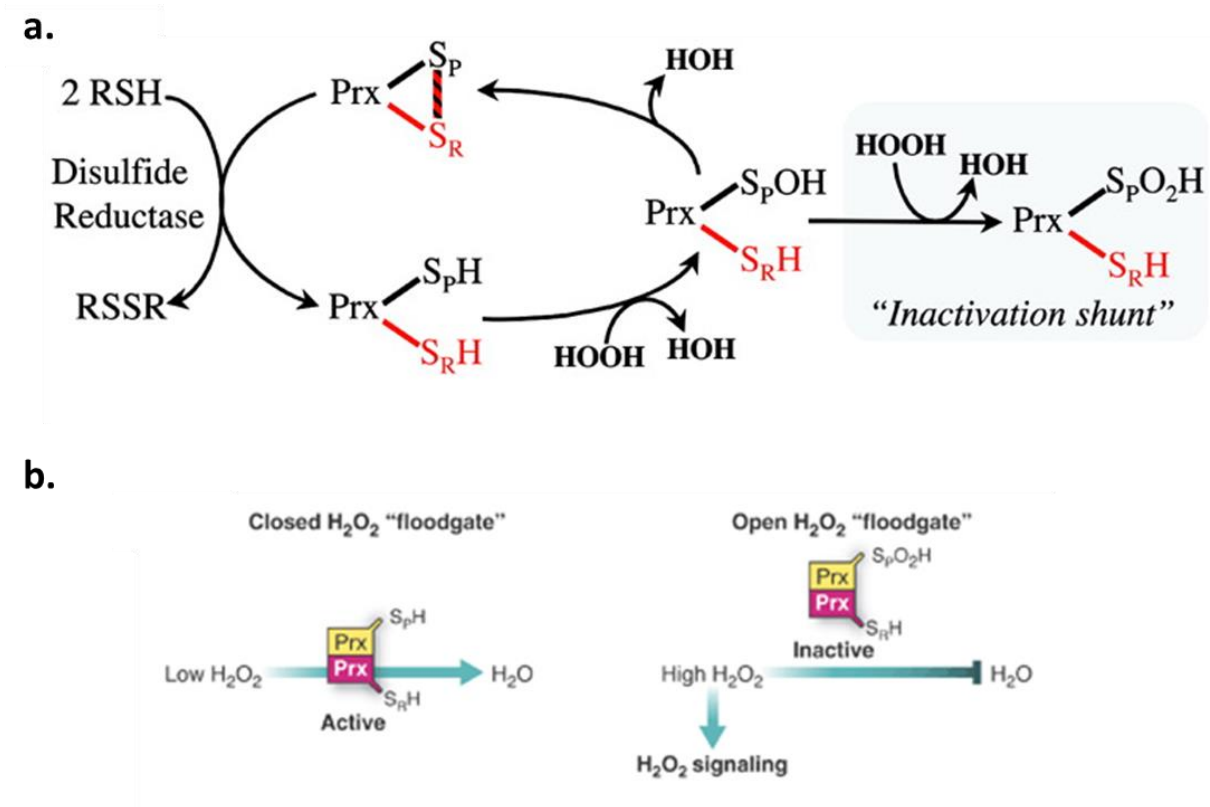

Figure 13 (adapted from Georgiou and Masip, 2003; Wood et al., 2003)**: Prx inactivation and Floodgate model** *(a) The* scheme of the Prx oxidation cycle. (b) *The floodgate model by which Prx are thought to regulate H_2O_2 signaling and redox biology. Under*

low H_2O_2 concentrations, Prx maintain redox homeostais by catalyzing the transformation of H_2O_2 into H_2O, preventing redox signaling. Under high H_2O_2 concentrations, Prx are oxidized, thus enabling it to participate in redox signaling.

In addition, it has further been shown that cells could indeed recycle the inactive sulfinic form of the Prx (Woo et al., 2003).The sulfiredoxin has been identified in yeast cells as the pivotal enzyme of sulfinic reaction (Biteau et al., 2003). Prx oxidation/ reversible inactivation can thus be viewed as a post-translational modification that can transiently modify the role of Prx (Schieber and Chandel, 2014).

Alternatively, upon oxidation, Prx can further transduce their oxidation to other proteins into the cytoplasm, acting as a redox signaling relay. It has been shown that the deletion of Prx was indeed largely precluding the oxidation of proteins into the cytoplasm (Stöcker et al., 2018). **Both the floodgate model, favouring H_2O_2-dependent redox signaling and the Prx-mediated redox relay are therefore thought to participate in redox signaling within cells.**

The case of Yap1 is a perfect illustration of how the oxidation of a protein can change its conformation and its function, ultimately triggering the transcription of dozens of genes ((Delaunay et al., 2000) see Ch1.2.). Since peroxiredoxins have a high affinity for H_2O_2 and are abundant in cells (Wood et al., 2003), they represent an ideal protein to mediate redox biology.

Indeed, it has been largely reported that the oxidation of Prx was involved in the activation of the oxidative stress response: Fomenko et al. reported that the **transcriptional changes** observed in a WT strain upon H_2O_2 exposure were **drastically reduced in strains lacking several thiol peroxidases** and were **close to be abolished in a strain lacking all thiol peroxidases** (transcriptional fold change score = 0.04 compared to 1.50 in a WT strain, see Fig 14) (Fomenko et al., 2011).

Thiol peroxidases are thus major regulators of the global transcriptional response to H_2O_2.

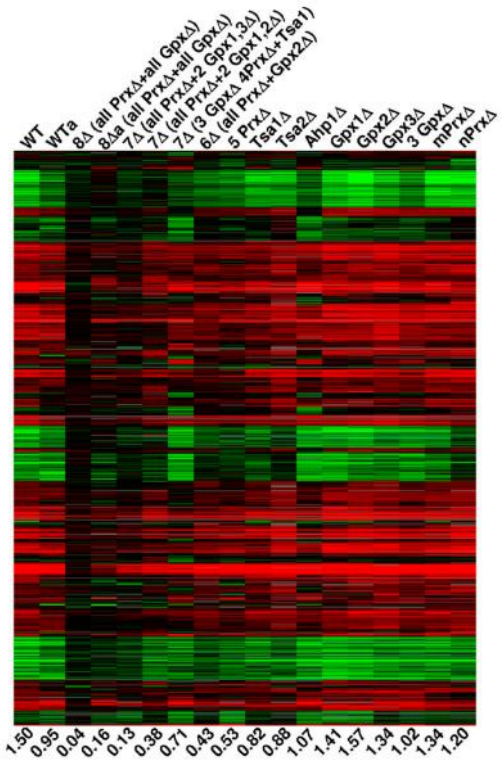

Figure 14 (from Fomenko et al., 2011): **Transcriptional profile of the response to H_2O_2 in several S. cerevisiae strains deleted for one or several Gpx/Prx**.

More specifically, it has been proposed that a Tsa1-dependent relay was required for the **repression of the major transcriptional regulator PKA in response to oxidative stress** (Molin et al., 2011; Roger et al., 2020). They observed that both redox modifications and Tsa1 were indeed destabilizing the activation loop of Tpk1, the main unit of PKA (Roger et al., 2020). However, the exact mechanism by which Tsa1 interacts with Tpk1 is still unclear. Importantly, authors showed that the oxidative stress sensitivity of the *tsa1*Δ mutant was rescued by the deletion of the gene *RAS2*

(that is an activator of the PKA pathway, see Ch1.4. for details), suggesting the major role of the signalling function of Tsa1 in its phenotype of H_2O_2 sensitivity.

In contrast, they had shown that the main peroxiredoxin Tsa1 had no role in H_2O_2 scavenging based on an external H_2O_2-scavenging assay (see Fig12). They concluded that the phenotype of sensitivity of the *tsa1*Δ mutant under H_2O_2 was related with its signalling function. However, a direct assessment of the internal redox state of *tsa1*Δ cells under H_2O_2 should help to confirm the non-necessity of its peroxidase activity under stress (as it has been done in the context of the glutathion system in Olin-Sandoval et al., 2019).

Moreover, if the *tsa1*Δ sensitivity under oxidative stress is not linked to its inability to scavenge H_2O_2 but rather to its inability to inhibit PKA, a clear understanding of the role of PKA inhibition under oxidative stress is still missing. Most surprisingly, in Molin et al., authors claimed that the inhibition of PKA led to an increase of H_2O_2 resistance by driving the expression of Srx1, thus favouring the reduction of Tsa1 and therefore its peroxidase activity (Molin et al., 2011). This model is in apparent contradiction with the fact that Tsa1 does not contribute to H_2O_2 scavenging.

Alternatively, it has been proposed in another study that the PKA inhibition under oxidative stress may be required to activate the expression of CTT1 (through the Msn2 regulon (Guan et al., 2012). In this model, the suppression of the Tsa1-dependent PKA inhibition may lead to a loss of the Ctt1-dependent H_2O_2 scavenging. The incapacity of the tsa1Δ to inhibit PKA and thus to over-express Ctt1 must therefore leads to a scavenging defect in the tsa1Δ mutant. Roger et al., 2020 showed that this is not the case based on scavenging assays.

The exact role of the PKA inhibition is therefore elusive and hardly explains the weak oxidative stress resistance of the *tsa1*Δ mutant without advocating its peroxidase function.

Overall**, those studies clearly identified the signalling function of Tsa1 as a determinant of the physiological behaviour of cells under oxidative stress, in particular the Tsa1-dependent inhibition of PKA.** However, the existing data do not enable to state whether the peroxidase function of Tsa1 also plays a role under oxidative stress and by which mechanism Tsa1 signalling drives oxidative stress resistance. It would be interesting to decipher whether redox signalling plays a role in the orchestration of oxidative stress resistance and stress tolerance.

d. The chaperone function

In addition its signaling function, it has been shown that the two main cytoplasmic Prx of yeast, Tsa1 and Tsa2, were mediating a **chaperone function** (Jang et al., 2004). Upon heat-shock or oxidative stress, Prx are prone to oligomerization (Schröder et al., 2000), forming high molecular weight (HMW) Prx complexes, compared to the basal low molecular weight of Prx (LMW). Jang et al. observed that the chaperone function was associated to the HMW form while the peroxidase function was mainly associated to the LMW. It has been proposed that the **chaperone function of Tsa1** may help in **preventing the aggregation of ribosomal proteins** and protect the cell from the toxicity that would result from their aggregation (Rand and Grant, 2006).

It has further been shown that the chaperone function of Tsa1 requires two inducible chaperone proteins, Hsp104 and Hsp70, and the sulfiredoxin Srx1 (Hanzén et al.,

2016) (see Fig15). By reacting with H_2O_2, Tsa1 forms a sulfenic acid (-SOH) on the C48S cysteine that will either form a disulfide bond with the resolving C171S cysteine or rather be further oxidized in a sulfinic acid (-SOOH). The recruitment of Tsa1 on H_2O_2-induced aggregates requires the peroxidatic C48S cysteine but not the resolving cysteine C171S (Hanzén et al., 2016). In addition, the chaperon function was reduced in a *tsa1YF*Δ mutant, wherein the sulfinylated form was rapidly resolved compared to a WT strain, strongly suggesting that Tsa1-SOOH was required for the chaperon function. Importantly, **this chaperon function has been suggested to extend yeast's lifespan independently** of the peroxidatic and genome stability functions of Tsa1 (Hanzén et al., 2016). However, its role in H_2O_2 stress response has not been explored by the authors.

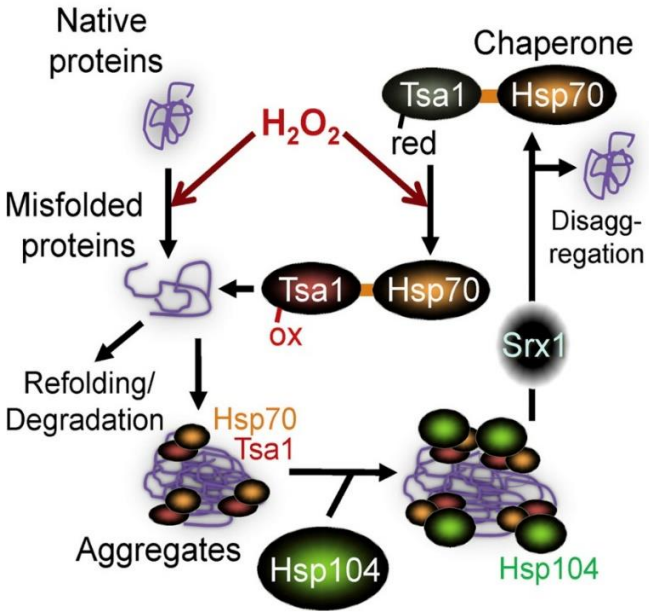

Figure 15 (from Hanzen et al., 2016): **The chaperone function of Tsa1**. *Upon oxidation, Tsa1 recruits the chaperon Hsp70 and binds to misfolded proteins. The Tsa1-Hsp70 complex then recruits the disaggregase Hsp104, counteracting the accumulation of the*

ubiquitinylated proteins. The reduction of Tsa1 by the sulfiredoxin Srx1 helps to clear H2O2-induced aggregates.

Our lab evaluated the role of each functions in the resistance to H_2O_2. We determined that the C48S cysteine was critical for adaptation and growth under H_2O_2 while the tsa1ΔYF mutant (no chaperon function) exhibited a WT phenotype under the same conditions (Goulev et al., 2017). **This tends to rule out the role of the chaperon function in oxidative stress resistance.**

3. Redox state and metabolism

The response of oxidative stress is often viewed within the prism of the transcriptional stress response. However, the oxidative stress response also includes massive metabolic changes that mostly serve NADPH production.

3.1. The pivotal role of NADPH for anabolism and redox homeostasis

In cells, **NADPH is an essential reducing compound**. In contrast to NADH, the electrons of NADPH are not used for the synthesis of ATP but mainly for **anabolic processes** such as the *de novo* synthesis of fatty acids, amino acids, and nucleotides. In addition to those anabolic processes, **NADPH** is necessary for the **scavenging of H_2O_2** since it furnishes reducing equivalent for both the thioredoxin and glutathion pathways (Chandel, 2015).

Since I already described the functioning of both the thioredoxin and glutathion pathways (see Ch1.2.2.3.), I will focus here on the anabolic processes that depend on NADPH and I will then discuss trade-offs that may result from the dual role of NADPH.

3.1.1. NADPH-dependent anabolic processes and trade-offs with redox state maintenance

Fatty acids are hydrocarbon chains that end with carboxylic acid groups that mainly serve in signal-transduction pathways and for the synthesis of hormones and lipids. The fatty-acid synthesis, that occurs in the cytosol, is largely dependent on NADPH since the synthesis of fatty acids from Acetyl-CoA requires two steps of reduction that are sustained by the oxidation of NADPH into NADP+ (Chandel, 2015). The overall reaction of the fatty acid synthesis pathway can be written as:

8 acetylCoA + 7 ATP + 14 NADPH + 6H+ → palmitate + 14 NADP+ + 8CoA + 6 H2O + 7 ADP + 7Pi

Another **NADPH-consuming anabolic pathway is the synthesis of nucleotides**. In particular, the synthesis of deoxyribonucleosides di-phosphate (dNDP) from nucleosides di-phosphate (NDP) requires a step of reduction that is fuelled by the ribonucleotide reductase (RR). The RR ends in an oxidized from, forming a disulfide bond. It is then reduced by thioredoxins and/or glutaredoxins that are themselves reduced by NADPH (Fig 16). There is therefore an **intrinsic trade-off between anabolic processes and redox homeostasis**: both of them critically require NADPH and thioredoxin and glutathion pathways (Chandel, 2015).

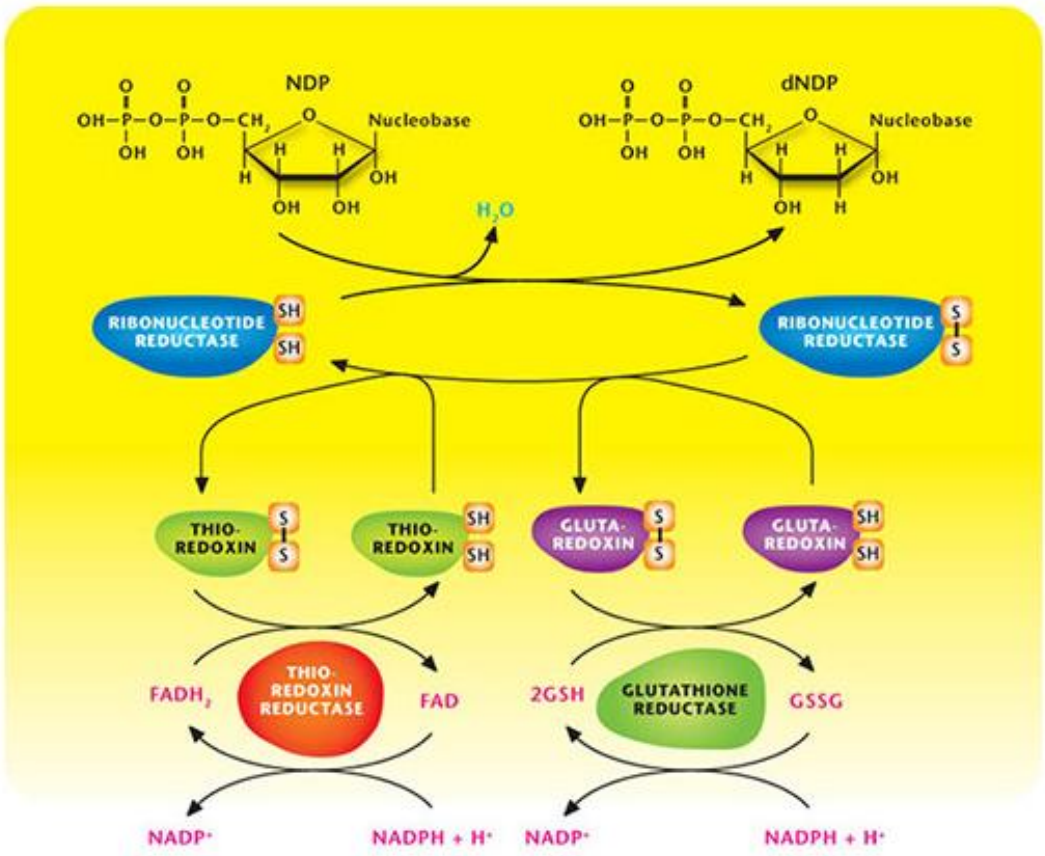

Figure 16 (from Navigating metabolism, N. Chandel): **The synthesis of dNDPs from NDPs by the ribonucleotide reductase (RR).** *During the process, the RR is oxidized and then reduced by both thioredoxin and glutathion pathways. Ultimately, the reduction of the machinery is sustained by NADPH.*

3.1.2. NADPH production: the central role of the pentose phosphate pathway

In order to perform anabolic processes, cells have different sources of NADPH**. The pentose phosphate pathway (PPP) represents the main source of NADPH in cells.** Once glucose is converted in glucose-6-phosphate, it enters the PPP. The two first reactions of this pathway (the oxidative phase of the PPP, see Fig 17) will reduce

two molecules of NADP+ into NADPH by oxidizing glucose-6-phosphate into ribulose-5-phosphate. Those 2 NADPH-generating reactions are catalysed by G6PDH (encoded by ZWF1 in *S. cerevisiae*) and 6PGD (encoded by GND1 in *S. cerevisiae*). Other metabolic NADPH-generating reactions include malic enzymes, isocitrate dehydrogenases and the one-carbon metabolism of serine (Chandel, 2015). In *S. cerevisiae*, the cytosolic aldehyde dehydrogenase is also a source of NADPH (Grabowska and Chelstowska, 2003).

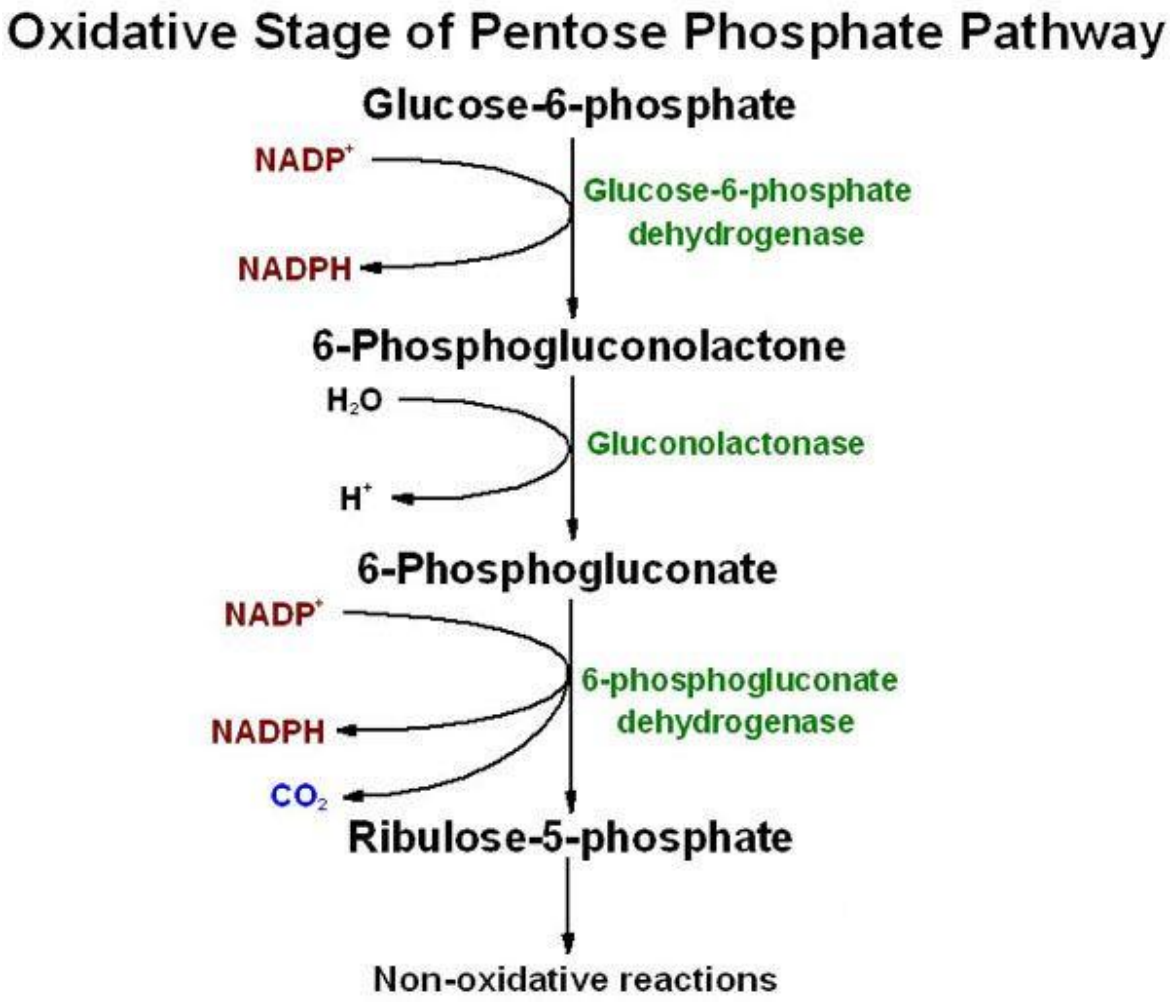

Figure 17 (from M. Javed Abbas MD): **Scheme of the oxidative branch of the Pentose phosphate pathway**

However, in *S. cerevisiae*, it has been shown that in mutant lacking the PPP, the NADPH demands could not be met by other pathways (Grüning et al., 2011; Olin-Sandoval et al., 2019; Ralser et al., 2007).

In line with that, the strain deleted for the first enzyme of the PPP, ***zwf1Δ*, has long been reported as sensitive to oxidative stress and slightly slow-growth** (Nogae and Johnston, 1990). More recent studies showed that the **basal redox state of the *zwf1Δ* strain is impaired** (Pastor-Flores et al., 2017; Zhang et al., 2016). The strain is also auxotroph for methionine, due to the high NADPH demand for methionine synthesis (Campbell et al., 2016).

Those phenotypes are likely due to the lack of NADPH resulting from the inhibition of the PPP in this strain. It has been shown that the cytosolic aldehyde dehydrogenase ALD6 was essential to maintain the viability of a strain deleted for ZWF1 (Grabowska and Chelstowska, 2003). Another study found that ALD6 was dispensable in the case of a growth on a respiratory medium that was maximizing the isocitrate dehydrogenase production of NADPH (Minard and McAlister-Henn, 2005).

A study similarly showed that the deletion of the PPP led to a reduction of the NADPH/NADP+ ratio in mammalian cells, testifying of an increased redox state. This also coincided with a reduction of the growth rate and a deficiency in folate synthesis in cells (Chen et al., 2019).

Overall, those studies thus pinpoint the crucial role of the PPP to sustain NADPH production and therefore the anabolic biosynthesis and the redox state of cells.

3.2. Metabolic rerouting in response to oxidative stress

In response to oxidative stress, when the redox homeostasis is threatened, several **adaptive mechanisms maximizing NADPH production** that enable the maintenance of homeostasis within cells have been reported (Christodoulou et al., 2018; Nikel et al., 2020; Peralta et al., 2015; Ralser et al., 2007). I will describe those metabolic adaptive processes in this part. Since NADPH production is mainly sustained by the PPP, increasing the carbon flux into the PPP represents a promising strategy to increase NADPH production under oxidative stress.

Metabolic pathways are a series of biochemical reactions that can either require or release energy. Enzymes can speed up the rate of those reactions, but it is thermodynamics that *in fine* dictates whether a reaction will require or release energy.

$$\text{Reactants} \xrightarrow{\text{Enzymes}} \text{Products} + (\Delta\ \text{Energy})$$

The occurrence and the rate of a given reactions will be determined by different parameters: the enzyme concentration, the metabolite concentration (the substrate and the product), but also the availability of energy (Chandel, 2015).

Interestingly, this means that any change in the conformation or availability of a given enzyme or a given metabolite can drastically change the repartition of the carbon fluxes within the different branches of the metabolic pathways.

Glucose-6-phosphate (G6P) is a hub metabolite that can either enter the glycolysis (to mainly produce ATP) or rather routes into the PPP to produce NADPH. In normal conditions, the larger part of G6P will enter glycolysis.

It has been shown that H_2O_2 induced the reversible S-thiolation of several metabolic enzymes by glutathion (Shenton and Grant, 2003). Among them, authors found that **GAPDH**, a major enzyme of the glycolysis, was **S-thiolated** while G6PDH, the first enzyme of the PPP, was intact. Interestingly, such an inhibition (reversible or not) of GAPDH must prevent the routing of carbon into the glycolysis and thus lead to the accumulation of substrates of the glycolysis, including G6P. Indeed, it had been measured that the metabolites upstream of GAPDH were enriched following an oxidative stress (Hyslop et al., 1988). **As a consequence, the flux of carbon may undergo a drastic rerouting into other metabolic pathways.**

Ralser et al. identified in a pioneer paper another inhibition of a glycolytic enzyme in response to oxidative stress: the triose-phosphate isomerase (TPI) (Ralser et al., 2007). Strikingly, they observed that both the inhibition of TPI or GAPDH coincided with an **increased activity of the PPP** due to the rerouting of carbon into it. Moreover, the synthetic inhibition of TPI increased diamide resistance (an oxidative stressor) but surprisingly did not change the response to H_2O_2 (Ralser et al., 2007). Since GAPDH is oxidized by H_2O_2 but not by diamide, authors speculated that the inhibition of TPI may be redundant with the H_2O_2-dependent inhibition of GAPDH. Importantly, this study demonstrated that metabolic fluxes were regulated at multiple levels in response to oxidative stress.

In a follow-up paper, authors have shown that the rerouting of carbon into the PPP could explain the maintenance of redox homeostasis when budding yeast cells transit from fermentation to respiration (Grüning et al., 2011). Indeed, respiration is accompanied by an important production of ROS in cells. Authors showed that this was compensated by an increased production of NADPH by the PPP due to a large-scale reorganization of metabolic fluxes in response to the cessation of fermentation. Accordingly, a *zwf1*Δ mutant strain could not maintain its redox balance in a respiratory medium.

If those observations pinpoint the critical role of metabolic regulation to sustain the redox state of cells, it is likely that those metabolic rerouting are controlled processes rather than a consequence of the H_2O_2 toxicity that may have impaired the metabolic pathways. Indeed, the S-thiolation of GAPDH is specific to the third isoform in *S. cerevisiae* (Tdh3) while the second isoform Tdh2 has 96% of homology with Tdh3. Moreover, the reactivity of GAPDH with H_2O_2 is very high compared to other enzymes (the second order of reaction of GADPH with H_2O_2 is ~10^2 – 10^3 M^{-1} s^{-1} while typical rates are around 10^1 for other enzymes (Stone, 2004; Winterbourn and Metodiewa, 1999)). Only the thiol peroxidases that have dedicated reaction mechanisms with H_2O_2 exhibit higher rates of reaction (~10^7 M^{-1} s^{-1}).

In a recent paper, it has been shown that GAPDH was indeed reacting with H_2O_2 by a specific mechanism that involves a proton relay promoting leaving group departure (Peralta et al., 2015). Lastly, authors demonstrated **the physiological role of the GAPDH sensitivity toward H_2O_2.** Together, those observations strongly suggest that the H_2O_2-mediated GAPDH inhibition is a conserved control regulatory mechanism in cells.

In addition to the inhibition of glycolysis, the PPP activity is regulated through a NADPH-mediated negative regulatory feedback (Fig 18). Indeed, it has been shown that NADPH was affecting the conformation of G6PDH, reducing the rate of the first reaction of the PPP. Under a high NADPH demand (like oxidative stress), the inhibition is alleviated and the NADPH production rises within seconds (Dick and Ralser, 2015a; Kuehne et al., 2015). This **self-inhibitory characteristics of NADPH** has been shown both in **mammalian cells** (Kuehne et al., 2015) and in ***E. coli*** (Christodoulou et al., 2018). Recently, a similar increase of the PPP carbon fluxes has been observed in ***Pseudomonas putida*** under hydrogen peroxide (Nikel et al., 2020). Indeed, authors observed that the NADPH production was exceeding the demands from ~50%. This surplus was routed into the glutathione pathway that in turn reduced H_2O_2.

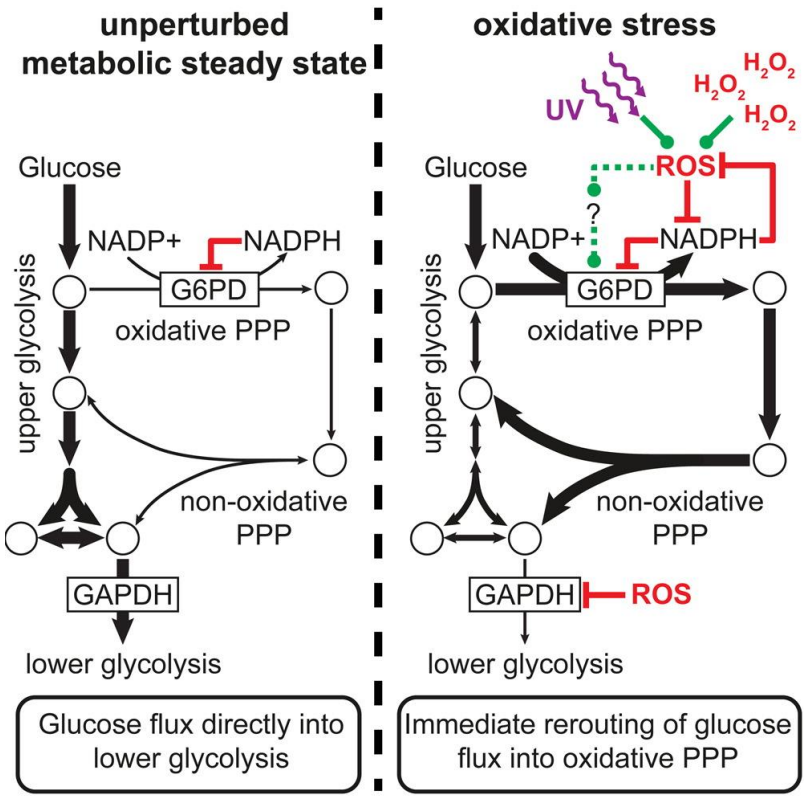

Figure 18 (from Kuehne et al., 2015): **NADPH negatively regulates the catalysis of the first reaction of the PPP by changing the conformation of G6PDH**. *Upon oxidative stress exposure, the NADPH concentration decreases, alleviating the downregulation of G6PDH thus routing carbon into the PPP. This feedback mechanism enables to adjust NADPH production to the demand and thus the maintenance of the NADPH concentration under oxidative stress.*

Overall, metabolic rerouting appears as a critical player of the response to oxidative stress. The PPP plays a major role in NADPH production and other pathways cannot fully compensate for its deficiency. Upon oxidative stress, different regulatory layers are rerouting carbon into the PPP. Among them, **GAPDH and G6PDH are two H_2O_2-dependent regulatory hubs that respectively inhibits the glycolysis and activates the PPP to increase NADPH production.**

3.3. An integrative view of H_2O_2 scavenging: the cooperation of metabolism rerouting and Yap1-dependent transcription

The PPP-dependent NADPH-production is therefore a central element of the redox homeostasis since it fuels the glutathion and thioredoxin cycles in reductive equivalents. **The NADPH-dependent antioxidant enzymes and the PPP rerouting following H_2O_2 exposure are thus largely cooperating to scavenge ROS.**

ROS scavenging is thus a complex mechanism integrating transcription and metabolic adaptions as central elements of the response. In the context of living cells, oxidative stress response requires a deep remodeling of the cellular physiology: both the transcriptional activity and the metabolic state must respond to the multiple demands to *in fine* maintain the internal redox state and cope with the stressor.

Such cross-talks between different fundamental aspects of the biology (transcription and metabolism) strongly motivates an integrative approach to shade the light on the complexity of the response.

4. General stress response and growth control mechanisms in response to environmental stressors

In addition to a H_2O_2-specific stress response, cells also respond to stressors using general plastic behaviours, independently of the nature of the stress. Those changes mainly include **drastic modifications of the growth status** and the **activation of a general stress response** coordinated by the growth control pathways of cells.

In this section, I will first describe those processes and their regulatory pathways. I will then show how they shape the physiological response of cells to stress, and more particularly in the context of oxidative stress response.

4.1. Protein Kinase A (PKA) controls a large regulatory network that coordinates growth inhibition with the general stress response activation

4.1.1. The environmental stress response paradigm

By screening the transcriptional changes in response to various stressors (H_2O_2, osmotic stress, heat-shock, starvation, etc.) in *S. cerevisiae*, it has been observed that a large set of genes (~900) exhibited a stereotypical response to all the stressors (Fig 19) (Gasch et al., 2000). Another work determined that approximatively 50% of the genome was included in at least one response to a given environmental change.

Furthermore, **~10% of the genome of *S. cerevisiae* was involved in the common stereotypical response found in response to all environmental stressors** (Causton et al., 2001). This common response includes a cluster of genes that is downregulated while another cluster is upregulated (Causton et al., 2001; Gasch et al., 2000). Those genes that are up- or down-regulated in response to most of environmental stressors have been historically called the “environmental stress response”, or the general stress response. In addition, both papers showed that the general stress response was to a large extent under the control of the transcription factors Msn2 and Msn4 (Causton et al., 2001; Gasch et al., 2000).

Together, those studies thus revealed that **environmental changes are accompanied by massive and stereotypical transcriptional changes, mediated in part by the regulon Msn2/4.**

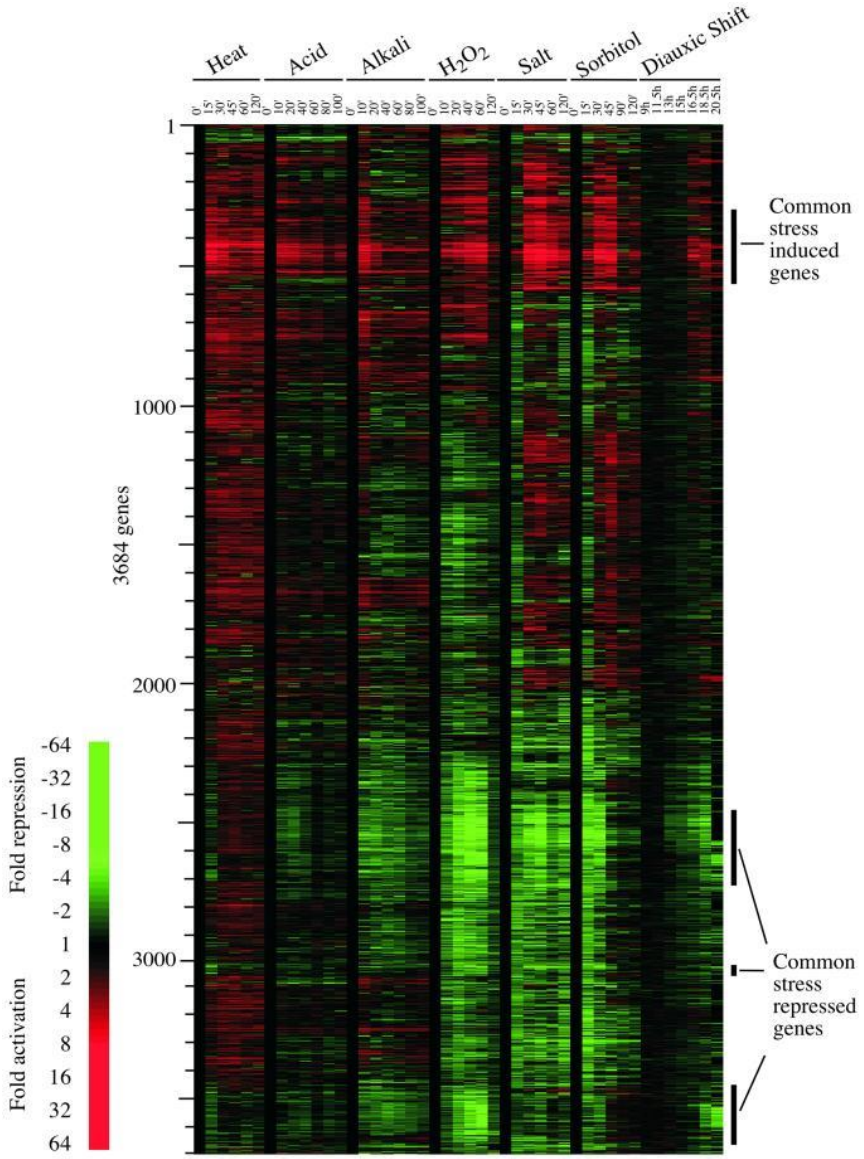

Figure 19 (from Causton et al., 2001): **RNA seq of the response of both WT and msn2/4Δ strains to various environemental perturbations.** *Two sets of genes exhibit a common response to most of the perturbations screened. One set is induced (in red) and one is downregulated (in green) in response to stressors.*

4.1.2. The coordination of growth and general stress response by the PKA pathway

In this part, I will briefly describe the growth regulatory network in *S. cerevisiae*. I will then mainly focus on one branch of this network, the PKA pathway, since it has a predominant role in response to stress compared to other growth pathways like TORC1, SNF1 and the HAP pathways (Hasan et al., 2002; Molin et al., 2011; Morano et al., 2012; Roger et al., 2020). Extensive reviews described the whole growth signaling network of *S. cerevisiae* (Broach, 2012; Conrad et al., 2014).

If the general stress response is largely dependent upon Msn2/4, its regulation is embedded in a larger regulatory network that involves the growth control pathways PKA and TORC1 (Broach, 2012). In this view, the **Msn2/4 regulon is only a downstream branch of the whole General Stress Response (GSR).**

PKA, TORC1 (through Sch9 signaling), SNF1 and the HAP complex are known as the main nutrient pathways that respond to glucose and metabolite availability (Broach, 2012) (Fig 20). The HAP complex and the SNF pathways mainly control the use of alternative carbon source and regulate the switch from fermentation to respiration in response to glucose deprivation (Broach, 2012; Hedbacker and Carlson, 2008; Mao and Chen, 2019). PKA and TORC1 are activated by the presence of glucose and 90% of the glucose-induced transcriptional changes can be recapitulated by activating PKA or the Sch9 branch, called PKB, of the TORC1 pathway (Zaman et al., 2009). If blocking Sch9 activation can be fully compensated by the PKA pathway activity, the contrary is not true, suggesting the predominant role of PKA for the activation of glucose-induced transcriptional changes (Broach, 2012; Zaman et al., 2009).

Moreover, the inhibition of PKA upon glucose starvation is required both for the accumulation of glycogen and for acquiring heat-shock resistance (Cameron et al., 1988; Cannon and Tatchell, 1987). Indeed, it has been shown that the inhibition of

PKA was required for the Msn2 relocation into the nucleus in response to starvation (Görner et al., 1998), therefore suggesting that the role of PKA in stress response is at least partially depending on the activation of the GSR (Broach, 2012; Morano et al., 2012; Pedruzzi et al., 2003).

More surprisingly, **the activation of the Msn2/4-dependent GSR largely participates to the growth inhibition** resulting from the inhibition of PKA (Smith et al., 1998a). In a mutant deleted for MSN2/4, authors showed that the growth defect resulting from PKA inhibition was partially rescued. Similarly, the deletion of the YAK1 kinase, that participates in the PKA-dependent activation of the GSR, also rescues the growth of a mutant deleted for tpk1, 2 and 3 (the three subunits of PKA) (Garrett and Broach, 1989). Altogether, those data demonstrate the important cross-talks between the growth control pathways and the activation of the GSR by Msn2/4. If PKA controls the nuclear localization of Msn2, the activation of the GSR seems to participate in the growth inhibition upon unfavourable environmental conditions.

The activation of the general stress response and the growth arrest observed in response to stress are therefore largely dependent on the PKA inhibition and the Msn2/4 regulon activation.

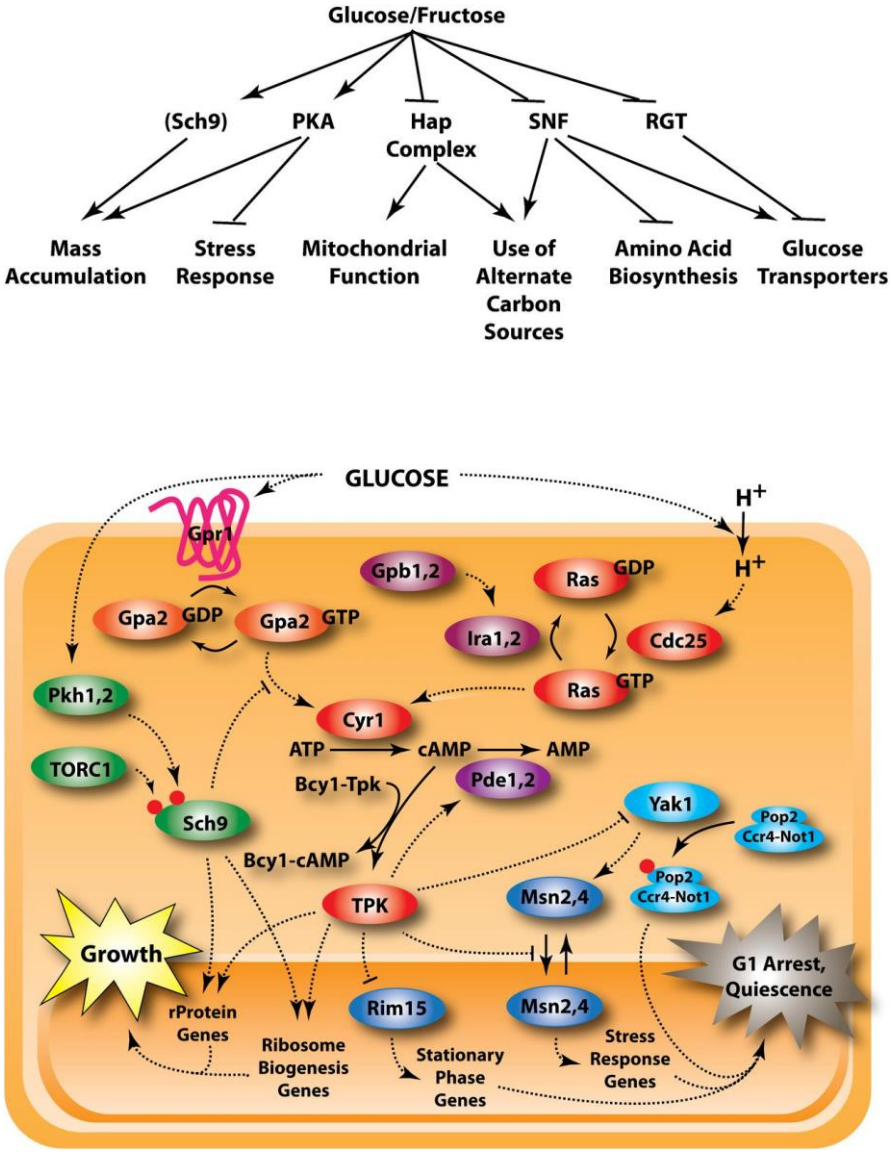

Figure 20 (adapted from Broach et al., 2012): **General growth control pathways and detailed schematic of the PKA pathway** *(a): The growth regulatory network of S. cerevisiae. PKA and TORC1 participates both in the activation of growth-related processes and the inhibition of the Msn2/4-dependent stress response. The HAP complex and the SNF/Rgt pathways mediates the activation of mitochondrial respiration and the consumption of secondary sugars, respectively. (b) Scheme of the PKA pathway and its downstream elements (mainly the Rim15 kinase and the Msn2/4 regulon).*

4.1.3. PKA controls the state of the translational machinery in response to stress

Upon environmental stressors, the PKA-dependent GSR activation inhibits cell growth. This arrest must be coordinated with other cellular processes to adapt the biological functions and the synthesis of biomolecules with the actual growth rate of cells. PKA is a central coordinator of those adaptive changes following growth inhibition. In particular, the translation machinery is a prominent determinant of the growth of cells.

a. Ribosome biogenesis

A first PKA-regulative layer controls the translation by regulating ribosome biogenesis. Its activity is controlled by PKA in a positive manner, thus offering an opposite regulation of the GSR activation and the activation of the translational apparatus and ribosome biogenesis. This enables a **reduction of the ribosome biogenesis when the GSR is activated** and thus the growth inhibition.

The nuclear localization of Sfp1, a transcription factor, is positively controlled by PKA (and TORC1). Sfp1 regulates at least 60 genes involved in ribosome assembly (Jorgensen et al., 2002), which activate the transcription of both ribosomal proteins and proteins involved in ribosome biogenesis (Marion et al., 2004). On the contrary, PKA (and TORC1) negatively regulates the nuclear localization of transcriptional factors Dot6, Tod6 and Stb3 that are themselves inhibiting the synthesis of ribosomal proteins (Lippman and Broach, 2009). Another layer of regulation of ribosomal proteins depends on the negative regulation exerted by PKA and TORC1 on the Yak1 kinase.

Yak1 phosphorylates and activates the transcription factor Crf1 that inhibits the transcription of ribosomal proteins (Martin et al., 2004). Upon environmental stress, PKA/TORC1-dependent inhibition of Yak1 is released and Crf1 inhibits ribosome biogenesis.

In addition, PKA regulates the synthesis of both RNA Pol II (Chang et al., 2004; Howard et al., 2003) and RNA Pol III (Cieśla et al., 2007; Moir et al., 2006) while TORC1 is involved in the control of RNA Pol I (Li et al., 2006; Mayer et al., 2004; Philippi et al., 2010). The demand in ribosomal RNA is thus coordinated with ribosome biogenesis through the control of Pol I and Pol III while the PKA-dependent inhibition of Pol II ensures the coordination of mRNA production with ribosome biogenesis.

Together, those mechanisms coordinate the inhibition of growth and the downregulation of the translational apparatus.

b. Translation inhibition and P-bodies formation

Another PKA-dependent layer of regulation directly inhibits translation in response to environmental stressors. It has been reported that **upon glucose starvation, protein synthesis was inhibited in a reversible manner** (Ashe et al., 2000). This inhibition was independent of any transcriptional processes and the global level of mRNA remained constant, suggesting a direct inhibition of translation upon glucose starvation. Further studies identified the Pat1/Dhh1 pathway as a key regulator of translation in response to glucose and amino acid starvations (Coller and Parker, 2005). **A mutant deleted for PAT1 and DHH1 cannot repress translation in starvation** while the overexpression of those genes constitutively inhibits translation (Coller and Parker, 2005). In addition, a *pat1*Δ*dhh1*Δ mutant cannot form P-bodies,

cytoplasmic foci containing non-translating mRNA complexed to repressors of translation and the mRNA decapping machinery (Buchan et al., 2008).

Importantly, it has been shown that the Pat1/Dhh1-dependent **formation of P-bodies** following starvation were **dependent upon the PKA pathway inhibition**. Authors showed that PKA was directly phosphorylating Pat1, preventing its role of scaffold in P-bodies. Moreover, a mutant deleted for PAT1 elicited a short survival in quiescence, suggesting the importance of both P-body formation and translational inhibition to survive prolonged starvation (Ramachandran et al., 2011).

In a recent paper, Bresson et al. showed that both in response to starvation and heat-shock, the binding of key initiators of translation on mRNA molecules was lost within seconds, thus preventing translation. This furnishes a striking evidence of the rapid translational shut-down following stress exposure (Bresson et al., 2020).

There is however no evidence of translational inhibition and P-body formation in response to other environmental stresses.

Overall, **the translation is therefore directly inhibited in response to starvation in a PKA-dependent manner**. If the function and the role of P-bodies are unclear upon stress exposure, is it likely that rapid translation arrest and storage of the translational machinery may have important functions.

4.2. The regulation of the PKA pathway

Before discussing the functional role of the PKA inhibition upon stress exposure, I will first describe how environmental stressors regulate the PKA activity.

4.2.1. Regulation in response to glucose availability

PKA works as a heterotetramer that contains two regulatory subunits Bcy1 and two catalytic subunits that are encoded by TPK1/2/3. While TPK 1, 2 and 3 have slightly different functions, one TPK gene is sufficient for viability in *S. cerevisiae* (Robertson and Fink, 1998), demonstrating their relative redundancy.

PKA is a cAMP-dependent kinase: cAMP binding to the regulatory sub-unit Bcy1 alleviates its inhibition since it induces the release of the two catalytic units of Tpk. The activity of **PKA is thus controlled by a tug-of-war between the binding of Bcy1 on the Tpk subunits and the binding of cAMP to Bcy1** (Fig 20) (Broach, 2012). cAMP is produced by an ATP-dependent synthesis by the adenylyl cyclase Cyr1 and degraded by the two phosphodiesterases Pde1 and Pde2. A study showed that the cAMP largely determines the state of activation of the PKA pathway (Nikawa et al., 1987).

The activity of Cyr1 is activated by the two homologs of the mammalian RAS gene, encoded by RAS1 and RAS2 in *S. cerevisiae* (Broach and Deschenes, 1990). Ras1/2 bound to GTP activates the Cyr1 activity. Cdc25 transforms the Ras protein bound to GTP into Ras-GDP, negatively regulating its activity. On the contrary, the two GTPase activating proteins Ira1/2 increase the Ras-GTP form, that in turn stimulates its activity (Fig 20). The whole activity of this pathways is modulated by glucose availability but the exact mechanism by which it occurs remains unclear (Broach, 2012; Broach and Deschenes, 1990). Another pathway participates to PKA regulation. Similarly to Ras1/2, Gpa2 bound to GTP activates the activity of the Cyr1 adenylyl cyclase (Peeters et al., 2006). Gpas2 interacts with Gpr1, a transmembrane G protein that activates Gpa2 activity in the presence of glucose in the environment.

The activity of PKA is therefore controlled by several layers that reacts to glucose availability. Those layers finally control the cAMP concentration that *in fine* regulates PKA activity. **Glucose availability is thus linked to the activation of PKA, the activation of growth, and the inhibition of the GSR.**

4.2.2. Redox-dependent control of the PKA activity

If the typical model involves glucose sensing as the modulator of the PKA activity, understanding **how PKA reacts to environmental stressors is also fundamental**. Indeed, in addition to its response to nutrient availability, PKA has also been reported to respond to multiple environmental stressors such as osmotic stress, ethanol, oxidative stress and heat-shock (Görner et al., 1998). How environmental stressors modulate PKA activity is still largely elusive. Moreover, the mechanism by which PKA regulates Msn2 localization in response to starvation is different than the one in response to other environmental stressors (Görner et al., 2002). In Görner et al., authors showed that Msn2 contains a Nuclear Localization Signal (NLS) sequence that is inhibited via a PKA-dependent phosphorylation. Upon starvation, Msn2 is dephosphorylated and relocates into the nucleus. However, upon environmental stressors, the dephosphorylation of the NLS sequence of Msn2 is not involved in the activation of the GSR.

The mechanisms that control both the inhibition of PKA and the activation of the GSR in response to environmental stressors are thus still unclear.

In response to oxidative stress, Boisnard et al. reported that thioredoxins were required for the nuclear translocation of Msn2 (Boisnard et al., 2009). A mutant strain

deleted for both *TRX*1/2 was not able to relocate Msn2 under 0.8 mM H_2O_2, but could still do it in response to osmotic stress (Boisnard et al., 2009), strongly suggesting an oxidative stress-specific mechanism. On the contrary, a mutant deleted for *TRR1* elicited a higher Msn2 relocalization than a WT strain. Finally, authors showed that the Trr1-dependent enrichment of Msn2-nuclear was dependent upon the presence of thioredoxins. Indeed, since the function of Trr1 is to reduce thioredoxins, **those observations strongly suggests that oxidized thioredoxins are responsible for the translocation of Msn2 into the nucleus in response to H_2O_2**. More surprisingly, authors showed that the Msn2 relocation was independent of the downregulation of the PKA activity under 0.8 mM H_2O_2. This Trx-dependent relay thus appears as a PKA-independent layer that can activates the GSR downstream of the PKA pathway.

In another paper, Bodvard et al. showed that the Msn2 nuclear localization observed in response to blue light was transduced through a H_2O_2 redox relay (Bodvard et al., 2017). In agreement with Boisnard et al., authors showed that the sensing and transduction of the signal was dependent upon thioredoxins. In a *trx1/2*Δ mutant, Msn2 was not relocated into the nucleus in response to light or direct H_2O_2 stimulation. Importantly, authors showed that the nuclear localization of Msn2 was lost in a *bcy1*Δ strain in response to 0.4 mM H_2O_2 but not under 0.8 mM H_2O_2. Interestingly, this suggests that **upon severe doses of H_2O_2, oxidized thioredoxins can bypass the strong activity of PKA** in the *bcy1*Δ mutant to induce the nuclear localization of Msn2. In addition, in both papers, authors pinpointed that the deletion of the main peroxiredoxin, Tsa1, also reduced the nuclear localization of Msn2 (Bodvard et al., 2017; Boisnard et al., 2009). **This suggests that the redox-signaling was transduced from H_2O_2 to Tsa1 and then to thioredoxins** (that reduces Tsa1). Once

oxidized, the mechanisms by which thioredoxins interact with Msn2 are still unclear. Importantly, authors showed that while the thioredoxin-dependent signal was independent of the PKA activity at 0.8 mM, it was however dependent upon it at lower doses (0.2 and 0.4 mM). At those low doses, the redox signaling routing through Tsa1 dephosphorylated Msn2 in a PKA-dependent manner. Authors showed that this redox signal was indeed inhibiting the nuclear localization of Tpk1 and 2, potentially alleviating the inhibitory regulation of Tpk1 and 2 on the Msn2 nuclear localization (Bodvard et al., 2017).

In a recent paper, Rodger et al. also reported that Tsa1 was inhibiting the activity of the PKA pathway in a redox-dependent manner (see also Ch1.2.4.1.) (Roger et al., 2020). Upon oxidative stress exposure, they showed that Tsa1 was transducing oxidation to the Tpk subunit of PKA, inducing the sulfenylation of two cysteine residues. The exact mechanism by which it happens and whether thioredoxins are required is however unclear.

Altogether, those results argue in favour of a multi-modal redox-dependent regulation of PKA activity and Msn2 localization. At low doses of H_2O_2, a redox signal negatively affects PKA and thus activates the Msn2 regulon. This seems to happen **through the action of oxidized thioredoxins (Bodvard et al., 2017) and also through the direct action of oxidized peroxiredoxins (Roger et al., 2020).**

At higher doses of H_2O_2, thioredoxins mediate a direct activation of the GSR, independently of the PKA activity (Bodvard et al., 2017; Boisnard et al., 2009).

Interestingly, those studies show **the existence of a redox-dependent coordination between the GSR and the state of oxidation of the thioredoxin** cycle, one of the prominent regulators of the redox state in cells.

In basal condition, the ratio of oxidation of thioredoxins is very low (Lee et al., 1999, Bodvard et al, 2017) due to the direct reduction of thioredoxins by NADPH. The increase of oxidized thioredoxins thus testifies a depletion of NADPH and a global increase of the redox state in cells. The inhibition of PKA by oxidized thioredoxins enables to restrict the activation of the GSR when the antioxidant machinery is overloaded and the redox homeostasis impaired. Since PKA inhibition leads to growth arrest, any non-necessary inhibition of PKA may have disastrous consequences for the cell fitness.

In this view, the **inhibition of PKA represents an 'alarm response'** that would be activated only if the H_2O_2-specific response cannot restore redox homeostasis. A similar organization of the σB stress response pathway has been reported in *E. coli*. The activation σB is only activated under sudden and large homeostatic disturbances while the stress-specific responses are activated alone in case of gradual perturbations (Young et al., 2013).

In my initial context, **it is likely that such a coordination between the GSR and the H_2O_2-specific stress response has a fundamental physiological function to adapt and survive to oxidative stress.**

4.3. The functional role of the general stress response (GSR)

In the following part, I will now focus on the physiological function of the GSR. I will first describe its downstream targets and the redundancy/complementarity existing with other stress response pathways. Then, I will discuss the physiological function of the GSR and by which mechanisms it helps to adapt and survive oxidative stress.

4.3.1. The targets of the Msn2/4 regulon and the cross-talks with other stress response pathways

a. The Stress Response Element (STRE)

Before demonstrating the large-scale transcriptomic response mediated by Msn2/4, it had been reported that Msn2 and 4 were key transcriptional factors (TF) in response to multiple environmental stressors. A conserved upstream activator sequence has been identified in several promoters of genes involved in stress response. This sequence, called the Stress Response Element (STRE), was first reported in the promoter of CTT1 (Marchler et al., 1993) and then in other genes such as DDR2 and HSP12 (Martínez-Pastor et al., 1996). Importantly, the **suppression of the STRE element inhibits the expression of those genes in response to stresses**. Later, Martinez-Pastor et al. found that the binding of Msn2/4 to the STRE element was required for the activation of those stress-inducible genes (Fig 21a and b). This has been further confirmed by Schmitt and Mcentee (Schmitt and Mcentee., 1996).

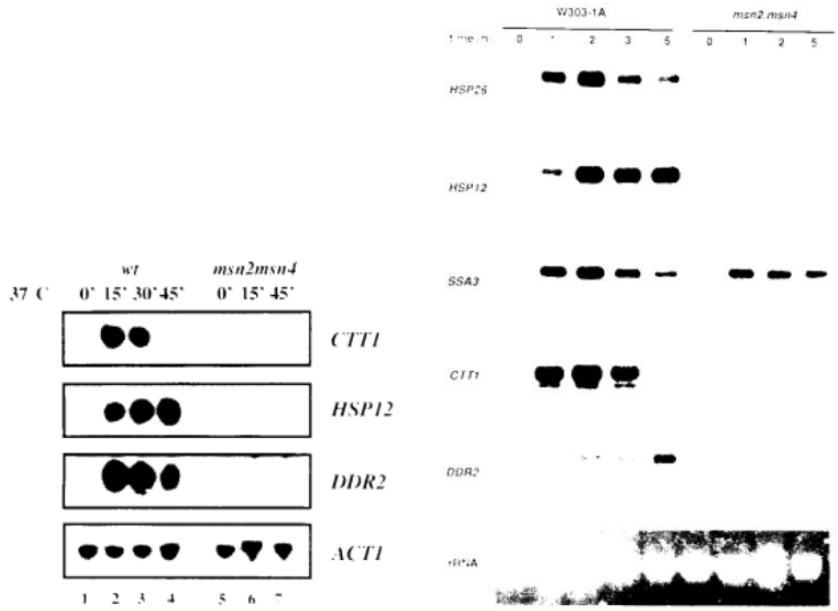

Figure 21 (adapted from Martinez-Pastor et al.): **The Msn2/4-dependent transcriptional stress response** (a) *Dynamical RNA expression of stress-inducible genes in response to a heat-shock (37°C). Total RNA was fractioned on an agarose gel by Northern blot hybridization.* (b) *Dynamical RNA expression of stress-inducible genes in response to starvation (same technic than in a). NB: The low image quality is coming from the original document.*

If the deletion of MSN2/4 critically disturbs the transcriptional changes upon stress exposure (Causton et al., 2001; Gasch et al., 2000), the Msn2/4 regulon is however largely overlapping and cooperating with other stress response pathways that can at least partially compensate for it. Hog1, the transcription factor mediating the osmotic stress response, has also been reported to bind to the STRE element (Schüller et al., 1994) and the downstream genes of both pathways are thus overlapping. CTT1 and HSP12 are thus also activated by the binding of Hog1 on the STRE element (Alepuz et al., 2001). More recently, AP Capaldi et al. showed that the activation of some promoters required both the binding of Hog1 and Msn2/4 to the STRE element while some promoters were activated by only one pathway (Capaldi et al., 2008). Interestingly, the authors showed that the cooperation of those pathways could drive a complex and conditions-dependent stress response (Capaldi et al., 2008).

b. Cross-talks with the Heat-shock response

Similarly, it has been shown that the transcription of several genes of the Heat-Shock response (HSR) could be activated by Hsf1 (the heat-shock specific TF) or rather by Msn2/4. For example, the promoter of the disaggregase protein Hsp104, that mediates

thermotolerance (Sanchez and Lindquist, 1990), possesses both the STRE element where Msn2/4 bind and the HSE element where Hsf1 binds. The deletion of both the Msn2/4 and the Hsf1 pathways is required to fully abolish the expression of Hsp104 (Grably et al., 2002). It is thus likely that the activation of the heat-shock response is indeed not specific to temperature increases but rather a part of the general stress response. Indeed, the expression of the main chaperon proteins Hsp70 and Hsp104 have been reported in several stress contexts.

c. Cross-talks with the oxidative stress response

The expression of the cytoplasmic catalase T **CTT1 is not only under the control of Yap1 but also under the control of Msn2/4** due to the presence of the STRE in its promoter (Marchler et al., 1993). Both the general stress response and the oxidative specific stress response mediated by Yap1 are thus thought to participate in H_2O_2 scavenging. However, the other antioxidants under the control of Yap1 like thiol peroxidases have not been reported to be part of the Msn2 regulon. The cross-talks of Msn2/4 with the Yap1 regulon thus seems minor compared to the one between Msn2/4 and the Hsf1 regulon.

Overall, the GSR therefore mediates a large-scale reorganization of the transitional expression within cells that is largely overlapping and interacting with the different specific stress response pathways. In addition, due to the large number of genes under the control of Msn2/4, a mechanistic understanding of the function of the regulon is still largely missing.

4.3.2. The physiological function of the GSR in adaptation and survival to present and future environmental changes

In the historical paper that reported the requirement of Msn2/4 for the expression of stress response genes, authors reported a pleiotropic stress sensitivity in the *msn2*Δ*msn4*Δ mutant (to starvation, heat-shock, osmotic stress, and oxidative stress) (Martínez-Pastor et al., 1996). Surprisingly, it has however been reported later that a mutant deleted for both MSN2 and MSN4 did not exhibit sensitivity to any environmental stressors (Berry and Gasch, 2008). Instead, authors claimed that the genes expressed upon a given stress provide a protective role for future stress exposures. In line with that, another study reported that only 7% of genes expressed in response to an acute stress were required for optimal growth under that stress (Giaever et al., 2002). Whereas the data from Martinez-Pastor et al. and those from Berry et al. are difficult to reconciliate, it can however be noticed that in both papers, the doses and the duration of stress imposed to cells have been arbitrarily chosen. Moreover, Berry et al. draw conclusions without submitting both the WT and the *msn2/4*Δ mutant strains to severe doses. We therefore cannot rule out that the stress conditions used in the Martinez-Pastor et al. paper may have been more discriminants than in the Berry et al. paper. In addition, the most important phenotype observed in the Martinez-Pastor et al. paper was in response to long-term starvation, a condition that is not tested in the Berry et al. paper. In the context of the alkaline stress, the sensitivity of the *msn2/4*Δ mutant has also been observed independently of those two papers (Casado et al., 2011). Overall, if the exact physiological function of the Msn2 regulon is still elusive, it does not seem to play a role in the survival and the adaptation to environmental stressors, at least in certain stress conditions.

4.3.3. The GSR in the context of oxidative stress

In this last subsection, I will focus in greater detail on the role of the GSR in response to oxidative stress and the potential mechanisms by which it participates to oxidative stress adaptation and/or survival.

In the context of oxidative stress, Hasan et al. evaluated the physiological consequences of the deletion of both the GSR (*msn2/4*Δ mutant strain) and the oxidative-specific stress response (*yap1*Δ). Interestingly, such comparative analysis has the advantage to give a biological significance to the physiological role of each stress response pathway. Indeed, the only comparison of a mutant strain to the WT is poorly informative since it cannot testify of the relative importance of a defence pathway compared to another.

Importantly, authors distinguished the fate of cells in response to both a short and severe bolus of H_2O_2 and a constant mild H_2O_2 exposure. In the first case, post-stress viability was quantified while in the second case the growth under stress was assessed. Those two assays can be interpreted as potential readouts of stress tolerance and stress resistance respectively (Brauner et al., 2016).

Authors strikingly observed that while **Yap1 was critical to grow under a mild oxidative stress**, the *msn2/4*Δ mutant elicited a smaller survival fraction than the *yap1*Δ mutant in response to a severe and short H_2O_2 bolus. More surprisingly, authors showed that **maintaining the activation of the PKA pathway was leading to a much higher oxidative stress sensitivity than the deletion of YAP1**. Similar observations have been made by Molin et al. that showed that while PKA inhibition

was required for oxidative stress resistance, the activation of Msn2/4 regulon was not. PKA inhibition is thus mainly participating in stress tolerance via a Msn2/4 independent mechanism.

This study thus provides evidence that the role of the general and the oxidative-specific stress responses are condition dependent and both participate in the physiological fate of cells under stress in a non-redundant manner. **While the Yap1-mediated antioxidant response seems critical for oxidative stress resistance, the GSR seems to be involved in oxidative stress tolerance.**

However, by which mechanism the GSR helps to survive to oxidative stress is largely unclear. Due to the presence of a STRE element on the promoter of CTT1 (Marchler et al., 1993), it has been suggested that the activation of the GSR could participate to H2O2 scavenging and thus explain the role of the GSR in the context of oxidative stress response (Morano et al., 2012). However, since Yap1 can also activate CTT1, this can hardly explain the non-redundant function of both the Msn2/4 and the Yap1 pathways. In addition, this could not account for the PKA-dependent but Msn2/4-independent oxidative stress tolerance.

Challenging the ability of a *msn2/4*Δ strain to maintain its redox state under a H_2O_2 challenge must enable to decipher whether the Msn2/4 regulon participates to oxidative stress response by a H_2O_2-scavenging dependent or independent mechanism.

Alternatively, since the GSR seems to be required in oxidative stress tolerance rather than in oxidative stress resistance (Hasan et al., 2002), the GSR might provide a

protective mechanism in response to stress, independent of any H_2O_2-scavenging activity. Trehalose synthesis is controlled by Msn2 and has been proposed as an efficient mechanism of stress protection by inducing the gelification of the cytoplasm. However, its mechanism of action remains debated (Gibney et al., 2015) and its physiological function has only been shown so far in response to heat shock (Li et al., 2018; Magalhães et al., 2018; Ziv et al., 2013) or dessiccation (Tapia et al., 2015) in *S. cerevisiae*. Protective mechanisms depending on stress response activation have been shown to be critical in the bacterial tolerance to antibiotics (Balaban et al., 2004a; Harms et al., 2016; Stewart et al., 2015). Growth arrest is another hallmark of bacterial tolerance. In my context, it is thus likely that the GSR participates through the inhibition of growth and protective mechanisms. However, it is largely unclear whether or not growth inhibition is required for GSR-dependent oxidative stress tolerance and which pathway might contribute.

5. Dynamics of the oxidative stress response and stress adaptation

5.1. The temporal orchestration of the oxidative stress response layers

Over the previous parts, I described three layers of response to oxidative stress: (1) the **transcriptional H_2O_2-specific stress response** mediated by **Yap1** that activates antioxidants (2) the **metabolic rerouting** of carbon into the **PPP** that increases NADPH production and (3) the **PKA-dependent GSR** that contributes to the inhibition of growth-related processes and the activation of the transcriptional **Msn2/4 regulon**. If those 3 layers of defense have been all described to participate in oxidative stress

tolerance and/or resistance, their timing of response following stress exposure are strongly different. It is thus likely that their physiological role is mandatory only in a given temporal window of the whole adaptive process.

5.1.1. The transcriptional layer: Yap1 and Msn2/4 regulon dynamics

Both Yap1 and Msn2/4 mediated pathways were reported to respond to the oxidative agent cumene hydroperoxide in *S. cerevisiae* (Sha et al., 2013). Authors found that the timing of activation of genes in the **Yap1 regulon was comprised between 6 and 20 minutes**. In Causton et al., 2001, authors realized a global transcriptional dynamical screen of the response to various stressors. They reported that the response to heat-shock was the fastest among all stressors tested **and fully occurred within 15 min following stress exposure**. On the contrary, the H_2O_2-mediated response was slightly slower (no precise timing furnished) than the other stress responses. Following those data, considering that the H_2O_2-mediated transcriptional stress response is in the order of magnitude of the dozens of minutes seems a reasonable approximation.

By probing the nuclear relocation time of both Msn2 and Yap1 in response to oxidative stress, it has been shown **that Msn2 relocation was delayed for minutes** (exact timing not provided) **compared to Yap1** (Granados et al., 2018). This suggests that the Yap1-specific stress response is the first transcriptional defense layer. Such temporal orchestration matches well with a Msn2 translocation mediated by the overload of the thioredoxin cycle and the oxidation of thioredoxins (Bodvard et al., 2017; Boisnard et al., 2009).

5.1.2. A PKA-dependent and transcription-independent layer

However, in addition to the Msn2-dependent transcriptional response, the GSR mediated by the inhibition of PKA includes transcription-independent mechanisms. The PKA-dependent translational arrest observed in response to starvation has been observed to be independent of new transcripts (Ashe et al., 2000). Authors recently reported that the decapping of eIF4A, eIF4B, and Ded1 was **abolished in 30 seconds following starvation, inducing a rapid translation arrest** (Bresson et al., 2020). In response to heat-shock, the inhibition went through the degradation of mRNA and was slower, taking up to 16 minutes. In the context of oxidative stress, it is not clear whether translation is similarly inhibited, and the timescale required to do so.

Overall, it is thus clear that the inhibition of **PKA can mediate a rapid response to stress, independently of the transcription**. Its functional role must be assessed to further decouple the different responses orchestrated by PKA over different timescales following stress exposure.

5.1.3. The metabolic rerouting layer

Similarly, it has been widely observed that the metabolic rerouting observed in response to stress is independent of the transcriptional machinery. Metabolic rerouting has been extensively studied in response to oxidative stress and the timescale of the response has been well characterized. To date, **the rerouting of carbon into the PPP is the fastest response to oxidative stress** that has been reported (Dick and Ralser, 2015). This rerouting is linked to the oxidation of enzymes of the glycolysis such as GAPDH (Peralta et al., 2015) and TPI (Ralser et al., 2007) and the inhibition

of G6PDH by NADPH (Christodoulou et al., 2018; Kuehne et al., 2015; Nikel et al., 2020). The rerouting has been shown to occur within seconds following oxidative stress exposure (Kuehne et al., 2015; Ralser et al., 2009). Following the blocking of glycolysis at the level of GAPDH and the activation of the PPP, it has been proposed that carbon may cycle into the upper glycolysis and the PPP to efficiently produce NADPH (Fig 22).

Interestingly, a transcriptional analysis found that **the transcription** of enzymes coding for the metabolism of the PPP was up-regulated within **4 to 7 minutes following H_2O_2 exposure** (Chechik et al., 2008). This may participate in the metabolic rerouting at a slower timescale, mediated by the Yap1 regulon (ZWF1, the genes coding for the first enzyme of the PPP is known to be part of the Yap1 regulon (Lee et al., 1999)). It also illustrates **the incapacity of the transcriptional layer to participate in the immediate stress response.**

Those studies therefore shade the light on the prominent role of the metabolic rerouting for the short-term response to stress, within the timescale of the seconds to minutes.

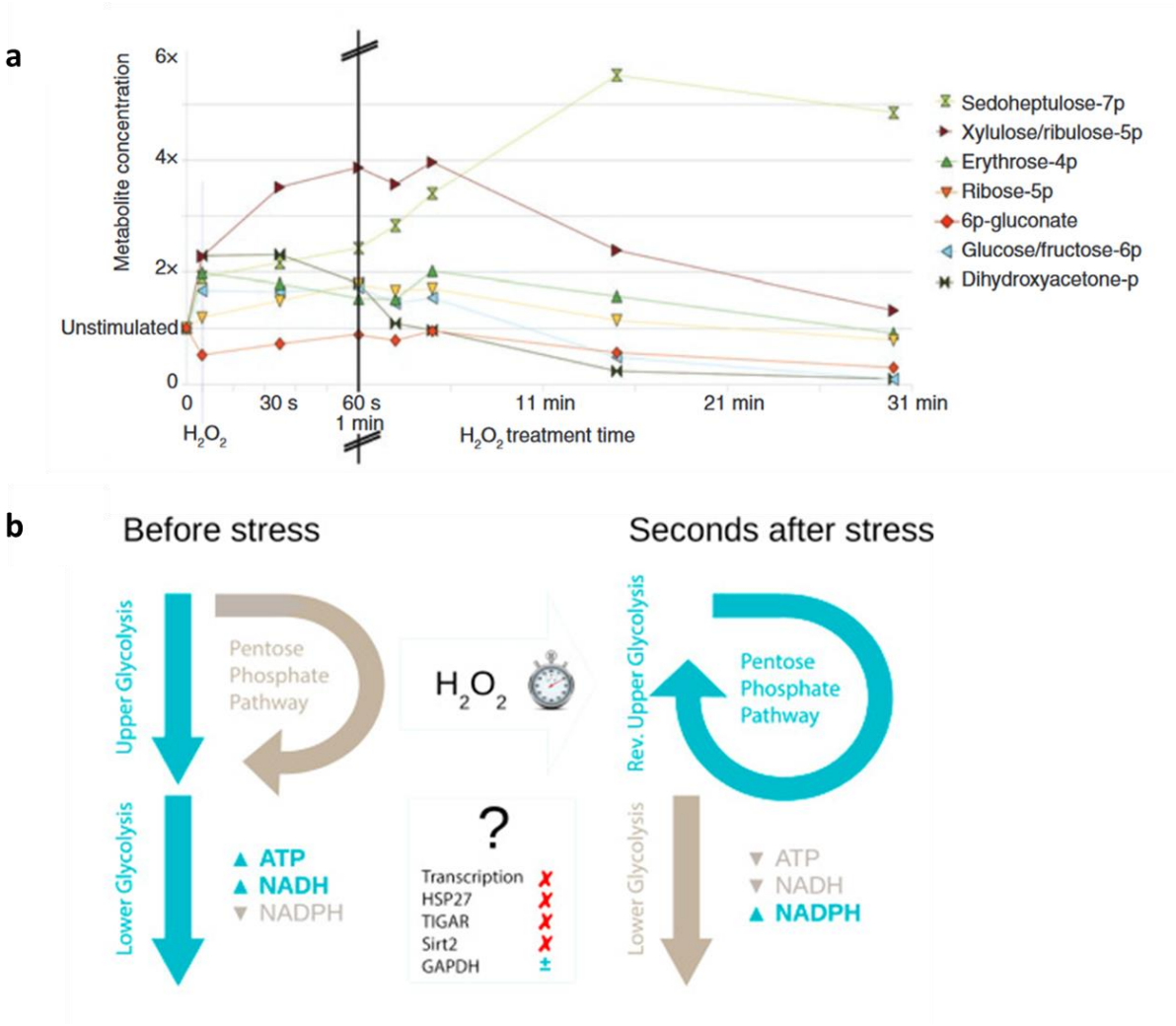

Figure 22 (adapted from Ralser et al. 2009 and Dick and Ralser 2015): **The cycling of carbon in PPP and neoglucogenesis is a oxidative stress response** *(a) Using a fast protocol to capture the rapid metabolic rerouting in response to H_2O_2, Ralser et al. found that metabolism adapted faster than 30 seconds. After dozens of minutes, the metabolic fluxes recovered their initial state, suggesting stress adaptation.* (b) *Scheme of the metabolic rerouting: upon H_2O_2 exposure, glycolysis is inhibited while the PPP is activated. This induces the cycling of carbon through the revert glycolysis and the PPP.*

5.1.4. Pre-conditioning and anticipatory strategies to bypass the slow dynamics of transcriptional stress responses

Due to the slow response of the transcriptional stress response, anticipatory strategies appear as a prominent alternative to protect against stressors.

Indeed, it has been suggested that the weak physiological defect found in a *msn2/4*Δ strain was explained by the inability of the regulon to respond fast enough to the stress (Berry and Gasch, 2008). On the contrary, it has been proposed that the **GSR could mediate cross-protection to future stress exposures**. It has been shown that a first stress was largely protecting against a second stress of a different nature (Berry and Gasch, 2008; Mitchell et al., 2009) (Figure 23a and b). In this view, **the state of the cell prior to stress exposure represents a first layer of response to stress.**

In Berry et al., authors showed that the **deletion of MSN2/4 largely impaired cross-protection.** Nevertheless, in those two papers, the coupling of stresses for which cross-protection was observed were surprisingly different and contradictory. With H_2O_2 as a secondary stressor, Berry et al. reported that NaCl conferred an important cross-protection against a future H_2O_2 challenge (Figure 23a.) while ethanol did not confer cross-protection to any secondary stresses. On the contrary, Mitchell et al. found no cross-protection between NaCl and H_2O_2 but an important one with heat-shock and ethanol (Fig 23b).

Globally, if the cross protective couples are not clearly identified, it is however widely accepted that stresses of different natures can cross-protect each other, in part due to the stereotypical activation of the Msn2/4 regulon in response to different environmental stressors.

However, anticipatory strategies are limited by two principal factors: the predictability of the environmental changes and the cost of fitness associated with the activation of the anticipatory strategy (Mitchell and Pilpel, 2011a; Perkins and Swain, 2009). Indeed, in a non-predictable environment, any anticipatory response may be unrelated to future environmental changes and therefore induce a loss of fitness in non-stressful environments without conferring advantage in response to random environmental changes. Based on cross-protective mechanisms observed in different microorganisms, Mitchell et al. showed with a mathematical model that the cost of anticipatory strategies was likely to exceed the gain of fitness associated with the strategy (Mitchell and Pilpel, 2011b).

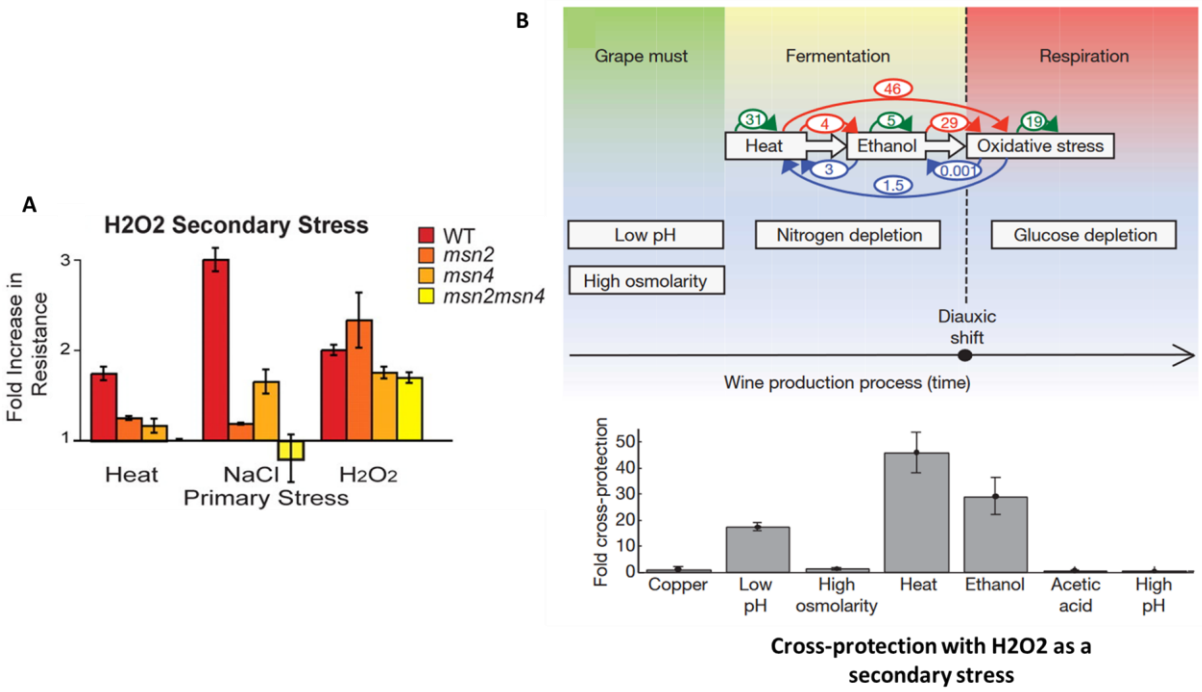

Cross-protection with H2O2 as a secondary stress

Figure 23 (adapted from Berry et al., 2008 and Mitchell et al., 2009): **Cross-protection observed between different couples of environmental stressors.** *(a) After different primary stresses, the fold resistance to H_2O_2 was measured in a WT strain and strain deleted for MSN2, MSN4 or both genes. All primary stresses increased survival to H_2O_2. Among those primary stresses, NaCl had the larger effect on H_2O_2. Data from Berry et al., 2008* (b) *The sequence of stress found in the ecological niche of S. cerevisiae and the cross-protection associated. With H_2O_2 as a secondary stressor, heat and ethanol conferred cross-protection to H_2O_2, but not osmotic stress. Authors argued that the couple conferring cross-protection has been selected by evolution in the ecological environment. Data from Mitchell et al., 2009.*

Overall, we have seen in this part that the response to oxidative stress can be subdivided into different layers that all respond with different timings. Their response time varies from seconds (metabolic rerouting and translation inhibition) to minutes or dozens of minutes for the activation of transcriptional regulons. Alternatively, pre-conditioning strategies can represent a way to bypass the slow response of transcription.

5.1.5. Functional role of the stress response dynamics

Importantly, the temporal decoupling of the stress response implies that the role of each layer may be restricted to specific temporal windows following stress exposure. Different layers could therefore accomplish a similar function but on a different timescale. Interestingly, this may help revealing the functional role of the redundancy of the H_2O_2 scavenging system in cells. Indeed, the efficiency of NADPH-dependent

H_2O_2 scavengers (thiol peroxidases) are dependent upon both their transcriptional expression (mediated by Yap1) and the metabolic rerouting into the PPP. On the contrary, cytochrome c peroxidase and catalases only depend on their own expression. Such differential dependency on metabolism may enable cells to respond to oxidative stress over a large temporal window.

NADPH-independent systems may have a critical role in the first seconds following stress to transiently buffer H_2O_2 before the metabolic rerouting occurs. This hypothesis is underpinned by the great efficiency of catalases under high H_2O_2 fluxes, a condition likely to be met right after H_2O_2 entered inside cells. After metabolic rerouting, NADPH-dependent systems are likely to play a crucial role due to the important flux of NADPH. Overall, the whole oxidative stress response can therefore not be considered as the simple sum of the different layers of response. Each response has a particular timing of activation and cannot work on the whole temporal window following stress exposure. It is therefore crucial to integrate a dynamical perspective in order to capture the complexity of the stress response.

In living cells, it is still largely unclear how this dynamic determines the evolution of the physiological state of cells and whether those layers are critically required for a specific temporal window.

5.2. Cell physiology as a relative timekeeper of the adaptation process

The following section will largely focus on the previous paper of our lab and will help to introduce the questions and motivations that drive my work. The questions and objectives of my work will be further developed and formalized in the section "Remaining questions and Objectives".

5.2.1. Acute stress and steady-state periods: a temporal view of stress tolerance and stress resistance

In the previous part, we described the dynamics of the stress response as the sum of the defense layers operating at different timescales following stress exposure. An interesting alternative to depict the stress response dynamics is to **distinguish stress periods depending on the physiological state of the cell** at a given moment.

Indeed, following a severe stress exposure impairing the redox equilibrium of cells, our lab previously described that the **growth of cells was transiently abolished before resuming at a maximal growth rate** (until irreversible growth cessation under H_2O_2 concentration higher than 0.5 mM) (Goulev et al., 2017). Additionally, authors reported that the recovery of growth was always preceded by the translocation of Yap1 into the cytoplasm, **suggesting a coupling between loss of redox homeostasis and growth inhibition** (Fig 24a). Those observations enable to define two distinct periods under stress, an acute period where the homeostasis of cells is impaired, and growth inhibited and a second period, where homeostasis is set back and growth recovers. Importantly, authors observed that **once growth had recovered, it never ceased later, suggesting that cells had reached a steady-state** (Goulev et al., 2017).

These two periods thus represent a promising framework to separate two fundamentally distinct physiological states under stress: the **acute period** corresponds to the period where the cell is in **an 'out of equilibrium' state** while the second period corresponds to the **recovery of homeostasis** and thus to a **steady**

state. In the case where cells do not adapt, the steady state is never reached, and the acute period continues until cells finally die.

While the ability to recover growth and reach a steady state corresponds to the resistance capacity of a cell (see general introduction), their ability to remain viable while not growing is referred as the tolerance capacity of cells (Brauner et al., 2016). Interestingly, it has been shown in different paper that cells could transiently survive at doses precluding their growth (Fomenko et al., 2011; Hasan et al., 2002). This strongly suggests that cells can tolerate oxidative stress without adaptation.

Overall, the temporal distinction between the acute stress period and a second period where growth recovers enable to distinguish two typical scenarios:

(1) Cells first exhibit a growth arrest and a redox imbalance during an acute and transient period and then undergo adaptation, to recover their initial homeostasis. The ability of cells to reach an equilibrium is set by the resistance capacity.

(2) Cells remain in the acute period as long as the stress continues. The ability of cells to remain alive in this ‘out of equilibrium’ state is set by the tolerance capacity of cells.

Interestingly, while the second scenario is often seen as a result of the inability of cells to adapt, it can rather represent a specific defense strategy to tolerate stressor over a long period of time. In several contexts, it has been shown that stress tolerance could drive cell survival independently of any mechanism of stress resistance (see general introduction).

In this view, **quiescence represents a prominent example of non-growing and extremely stress tolerant state**. Indeed, it has been widely observed that quiescent cells could tolerate extreme doses of H_2O_2, up to 50 mM for several hours (Gray et al., 2004a; Klosinska et al., 2011; Quan et al., 2015), so concentrations that are two orders of magnitude higher that the dose required to inhibit growth in Goulev et al. 2017 (MIC = 0.6 mM). However, **the mechanism associated with such tolerance is not clear** and whether the arrest of growth (no resistance) is critically required to access to stress tolerance. In the context of antibiotic stress tolerance, the relation between growth arrest and tolerance has also been largely described (see general introduction).

In the context of oxidative stress, whether tolerance represents a prominent strategy for stress survival and the mechanisms underpinning it are largely unclear. Further studies are required to characterize and evaluate the role of stress tolerance under H_2O_2.

5.2.2. Stress pattern dynamics sets the ability of cells to reach an equilibrium under stress

Another important question is what drives the transition from the acute stress period to the following steady state period.

By gradually increasing H_2O_2 concentration (ramp assay) instead of sharply submitting cells to stress (step assay), Goulev et al. observed that the acute period could be bypassed (Fig 24a, b and c). In the ramp assay, cells did not arrest their growth and could adapt until doses that were 10 times higher than the concentration which

inhibited growth in response to a sharp stress increase (Fig 24b). Moreover, the acute burst of Yap1 into the nucleus was not observed (Fig 24b).

Altogether, those observations strongly suggest that the initial loss of redox homeostasis during the acute stress period greatly limits the adaptive capacity of cells. The resistance limit is therefore not directly dependent on the maximal scavenging capacity of cells once at steady state but rather on the slow response dynamics of the Yap1 regulon. In agreement with that, authors showed that a *yap1*Δ strain could not grow under stress, even in the ramp assay (Goulev et al., 2017).

Most importantly, it suggests that **the ability to tolerate the stressor during the acute period of stress determines the ability to reach a steady state**, demonstrating the cross-talks between tolerance and resistance in the context of oxidative stress. It is therefore likely that while the Yap1-mediated transcriptional response is required to reach a steady state, other response layers play a role in acute stress tolerance at a much shorter timescale.

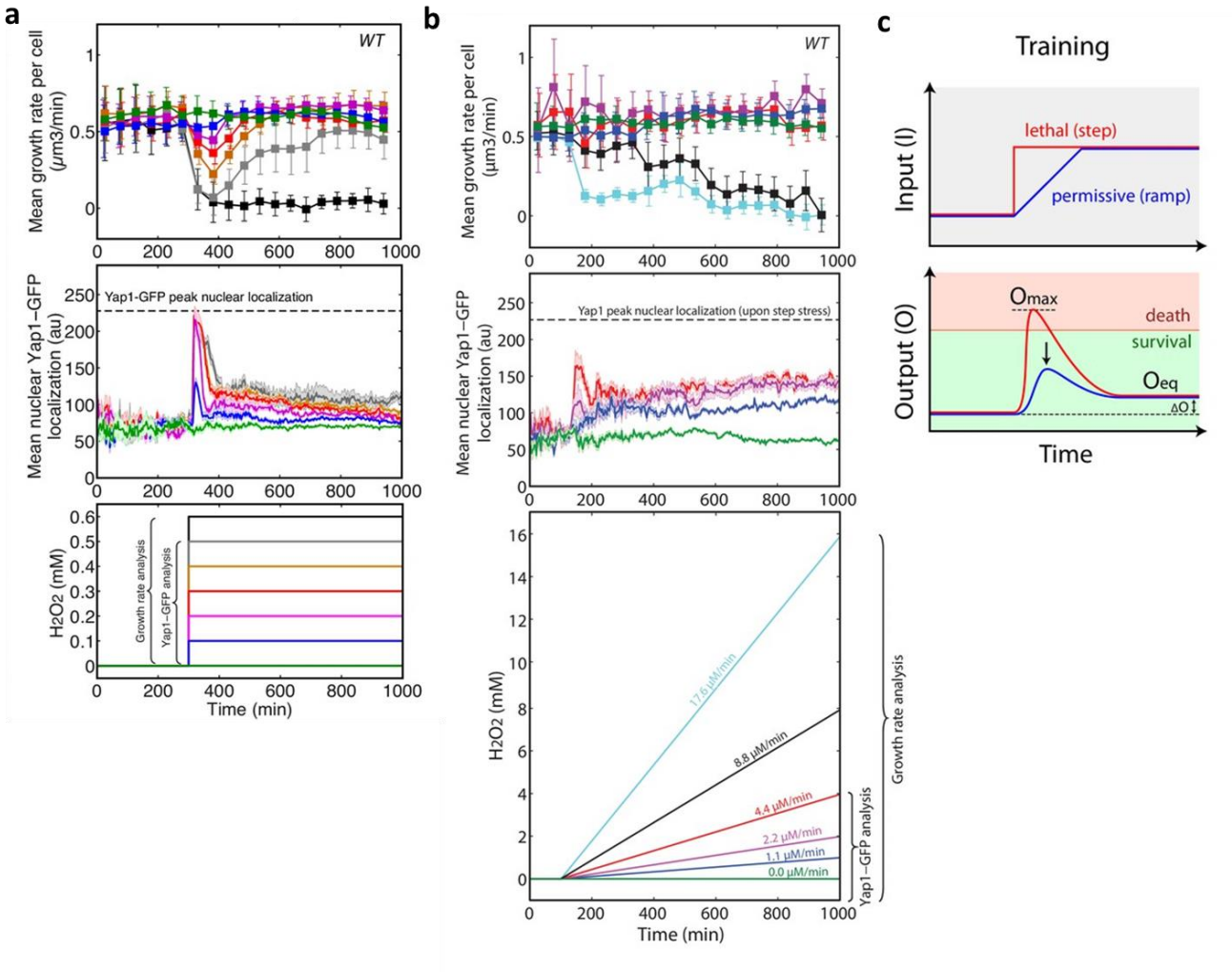

Figure 24 (adapted from Goulev et al., 2017): **Single yeast cells imaged and followed over time in response to an oxidative stress in a microfluidic device.** *(a) When exposed to a sharp oxidative stress (step), cells exhibited a transient growth arrest and an important translocation of Yap1 into the nucleus, testifying of a transient redox imbalance. After a while, growth recovers and Yap1 returns into the cytoplasm. At 0.6 mM H_2O_2, growth was precluded. (b) When exposed to a gradual H_2O_2 stress increase (ramp), the growth of cells did not stop and Yap1 was only slightly relocated into the nucleus. In those conditions, cells could grow until 7.3 mM H_2O_2, so for doses 10 times higher than in the step assay. (c) Scheme of the behaviour observed. This mechanism by which cells adapt to important doses of stress by a gradual increase of the concentration has been called 'training'.*

5.2.3. Are oxidative stress tolerance and stress resistance antagonistic properties?

Indeed, studying the mechanisms involved in each process is critical in order to get better understanding of the sequence of events that drives stress survival and adaptation. Moreover, it is not clear whether the state required to tolerate stress is compatible with the one required to proliferate actively under stress. Stated differently, does oxidative stress tolerance and stress resistance are antagonistic properties?

From a theoretical point of view, several mechanisms that have been described to participate in the stress response appear largely antagonistic with the active proliferation of cells under stress, and thus to stress resistance.

For example, the metabolic rerouting that occurs following H_2O_2 exposure is likely to be detrimental for cellular fitness. The **cycling of carbon into the upper glycolysis and the PPP is not favourable to ATP production** and thus may be detrimental for long term stress adaptation. In line with that, Ralser et al., 2009, reported that the **metabolic fluxes return to their initial state after ~30 minutes**.

Similarly, the PKA-dependent activation of the GSR is known to inhibit growth and translational activity (see Ch1.4.) Its activation thus clearly seems incompatible with stress resistance.

Therefore, it is often assumed that the activation of those responses is restricted to the acute phase of stress and only helps cells to transition toward a steady state where growth can resume. However, it is unclear whether those stress responses are

required during the acute period for stress tolerance *per se* or rather help cells to recover growth, thus participating to stress resistance.

In the case where the mechanisms driving oxidative stress tolerance and stress resistance would be different, **it is likely that the transition toward a steady state under stress initially requires a cost in cell survival**.

Moreover, this dynamical view implies that the physiological transition of cells from a tolerant state to the recovery of growth is tightly coordinated with their redox state. Indeed, it is likely that the recovery of canonical functions and growth while the redox state of cells is still impaired may lead to dramatic consequences for cells. In line with that, it has been shown that key constituents of the growth machinery, such as ribosomes, could be targeted and oxidized by hydrogen peroxide, causing irreversible damages for cells.

In this view, the control of the GSR activation by the state of oxidation of the antioxidants (thioredoxin and peroxiredoxins) appears as a pivotal control of the coordination between the redox state and the growth status of cells.

5.3. A methodological perspective: following stress response dynamics at the single-cell level in a controlled environment

To finish this introduction, I will now motivate the single-cell microfluidic-based approach that has been used in the following work. The scope of this section is not to present microfluidics from a technical point of view but rather to justify its necessity in the context of the oxidative stress response. I will focus on three critical points: the necessity to observe the whole dynamics of the stress response process over a long timescale, the necessity to access to a single-cell resolution and the ability to

dynamically control the stress conditions and patterns. I will then discuss the limitations of such approaches in the context of stress response.

Briefly, microfluidics-based imaging consists in trapping cells into micro-chambers (Fig 25a). Those chambers are confined between a coverslip and a transparent polymer, PDMS. Cells trapped into the chambers can therefore be imaged with standard inverted microscope, both in bright field or phase contrast imaging and fluorescence imaging. Importantly, cells trapped into those chambers can remain in a perfectly physiological state and grow at their maximal growth rate (Goulev et al., 2017). Such assay is consistent with **long-term imaging** within the timescales of hours or days.

5.3.1. Microfluidics enables stable conditions over time and the use of stress pattern modulations

Medium is continuously perfused within the microfluidics chip with a rate sufficient to consider the consumption of nutrients stable. Similarly, in the case of a stress condition, we showed that **H_2O_2 stress concentration could remain barely constant over time** (Fig 25b, open circle). Indeed, in the case of the oxidative stress, this aspect is particularly crucial since cells in a bulk culture can rapidly degrade H_2O_2 (see Fig 25b, filled circle). This approach prevents to conclude whether cell adaptation results from the external modification of the environment or rather from the internal re-organization of cells that were enabled to cope with the stressor.

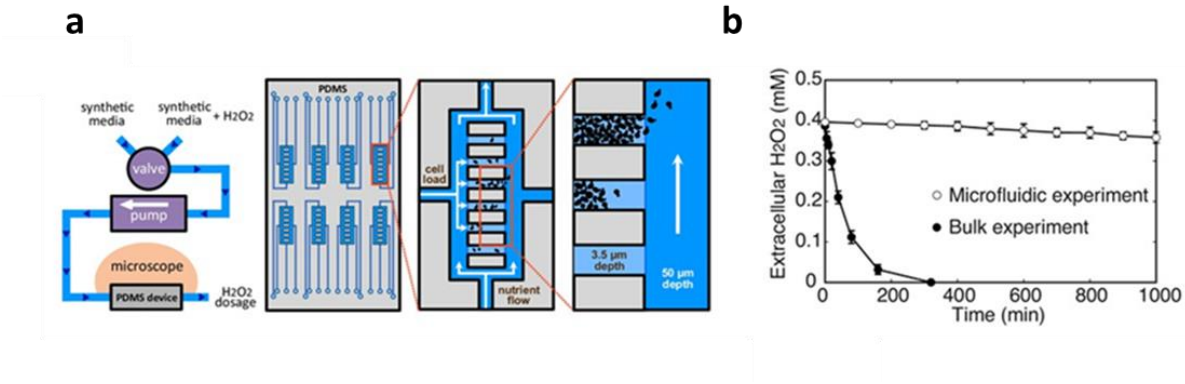

Figure 25 (adapted from Goulev et al. 2017): **Microfluidic device and H_2O_2 stability** *(a) Scheme of the microfluidics device used in this study. Cells can grow in a micro-chamber and are fed by the continuous flow imposed by the peristaltic pump. (b) Temporal evolution of the H_2O_2 concentration in a tank medium containing cells (bulk experiment, filled circles) or in the tank medium fuelling cells in the microfluidic device (open circles).*

Another great advantage of microfluidics-based approaches is **the ability to control the stress pattern over time**. Indeed, I previously showed in this introduction that the rate of stress exposure could drastically shape the response of cells to the stressor. Modulating the stress pattern dynamics previously led to the understanding of non-intuitive system-level properties of the homeostatic systems of cells (Mitchell et al., 2015; Muzzey et al., 2009; Young et al., 2013).

5.3.2. Microfluidics enables to follow the dynamics of the stress response at the single-cell level

In this introduction, we saw that the oxidative stress response is composed of several embedded layers that all respond over different timescales, from seconds to hours, including the initial state of cells that can also determines the fate of cells to future stresses (see Ch1.5.1.). If classical assays can follow such dynamical processes, they

cannot do so at the single-cell level. Following single-cell response confers the great advantage to link the stress response to cells with a given cell fate. Doing so, it has been shown that cell to cell heterogeneities could predict the future behaviours of cells based on a pre-stress marker (Levy et al., 2012; Mitosch et al., 2017). Indeed, heterogeneities are widely observed in the context of stress response since bet-hedging is a common colony-scale behaviour adopted by microorganisms (Balaban et al., 2004a; Levy et al., 2012; Venturelli et al., 2015; Ziv et al., 2013).

5.3.3. Single-cell resolution enables to decouple stress resistance and stress-tolerance

In our context, another non-negligible aspect to consider is the ability, thanks to the single-cell resolution, to decipher between distinct routes that lead to a final identical state. Indeed, from a bulk experiment, it is not possible to distinguish between two populations with different survival rates and proliferation rates under stress.

As an example, let's imaging a first population, where 5% of the population would have survived and where surviving cells would have done an average of 3 divisions within 8 hours. Observing cells after 8h, the number of viable cells compared to the initial population would be $5*2^3 = 40\%$.

Now imagining another population, with 20% survival but with surviving cells doing in average one division, the number of viable cells compared to the initial population after 8h would be $20*2^1 = 40\%$.

To decipher between such situations, it is therefore required to access to the individual fate trajectory of single cells over the whole adaptation process. Cells born before stress can be tracked and isolated from daughter cells born under stress, therefore

distinguishing between the in-stress capacity of cells and their ability to survive, independently of their proliferative capacity (Fig 26).

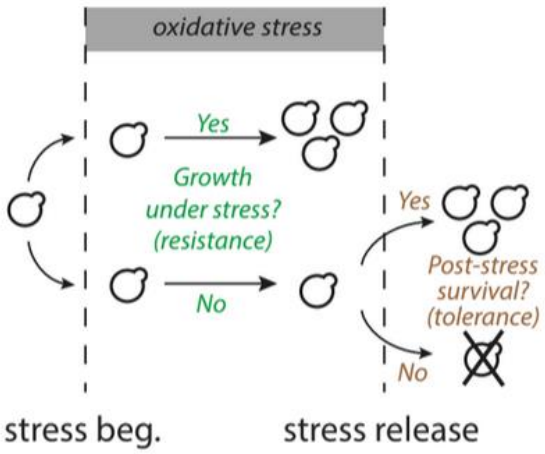

Figure 26: Scheme of the single-cell approach to decipher the proliferative capacity and the post-stress survival of cells.

REMAINING QUESTIONS AND OBJECTIVES OF THE WORK

Cells are open systems that exchange information, energy, and matter with their environment. Those interactions are mandatory to fuel and regulate intracellular processes but can also be at the onset of various stresses for cells, i.e. the loss of their internal homeostasis. To avoid these deleterious effects, cells developed plastic stress responses that enable to maintain their homeostasis under changing environments. Ultimately, it must enable the organism to adapt to stress, i.e. to recover its basal physiological functions and thus maximize its fitness in the presence of the stressor, a mechanism called stress resistance.

However, we saw that in multiple situations (see general introduction), microorganisms could ‘tolerate’ the stressors without adapting, thus remaining in an ‘out-of-homeostasis’ vegetative state until the stressor ceases. While such a state cannot enable ‘infinite’ survival under stress, it can represent a valuable strategy when adaptation is precluded.

In this chapter, we have seen that the budding yeast *S. cerevisiae* was responding to oxidative stress through a multiplexed network that is largely known. Among the mechanisms involved, the core H_2O_2 homeostasis system, composed of the sense-and-signal Yap1-transcriptional regulon as well as the carbon rerouting into the PPP, ensures H_2O_2 scavenging and the maintenance of redox homeostasis. Additional layers exist, such as the general stress response mediated by the inhibition of PKA, including the activation of the Msn2 regulon and the arrest of growth and growth-related processes.

If the organization and the actors of the oxidative stress response are remarkably well known, several discrepancies limit its understanding.

First, the role of antioxidants upon H_2O_2 stress exposure is not clearly established. In particular, the role of peroxiredoxins has been largely debated and the role of its peroxidase function seems to play a minor role compared to its redox-signaling function. Similarly, the role of the GSR is largely unclear and whether its function is linked to H_2O_2 scavenging is not known.

Most importantly, those different actors have been hardly linked to precise physiological function upon stress exposure. The fundamental distinction between stress survival and stress adaptation has been only very rarely considered in the context of oxidative stress. As a consequence, whether antioxidants and other stress response proteins underpin stress resistance and/or stress tolerance is largely unknown.

Finally, how stress tolerance and stress resistance are coordinated with each other in response to stress and in which extend they interact with the homeostatic system of cells (the H_2O_2 scavenging system in our context) have not been explored yet.

In this work, I aimed at achieving the following objectives:

a. Decouple the core modules of genes involved in oxidative stress tolerance and/or resistance

The first objective of this work was to demonstrate that both tolerance and resistance could represent effective strategies to cope and survive to oxidative stress.

Then, I aimed at identifying and decoupling the players involved in each mode of stress defense.

Based on the important knowledge existing on stress response pathways involved in the oxidative stress response, I envisioned to drive a 'candidate approach' screening. In particular, I aimed at identifying the role of genes comprised within the H_2O_2 specific stress response mediated by Yap1 and the GSR mediated by the inhibition of PKA and the Msn2 regulon.

b. Linking redox homeostasis to cell fate under oxidative stress

As a second objective, I aimed at understanding the relation between the ability of cells to maintain their redox homeostasis under stress and their physiological fate, i.e. to tolerate and/or to adapt the stressor.

This should enable to discriminate among the core module of genes involved in H_2O_2 scavenging (homeostatic function) and the ones involved in a protective function, independently of the maintenance of the redox homeostasis.

c. Architecture and orchestration of stress tolerance and stress resistance defense processes in a context of a homeostatic system

Finally, I aimed at deciphering how the mechanisms involved in stress resistance and those involved in stress tolerance 'talk to each other' and are coordinated with redox homeostasis. Indeed, the context of hydrogen peroxide response is an ideal context to study how cells coordinate their physiological fate to their homeostasis since Prxs have been shown to exhibit both H_2O_2 scavenging and redox-signaling functions (as

well as Trx). We therefore hypothesized that the Prx cycle may play a predominant role in transducing redox homeostasis to cell fate under H_2O_2.

d. Challenging the antagonistic nature of oxidative stress resistance and tolerance

In several contexts, it has been suggested that tolerance may be associated with an inhibition of growth and a reduced metabolic activity, suggesting an antagonistic relation between the processes of stress tolerance and resistance. In the context of oxidative stress, I thus aimed at exploring such a relation in the light of the core modules of genes associated with both defence strategies.

RESULTS

A trade-off between stress resistance and tolerance underlies the adaptive response to hydrogen peroxide

Basile Jacquel[1234*], Audrey Matifas[1234], Gilles Charvin[1234*]

Affiliations:

1) Department of Developmental Biology and Stem Cells, Institut de Génétique et de Biologie Moléculaire et Cellulaire, Illkirch, France

2) Centre National de la Recherche Scientifique, UMR7104, Illkirch, France

3) Institut National de la Santé et de la Recherche Médicale, U964, Illkirch, France

4) Université de Strasbourg, Illkirch, France

*: Corresponding authors : charvin@igbmc.fr, jacquelb@igbmc.fr

Abstract

In response to environmental stress, cellular defense strategies may be divided into two categories: those, as in homeostatic systems, that seek to maintain cell proliferation by degrading the stressor (i.e. resistance); and those that ensure cell survival (i.e. tolerance), even if this is often at the expense of cell proliferation. In this study, we have explored the genetic bases of the antagonism between resistance and tolerance in the response to hydrogen peroxide (H_2O_2) in budding yeast. We show that inactivation of protein kinase A (PKA) mediated by H_2O_2 signaling induces an abrupt transition from normal homeostatic function to a stress-tolerant state by protecting the growth machinery, thus maximizing cellular fitness in a changing environment. This model system paves the way for the development of antiproliferative strategies in which both resistance and tolerance mechanisms could be independently targeted to prevent relapse.

Introduction

Cell responses to stress are based on multifaceted strategies that promote physiological adaptation in changing environments. A large class of defense mechanisms against both environmental and endogenous insults (e.g. oxidative (Veal, Day, and Morgan 2007; Toledano et al. 2004; Toledano, Planson, and Delaunay-Moisan 2010), hyperosmolarity (Hohmann 2002) use sense-and-respond regulatory systems that work according to the homeostatic framework: cells attempt to restore a preexisting optimal cellular state by removing the cause of internal stress. In this scenario, the role of the homeostatic system is to restore or to maintain proliferation under stress, i.e. to reach a state of "stress resistance" (Brauner et al. 2016; Balaban et al. 2019). Whereas such regulatory mechanisms may drive excellent adaptive properties at steady-state(Goulev et al. 2017; Muzzey et al. 2009; Milias-Argeitis et al. 2011), they usually suffer from a number of limitations, including a limited homeostatic range and a slow response time (e.g. slow transcriptional activation(Goulev et al. 2017)), which restricts the cell's ability to deal with abrupt unpredictable environmental changes.

An alternative defense scheme, referred to as "stress tolerance" (Brauner et al. 2016), has been described whereby a population of cells can survive a transient physiological threat without necessarily fighting the intrinsic cause of internal stress. In this framework, cell survival is usually associated with arrested proliferation and reduced metabolism, as commonly observed in the context of cellular dormancy (Gray et al. 2004), or in specific cases of heterogeneous cellular behaviours (e.g. bacterial persistence (Bigger 1944; Balaban et al. 2004), bet-hedging (Slatkin 1974; Levy, Ziv,

and Siegal 2012)). Stress response strategies can thus be split into those that seek to maintain cell proliferation under stress (resistance) versus those that ensure cell survival (tolerance), see Fig. 1A. The former may *a priori* maximize cellular fitness, however, their intrinsic limitations (e.g. homeostatic failure) expose the cells to damages and death. In the latter, cell survival comes at the expense of reduced cellular proliferation. Altogether, stress resistance and tolerance mechanisms thus appear as antagonistic cellular strategies of fitness maximization in response to stress, and, so far, how cells deal with such antagonism has not been investigated.

Redox homeostasis is an essential feature that ensures reliable cellular function in cells experiencing redox perturbations of both external and internal origin(Veal, Day, and Morgan 2007; Toledano et al. 2004). In yeast, the control of hydrogen peroxide concentration is achieved through a transcriptional sense-and-respond homeostatic system based on the Yap1 transcription factor(Lee et al. 1999; Delaunay, Isnard, and Toledano 2000; Kuge and Jones 1994). The Yap1 regulon drives the expression of about one hundred genes(Godon et al. 1998; Gasch et al. 2000; Lee et al. 1999), including antioxidant enzymes with somewhat overlapping H_2O_2 scavenging functions(Jiang and English 2006; Chae, Chung, and Rhee 1994; Pedrajas et al. 2000; Wong et al. 2002; Iraqui et al. 2009). Additional regulations participate in the restoration of internal redox balance: first, glycolysis rerouting to the pentose phosphate pathway (PPP) leads to increased production of NADPH (Ralser et al. 2007; Kuehne et al. 2015), which is the ultimate electron donor involved in H2O2 buffering in the peroxidatic cycle (Hall, Karplus, and Poole 2009); then, the inhibition of the protein kinase A (PKA) pathway, which is a major hub for cell proliferation control(Broach 2012) and general stress response (Gasch et al. 2000), contributes to the adaptation to oxidative stress(Hasan et al. 2002) and is connected to the H_2O_2

signaling response through various putative mechanisms (Boisnard et al. 2009; Molin et al. 2011; Bodvard et al. 2017; Roger et al. 2020). Therefore, the response to H_2O_2 provides an ideal context in which to decipher whether and how resistance and tolerance mechanisms coordinate to shape an integrative adaptive stress response.

To address this question, we have used live-cell imaging and microfluidics approaches to develop combined proliferation and survival assays that elicit the distinction between H2O2-resistant and tolerant cellular behaviours. Using a candidate-gene screen, we have classified the main players involved in H_2O_2 stress response into functional categories that highlight their respective roles in adaptation to this stressor. Specifically, our study unraveled the existence of a strong antagonism between resistance and tolerance, that was exacerbated by mutations that affect NADPH fueling in the peroxidatic cycle (e.g. *zwf1* and *trr1* mutants). Further results allowed us to decipher the genetic bases of H_2O_2 tolerance and its interplay with H_2O_2 signaling. Altogether, our study thus revealed how the integrated cellular response to H_2O_2 results from a trade-off between the homeostatic system that ensures cell proliferation and a mechanism that prevents cell death by protecting the growth machinery. This model system paves the way for developing anti-proliferative strategies in which both resistance and tolerance mechanisms could be independently targeted to improve therapeutic efficiency.

Results

Resistance and tolerance are distinct properties of the response to hydrogen peroxide

To determine whether stress resistance and tolerance are relevant and distinct physiological properties of the H_2O_2 stress response, we needed to establish whether yeast could tolerate (i.e. survive) H_2O_2 doses beyond its ability to resist (i.e to proliferate). To this end, we measured yeast resistance to H_2O_2 as the threshold concentration beyond which cell proliferation arrests, which is also referred to as the Minimum Inhibitory Concentration (or MIC) (Brauner et al. 2016; Balaban et al. 2019). Importantly, since H_2O_2 is a quite unstable compound, measuring the MIC for H_2O_2 required a microfluidic chamber with constant medium replenishment in order to maintain a constant concentration of the stressor, as previously described (Goulev et al. 2017).

Using time-lapse microscopy, we followed the proliferation of individual cells under continuous H_2O_2 exposure (starting at t=0). We found that, whereas cells were able to resume proliferation after a lag when exposed to 0.5mM, a 1mM concentration fully arrested cell growth, at least up to 16 hours (Fig. 1B). This indicated that the MIC was between 0.5mM and 1mM, in agreement with previous measurements(Goulev et al. 2017). In contrast, cell growth resumed after a 1h stress pulse at 1mM, indicating that a fraction of the cells managed to survive above the MIC, despite the lack of resistance (Fig. 1C). Interestingly, when varying the duration τ of stress exposure (see Fig. 1D with τ = 4h), the survival fraction (see Material and Methods for details) displayed a similar decay at both 0.5mM and 1mM for $\tau \leq 2h$, suggesting that cell survival (i.e. tolerance) was somewhat independent of stress resistance (Fig. 1E). For $\tau > 3h$, cell survival plateaued at 0.5mM but further decreased at 1mM, due to growth recovery and population adaptation at 0.5mM.

Altogether, the independent assessment of both proliferation and survival, as performed using our single-cell tracking methodology, revealed that resistance and tolerance are two distinct aspects of cell behaviour in response to H_2O_2.

A genetic screen identifies mutants that combine a severe resistance defect with a hyper-tolerance phenotype

In order to decipher the respective genetic determinants of tolerance and resistance, we designed a candidate-gene approach in which we systematically measured proliferation and survival in mutants that have been previously reported as "sensitive" to H_2O_2. Importantly, the survival assays at 0.5mM revealed that cells displayed a two-step response to stress (Fig. 1): an acute period, characterized by arrested growth and high mortality rate, followed by a steady-state, in which cell proliferation resumed yet no further mortality was observed. Therefore, in order to further discriminate between the role of individual genes in the acute versus steady-state response, we used a methodology whereby survival and proliferation were compared between stepping (i.e acute stress regime) and ramping (i.e. steady-state regime but no acute period, see Fig. S2A) stress patterns after a 4-hour exposure at 0.5mM (see Fig. 2A and Fig. S2B and (Goulev et al. 2017)). Cell proliferation was assayed by measuring the total biomass produced by surviving cells only during stress exposure (Fig. 2B), and tolerance was calculated as a fraction of initial cells that resumed or maintained growth after the stress (Fig. 2C, see Materials and methods for details).

We screened 14 genes directly involved in H_2O_2 defense such as Yap1, players associated with the peroxidatic cycle of 2-Cys peroxiredoxins (e.g. the peroxiredoxin

Tsa1 (Wong et al. 2002), the thioredoxins Trx1/2 (Boisnard et al. 2009), the thioredoxin reductase Trr1 (Chae, Chung, and Rhee 1994)), other antioxidant genes (e.g the catalase Ctt1 (Guan et al. 2012) and the mitochondrial peroxidase Ccp1 (Jiang and English 2006)), genes driving the general Environmental Stress Response (or ESR, e.g. Msn2/4 (Boisnard et al. 2009; Hasan et al. 2002)),or specific mutants that were observed to be sensitive to H202 (such as the phosphodiesterase Pde2 (Hasan et al. 2002)) (see Fig. S2C). Results were displayed by plotting the mean survival and resistance for each mutant analyzed under step and ramp conditions, Fig. 2D and 2E.

We first verified that the *yap1Δ* mutant displayed poor proliferation and survival under these stress conditions, Fig. 2D and 2E, in agreement with previous studies (Delaunay, Isnard, and Toledano 2000). Then, we noticed that mutants could be classified into two different groups (see the shaded area on Fig. 2D and E): the first group (see the yellow shaded area on Fig. 2D and 2E) included mutants with mild (e.g. glr1*Δ)* to severe (e.g. ctt1*Δ*) proliferation and survival defects compared to WT. Importantly, both proliferation and survival increased significantly for this group of mutants when comparing step to ramp assays (see the deviation off the diagonal in Fig. 2D and 2E). This indicates that these mutants, in spite of their variable defects in the presence of acute stress, all displayed some level of adaptation at steady-state, hence were referred to as “adapters”. In this category, proliferation and survival seemed to be affected somewhat proportionally, i.e. none of the corresponding genes had a role specifically associated with either stress tolerance or resistance (with the probable exception of pde2Δ, which displayed a reduced tolerance yet a resistance similar or even superior to WT).

In contrast to the first category, we found a second group of mutants (referred to as “non-adapters”) that spread along the diagonal on both survival and proliferation panels (Fig. 2D and 2E). This indicated that submitting the cells to a ramp (where the acute stress period is removed) did neither improve proliferation nor survival in these mutants, compared to a step, indicating that the corresponding genes were required to reach an adapted steady-state under stress. All these mutants also shared a greatly reduced resistance compared to WT and the group of adapters (Fig. 2E). Interestingly, genes in this non-adapter group were all associated with the biochemical pathway of NADPH-dependent peroxidases: following their reaction with H_2O_2, oxidized Tsa1 and Tsa2 are reduced by the thioredoxins Trx1 and Trx2, which in turn, react with the thioredoxin reductase Trr1. Trr1 is reduced by NADPH which is mainly synthesized upon glucose rerouting into the pentose phosphate pathway (PPP) by the glucose-6-phosphate dehydrogenase (G6PD, or Zwf1). Therefore, these results suggested that this biochemical pathway is the primary effector of H_2O_2 homeostasis.

To further test this hypothesis, we integrated a transcriptional Srx1pr-GFP-degron reporter in each mutant strain tested above (Srx1 encodes a sulfiredoxin, the expression of which is regulated by Yap1), as a proxy for the activation of the Yap1 and H2O2 imbalance. Strains were submitted to a mild 0.1mM H_2O_2 step to ensure the cell's ability to drive a transcriptional response even in low-resistance mutants. Under these conditions, the WT strain displayed a transient burst of GFP fluorescence, followed by a recovery period leading to a steady-state level comparable to the pre-stress level (Fig. 2F). Such decay in fluorescence, which implies deactivation of the Yap1 regulon indicated that the internal H_2O_2 balance was restored. By quantifying the amplitude of the fluorescence drop during the period from burst to steady-state, we

defined an "H_2O_2 adaptation index" to quantitatively assess the ability of each mutant to restore H_2O_2 balance (see sample data obtained with specific mutants on Fig. 2F), and we plotted these measurements against the stress ramp resistance data displayed above (Fig. 2G). This analysis revealed that the restoration of H2O2 balance was strongly impaired in the group of non-adapters defined above, in contrast to adapters, which were less severely affected. Furthermore, the correlation between H_2O_2 balance and resistance was quite good (Fig. 2G, r^2=0.79). Therefore, this analysis further demonstrated the specific role of the peroxiredoxin pathway in promoting both H_2O_2 homeostasis and stress resistance at the steady state.

However, in spite of their belonging to the same group, we noticed that non-adapters mutants displayed very heterogeneous tolerance phenotypes, which could not be explained by differences in H_2O_2 homeostasis (Fig. 2G and Fig. S2D). In addition, two of them (i.e zwf1*Δ*, trr1*Δ)* had an unexpected ~3-5 fold higher survival fraction than that of the WT (Fig. 2D). Such dramatically increased tolerance was consistently observed with an H_2O_2 exposure of up to 128mM (i.e. well above the MIC of the WT, Fig. S2E, and Fig. S2F), i.e. under conditions in which the cells were unlikely to trigger any active response. Therefore, our screen unraveled mutants in which a pronounced H_2O_2 resistance defect, together with a loss of H_2O_2 homeostasis, was associated with a hyper-tolerant phenotype, hence further validating the necessity to disentangle mechanisms of resistance and tolerance during the H_2O_2 stress response.

A dynamic and reversible antagonism between redox imbalance, proliferation, and survival in the *zwf1Δ* mutant

How can mutants display both a severe resistance defect and a much stronger tolerance than WT? By focusing specifically on the *zwf1Δ* mutant, we sought to address this conundrum by characterizing further the interplay between proliferation control, H_2O_2 imbalance, and tolerance in this background.

By measuring the MIC of the *zwf1Δ* mutant using both colony growth assays (Fig. 3A and 3B) and quantification of single-cell division frequency (Fig. 3C), we observed a graded dose-dependent reduction in cell proliferation with increasing H2O2 levels, and cell growth and division were fully arrested above 0.3mM (i.e. $MIC_{zwf1\Delta}$ = 0.3 mM). This growth defect under constant H_2O_2 could not be explained by a potential limitation in the NADPH level (which could be detrimental to anabolic processes), since the *trr1Δ* mutant, in which NADPH levels are not impaired, displayed the same phenotype as *zwf1Δ* (Fig S3A). Concomitantly, we observed a dose-dependent increase in the mean transcriptional activation of Srx1 under H_2O_2 stress (as well as a persistent nuclear relocation of Yap1-GFP, see Fig. S3B), the upregulation of which was much larger than that of the WT (Fig. 3D). Interestingly, both cell proliferation and Srx1pr activation distributions obtained in the presence (0.1mM) or absence of H_2O_2 stress displayed large cell-to-cell variability (Fig 3C and D). Under these conditions, tracking single cells over multiple divisions revealed an erratic division pattern with alternating prolonged cell cycles with high Srx1 expression followed by a recovery period and cell cycle durations close to normal (Fig. 3E). In support of this observation, we observed a negative correlation between the division frequency and Srx1 expression level in the mutant but not in the WT (R^2 (*zwf1Δ*) = 0.73 and R^2(WT) = 0.02, respectively, at 0 mM H2O2, see Fig. 3F). Altogether, these results thus suggested the existence of a dynamic - and reversible - antagonism between cell growth and H_2O_2 balance. It also

raised the hypothesis that cell cycle arrests observed in the *zwf1Δ* mutant could either result from an active growth control regulatory process or, alternatively, from cellular dysfunctions due to a potentially toxic H_2O_2 imbalance.

To test these hypotheses, we turned to fluorescent markers of protein oxidation to investigate whether proteins in the *zwf1Δ* mutant were more oxidized than in WT and if this could compromise cellular function. To this end, first, we monitored the formation of fluorescence foci using the Tsa1-GFP fusion in cells exposed to a continuous 0.5mM H_2O_2 concentration. Indeed, Tsa1 has been shown to induce the formation of supramolecular assemblies when super-oxidized in response to moderate to severe H_2O_2 levels (Jang et al. 2004; Hanzén et al. 2016). In the WT, we observed a progressive formation of protein aggregates in response to stress, followed by a decrease that was presumably due to the adaptation to stress (Fig. 3G and H). Instead, in the *zwf1Δ* mutant, aggregation was much faster and turned out to be irreversible over an 8-hour window. We obtained similar results with the Hsp104-GFP marker (Fig 3I and J), which was used as a generic marker of protein aggregation (Hsp104 is a disaggregase that binds misfolded aggregated proteins), and is known to form localized foci in response to H_2O_2 (Erjavec et al. 2007). This suggested that part of the proteome is irreversibly oxidized in the *zwf1Δ* mutant under stress. However, by releasing the cells into a stress-free medium, we observed a progressive disaggregation of Hsp104-GFP that coincided with (Fig. 3K and L) or even preceded (Fig.S3C) cell cycle re-entry, indicating that the cellular oxidation was reversible and that the restoration of an internal H_2O_2 balance elicited the recovery of cell proliferation. Altogether, these results suggested that, in the *zwf1Δ* mutant, cell

proliferation was tightly associated with the internal H_2O_2 imbalance through a putative regulatory mechanism.

Then, we asked whether the variable levels of H_2O_2 imbalance within *zwf1Δ* cells, which were reported even in the absence of stress (Fig. 3D), would predict the tolerance to acute H_2O_2 stress (1 hour at 64mM). Using either Srx1-GFP or Tsa1-GFP fusions as read-outs of internal H2O2 imbalance (Fig 3M), we plotted the survival fraction as a function of the normalized expression level of each reporter (data were pooled then binned in groups of N=46 events). This experiment revealed that cells with a greater H_2O_2 imbalance displayed enhanced tolerance, in agreement with the hyper-tolerant phenotype of the *zwf1Δ* mutant compared to WT (Fig 3N). Altogether, these single-cell analyses further confirmed the strong antagonism between resistance, H_2O_2 imbalance, and tolerance, and suggested the existence of a regulatory mechanism that couples all three features of the H_2O_2 stress response.

A thioredoxin-dependent PKA inhibition drives stress tolerance in part by protecting the growth machinery under H2O2 stress

The Ras - cyclic AMP (cAMP) - protein kinase A (PKA) pathway is a major proliferation control hub that transduces nutrient signals to regulate the transcriptional activation of ribosomes and protein synthesis (Broach 2012; Conrad et al. 2014; Tamaki 2007). In addition, PKA inhibition controls the stress response in part by inducing the nuclear relocalization of the Msn2/4 transcription factor (Boisnard et al. 2009; Jacquet et al. 2003), which drives the expression of hundreds of genes in response to various stressors (Gasch et al. 2000). In the specific context of oxidative stress, maintaining a

high PKA activity has long been observed to induce H_2O_2 sensitivity (Hasan et al. 2002), and recent studies proposed a mechanism whereby H_2O_2 signaling through either peroxiredoxins or thioredoxins controls PKA activation and hence the downstream general stress response (Bodvard et al. 2017; Roger et al. 2020). Therefore, In the following, we sought to decipher the role of PKA in controlling both H2O2 resistance and tolerance.

We reasoned that, if cell proliferation is arrested in the *zwf1Δ* mutant due to PKA inhibition, alleviating this inhibition may rescue growth under stress conditions. To test this hypothesis, first, we deleted the phosphodiesterase Pde2, which drives the linearization of cAMP and thus inactivates PKA. By quantifying the nuclear shuttling of an Msn2-GFP fusion as a readout of PKA activation, we first checked that Msn2-GFP transiently relocalized to the nucleus in response to a 0.5mM H_2O_2 step in the WT (Fig. 4A), in agreement with the reversible proliferation arrest observed in Fig.1. In the *zwf1Δ* mutant, instead, Msn2-GFP was found to be at least partially nuclear at all times during stress exposure, consistently with prolonged PKA inhibition (Fig. 4A). Strikingly, Msn2-GFP remained almost fully cytoplasmic throughout the experiment in the *zwf1Δ pde2Δ* double mutant (Fig. 4A and S4B), similarly to the single *pde2Δ* mutant (Fig. S4A and S4B), suggesting that deleting Pde2 reactivated PKA in the *zwf1Δ* mutant.
Then, to directly check whether forced PKA activation could rescue cell growth, we compared the growth of these mutants in response to a low H_2O_2 (0.1mM) dose (i.e. lower than the MIC of the *zwf1Δ* mutant). We found that, unlike *zwf1Δ,* the *zwf1Δ pde2Δ* double mutant recovered a proliferation similar to WT (Fig. 4B), thus clearly demonstrating that the H_2O_2-dependent growth arrest in the *zwf1Δ* mutant is controlled by PKA inhibition and may not be interpreted as the consequence of toxicity associated

with H_2O_2 imbalance. Moreover, using an Srx1pr-GFP-deg reporter integrated into the *zwf1Δ pde2Δ* double mutant, we observed a rescue of the H_2O_2 imbalance under these conditions (Fig. 4C), indicating that, unexpectedly, preventing PKA inhibition induced recovery of the H_2O_2 homeostatic function (Fig. S4C). This result also suggested that Zwf1-independent sources of NADPH (Minard et al. 1998) could successfully fuel H_2O_2 detoxification in the *zwf1Δ pde2Δ* background at low-stress doses, and, conversely, that the restoration of H_2O_2 balance in the *zwf1Δ* mutant at low dose was prevented by PKA inhibition.

Next, to further assess the role of PKA inhibition in the H_2O_2 stress response, we asked whether deleting Pde2 in the *zwf1Δ* mutant would also abolish its hyper-tolerant phenotype. Indeed, we found that the *pde2Δ* deletion was epistatic to *zwf1Δ* for survival at 0.5mM H_2O_2 step (Fig. 4D), as well as at much higher stress concentrations (Fig. S4D). Further experiments using ramping stress exacerbated the genetic interactions between *pde2Δ* and *zwf1Δ* (since the *pde2Δ* mutant has no tolerance defect in ramps) and these two genes turned out to be synthetic lethals under stress after the addition of cAMP (which drives PKA activation further) (Fig 4E). Altogether, these results demonstrated that H_2O_2 hyper-tolerance in the *zwf1Δ* mutant requires PKA inhibition.

How is the internal H_2O_2 signal relayed to mediate PKA inhibition in response to stress? Recent studies have proposed that peroxiredoxins in their oxidized form (or, alternatively, thioredoxins) may inactivate PKA through a redox-dependent mechanism (Bodvard et al. 2017; Roger et al. 2020). To test this model in the context of stress tolerance, we investigated whether the deletion of thioredoxins or

peroxiredoxins would be epistatic to the *zwf1Δ* mutant in survival assays. When submitted to step stress, we found that the hyper-tolerant phenotype of both *zwf1Δ* and *trr1Δ* mutants under step stress was abolished in the *trx1/2Δ zwf1Δ* and *trx1/2Δ trr1Δ* mutants, respectively (Fig. 4F), and similar results were obtained with ramps (Fig. 4F). Importantly, the quantification of nuclear Msn2-GFP localization confirmed that PKA was no longer inhibited in the *trx1/2Δ zwf1Δ* mutant under stress (Fig.S4E). Furthermore, knocking out all three peroxiredoxins Tsa1, Tsa2, and Ahp1, but not Tsa1 alone, abolished the hyper-tolerant phenotype of the *zwf1Δ* mutant. Deleting Tsa1 alone also failed to prevent PKA inhibition in the *zwf1Δ* background (Fig.S4F), suggesting that Tsa1 itself would not be the relay mediating PKA inactivation. In this scenario, the loss of hyper-tolerance observed in the *tsa1Δ tsa2Δ ahp1Δ zwf1Δ* mutant could be interpreted as the fact that thioredoxins may no longer be oxidized in the absence of their major substrate (i.e. peroxiredoxin). Therefore, these results suggested that thioredoxins are the main player relaying H_2O_2 signals to PKA and eliciting stress tolerance.

Last, we wondered by which mechanism PKA inhibition would drive cellular protective effects leading to stress tolerance. To this end, we sought to identify genes downstream of PKA whose deletion would abolish the hyper-tolerant phenotype of the *zwf1Δ* mutant (Fig. 4G). We found that an *msn2/4Δ* mutant was epistatic to the *zwf1Δ* mutant for tolerance (Fig. 4H), presumably because of the pleiotropic roles of Msn2/4 in the general stress response (Gasch et al. 2000). Interestingly, tolerance was also abolished in the triple mutant *pat1Δ dhh1Δ zwf1Δ* (Fig. 4H). This suggested that Pat1 and Dhh1, which are involved in the formation of P-bodies and stress granules (Nissan et al. 2010; Decker and Parker 2012), may contribute to protect the translation

machinery in the presence of H2O2 - even though no such epistasis was observed by mutating Gcn2, which controls translation initiation (Garcia-Barrio et al. 2000), see Fig. 4H). To check this hypothesis further, using a Pat1-GFP fusion as a reporter of P-bodies formation, we observed a stronger aggregation of this marker in the *zwf1Δ* mutant compared to WT under stress, consistently with its highly tolerant phenotype (Fig. 4I and S4G). Conversely, any mutation that prevented PKA inhibition decreased the aggregation level of Pat1-GFP back to the WT level or lower (Fig. 4I). This result suggested that P-bodies and stress granules formation contributes to the establishment of tolerance by protecting the growth machinery under H2O2 stress.

Altogether, the analysis of the genetic determinism of the hyper-tolerant phenotype in the *zwf1Δ* mutant thus unraveled the antagonistic roles of PKA in orchestrating the response to H2O2 stress: whereas the growth inhibition mediated by PKA leads to cell survival in part by protecting the translation machinery, it comes at the expense of the H2O2 homeostatic system, which requires cell growth to function (Fig. 4B).

A PKA-dependent fitness trade-off between resistance and tolerance

Since stress tolerance requires stopping proliferation while stress resistance aims to maximize it, cells have to decide which of the two possible strategies is the most appropriate depending on the level of stress. To explore this decision-making process further, we sought to compare the cellular fitness between two strains which were engineered to display a unique defense strategy (i.e. either resistance or tolerance) by controlling PKA activation status. For this, we measured the overall cellular fitness, defined as the total biomass produced during a given interval, in the *zwf1Δ* mutant (i.e.

inhibited PKA) versus the *pde2Δ zwf1Δ* mutant (i.e. activated PKA), during and after an H2O2 exposure to various levels.

Below the $MIC_{zwf1\Delta\ /\ pde2\Delta\ zwf1\Delta}$ (i.e. < 0.3mM, Fig 3B and FigS5A), there was no difference in survival between the two mutants (Fig. 5A and C), yet cell proliferation was greater, so the overall fitness was higher for the *pde2Δ zwf1Δ* strain than in the single mutant due to the rescue of PKA activation (Fig. 5B) and recovery of H_2O_2 homeostatic function (Fig. 4B).

At higher stress concentrations, cell growth was inhibited in both mutants to the same extent, so the fitness *during* stress exposure was identical (Fig. 5B and S5B). Yet, under these conditions, cell survival was dramatically impaired in the *pde2Δ zwf1Δ* background, but not the *zwf1Δ* mutant, due to the activation of PKA (in agreement with results in Fig. 4D). As a result, cellular fitness measured *after* stress exposure turned to the advantage of the *zwf1Δ* mutant for stress concentrations above 0.4mM (Fig 5B). Overall, transposed to the WT context, these results suggest that the abrupt shift from resistance (high PKA activity, functional H2O2 homeostatic system) to tolerance (low PKA activity, halted homeostatic system) at the MIC maximizes cellular fitness, by preventing the massive decrease in survival that would occur if cells tried to maintain proliferation (Fig 5D and S5C).

Discussion

In this study, we have used a single-cell time-lapse methodology to investigate the mechanisms that underlie the adaptation to oxidative stress in budding yeast. Our analysis reveals that the ability of the cells to grow under stress (resistance) is distinct from its ability to survive the stressor (tolerance), and we show that each of these

aspects is determined by different mechanisms. Importantly, this distinction could not be operated without the use of longitudinal analyses, which are essential to determine the fate of individual cells in response to stress. In contrast, H_2O_2 "sensitivity" assays based on plate measurement, even though they can be very quantitative, do not allow one to discriminate between resistance and tolerance, since both control cellular fitness and biomass production. Hence classical analyses could not correctly assess the behaviour of mutants, such as the hyper tolerant *zwf1Δ*, that were previously characterized as sensitive to H_2O_2.

The lack of distinction between tolerance and resistance might in part explain why the detailed role of classical redox players in the adaptation to oxidative stress has remained elusive, despite an extensive characterization of their specific biochemical functions. Here our candidate-gene genetic screen allows us to classify mutants according to their respective functional roles. Importantly, it reveals that specific mutations may impair the H_2O_2 homeostatic core hence decrease cellular resistance yet contribute to enhance the cellular tolerance to H_2O_2. Unraveling such a priori antagonistic role is key to reach an integrative understanding of the H_2O_2 defense mechanisms.

Our study clearly unravels the existence of distinct stress response mechanisms that drive different cellular behaviours: resistance, which marks the ability to grow under stress, appears to be directly linked to the ability to restore an internal H_2O_2 balance; tolerance, which can be defined as the ability to survive under stress, is a distinct property that is based on PKA inhibition. Knowing the intrinsic limitations associated with the H_2O_2 homeostatic system, cellular resistance is maximized under either low H_2O_2 levels or when H_2O_2 levels are progressively increased (i.e. ramping stress). In

contrast, in response to acute H_2O_2 steps larger than 0.6mM, tolerance is the main defense mechanism. The coordination of these two processes is what drives the overall response to H_2O_2.

The role of PKA in response to oxidative stress has long been reported and has been recently refined by providing genetic and biochemical evidence that its inhibition is mediated either by peroxiredoxins or thioredoxins, which relay H_2O_2 signals. The model generally assumed in the literature is that the function of PKA inhibition was mostly to trigger the environmental stress response through the activation of Msn2/4. Here, in addition, we propose that it is required to protect the growth machinery by the formation of P-bodies and stress granules, which would be otherwise exposed to H_2O_2 and hence generate damages that would compromise cell survival.

The diverse functions of peroxiredoxins (as well as related partners involved in this biochemical pathway) have been thoroughly documented. Among them, the role of Tsa1 as an H_2O_2 signaling molecule (in particular for PKA inhibition) has received considerable attention. This contributed to toning down its importance as an H_2O_2 scavenging enzyme. Here, our results emphasize that both functions are equally important: the peroxidase function is essential (in contrast to the catalase Ctt1) for homeostatic system function and hence resistance, whereas Tsa1/Trx signaling to PKA is the key mechanism that drives tolerance.

Tolerance and resistance display some functional overlap at intermediate stress levels, as the transient activation of the Yap1 regulon (which is a mark of the homeostatic system) is concomitant with the inhibition of cell growth, as monitored

using cell cycle arrest and the activation of Msn2-GFP. Yet, these two mechanisms are antagonistic since resistance aims at maximizing cellular fitness by limiting cellular damages and therefore ensuring cell growth, while tolerance is based on the downregulation of cell growth. Therefore, this study provides an interesting example of a stress response strategy that is based on a tradeoff between growth and survival.

Interestingly, while stress response mechanisms are often associated with tolerance in antibiotics research, studies that focus on physiological homeostatic systems rather try to understand the determinants of resistance. Our analysis of the H_2O_2 stress response shows that resistance and tolerance are intertwined elements with overlapping molecular bases, both of which contribute to cellular fitness. Importantly, mutations that impair resistance (e.g. zwf1) do not necessarily affect tolerance and can even enhance it. Conversely, limiting tolerance by preventing PKA inhibition (e.g. pde2) does not necessarily impair cellular resistance (pde2 mutant has no growth defect in H_2O_2 ramps). However, altering both resistance and tolerance leads to a strong fitness defect no matter the temporal stress profile. Many cancer therapies are based on drugs that impair cellular function, thus leading to resistance defects. Yet, tolerance mechanisms can be responsible for relapses after the treatment. Targeting both aspects of stress response could provide an interesting framework to prevent relapse in cancer therapeutic strategies.

Material & Methods

Strains construction

All strains were issued from the S288C background (Sikorski and Hieter, 1989; Huh et al., 2003), derived from BY4741 or BY4742. The list of strains is detailed in Supplementary file 1. Simple mutant strains were all issued from the BY4742 delta collection (invitrogen). The *trx1*Δ *trx2*Δ and the *tsa1*Δ*tsa2*Δ*ahp1*Δ strains were gifts from the Toledano Lab and were also derived from S288c. The strain *msn2*Δ*msn4*Δ *was Dr.* Li Wei and was also derived from S288c*.* The strain *pat1*Δ *dhh1*Δ was a gift from the Roy Parker lab and was derived from S288c. All strains have been checked by PCR with oligos targeting the kanMX4 cassette.

The transcriptional reporter strains carrying the *SRX1pr-sfGFP-deg* were generated by a one-step cloning-free method (Huber et al., 2014) in the corresponding mutant strain issued from the BY4742 delta collection (invitrogen).

The double mutants (*X*Δ *zwf1*Δ*::natMX4*) were obtained by substituting the entire ZWF1 gene by a natMX4 cassette in the corresponding *X*Δ*::kanMX4* strain from the BY4742 delta collection (invitrogen). The mutants *tsa1*Δ*tsa2*Δ*ahp1*Δ*zwf1*Δ*::natMX4, trx1*Δ*trx2*Δ*zwf1*Δ*::natMX4, pat1*Δ*dhh1*Δ*zwf1*Δ*::natMX4,* and *trx1*Δ*trx2*Δ*trr1*Δ*::natMX4* were obtained following the same procedure, substituting the ZWF1 or the TRR1 gene by a natMX4 cassette in the corresponding strain. The triple mutant *msn2*Δ*msn4*Δ*zwf1*Δ was obtained by crossing X-03 (*msn2*Δ*msn4*Δ) with BJ2-28 (*zwf1*Δ).

The protein fusion GFP strains were obtained from the BY4741 Invitrogen collection. The strains HSP104-GFP *zwf1*Δ*::natMX4* was obtained by substituting the

entire ZWF1 gene by a natMX4 cassette in the corresponding protein fusion GFP strain (from invitrogen).

The PAT1-GFP::URA, PAT1-GFP::URA *zwf1*Δ, PAT1-GFP::URA *zwf1*Δ*pde2*Δ, PAT1-GFP::URA *pde2*Δ and PAT1-GFP::URA *trx1*Δ*trx2*Δ strains have been obtained by fusing GFP at the C terminal of the PAT1 gene in the corresponding mutant strains.

List of strains

Name	Mat	Background	Genotype	Origin
SF1.39	α	S288C	his3Δ1; leu2Δ0; lys2Δ0; ura3Δ0	Euroscarf
YG2.16	α	S288C	his3Δ1; leu2Δ0; lys2Δ0; ura3Δ0 ctt1::NatMX	Euroscarf
YG2.13	α	S288C	his3Δ1; leu2Δ0; lys2Δ0; ura3Δ0 ccp1::NatMX	Euroscarf
BJ2.6	α	S288C	his3Δ1; leu2Δ0; lys2Δ0; ura3Δ0 pde2::NatMX	Euroscarf
BJ2.53	α	S288C	his3Δ1; leu2Δ0; lys2Δ0; ura3Δ0 yak1::NatMX	Euroscarf
BJ2.58	α	S288C	his3Δ1; leu2Δ0; lys2Δ0; ura3Δ0 glr1::NatMX	Euroscarf
YG2.36	α	S288C	his3Δ1; leu2Δ0; lys2Δ0; ura3Δ0, tsa1::KanMX	Euroscarf
YG2.4	α	S288C	his3Δ1; leu2Δ3, trx1::URA3, trx2::KAN	Michel Toledano lab
yRP2069	a	S288C	his3Δ1; leu2Δ; ura3Δ, pat1:: KanMX4 dhh1:: KanMX4	Roy Parker Lab
X.26	α	S288C	his3Δ1; leu2Δ0; lys2Δ0; ura3Δ0 yap1::NatMX	Euroscarf
X2.3	α	S288C	leu2Δ0, tsa1::TRP1, tsa2::URA3, ahp1::KanMX	Michel Toledano lab
X.03	a	S288C	trp1Δ1; ura3Δ52, msn2::HIS3, msn4::LEU2	C. Godon
BJ2.28	α	S288C	his3Δ1; leu2Δ0; lys2Δ0; ura3Δ0, zwf1::KanMX	Euroscarf
YAM4-48	α	S288C	his3Δ1; leu2Δ0; lys2Δ0; ura3Δ0, srx1p-sfGFP-deg-NatMX	This study
YAM4-47	α	S288C	his3Δ1; leu2Δ0; lys2Δ0; ura3Δ0, tsa1::KanMX4, srx1p-sfGFP-deg-NatMX	This study

YAM4-46	α	S288C	his3Δ1; leu2Δ0; lys2Δ0; ura3Δ0, yap1::KanMX4, srx1p-sfGFP-deg-NatMX	This study
YAM4-41	α	S288C	trp1Δ1; ura3Δ52, msn2::HIS3, msn4::LEU2, srx1p-sfGFP-deg-NatMX	This study
YAM4-50	α	S288C	his3Δ1; leu2Δ0; lys2Δ0; ura3Δ0, glr1::KanMX4, srx1p-sfGFP-deg-NatMX	This study
YAM4-52	α	S288C	his3Δ1; leu2Δ0; lys2Δ0; ura3Δ0, pde2::KanMX4, srx1p-sfGFP-deg-NatMX	This study
YAM4-57	α	S288C	leu2Δ0, tsa1::TRP1, tsa2::URA3, ahp1::KanMX, srx1p-sfGFP-deg-NatMX	This study
YAM4-58	α	S288C	his3Δ1; leu2Δ0; lys2Δ0; ura3Δ0,srx1::KanMX4, srx1p-sfGFP-deg-NatMX	This study
YAM4-59	α	S288C	his3Δ1; leu2Δ3, trx1::URA3, trx2::KAN, srx1p-sfGFP-deg-NatMX	This study
YAM4-61	α	S288C	his3Δ1; leu2Δ0; lys2Δ0; ura3Δ0, zwf1::KanMX4, srx1p-sfGFP-deg-NatMX	This study
YAM4-63	α	S288C	his3Δ1; leu2Δ0; lys2Δ0; ura3Δ0, yak1::KanMX4, srx1p-sfGFP-deg-NatMX	This study
YAM5-1	α	S288C	his3Δ1; leu2Δ0; lys2Δ0; ura3Δ0, ctt1::KanMX4, srx1p-sfGFP-deg-NatMX	This study
YAM5-60	α	S288C	his3Δ1; leu2Δ0; lys2Δ0, pde2::KanMX4, trr1::NatMX, srx1p-sfGFP-deg-URA3	This study
YAM5-10	α	S288C	his3Δ1; leu2Δ0; lys2Δ0; ura3Δ0, pde2::KanMX4, zwf1::NatMX	This study
YAM5-12	α	S288C	his3Δ1; leu2Δ3, trx1::URA3, trx2::KAN, zwf1::NatMX	This study
YAM5-13	α	S288C	his3Δ1; leu2Δ0; lys2Δ0; ura3Δ0, tsa1::KanMX4, zwf1::NatMX	This study
YAM5-56	α	S288C	his3Δ1; leu2Δ0; lys2Δ0; ura3Δ0, gcn2::KanMX4, zwf1::NatMX	This study
YAM5-58	α	S288C	his3Δ1; leu2Δ0; lys2Δ0; ura3Δ0, pat1:: KanMX , dhh1:: KanMX , zwf1::NatMX	This study
YAM5-38	a	S288C	leu2Δ0; lys2Δ0; ura3Δ0, PAT1-GFP-HIS3, zwf1::NatMX	This study
BJ3.1	a	S288C	leu2Δ0; lys2Δ0; ura3Δ0 zwf1::KnMX Tsa1-GFP-HIS	This study
BJ3.54		S288C	leu2Δ0; lys2Δ0; ura3Δ0 zwf1::KnMX Hsp104-GFP-HIS	This study
X.32	a	S288C	leu2Δ0; lys2Δ0; ura3Δ0 Tsa1-GFP-HIS	This study
HSP104-HGP	a	S288C	his3Δ1; leu2Δ0; met15D0; ura3Δ0; HSP104-GFP::His3MX6	Huh et al., 2003
YAM5-47	α	S288C	his3Δ1; leu2Δ0; lys2Δ0; ura3Δ0, trr1::NatMX	This study
YAM5-44	α	S288C	his3Δ1; leu2Δ0; lys2Δ0, trx1::URA3, trx2::KAN, trr1::NatMX	This study
YAM5-49	α	S288C	his3Δ1; leu2Δ0; lys2Δ0; ura3Δ0, tsa1::KanMX4, trr1::NatMX	This study
YAM5-55	α	S288C	his3Δ1; leu2Δ0; lys2Δ0; ura3Δ0, pde2::KanMX4, trr1::NatMX	This study

YAM5-51	α	S288C	his3Δ1; leu2Δ0; lys2Δ0; ura3Δ0, srx1p-sfGFP-deg-NatMX, trr1::KanMX	This study
GC9.8	a	S288C	leu2Δ0; ura3Δ0; met15Δ0 MSN2-GFP-HIS	invitrogen
BJ4.22	a	S288C	leu2Δ0; ura3Δ0; MSN2-GFP-HIS tsa1::KanMX	This study
BJ4.23	a	S288C	leu2Δ0; MSN2-GFP-HIS trx1::URA3, trx2::KanMX	This study
BJ3.21	a	S288C	leu2Δ0; ura3Δ0; MSN2-GFP-HIS zwf1::KnMX tsa1::KanMX	This study
BJ4.26	a	S288C	leu2Δ0; ura3Δ0; MSN2-GFP-HIS zwf1::KnMX trx1::URA3, trx2::KAN	This study
BJ2.61	a	S288C	leu2Δ0; ura3Δ0; MSN2-GFP-HIS zwf1::NatMX	This study
BJ4.24	a	S288C	leu2Δ0; ura3Δ0; MSN2-GFP-HIS pde2::KnMX	This study
BJ3.19	a	S288C	leu2Δ0; ura3Δ0, MSN2-GFP-HIS zwf1::KnMX pde2:: KnMX	This study
YAM6-1	α	S288C	leu2Δ0; lys2Δ0; ura3Δ0 PAT1-GFP-HIS3	This study
YAM6-9	α	S288C	leu2Δ0; trx1::URA, trx2::KanMX, PAT1-GFP-HIS3	This study
YAM6-3	α	S288C	leu2Δ0; lys2Δ0; ura3Δ0, PAT1-GFP-HIS3, zwf1::NatMX	This study
YAM6-5	α	S288C	leu2Δ0; lys2Δ0; ura3Δ0, PAT1-GFP-HIS3, pde2::NatMX	This study
YAM6-7	α	S288C	leu2Δ0; lys2Δ0; ura3Δ0, PAT1-GFP-HIS3, pde2::KanMX , zwf1::NatMX	This study
YAM6-11	α	S288C	leu2Δ0; trx1::URA, trx2::KanMX, zwf1::NatMX , PAT1-GFP-HIS3	This study

Microscopy

Microfabrication and microfluidics setup

The microfluidic chips design was the same as the one used and described in Goulev et al., eLife, 2017. Microfluidics chips were PDMS replicas of the master mold. The chip was covalently bonded to a 24 × 50 mm coverslip with the use of a Plasma activator (Diener, Germany). The microfluidic chip was connected to a peristaltic pump (Ismatec, Switzerland) within one hour following the plasma activation with Teflon tubing. The rate of the pump was set between 20 and 60 µL/min. Switches of media were done manually. Linear ramps of medium containing H_2O_2 were done as described in Goulev et al., Methods Cell Biol 2018.

Growth medium and H2O2 preparation

For bulk cultures and microfluidics experiments, yeast was grown at 30°C in synthetic complete 2% dextrose supplemented with amino-acids.

The H_2O_2 (Hydrogen peroxide solution 35wt. % in H_2O, 349887–500 ML, Sigma) solutions were prepared as described in Goulev et al., eLife 2017. Briefly, solutions were prepared no more than 1h before the experiment. H_2O_2 was mixed with SCD media at the required concentration and kept on ice prior to the experiment. The H_2O_2 concentration was checked at the end of the experiment and we found no

Time-lapse microscopy

For time-lapse imaging, cells were pre-grown overnight at 30°C. Overnight cultures were then diluted and grown for 4 to 6h to mid-log phase and were injected in the

microfluidics device. Cells were let at least 1-2h before the beginning of the experiment. Images were taken using an inverted Zeiss Axio Observer Z1 or a Zeiss Axiovert. The focus was maintained using a software custom algorithm developed on MatLab. Fluorescence images were taken using a LED light (CoolLed, LumenCor). The objectives used were a 63x N.A. 1.4 objective (with Zeiss Axio Observer Z1) or a 40x N.A. 1.4 objective (Zeiss Axiovert) and an EM-CCD Luca-R camera (Andor). Multi-Position imaging was enabled by an automated stage (up to 80 positions). For all experiments, one image was acquired every 10 or 15 min except for the determination of the SRX1pr-GFP-deg expression. For that, one image was taken every 5 or 10 min.

The temperature was set to 30°C during the whole experiment using both a custom objective heater (controlled with a 5C7-195, Oven Industries) and a holder heater (controlled using a custom Arduino module).

Cell segmentation and cell mapping

Raw images were imported and processed on MatLab using a free access custom software (phyloCell, available on GitHub, Charvin 2017). The software was used to segment and track cells over time. Segmentation and tracking were corrected manually with the phyloCell interface when needed. Data analysis was then done following the detailed procedures developed below.

Data analysis

All the data analyzed in this study came from at least two independent experimental replicates. All the data have been extracted from microfluidics experiments.

Analysis of physiological parameters

Post-stress survival fraction

For post-stress survival quantifications, only the cells present at the beginning of the stress were included. All cells born during the stress or after the stress were excluded. Following this procedure, the post-stress survival fraction was assessed independently of the proliferative capacity of cells under stress. The survival fraction was thus assessed by determining the fraction of cells born before stress exposure able to form a proliferate after the release of stress.

To evaluate their ability to reproliferate after stress, we checked whether each cell was forming two new buds within the 15h following the stress release. Counting two buds enable to not include cells that remain stuck in G2/M during their first post-stress division due to a DNA-damage checkpoint arrest (Goulev et al., 2017).

Each single survival fraction included at least 100 cells (except for trx1/2 delta where some conditions included only between 50 to 100 cells). Importantly, we are conscious that very small fractions of cells may not be captured in our microfluidic assay due to the relatively small number of cells (~10^2 to 10^3). Survival fraction of persister cells as small as 1/10^5 cells have been reported in different contexts.

Normalized proliferation during stress

Proliferation under stress was assessed by measuring the fold cell number during the stress period for each cell present at the beginning of the stress period, based on the segmentation and the mapping of single-cells. Importantly, cells were included only if

they had survived after the stress to avoid the possibility that the proliferative measurement would reflect a survival deficiency rather than a proliferative defect. Following this procedure, the proliferation under stress was assessed independently of the survival fraction. The readout was called ‘Normalized cell proliferation’ since it reflected a ‘fold increase’.

Proliferative capacity

The proliferative capacity represents the normalized proliferation during stress relative to the WT score in the same stress conditions.

Bud to bud frequency quantification

The bud to bud frequency was calculated as the inverse of the time measure between the formation of two successive buds (proxy of cell cycle duration). For the in-stress condition, only the new bud formed after 6h under stress were included to avoid taking into account cells that would still be in the acute phase of stress.

Colony proliferation

Colony proliferation was measured by counting the number of cells over time under stress normalized by the number of cells present at the onset of stress exposure.

MDK99

The minimal duration for killing 99% of the population has been assessed based on 2 to 4 independent microfluidic experiments for each condition tested. The survival

fraction was assessed as described in the section ‘Post-stress survival fraction’. The represented MDK99 corresponds to the mean survival fraction of the different replicates. Each independent replicate included at least 100 cells. Importantly, the significance of the difference between the survival fraction measured and the fixed survival limit of 1% has not been tested statistically due to the low number of replicates (2 for some conditions). The observed MDK99 must therefore be viewed as a qualitative assay. We explain this choice by a large number of experiments that would have been required to screen the whole range of H_2O_2 concentrations and durations with at least 3 replicates. However, we found that the MDK99 measured for the zwf1 delta strain was at least 4 times higher than the one required to kill the WT population from 1 to 64mM. Such differences over several log2 scales strongly suggest the sufficiency of our qualitative assessment.

MIC

The minimal duration to inhibit the growth of the population was routinely assessed by the incapacity of cells to recover an exponential growth within 12 h following stress exposure. We tested in three independent replicates that at 0.3 mM (the smallest dose at which a zwf1 delta population did not grow) that the growth did not recover within 24h following stress exposures under H_2O_2. A 12 h arrest was therefore considered as a ‘definitive’ arrest in the case the stress would be maintained.

Fluorescence analysis

Yap1 and Msn2 nuclear localization quantification

Camera background was first subtracted from the GFP signal. Yap1-sfGFP and Msn2-GFP nuclear localization were then quantified as described in Cai et al., Nature, 2008. Briefly, the nuclear localization score was measured by the difference between the mean intensity of the 5 brightest pixels in the segmented cell and the mean intensity of all other pixels in the same segmented area.

Quantification Hsp104-GFP, Tsa1-GFP, and Pat1-GFP aggregates

The relative aggregation scores of protein-GFP were quantified at the single-cell level (based on the cell segmentation) using the same methodology as for Yap1 and Msn2 nuclear scores. The relative quantification of GFP foci upon stress exposures had been previously assessed following a similar method in S. Saad et al., Nat Cell Biol, 2017. We checked that the dynamics was not depending on the number of pixels accounting for the GFP foci. The averaged signal represents the mean of all cells present in the different field of view (multi-position acquisition).

Quantification of the SRX1pr-GFP-deg signal and H_2O_2 adaptation index quantification

The SRX1pr-GFP-deg signal was assessed at the single-cell level (based on the segmentation). The GFP signal of each cell was obtained by quantifying the mean fluorescence of the pixels included in the segmented cell area.

The redox adaptation index (RAI) was quantified at the single-cell level. For each cell, the mean GFP value after 5h under 0.1 mM H_2O_2 was divided by the mean GFP value after 1h under 0.1 mM H_2O_2. The score was then quantified relative to the WT and

plotted as HAI (delta strain) / HAI (WT). A small H_2O_2 adaptation index represents a weak ability to rescue redox equilibrium.

The dose of H_2O_2 was chosen as low as 0.1 mM so that every strain included could grow under stress, testifying of their adaptation. We checked that the SRX1pr-GFP was not expressed under H2O2 in a yap1 delta strain (data not shown), testifying of the specificity of the transcriptional response toward the Yap1 regulon and H_2O_2 sensing.

References

Balaban, Nathalie Q., Sophie Helaine, Kim Lewis, Martin Ackermann, Bree Aldridge, Dan I. Andersson, Mark P. Brynildsen, et al. 2019. “Definitions and Guidelines for Research on Antibiotic Persistence.” *Nature Reviews. Microbiology* 17 (7): 441–48.

Balaban, Nathalie Q., Jack Merrin, Remy Chait, Lukasz Kowalik, and Stanislas Leibler. 2004. “Bacterial Persistence as a Phenotypic Switch.” *Science* 305 (5690): 1622–25.

Bigger, Joseph. 1944. “TREATMENT OF STAPHYLOCOCCAL INFECTIONS WITH PENICILLIN BY INTERMITTENT STERILISATION.” *The Lancet* 244 (6320): 497–500.

Bodvard, Kristofer, Ken Peeters, Friederike Roger, Natalie Romanov, Aeid Igbaria, Niek Welkenhuysen, Gael Palais, et al. 2017. “Light-Sensing via Hydrogen Peroxide and a Peroxiredoxin.” *Nature Communications* 8 (March): 14791.

Boisnard, Stéphanie, Gilles Lagniel, Cecilia Garmendia-Torres, Mikael Molin, Emmanuelle Boy-Marcotte, Michel Jacquet, Michel B. Toledano, Jean Labarre, and Stéphane Chédin. 2009. “H2O2 Activates the Nuclear Localization of Msn2 and Maf1 through Thioredoxins in Saccharomyces Cerevisiae.” *Eukaryotic Cell* 8 (9): 1429–38.

Brauner, Asher, Ofer Fridman, Orit Gefen, and Nathalie Q. Balaban. 2016. “Distinguishing between Resistance, Tolerance and Persistence to Antibiotic Treatment.” *Nature Reviews. Microbiology* 14 (5): 320–30.

Broach, James R. 2012. “Nutritional Control of Growth and Development in Yeast.” *Genetics* 192 (1): 73–105.

Chae, H. Z., S. J. Chung, and S. G. Rhee. 1994. “Thioredoxin-Dependent Peroxide Reductase from Yeast.” *The Journal of Biological Chemistry* 269 (44): 27670–78.

Conrad, Michaela, Joep Schothorst, Harish Nag Kankipati, Griet Van Zeebroeck, Marta Rubio-Texeira, and Johan M. Thevelein. 2014. “Nutrient Sensing and Signaling in the Yeast Saccharomyces Cerevisiae.” *FEMS Microbiology Reviews* 38 (2): 254–99.

Decker, Carolyn J., and Roy Parker. 2012. “P-Bodies and Stress Granules: Possible Roles in the Control of Translation and mRNA Degradation.” *Cold Spring Harbor Perspectives in Biology* 4 (9): a012286.

Delaunay, A., A. D. Isnard, and M. B. Toledano. 2000. “H2O2 Sensing through Oxidation of the Yap1 Transcription Factor.” *Science’s STKE: Signal Transduction Knowledge Environment* 19 (19): 5157.

Erjavec, Nika, Lisa Larsson, Julie Grantham, and Thomas Nyström. 2007. “Accelerated Aging and Failure to Segregate Damaged Proteins in Sir2 Mutants Can Be Suppressed by Overproducing the Protein Aggregation-Remodeling Factor Hsp104p.” *Genes & Development* 21 (19): 2410–21.

Garcia-Barrio, M., J. Dong, S. Ufano, and A. G. Hinnebusch. 2000. “Association of GCN1-GCN20 Regulatory Complex with the N-Terminus of eIF2alpha Kinase GCN2 Is Required for GCN2 Activation.” *The EMBO Journal* 19 (8): 1887–99.

Gasch, A. P., P. T. Spellman, C. M. Kao, O. Carmel-Harel, M. B. Eisen, G. Storz, D. Botstein, and P. O. Brown. 2000. “Genomic Expression Programs in the Response of Yeast Cells to Environmental Changes.” *Science’s STKE: Signal Transduction Knowledge Environment* 11 (12): 4241.

Godon, C., G. Lagniel, J. Lee, J. M. Buhler, S. Kieffer, M. Perrot, H. Boucherie, M. B. Toledano, and J. Labarre. 1998. “The H2O2 Stimulon in Saccharomyces Cerevisiae.” *The Journal of Biological Chemistry* 273 (35): 22480–89.

Goulev, Youlian, Sandrine Morlot, Audrey Matifas, Bo Huang, Mikael Molin, Michel B. Toledano, and Gilles Charvin. 2017. “Nonlinear Feedback Drives Homeostatic Plasticity in H2O2 Stress Response.” *eLife* 6 (April). https://doi.org/10.7554/eLife.23971.

Gray, Joseph V., Gregory A. Petsko, Gerald C. Johnston, Dagmar Ringe, Richard A. Singer, and Margaret Werner-Washburne. 2004. “‘Sleeping Beauty’: Quiescence in Saccharomyces Cerevisiae.” *Microbiology and Molecular Biology Reviews: MMBR* 68 (2): 187–206.

Guan, Qiaoning, Suraiya Haroon, Diego González Bravo, Jessica L. Will, and Audrey P. Gasch. 2012. “Cellular Memory of Acquired Stress Resistance in Saccharomyces Cerevisiae.” *Genetics* 192 (2): 495–505.

Hall, Andrea, P. A. Karplus, and Leslie B. Poole. 2009. “Typical 2-Cys Peroxiredoxins--Structures, Mechanisms and Functions.” *The FEBS Journal* 276 (9): 2469–77.

Hanzén, Sarah, Katarina Vielfort, Junsheng Yang, Friederike Roger, Veronica Andersson, Sara Zamarbide-Forés, Rebecca Andersson, et al. 2016. “Lifespan Control by Redox-Dependent Recruitment of Chaperones to Misfolded Proteins.” *Cell* 166 (1): 140–51.

Hasan, Rukhsana, Christophe Leroy, Anne-Dominique Isnard, Jean Labarre, Emmanuelle Boy-Marcotte, and Michel B. Toledano. 2002. “The Control of the Yeast H2O2 Response by the Msn2/4 Transcription Factors.” *Molecular Microbiology* 45 (1): 233–41.

Hohmann, Stefan. 2002. “Osmotic Stress Signaling and Osmoadaptation in Yeasts.” *Microbiology and Molecular Biology Reviews: MMBR* 66 (2): 300–372.

Iraqui, Ismail, Guy Kienda, Jérémie Soeur, Gérard Faye, Giuseppe Baldacci, Richard D. Kolodner, and Meng-Er Huang. 2009. “Peroxiredoxin Tsa1 Is the Key Peroxidase Suppressing Genome Instability and Protecting against Cell Death in Saccharomyces Cerevisiae.” *PLoS Genetics* 5 (6): e1000524.

Jacquet, Michel, Georges Renault, Sylvie Lallet, Jan De Mey, and Albert Goldbeter. 2003. “Oscillatory Nucleocytoplasmic Shuttling of the General Stress Response Transcriptional Activators Msn2 and Msn4 in Saccharomyces Cerevisiae.” *The Journal of Cell Biology* 161 (3): 497–505.

Jang, Ho Hee, Kyun Oh Lee, Yong Hun Chi, Bae Gyo Jung, Soo Kwon Park, Jin Ho Park, Jung Ro Lee, et al. 2004. “Two Enzymes in One; Two Yeast Peroxiredoxins

Display Oxidative Stress-Dependent Switching from a Peroxidase to a Molecular Chaperone Function." *Cell* 117 (5): 625–35.
Jiang, Heng, and Ann M. English. 2006. "Phenotypic Analysis of the ccp1Δ and ccp1Δ-ccp1W191F Mutant Strains of Saccharomyces Cerevisiae Indicates That Cytochrome c Peroxidase Functions in Oxidative-Stress Signaling." *Journal of Inorganic Biochemistry* 100 (12): 1996–2008.
Kuehne, Andreas, Hila Emmert, Joern Soehle, Marc Winnefeld, Frank Fischer, Horst Wenck, Stefan Gallinat, et al. 2015. "Acute Activation of Oxidative Pentose Phosphate Pathway as First-Line Response to Oxidative Stress in Human Skin Cells." *Molecular Cell* 59 (3): 359–71.
Kuge, S., and N. Jones. 1994. "YAP1 Dependent Activation of TRX2 Is Essential for the Response of Saccharomyces Cerevisiae to Oxidative Stress by Hydroperoxides." *The EMBO Journal* 13 (3): 655–64.
Lee, J., C. Godon, G. Lagniel, D. Spector, J. Garin, J. Labarre, and M. B. Toledano. 1999. "Yap1 and Skn7 Control Two Specialized Oxidative Stress Response Regulons in Yeast." *The Journal of Biological Chemistry* 274 (23): 16040–46.
Levy, Sasha F., Naomi Ziv, and Mark L. Siegal. 2012. "Bet Hedging in Yeast by Heterogeneous, Age-Correlated Expression of a Stress Protectant." *PLoS Biology* 10 (5): e1001325.
Milias-Argeitis, Andreas, Sean Summers, Jacob Stewart-Ornstein, Ignacio Zuleta, David Pincus, Hana El-Samad, Mustafa Khammash, and John Lygeros. 2011. "In Silico Feedback for in Vivo Regulation of a Gene Expression Circuit." *Nature Biotechnology* 29 (12): 1114–16.
Minard, K. I., G. T. Jennings, T. M. Loftus, D. Xuan, and L. McAlister-Henn. 1998. "Sources of NADPH and Expression of Mammalian NADP+-Specific Isocitrate Dehydrogenases in Saccharomyces Cerevisiae." *The Journal of Biological Chemistry* 273 (47): 31486–93.
Molin, Mikael, Junsheng Yang, Sarah Hanzén, Michel B. Toledano, Jean Labarre, and Thomas Nyström. 2011. "Life Span Extension and H(2)O(2) Resistance Elicited by Caloric Restriction Require the Peroxiredoxin Tsa1 in Saccharomyces Cerevisiae." *Molecular Cell* 43 (5): 823–33.
Muzzey, Dale, Carlos A. Gómez-Uribe, Jerome T. Mettetal, and Alexander van Oudenaarden. 2009. "A Systems-Level Analysis of Perfect Adaptation in Yeast Osmoregulation." *Cell* 138 (1): 160–71.
Nissan, Tracy, Purusharth Rajyaguru, Meipei She, Haiwei Song, and Roy Parker. 2010. "Decapping Activators in Saccharomyces Cerevisiae Act by Multiple Mechanisms." *Molecular Cell* 39 (5): 773–83.
Pedrajas, J. R., A. Miranda-Vizuete, N. Javanmardy, J. A. Gustafsson, and G. Spyrou. 2000. "Mitochondria of Saccharomyces Cerevisiae Contain One-Conserved Cysteine Type Peroxiredoxin with Thioredoxin Peroxidase Activity." *The Journal of Biological Chemistry* 275 (21): 16296–301.
Ralser, Markus, Mirjam M. Wamelink, Axel Kowald, Birgit Gerisch, Gino Heeren, Eduard A. Struys, Edda Klipp, et al. 2007. "Dynamic Rerouting of the Carbohydrate Flux Is Key to Counteracting Oxidative Stress." *Journal of Biology* 6 (4): 10.
Roger, Friederike, Cecilia Picazo, Wolfgang Reiter, Marouane Libiad, Chikako Asami, Sarah Hanzén, Chunxia Gao, et al. 2020. "Peroxiredoxin Promotes Longevity and H2O2-Resistance in Yeast through Redox-Modulation of Protein Kinase A." *eLife* 9 (July). https://doi.org/10.7554/eLife.60346.
Slatkin, Montgomery. 1974. "Hedging One's Evolutionary Bets." *Nature* 250 (5469): 704–5.

Tamaki, Hisanori. 2007. “Glucose-Stimulated cAMP-Protein Kinase A Pathway in Yeast Saccharomyces Cerevisiae.” *Journal of Bioscience and Bioengineering* 104 (4): 245–50.

Toledano, Michel B., Agnès Delaunay, Ludivine Monceau, and Frédérique Tacnet. 2004. “Microbial H2O2 Sensors as Archetypical Redox Signaling Modules.” *Trends in Biochemical Sciences* 29 (7): 351–57.

Toledano, Michel B., Anne-Gaëlle Planson, and Agnès Delaunay-Moisan. 2010. “Reining in H(2)O(2) for Safe Signaling.” *Cell* 140 (4): 454–56.

Veal, Elizabeth A., Alison M. Day, and Brian A. Morgan. 2007. “Hydrogen Peroxide Sensing and Signaling.” *Molecular Cell* 26 (1): 1–14.

Wong, Chi-Ming, Yuan Zhou, Raymond W. M. Ng, Hsiang-Fu Kung Hf, and Dong-Yan Jin. 2002. “Cooperation of Yeast Peroxiredoxins Tsa1p and Tsa2p in the Cellular Defense against Oxidative and Nitrosative Stress.” *The Journal of Biological Chemistry* 277 (7): 5385–94.

Figures

Figure 1

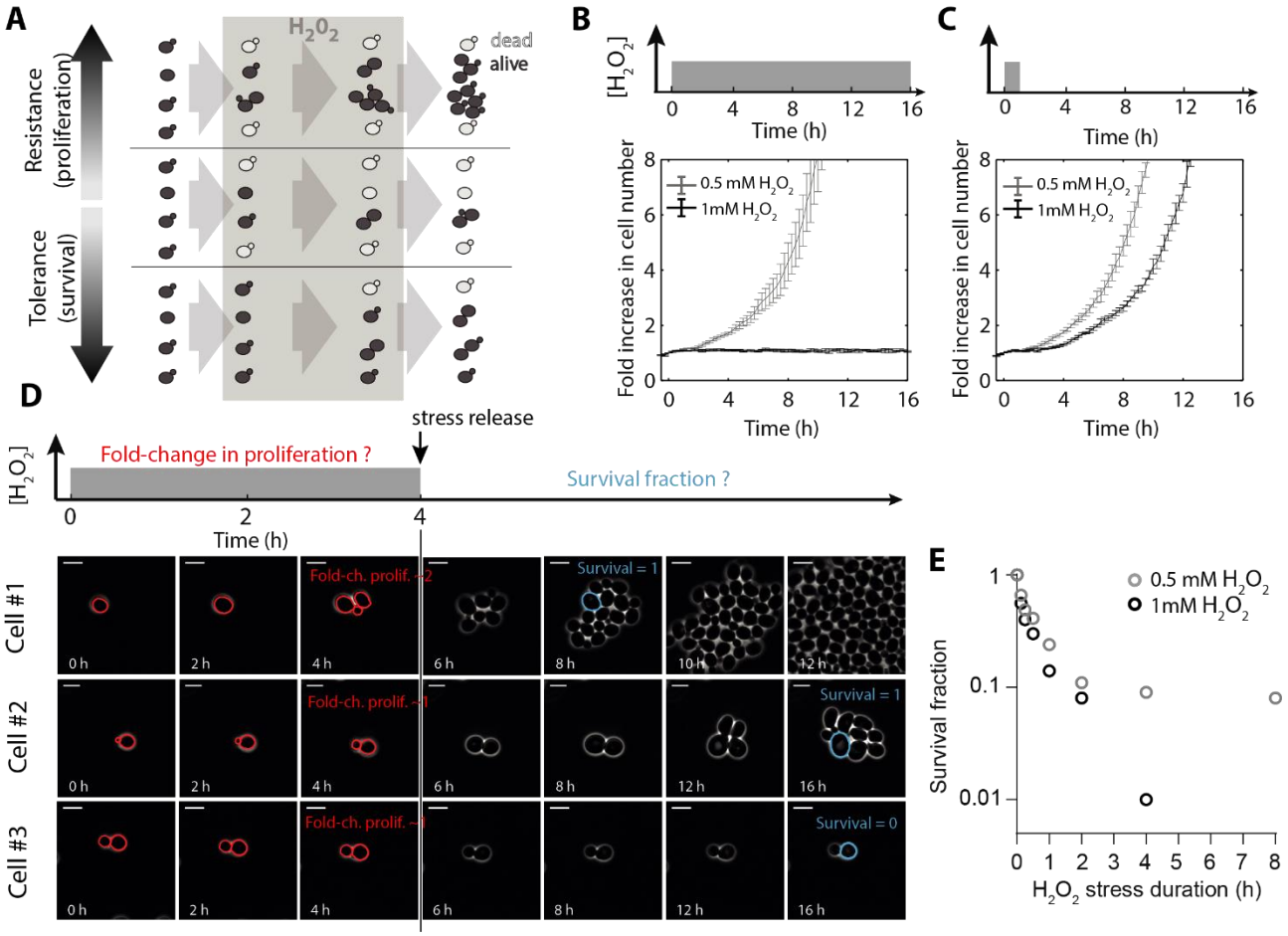

Figure 1: Resistance and tolerance are distinct properties of the response to hydrogen peroxide

(A) Schematic representation of the difference between oxidative stress tolerance (ability of cells to survival to stress without proliferation) and stress resistance (ability of cells to proliferate and adapt under the stressor). **(B)** and **(C)** Fold change in cell number under H_2O_2. In B, stress continues until the end of the experiment. In C, stress is released after 1h. Time is normalized from stress beginning. Stripes indicate the stress pattern and the H_2O_2 concentration. Error bars represent the SEM of N=3 independent technical replicates. **(D)** Time course of single yeast cell's behaviour under H_2O_2 and after stress release (duration of H_2O_2 bolus = 4h). The single-cell approach enables to distinguish Fold change proliferation (in red) from post-stress survival (in blue). The ability of a cell (born before that the stress begins) to form a colony after stress release account for one surviving event. **(E)** Survival fraction of WT cells for different stress duration (from 0 to 8h) and different concentrations (0.5 mM and 1 mM, below and above the MIC(WT), respectively). Log scale.

Figure 2

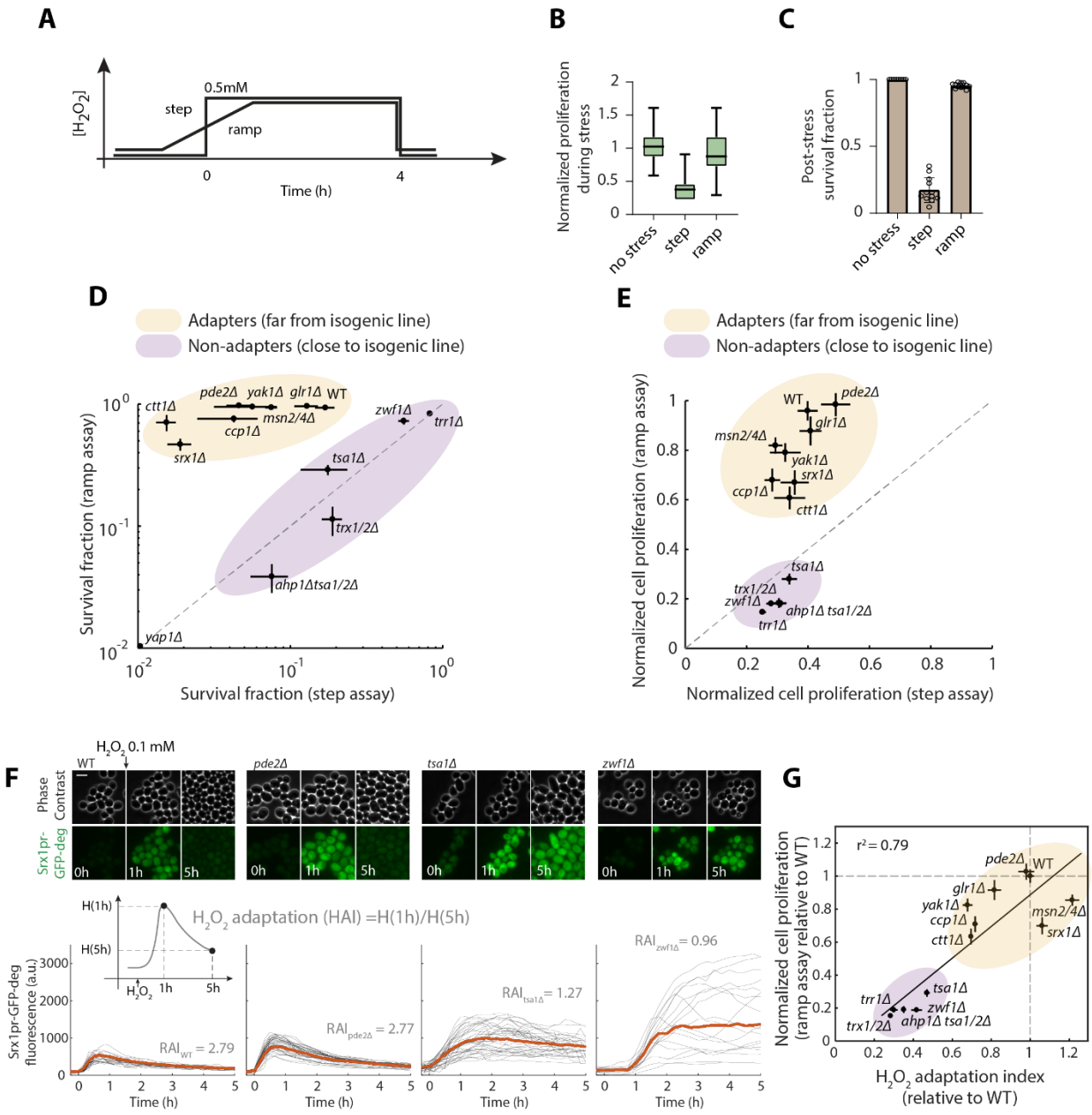
A
[H2O2]
0.5mM
step
ramp
0
4
Time (h)
B
Normalized proliferation during stress
no stress
step
ramp
C
Post-stress survival fraction
no stress
step
ramp
D
Adapters (far from isogenic line)
Non-adapters (close to isogenic line)
Survival fraction (ramp assay)
Survival fraction (step assay)
pde2Δ yak1Δ glr1Δ WT
msn2/4Δ
ccp1Δ
ctt1Δ
srx1Δ
zwf1Δ
trr1Δ
tsa1Δ
trx1/2Δ
ahp1Δtsa1/2Δ
yap1Δ
E
Adapters (far from isogenic line)
Non-adapters (close to isogenic line)
Normalized cell proliferation (ramp assay)
Normalized cell proliferation (step assay)
WT
pde2Δ
glr1Δ
msn2/4Δ
yak1Δ
srx1Δ
ccp1Δ
ctt1Δ
tsa1Δ
trx1/2Δ
zwf1Δ
ahp1Δ tsa1/2Δ
trr1Δ
F
H2O2 0.1 mM
WT
pde2Δ
tsa1Δ
zwf1Δ
Phase Contrast
Srx1pr-GFP-deg
0h
1h
5h
H(1h)
H(5h)
H2O2 adaptation (HAI) =H(1h)/H(5h)
Srx1pr-GFP-deg fluorescence (a.u.)
RAIWT = 2.79
RAIpde2Δ = 2.77
RAItsa1Δ = 1.27
RAIzwf1Δ = 0.96
Time (h)
G
r² = 0.79
Normalized cell proliferation (ramp assay relative to WT)
H2O2 adaptation index (relative to WT)
pde2Δ
WT
glr1Δ
yak1Δ
ccp1Δ
ctt1Δ
msn2/4Δ
srx1Δ
trr1Δ
tsa1Δ
zwf1Δ
trx1/2Δ
ahp1Δ tsa1/2Δ

Figure 2: A genetic screen identifies mutants that combine a severe resistance defect with a hyper-tolerance phenotype

(A) Schematic of the stress-pattern modulation methodology used. Cells were exposed to two transient boluses of 0.5 mM H_2O_2, increasing the stress concentration sharply (step assay) or slowly (ramp assay). **(B)** Quantification of the normalized cell proliferation under stress (see also Methods). N = 12 independent replicates, n>100 for each replicate **(C)** Quantification of the post-stress survival in both step and ramp assays (see also Methods). N = 12 independent replicates, n>100 for each replicate **(D)** Quantification of the post-stress survival in the mutants screened both in the step and the ramp assays. Log scale. **(E)** Quantification of the normalized cell proliferation in mutant strains screened both in the step and the ramp assays. **D** and **E**; the dashed line represents the condition with a similar response in both step and ramp assays, the yellow circle represents adapter strains, exhibiting a response at least 1.5 times better in the ramp assay, the purple circle represents non-adapter strains, not filling the criterion sub-cited. **(F)** Time series of strains carrying PrSRX1-GFP-deg, imaged in phase contrast, and GFP fluorescence. Curves represent the corresponding quantification of the median GFP signals within single cells (black lines) and the median response within the population. The single-cells traces are only representative and do not include all trajectories included in the median value. (n>50 cells for each condition). The H_2O_2 adaptation index (HAI) is calculated as the mean GFP value after 1h under stress divided by the mean GFP value after 5h under stress (H_2O_2 0.1 mM). **(I)** Quantification of the proliferative capacity of cells in the ramp assay as a function of the H_2O_2 adaptation index, both parameters relative to the WT score. The R^2 value represents the square of the correlation between the response values and the predicted response values with a linear fitting. B, C, D, E, G; error bars represent the SEM of independent technical replicates.

Figure 2 Supp.

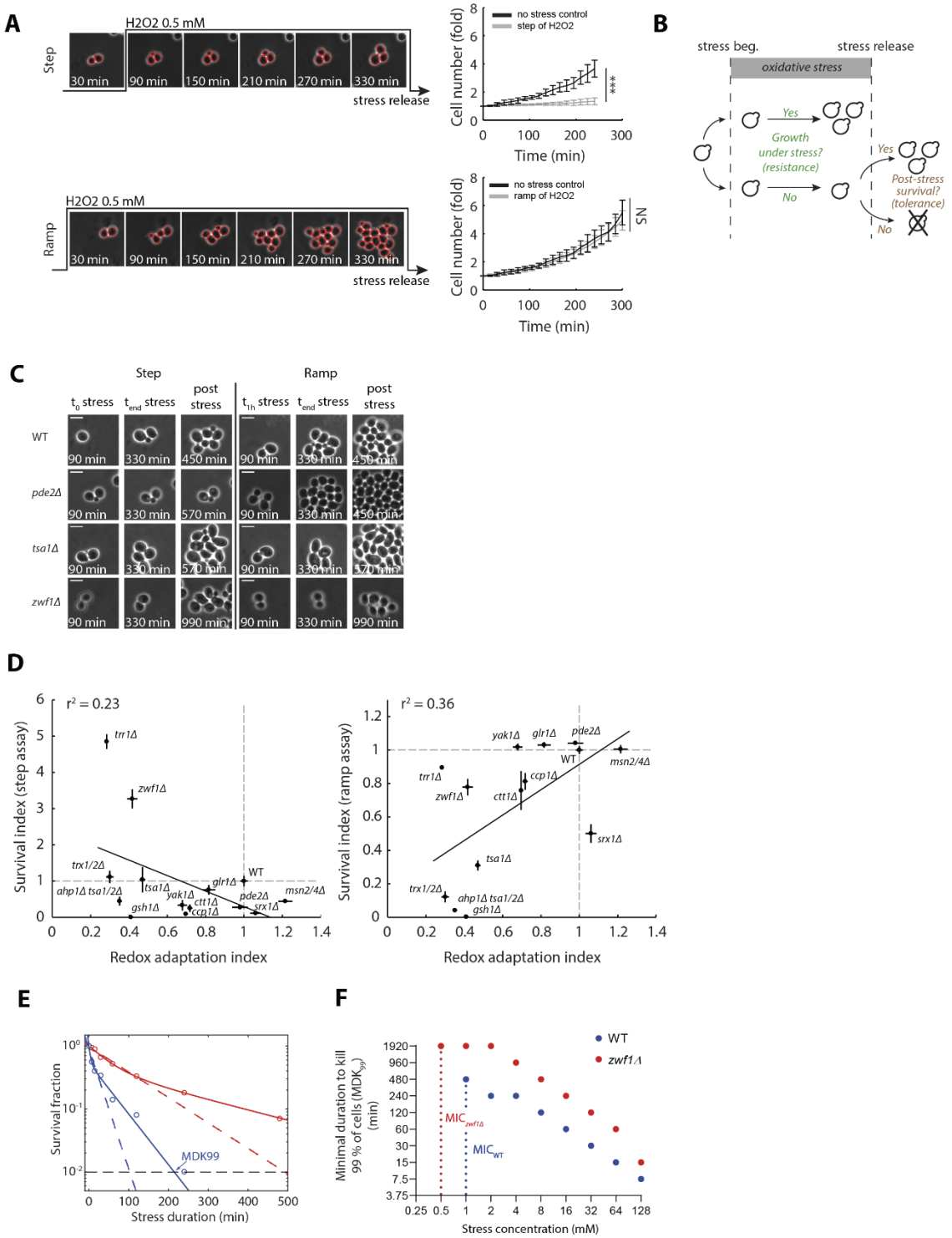

(A) Typical images sequence of a BY4742 Wild Type strain observed by time-lapse microscopy in a microfluidic device (phase contrast). The strain is observed in the step and the ramp assays. Growth is greatly impacted in the step assay compared to the ramp assay. The white bar represents 6.2 µm. Fold cell number under step and ramp assays are quantified on the right panels. Error bar represents the SEM on independent technical replicates. **(B)** Scheme of the experimental protocol to distinguish stress resistance and stress tolerance. Proliferation under stress and post-stress survival were quantified as two independent readouts of oxidative stress resistance and oxidative stress tolerance, respectively (see also Methods). **(C)** Time course under and after H_2O_2 stress exposure in step and ramp assays. **(D)** Quantification of the post-stress survival of cells in response to step and ramp assays as a function of the H_2O_2 adaptation index, both parameters relative to WT score. The r^2 value represents the square of the correlation between the response values and the predicted response values with a linear fitting. **(E)** Survival fraction kinetics of both a WT and a zwf1Δ strain in log scale as a function of the stress duration. MDK99 represents the minimal duration of stress to kill 99% of the population (see Methods). The dashed line is an exponential fit, the continuous line a bi-exponential fit. **(F)** Screen of the MDK99 for WT and zwf1Δ strains in response to different doses of H_2O_2, from 0.25 to 128 mM. At least 2 independent technical replicates were averaged for each time point.

Figure 3

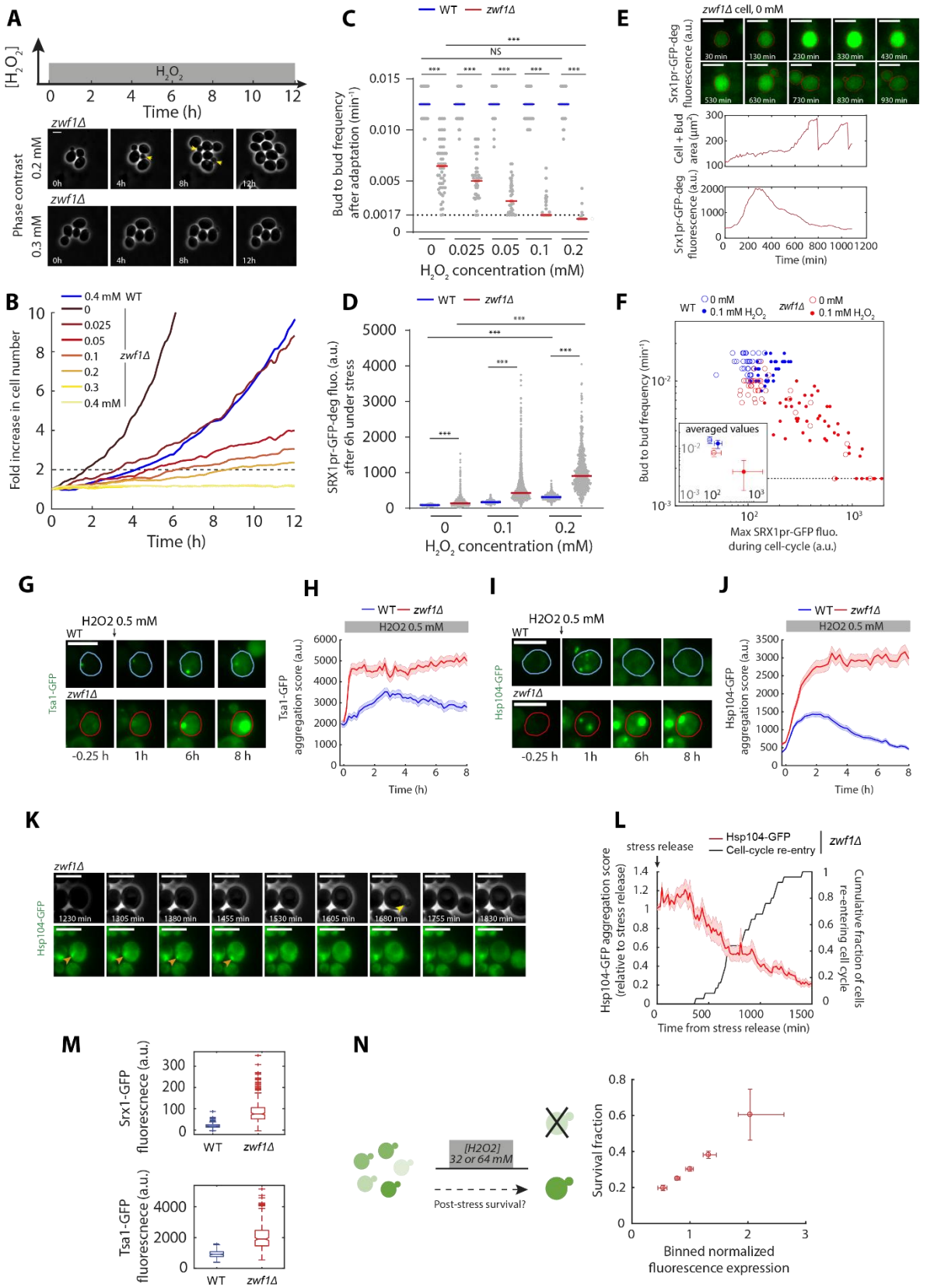
A
B
C
D
E
F
G
H
I
J
K
L
M
N
Time (h)
Fold increase in cell number
Bud to bud frequency after adaptation (min-1)
H2O2 concentration (mM)
SRX1pr-GFP-deg fluo. (a.u.) after 6h under stress
Srx1pr-GFP-deg fluorescence (a.u.)
Cell + Bud area (µm²)
Bud to bud frequency (min-1)
Max SRX1pr-GFP fluo. during cell-cycle (a.u.)
averaged values
H2O2 0.5 mM
Tsa1-GFP
Hsp104-GFP
Tsa1-GFP aggregation score (a.u.)
Hsp104-GFP aggregation score (a.u.)
stress release
Cell-cycle re-entry
Hsp104-GFP aggregation score (relative to stress release)
Cumulative fraction of cells re-entering cell cycle
Time from stress release (min)
Srx1-GFP fluorescnece (a.u.)
Tsa1-GFP fluorescnece (a.u.)
[H2O2] 32 or 64 mM
Post-stress survival?
Survival fraction
Binned normalized fluorescence expression

Figure 3: A dynamic and reversible antagonism between redox imbalance, proliferation, and survival in the *zwf1Δ* mutant

(A) Time series of a zwf1Δ strain in response to 0.2 and 0.3 mM H_2O_2. New buds formed under stress are marked with the yellow arrow. **(B)** Determination of the resistance limit of a zwf1Δ strain. The fold cell number is quantified under various H_2O_2 stress concentrations to assess the MIC (from 0 to 0.4 mM, MIC ~ 0.3 mM). The response of a WT strain at 0.4 mM is also represented. **(C)** Single-cell quantification of the bud to bud frequency (see Methods) under the indicated dose of stress after cells reached equilibrium, in both WT and *zwf1*Δ strains. The quantification has been made only for doses permissive with the growth of a zwf1Δ strain (until 0.2 mM H_2O_2). The lines represent the median value within the population **(D)** Quantification of the median SRX1pr-GFP-deg fluorescence expression inside single yeast cells, 6h after being submitted to the indicated dose of H_2O_2. The lines (blue and red) represent the median value within the corresponding population. The dashed line represents the lowest frequency considered (0.0017 min^{-1}). Cell to cell frequency smaller than 0.0017 min^{-1} (cell-cycle duration of 10h) were arbitrarily set at this limit frequency. (C) and (D), Man-Whitney U test, NS for p>0.05), *** for p<0.0001 **(E)** Time series of a single zwf1Δ mutant cell evolving in a no-stress condition. The area of the cell was quantified over time by including the bud until mitosis. The corresponding averaged fluorescence expression of the SRX1pr-GFP reporter is also represented concomitantly. **(F)** Bud to bud frequency in single cells as a function of the maximal fluorescence expression of the SRX1pr-GFP-deg reporter during the corresponding cell cycle. Log scale. Open circles correspond to cells evolving without H_2O_2 (WT in blue, zwf1Δ in red), filled circles correspond to cells evolving under 0.1 mM H_2O_2 (WT in blue, zwf1Δ in red). For the in-stress condition, cell-cycle events were only included after 6h under stress to ensure cells had reached equilibrium. The inset corresponds to the average values of each condition. Axes are the same as the main graph. **(G) and (I)** Time series of Tsa1-GFP in WT and *zwf1*Δ strains and Hsp104-GFP respectively, under 0.5 mM H_2O_2. Stress duration is indicated with the stripe. The time is normalized to stress the beginning. The white bar represents 6.2 µm. (**H)** and **(J)** The corresponding quantification of the aggregation score of both protein-GFP reporters under stress (see Methods). Mean GFP signal in the population +/- SEM are represented by the bold lines and the small lines respectively **(K)** Time series of a zwf1Δ recovering growth after stress release (after 16h under stress). The Hsp104-GFP aggregates is represented with oranges arrows. The first bud observed after stress release is marked with a yellow arrow. The white bar represents 6.2 µm. **(L)** The corresponding Hsp104 aggregation score after stress release. Only cells that adapted were included in the analysis. The Hsp104 aggregation score was normalized by the value measured at the moment of stress release in every single cell to follow the following aggregation decrease. The bold and small red lines represent respectively the mean value and the SEM of the Hsp104 aggregation score within the post-stress surviving population. The black line represents the cumulative fraction of cells that re-entered in the cell-cycle (see Methods). **(M)** Boxplot representations of the basal (before sterss) Srx1-GFP and Tsa1-GFP signals in WT and *zwf1*Δ strains. **(N)** Signals from (M) are normalized from the median and then pooled as a proxy of redox basal imbalance and is used to predict post stress survival. Single cells are binned in categories in function of their pre-stress GFP expression and survival score is plotted in each binned population.

Figure 3 Supp

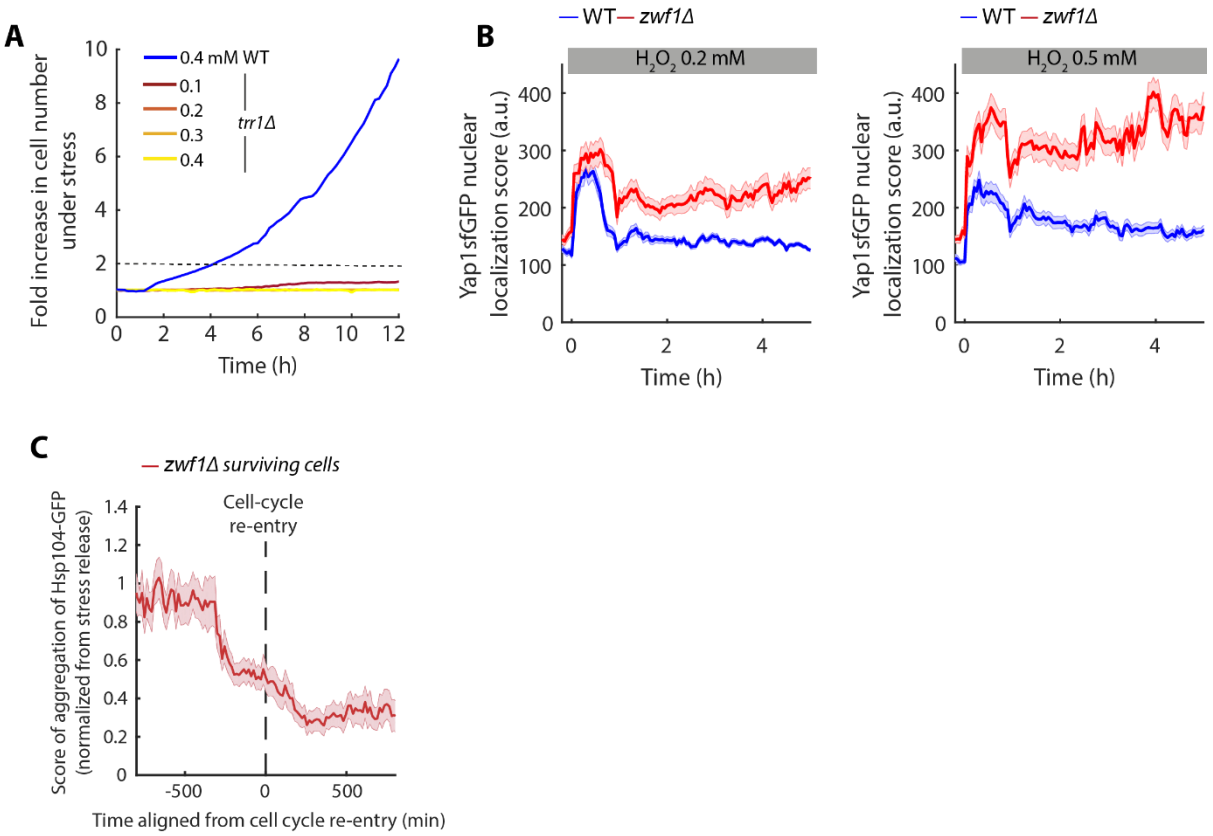

(A) Determination of the resistance limit of a trr1Δ strain. The fold cell number is quantified under various H_2O_2 stress concentrations to assess the MIC (from 0 to 0.4 mM, MIC < 0.1 mM). The response of a WT strain at 0.4 mM is also represented. **(B)** Yap1sf-GFP nuclear localization score (see Methods) in WT and zwf1Δ strains under 0.2 or 0.5 mM H_2O_2. Stripes indicate the stress period. **(C)** Same signal than in **(L)** in Fig.4 but single-cell trajectories are aligned from their respective time of cell cycle re-entry. This enables to observe the disaggregation that is preceding cell-cycle re-entry.

Figure 4

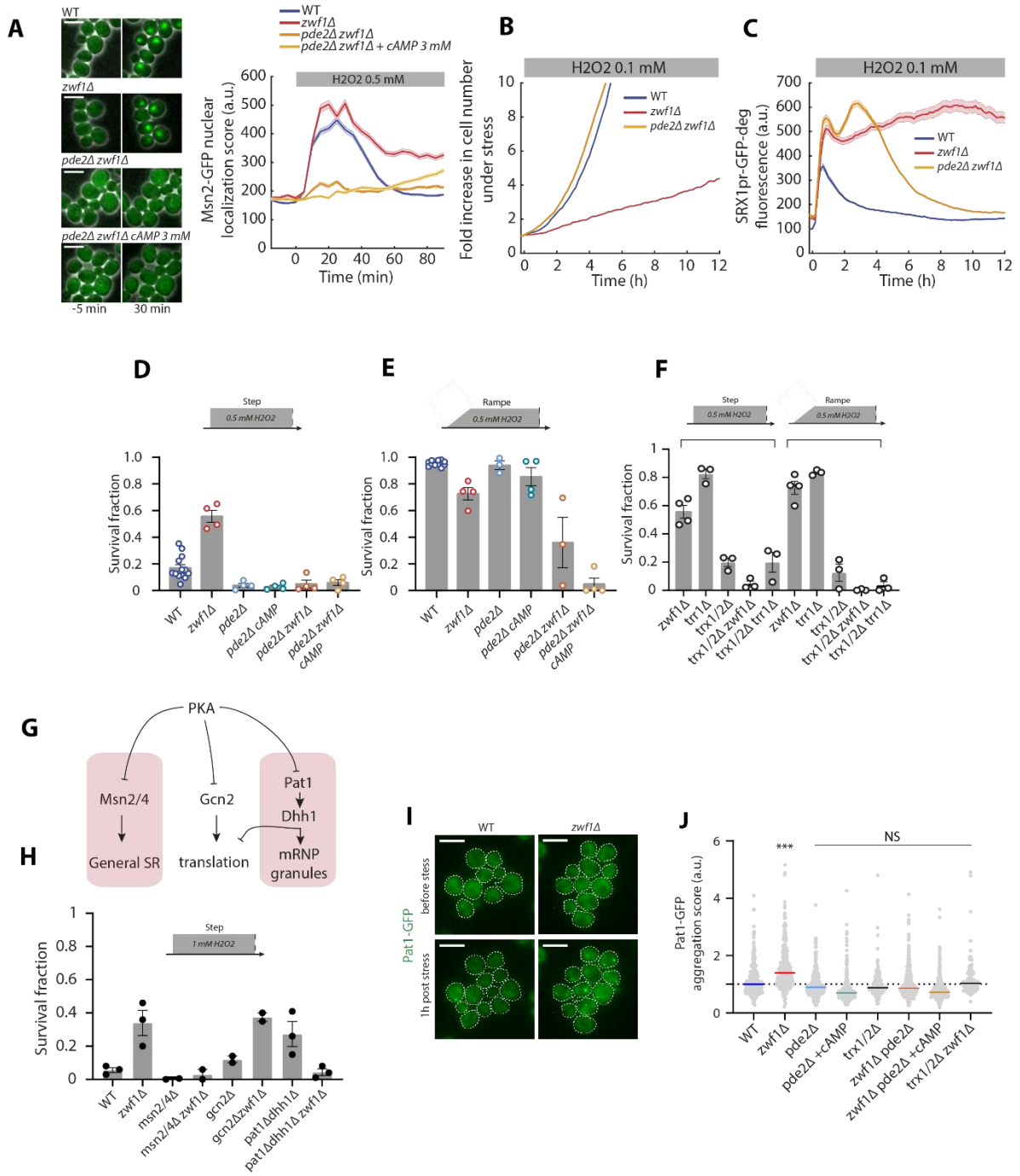
A
WT
zwf1Δ
pde2Δ zwf1Δ
pde2Δ zwf1Δ cAMP 3 mM
-5 min
30 min
WT
zwf1Δ
pde2Δ zwf1Δ
pde2Δ zwf1Δ + cAMP 3 mM
H2O2 0.5 mM
Msn2-GFP nuclear localization score (a.u.)
Time (min)
B
H2O2 0.1 mM
Fold increase in cell number under stress
Time (h)
C
H2O2 0.1 mM
SRX1pr-GFP-deg fluorescence (a.u.)
Time (h)
D
Step
0.5 mM H2O2
Survival fraction
WT
zwf1Δ
pde2Δ
pde2Δ cAMP
pde2Δ zwf1Δ
pde2Δ zwf1Δ cAMP
E
Rampe
0.5 mM H2O2
Survival fraction
F
Step
Rampe
0.5 mM H2O2
Survival fraction
G
PKA
Msn2/4
Gcn2
Pat1
Dhh1
mRNP granules
General SR
translation
H
Step
1 mM H2O2
Survival fraction
I
WT
zwf1Δ
Pat1-GFP
before stress
1h post stress
J
Pat1-GFP aggregation score (a.u.)
***
NS

Figure 4: A thioredoxin-dependent PKA inhibition drives stress tolerance in part by protecting the growth machinery under H2O2 stress

(A) On the left, time series of Msn2-GFP merged with the phase-contrast signal. The white bar represents 6.2µm. Time is normalized from stress beginning. On the right, the corresponding quantification of the nuclear score of Msn2-GFP over time. The stripe indicates the stress pattern. The time is normalized from stress beginning. Mean GFP aggregation score in the population +/- SEM is represented by the bold lines and the small lines respectively**. (B)** Quantification of the colony proliferation under stress in the stress condition indicated by the stripe (0.1 mM H_2O_2). One experimental replicate is represented on the panel **(C)** Quantification of the SRX1pr-GFP-deg mean fluorescence signal within cells. Mean GFP fluorescence in the population +/- SEM is represented by the bold lines and the small lines, respectively. **(D)** and **(E)** Post-stress survival fraction in a step assay (D) and in a ramp assay (E). Open circles represent independent technical replicates, and the bar represents the mean value of the replicates (n>100 for each replicate). Error bar represents the SEM. Stripes represent stress patterns. **(F)** Survival fractions in both step and ramp assays in the indicated mutants. N>3 (at least) independent technical replicates for each condition. Stripes represent stress patterns. **(G)** Scheme of the PKA pathway downstream elements screened for tolerance in both a WT and a *zwf1*Δ contexts. Red squares represent the downstream elements required for the increased oxidative stress tolerance observed in a *zwf1*Δ strain. **(H)** Post stress survival fractions in response to a 2h H_2O_2 stress bolus (1 mM). Filled circles represent technical replicates (N = 2 or 3, n>100 per replicate), error bar represents the SEM of replicates. **(I)** Pat1-GFP before and under 1 mM H_2O_2 stress (1h after stress beginning) in a WT and a zwf1Δ strains. For zwf1Δpde2Δ, zwf1Δpde2Δ + cAMP 3mM and zwf1Δtrx1/2Δ strains, the in-stress condition only is represented. Dash white circle indicates cellular contours. **(J)** Quantification of the Pat1-GFP aggregation score within the corresponding populations, relative to the WT score (see Methods). The line indicates the median within the population. The statistical analysis used a one-side Man Whitney U test to challenge whether each mutant had a greater aggregation or not than the WT strain. Only the zwf1Δ score was significantly greater than the WT score ($p<0.0001$,***). Other p-values were > 0.05 (NS).

Figure 4 Supp

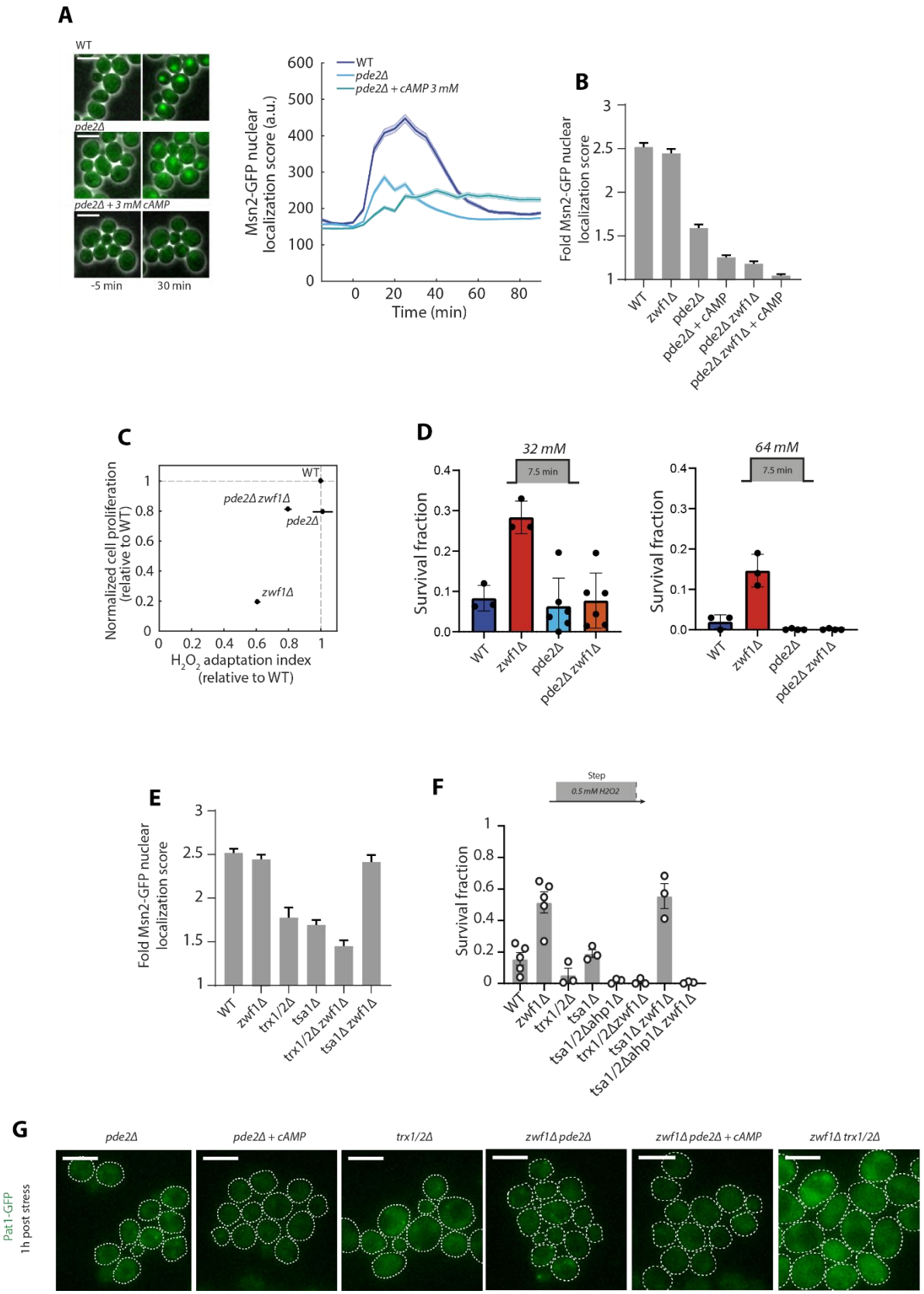

(A) On the left, the time series of Msn2-GFP merged with the phase-contrast signal. The white bar represents 6.2µm. Time is normalized from stress beginning. On the right, the corresponding quantification of the nuclear score of Msn2-GFP over time. The stripe indicates the stress pattern. The time is normalized from stress beginning. Mean GFP aggregation score in the population +/- SEM is represented by the bold lines and the small lines, respectively. **(B) and (E)** The fold enrichment in the Msn2-GFP nuclear score between pre-stress condition and 30min after stress beginning. The bar represents the mean and error bar the SEM within the population (n>50 for each condition) **(C)** Proliferative capacity under stress as a function of the redox adaptation index, both relative to WT strain. Two or three technical replicates were pooled for the WT, zwf1Δ, pde2Δ, and zwf1Δpde2Δ strains, Error bar for the H_2O_2 adaptation index represents the SEM within the population (pooled experiments). **(D)** Post-stress survival quantification. The stress pattern is indicated with the scheme (7.5 min, 32 or 64 mM). Filled circles represent independent technical replicates, the error bars represent the SEM. **(G)** Pat1-GFP under 1 mM H_2O_2 stress (1h after stress beginning) in pde2Δ, pde2Δ + cAMP 3mM and trx1/2Δ strains, the in-stress condition only is represented. Dash white circle indicates cellular contours.

Figure 5

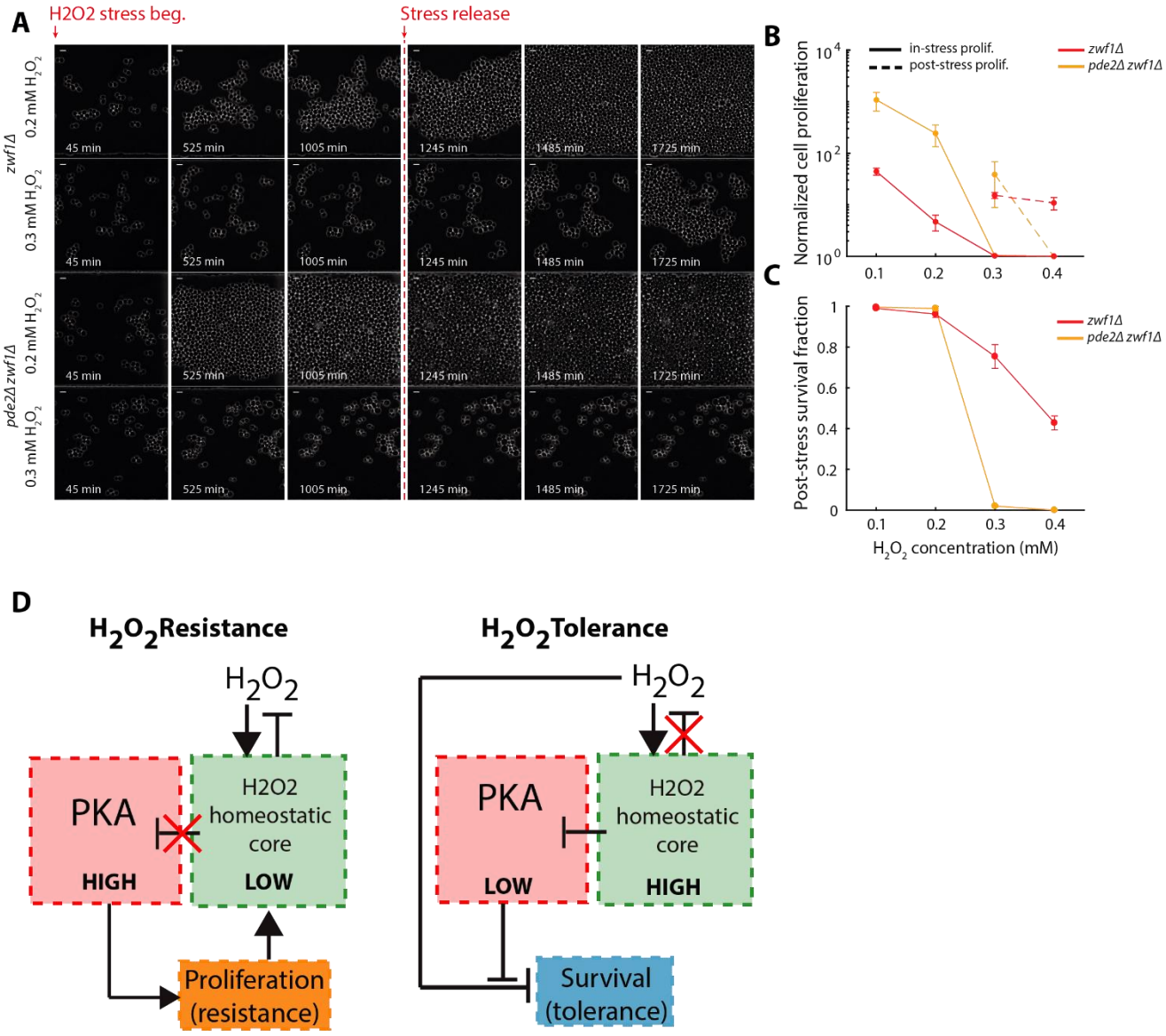

Figure 5: A PKA-dependent fitness trade-off between resistance and tolerance

(A) Time series of *zwf1*Δ and *zwf1Δpde*2Δ (+cAMP 3 mM) mutant strains under and after 0.2 or 0.3 mM H_2O_2. Stress beginning and stress release are indicated by the red arrows and the red dash line. The white bar represents 6.2µm. **(B)** The corresponding normalized cell proliferation integrated over 16h under (full line) and 16h after stress (dash-line) as a function of H_2O_2 concentration (from 0.1 to 0.4 mM) Error bars represent the SEM of 3 independent technical replicates **(C)** Post-stress survival fractions as a function of H_2O_2 concentration. Error bars represent the SEM of 3 independent technical replicates. **(D)** Schematic of the biological model representing the antagonism between oxidative stress tolerance and stress resistance.

Figure 5 Supp

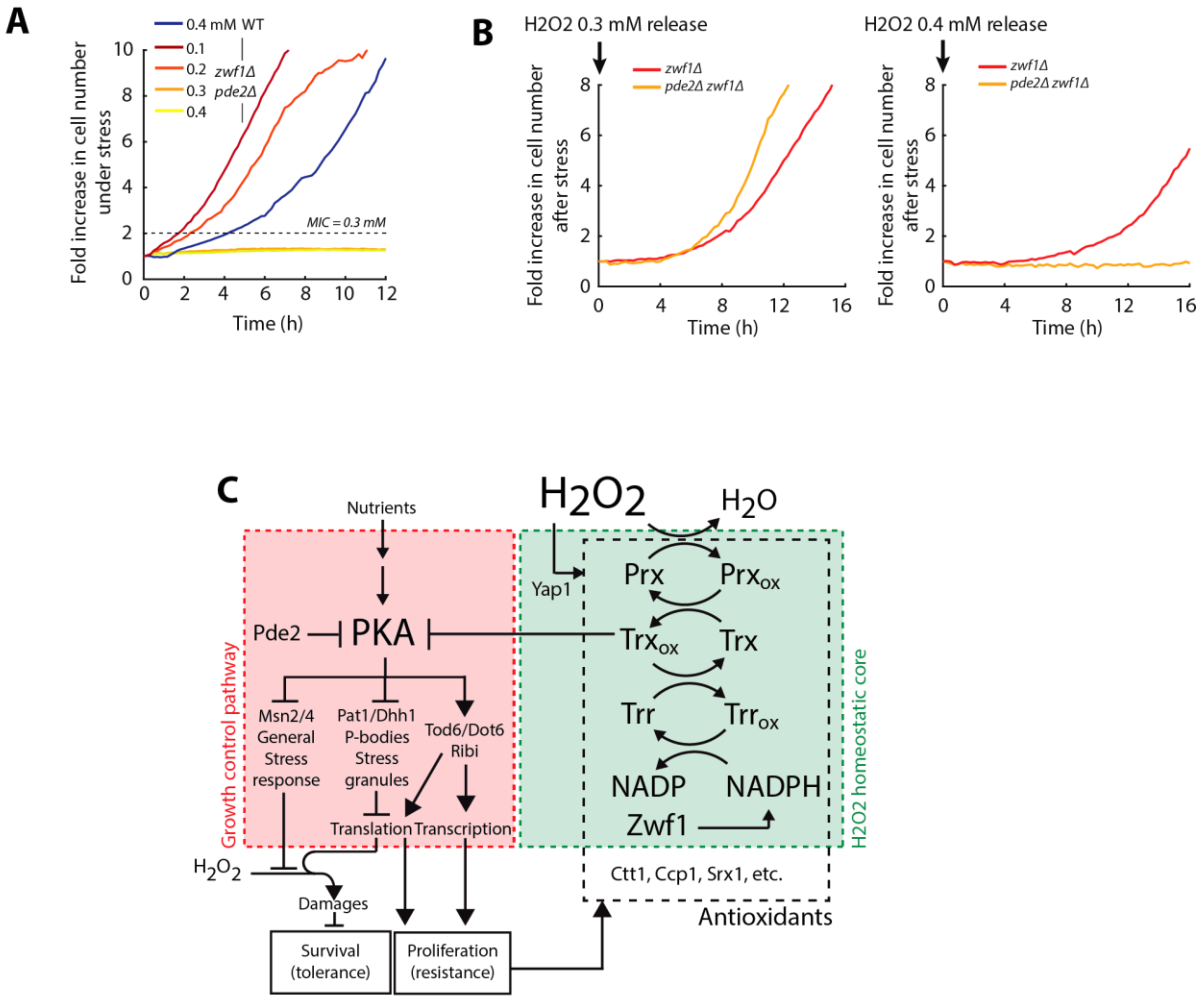

(A) Determination of the resistance limit of a *zwf1*Δ *pde2*Δ strain. The fold cell number is quantified under various H_2O_2 stress concentrations to assess the MIC (from 0 to 0.4 mM, MIC ~ 0.3 mM). The response of a WT strain at 0.4 mM is also represented. **(B)** Fold increase in cell number following stress release (H_2O_2 0.3 mM or 0.4 mM) in the indicated strains. **(C)** Schematic of the signaling network controlling the antagonism between oxidative stress resistance and tolerance.

DISCUSSION

Using a microfluidic-based single-cell methodology, we identified in this work the core stress response modules underpinning oxidative stress resistance and oxidative stress tolerance. Most importantly, we unravelled how both properties depend upon antagonistic cell states coordinated by the state of oxidation of the Prx cycle.

a. Methodological aspects and general dynamics of the oxidative stress response

From a methodological point of view, the use of stress pattern modulations was a decisive element to distinguish the physiological response of cells during the acute phase of stress (that greatly impairs both proliferative capacity and survival) from their ability to reach a steady-state equilibrium under stress and thus to adapt. Indeed, we previously showed that since the ability of yeast cells to adapt was limited by the acute period following brutal stress exposure rather than their intrinsic ability to deal with H_2O_2 scavenging at steady-state (Goulev et al., 2017). Challenging the oxidative stress resistance of cells in response to a sharp step of H_2O_2 may therefore result in misinterpreting an acute tolerance defect (that would preclude cells to reach a steady-state) with an intrinsic inability of cells to adapt (low stress resistance).

Our approach enabled to identify pure non-resistant mutants (deleted for a gene in the Prx cycle) and pure non-tolerant mutants (deleted for one NADPH-independent antioxidant enzyme or unable to inhibit PKA or activate the GSR). This strongly suggests that that oxidative stress resistance only depends upon the H_2O_2 specific

stress response while stress tolerance requires both the H_2O_2 specific and the GSR. Interestingly, another study that uses stress patterns modulation found a similar organization of the stress response to different environmental stressors in *E. coli* (Young et al., 2013): the specific stress response was required in response to ramp at equilibrium under stressors while the GSR was only activated during an important homeostatic imbalance. Such similarities among different microorganisms may suggest a general scheme in the organization of the stress response of microorganisms.

b. The Prx cycle sustains stress resistance and redox homeostasis

Now going deeper into the biological findings of this study, we revealed how the Prx cycle and the synthesis of NADPH were both critically required for oxidative stress resistance while largely dispensable for oxidative stress tolerance. We showed that the inhibition of the Prx cycle, from the most upstream inhibition (*zwf1*Δ) to the most downstream one (*tsa1*Δ) inhibited stress resistance and the ability of cells to reach a steady state under stress, independently of the acute stress period. Those results confirmed observations made by our lab in Goulev et al., 2017, that already identified Prxs and thioredoxins as critical determinant of H_2O_2 stress adaptation. However, the critical role of both upstream genes *ZWF1* and *TRR1* reported in this study strongly pointed toward the requirement of NADPH-reductive power for stress resistance. In agreement, we further showed with our internal redox sensor (SRX1pr-GFP-degron) that the capacity to scavenge H_2O_2 was largely dependent upon the Prx Cycle, thus linking H_2O_2 scavenging to stress resistance.

On a physiological point of view, the fact that the Prx cycle is involved in growth under stress (stress resistance) agrees with the data published in Fomenko et al., 2011. They showed that the deletion of all thiol peroxidases in yeast cells drastically affected the ability of cells to grow under stress while only slightly impairing survival under high doses of H_2O_2 (also see c. for the discussion about tolerance). This is also in line with previous results showing a growth defect in a *tsa1*Δ mutant under H_2O_2 (Lee et al., 1999b).

Recently, it had been suggested in Roger et al., 2020, that the peroxidase function was not participating in the sensitivity phenotype observed in a *tsa1*Δ mutant. Authors had observed that a *tsa1*Δ mutant was scavenging H_2O_2 in a WT manner (Ch1.2.). The discrepancy between this observation and our data showing that the inability of the *tsa1*Δ strain to recover redox homeostasis under a small dose of H_2O_2 (0.1 mM) is hard to explain. However, we argue that in our study, we screened most of antioxidants known in the yeast in similar and standardized conditions. Doing so, we only found the Prx cycle to affect H_2O_2 scavenging. We can therefore conclude that in our context, Prx are the main enzymes involved in the scavenging of H_2O_2.

Altogether, our results thus demonstrate that the oxidative stress adaptation (resistance capacity) is critically depending upon the peroxidase activity of Prxs. Overall, our study agrees well with a model where stress resistance capacity and thus H_2O_2 stress adaptation are intimately linked to the recovery of redox homeostasis under stress, achieved by the peroxidase activity of Prx and their recycling by the Prx cycle.

c. PKA and NADPH-independent antioxidants drive oxidative stress tolerance

In striking contrast to what is described above, we found that stress tolerance was largely independent of the redox homeostasis maintenance and the Prx cycle. It was mostly the PKA-dependent general stress response as well as NADPH-independent antioxidants that governed oxidative stress tolerance.

Surprisingly, if Ctt1 and Ccp1 were found to be required for stress tolerance, in particular during the acute phase of stress, no scavenging defects were associated to their deletion. We hypothesize that the relatively slow response dynamics of our transcriptional-based redox sensor (SRX1pr-GFP-degron) may have missed an increased H_2O_2 imbalance during the first seconds/minutes of stress exposure in those mutants. The preponderant role of Ctt1 during the acute phase of stress tolerance is in consistent with its efficient scavenging function under high H_2O_2 fluxes (Fourquet et al., 2008; Martins and English, 2014). Nevertheless, further studies are required to demonstrate whether a scavenging defect is associated to the sensitivity of a *ctt1*Δ mutant during the acute period of stress.

Importantly, our observations pinpoint **the essential role of NADPH-independent antioxidant for stress tolerance, whereas stress resistance depends upon the NADPH-dependent Prx cycle.** The dependency upon NADPH production therefore seems to dictate the physiological role of antioxidants. We can therefore hypothesize that Ctt1 and Ccp1 may have a predominant role within seconds following stress exposure when the PPP-rerouting furnishing NADPH is still not activated. Alternatively, the Yap1-dependent transcriptional expression of Prxs may set the time

at which a switch will operate between a catalase-based scavenging and a Prx-based scavenging.

The requirement of the inhibition of PKA and the activation of the Msn2/4 regulon for oxidative stress tolerance agrees well with previous data showing the extreme sensitivity of mutants with a high PKA activity as well as the sensitivity of the *msn2/4*Δ mutant upon H_2O_2 stress exposure (Hasan et al., 2002). In our study, no scavenging functions were associated to the GSR, thus rendering unlikely the hypothesis in which the Msn2/4 regulon participates in H_2O_2 stress response by activating a Ctt1-dependent H_2O_2 scavenging (Guan et al., 2012; Morano et al., 2012). However, as for the *ctt1*Δ, we may have missed an acute scavenging defect explaining the msn2/4Δ phenotype.

More surprisingly, the high survival of the *zwf1*Δ and *trr1*Δ mutants under H_2O_2 gretly challenges the homeostatic framework vision (in which the physiological cell fate under stress is thought to be dependent upon the maintenance of redox homeostasis). Indeed, those mutants had been largely reported as sensitive to H_2O_2 (Campbell et al., 2016; Grüning et al., 2011; Jamieson, 1998; Slekar et al., 1996; Toledano et al., 2013) based on their incapacity to grow under H_2O_2. This was explained by the PPP-dependent (thus ZWF1 dependent) production of NADPH that is thought to play a critical role during the acute period of stress (Dick and Ralser, 2015; Ralser et al., 2007). It was therefore highly surprising to observe that the *zwf1*Δ mutant was less sensitive during the acute stress period that a WT strain. If the role of Zwf1 in NADPH synthesis is likely to be critical for H_2O_2 adaptation (explaining the low resistance of a *zwf1*Δ mutant), our study revealed that the low resistance of this mutant was largely

compensated by its large stress tolerance, a mechanism found to be independent of redox scavenging.

For a large set of H_2O_2 concentrations, the high tolerance of the mutant was able to compensate for its low resistance, **thus reveals a non-intuitive and previously unknown phenotype of growth arrest coupled with a high survival capacity under H_2O_2.**

Importantly, we observed that ***zwf1*Δ yeast cells could reversibly switch into a state of very slow growth, high redox imbalance, and increased survival to H_2O_2.** From a phenomenological point of view, this phenotype thus strongly echoes with persister bacterial cells (Balaban et al., 2004) that can tolerate high doses of antibiotics for several hours in a vegetative state.

The **reactivation of the PKA pathway in a *zwf1*Δ mutant led to a rescue of proliferation under small doses of stress but a massive loss of tolerance under high doses of stress**. This therefore strongly suggests **an intrinsic antagonism between the state of growth/proliferation and the state of oxidative stress tolerance.** Similarly, the transition toward a state of persistence in bacteria has been largely linked to a reduced growth activity (Amato et al., 2013; Fisher et al., 2017; Radzikowski et al., 2016) and the activation of GSR pathways (Harms et al., 2016; Radzikowski et al., 2016).

Those similarities suggest the existence of **universal stress tolerance mechanisms** among different stressors and microorganisms.

In our context, we observed that at least two downstream mechanisms of PKA, the Msn2 regulon activation and the formation of P-bodies, were required to tolerate H_2O_2

in a zwf1Δ non-resistant mutant. Those two pathways are intimately linked to growth arrest and inhibition of growth related processes (Ashe et al., 2000; Buchan et al., 2008; Coller and Parker, 2005; Smith et al., 1998). We therefore propose that stress tolerance might be associated with the protection of the growth machinery upon stress exposure. It is likely that stress tolerance may require the protection of several structures rather than a specific one. Indeed, any impairment in the growth machinery can lead to dramatic consequences for cells since oxidation can potentially attacks a large variety of structures. It has been reported that oxidative stress could damage ribosomal proteins as well as rRNA within ribosomes (Gonskikh and Polacek, 2017; Rand and Grant, 2006a; Shcherbik and Pestov, 2019). The numerous potential targets of H_2O_2 may explain why two different pathways downstream of PKA are required to tolerate a redox imbalance. **It is indeed likely that multiple other protective layers (downstream of PKA?) are associated with stress tolerance.**

Overall, those observations therefore **demonstrate the antagonism between the active proliferation of cells under oxidative stress and their capacity to tolerate redox imbalance.** Indeed, following our model, the rescue of growth while the redox homeostasis is impaired may lead to dramatic consequences for cells. This explains the extreme stress sensitivity of the double mutant *zwf1*Δ *pde2*Δ, in which the redox homeostasis is lost while the growth processes downstream of PKA are reactivated.

d. The antithetic functions of the Prx cycle encodes at the molecular level the antagonism between stress resistance and stress tolerance

Our study thus highlights the crucial need in coordinating both growth recovery and redox homeostasis under stress.

In the light of our data, we want to propose a biological model (inspired from the floodgate model from Woods et al., 2003) that aims at **linking the dual function of the Prx cycle** (H_2O_2 scavenging and redox signalling) **to the decision-making process underpinning the antagonism between stress resistance and stress tolerance**.

In Woods et al., 2003 (see Ch1.3. Redox signalling and the scheme below), authors proposed upon low doses of H_2O_2, Prx may works as H_2O_2 scavenger while at higher doses, their rapid oxidation may lead to 'open a floodgate' to favour H_2O_2-mediated redox signalling, highlighting the dual function of Prx depending of the internal H_2O_2 concentration.

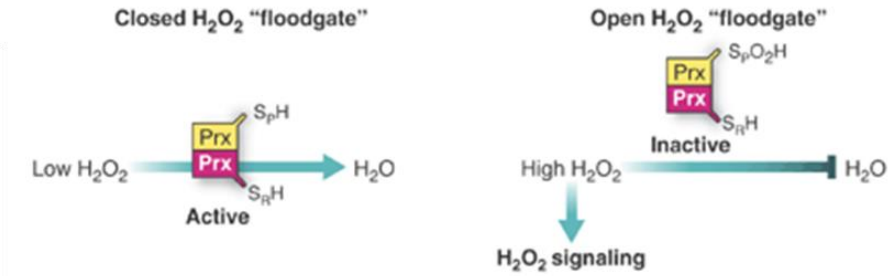

Figure (replicated from 13b): The classical 'Floodgate model' *from Wood et al., 2003.*

Here, we propose that this H_2O_2 floodgate represents the decision-making system determining whether cells 'resist' oxidative stress or rather 'tolerate' it, depending on whether the floodgate is closed or open.

(1) Floodgate closed: the cell resist

In the ‘close floodgate’ situation, the reduction of H_2O_2 by the Prx cycle enables to maintain the redox balance of cells. As we have shown, this is largely achieved by the peroxidase activity of Prx (and the reduction of Prx by the Prx cycle). In this situation, the redox signalling is “off” and the PKA pathway activated: cells have reached a steady state under H_2O_2. **Cells resist to oxidative stress.**

(2) Floodgate open: the cell tolerates

In the ‘open floodgate’ situation, Prx and Trx are oxidized. The redox signalling is ‘on’ and triggers the inhibition of PKA and the activation of the general stress response. Growth is inhibited and the growth machinery protected. **Cells tolerate oxidative stress.**

Interestingly, this model explains **how the antagonism between the state of resistance and the state of resistance is encoded at the molecular level by the two antithetic functions of the Prx cycle**. Stress resistance requires redox homeostasis, and thus an efficient H_2O_2 scavenging by the Prx. The floodgate is ‘closed’. If the floodgate is ‘open’, it necessarily means that the Prx cycle is overloaded and thus that the conditions to resist are not met. Additionally, it means that the redox signalling inhibits PKA and the cell tolerate. **Both tolerance and resistance are thus antagonized by the inability of the Prx cycle to accomplish both scavenging and redox-signalling functions at the same time.**

The ‘open floodgate’ situation explains the transient growth arrest observed during the acute stress period (Goulev et al., 2017) before steady-state adaptation as well as the

high tolerance of non-resistant mutants as *zwf1*Δ and *trr1*Δ that compensate by downregulating the PKA pathway and the growth-related mechanisms.

Interestingly, this bimodal model can explain the discrepancy with others study that found the H2O2 sensitivity of a *tsa1*Δ mutant was associated with its signalling function (Roger et al., 2020). We envisioned that depending on the experimental conditions used, authors may have been in a situation where the floodgate is 'open', and thus the signalling functions largely explain the phenotype observed. Unfortunately, the conditions used in this paper are too different from ours to determine whether stress tolerance or stress resistance dominate in their context.

A last point we want to address here is the distinct roles of the three Prxs as well as Trxs for both H_2O_2 scavenging and redox signalling functions.

In our work, we observed that stress resistance was barely the same in both a *tsa1*Δ mutant and a tsa1/2Δahp1Δ triple mutant. This tends to suggest that the peroxidase activity that sustains stress resistance is largely depending upon the main Prx Tsa1. This largely agrees with the literature, since Ahp1 is thought to be mostly required against lipid peroxides (Lee et al., 1999b). **Tsa1 is therefore the key determinant of stress resistance in the 'closed floodgate situation'.**

However, we observed that the tolerance of the triple mutant *tsa*1/2Δ*ahp1*Δ was very weak while the one of a *tsa1*Δ mutant was close to the WT one. This suggests that Tsa2 and Ahp1 can compensate for the Tsa1 for signalling function and that all Prx participate in redox signalling. This agrees well with the data in Fomenko et al., 2011 where authors showed the additive function (and thus the overlapping) of thiol peroxidases in mediating redox signalling.

However, the low tolerance of the triple deleted mutant could be alternatively explained by the role of oxidized thioredoxins in mediating the redox signal (instead or in addition of Prx). Indeed, in a *tsa1/2*Δ*ahp1*Δ, thioredoxins lose their principal subtracts (Prx) and cannot be oxidized.

The loss of tolerance of the *zwf1*Δ mutant when deleting all thioredoxins or all Prx strongly argue in favour of the second situations: if thioredoxins are not oxidized (deletion or no substrate), the redox signalling and the stress tolerance is lost. This agrees well with Boisnard et al., 22009 where authors found that thioredoxins were required to activate Msn2 under oxidative stress.

Oxidized thioredoxins are thus the pivotal signalling player of stress tolerance In the 'closed floodgate' situation.

Overall, the proposed model therefore gives a physiological perspective to the initial floodgate model proposed in Wood et al., 2003, linking stress resistance and tolerance to the ambivalent functions of the Prx cycle (Tsa1 scavenging vs oxidized thioredoxin-mediated redox signalling). We envision that such coordination between stress tolerance and resistance represents a general scheme of the orchestration of stress response pathways in microorganisms.

e. Relevance of our work in a cancer therapeutic context

Targeting the mechanisms that coordinate the homeostatic system of cells with their physiological fate thus appears as a promising strategy in pathological contexts to potentialize the effects of therapeutic drugs. Indeed, as we have shown in this paper, by identifying the core modules of genes underpinning stress resistance and tolerance,

we could build a strain close to synthetic lethality (*zwf1*Δ*pde2*Δ) in conditions where any of the single deleted mutant exhibited a survival defect. Unravel the system-level architecture of the stress response can therefore identify non-intuitive Achillean heels in the system.

In particular, redox biology is at the heart of tumorigenesis and cancer biology (Reczek and Chandel, 2017; Schieber and Chandel, 2014). ROS signalling can promote pro tumorigenic signals that induce cancer cell proliferation and survival. However, ROS can also have anti tumorigenic properties and induce an oxidative stress-mediated cell death (Panieri and Santoro, 2016; Reczek and Chandel, 2017) (Fig 27). As a consequence of those antagonistic effects of ROS, many antioxidants therapies led to failure of clinical trials.

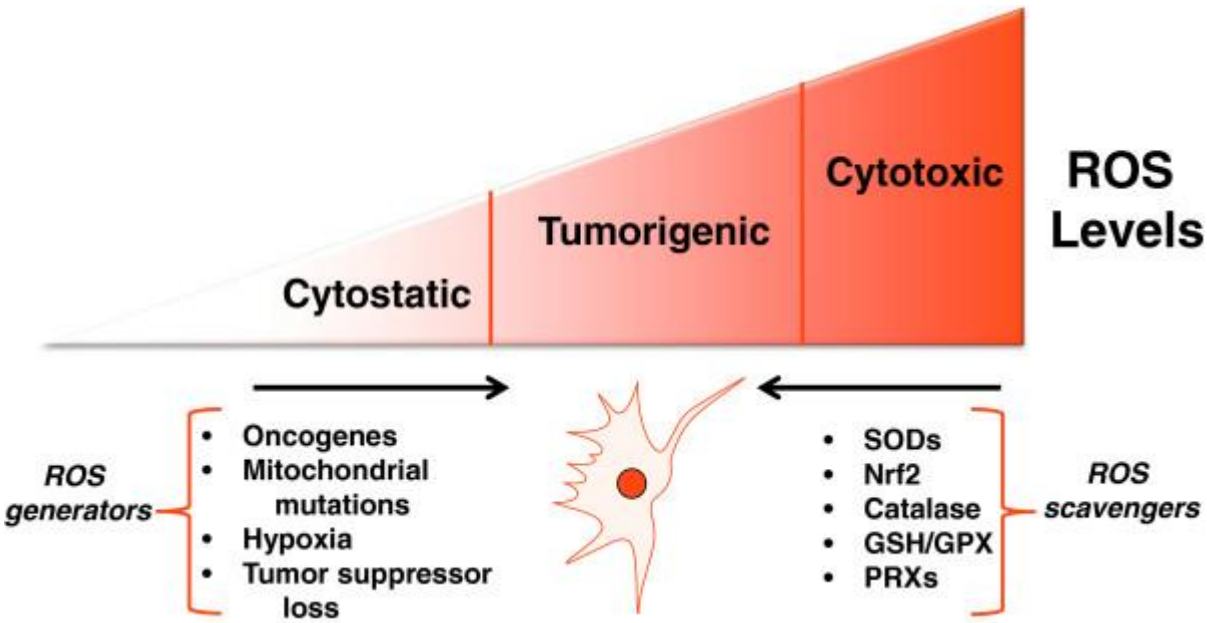

Figure 27 (Sullivan and Chandel, 2014): **Scheme of the antagonistic role of ROS in tumorigenesis**. *High doses of ROS can induce oxidative stress and cell death while mild ROS levels promote tumorigenesis.*

In addition, to cope with their high proliferation and high metabolic demand, cancer cells have an increased production of ROS that is compensated by high levels of antioxidants and an important PPP-dependent production of NADPH (Panieri and Santoro, 2016). This particular redox environment has been suggested to potentialize the susceptibility of cancer cells to ROS because their homeostasis redox systems work at saturation (Glasauer and Chandel, 2014; Panieri and Santoro, 2016; Reczek and Chandel, 2017). This makes pro-oxidant cancer therapy another appealing strategy. Recently, the inhibition of the PPP-dependent NADPH production by an inhibitor of G6PDH (ZWF1 in yeast cells), polydatin, showed promising results in cancer cell lines and cancer cell mouse models (Mele et al., 2018).

Such pro-oxidant therapies aim at inducing a redox imbalance inside cells by saturating their redox homeostatic system. Drug therapies inhibiting the tolerance of cells to oxidative stress may offer an important synergistic effect to pro-oxidant therapies. Moreover, due to the intrinsic ROS production in cancer cells and the dependency of tumorigenesis upon ROS signals, we speculate that lowering their oxidative stress tolerance would induce an irreconcilable antagonism between their critical needs for ROS and their incapacity to tolerate them.

We envision that identifying the system-level orchestration of stress resistance and tolerance in pathological contexts may help in designing new combinatorial drug strategies to potentialize the effect of antitumoral therapies.

Chapter 2: A pH-driven cytoplasmic phase transition underlies a cell fate divergence during the budding yeast life cycle

INTRODUCTION

This work represents a side project initiated during the PhD. It will be introduced more briefly than the Chapter 1.

1. The state of quiescence: a reversible response program to exit the cell-cycle

The proliferation of microorganisms is tightly linked to the availability of nutrients in their ecological habitat. Upon nutrient starvation, eukaryotic and prokaryotic cells can enter a stable and nonproliferating state, called quiescence. Within this state, cells can survive extended period of time, until years, and finally reproliferate when environmental conditions become more favourable (Gray et al., 2004a).

S. cerevisiae represents a prominent model for the study of quiescence. It is a well-known eukaryotic cells model. In addition, the pathways involved in its entry into quiescence seem to be conserved among other eukaryotic cells (mostly PKA and TOR pathways) (de Virgilio, 2012). Finally, since microbial cells spend most of their life in their natural habitat into quiescence (Gray et al., 2004a; Sagot and Laporte, 2019), the

state of quiescence in *S. cerevisiae* may have been tightly selected by evolution to favour its long-term survival.

Quiescent cells have long been thought to be G1 arrested cells, entering in a non-proliferative G0 state (Fig 28a) (PRINGLE and R., 1981). However, it has been further established in S. cerevisiae that yeast cells could enter quiescence in a budding state (5-10% of a yeast cell quiescent population (Fig 28b) (Laporte et al., 2011)). The entry into quiescence from the G2 state has been further observed in other microorganisms such as *Cryptococcus neoformans* and *Tetrahymena pyriformis* (Sagot and Laporte, 2019). It has been found that instead of the cell cycle state, it was rather the metabolic status of the cells was determining the entry of cells into quiescence (Laporte et al., 2011).

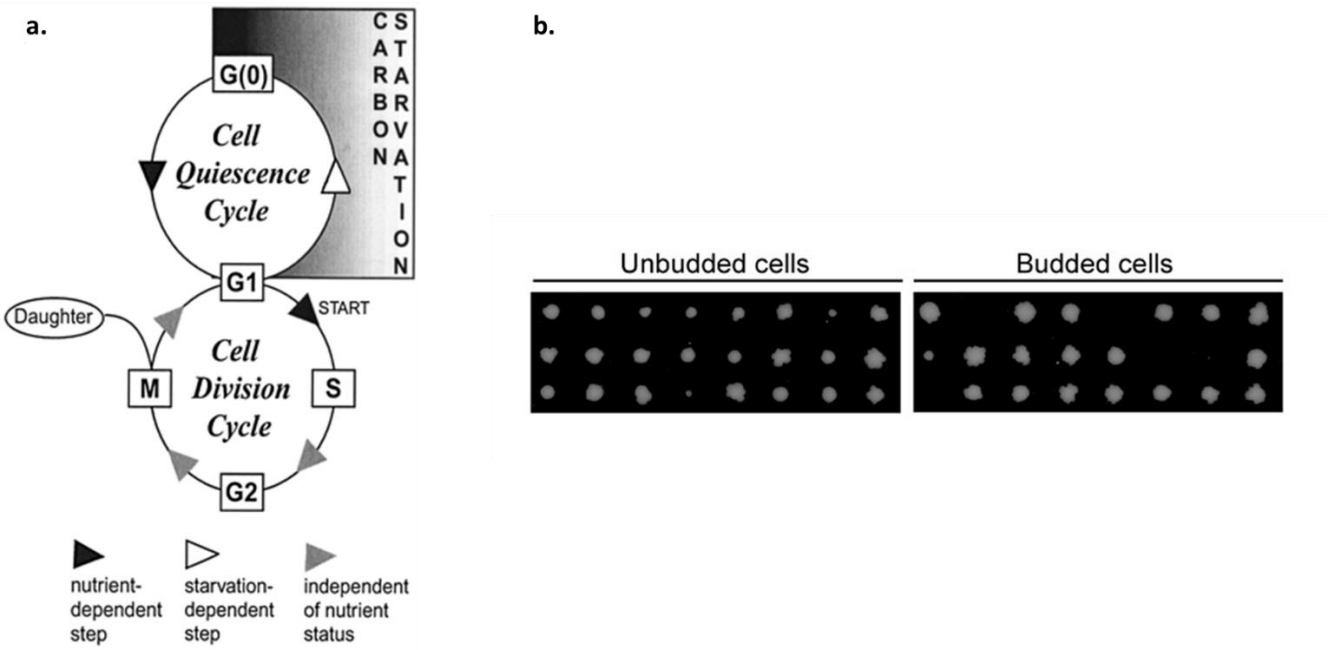

Figure 28 (adapted from Gray et al., 2004 and Laporte et al., 2011): **Relation between quiescence and the cell-cycle and the metabolic status of cells** (a) *Scheme of the historical relation between quiescence entry and the cell-cycle.* (b) *Re-entry into the cell cycle*

of budding yeast cells after 7 days of quiescence. Both unbudded and budded cells can survive an extended period of time under quiescence.

The entry into quiescence largely is dependent upon the PKA and TORC1 pathways. Indeed, their role in the integration of nutrient signals make them prominent hub regulators of the metabolic status of cells and therefore of quiescence entry (see Chapter 1 for details about the PKA pathways) (de Virgilio, 2012).

It has been shown that the activation of the PKA pathway precluded the entry of cells into quiescence upon starvation. On the contrary, the inhibition of the PKA and TORC1 pathway is thought to be sufficient to drive cells into a pseudo-quiescent state (Conrad et al., 2014; Tatchell, 1986; Thevelein and De Winde, 1999; de Virgilio, 2012). More recent studies found that the Rim15 kinases was the downstream hub of both PKA and TORC1 signalling (Bontron et al., 2013; Cao et al., 2016). Rim15 controls a large downstream signalling cascade involving among others the stress response transcription factor Gis1. Overall, this cascade is thought to induce both the inhibition of growth-related processes such as ribosome biogenesis, both translational and transcriptional activities, and the activation of stress response pathways (Broach, 2012; Broach and Deschenes, 1990; de Virgilio, 2012) (also see Ch.1.4.). The inhibition of this cascade had been found to drastically impair the viability of cells into quiescence (Cao et al., 2016; Quan et al., 2015; Ramachandran et al., 2011).

Overall, the state of quiescence therefore represents a non-growing state reached by cells to survive to extended period of times under starvation.

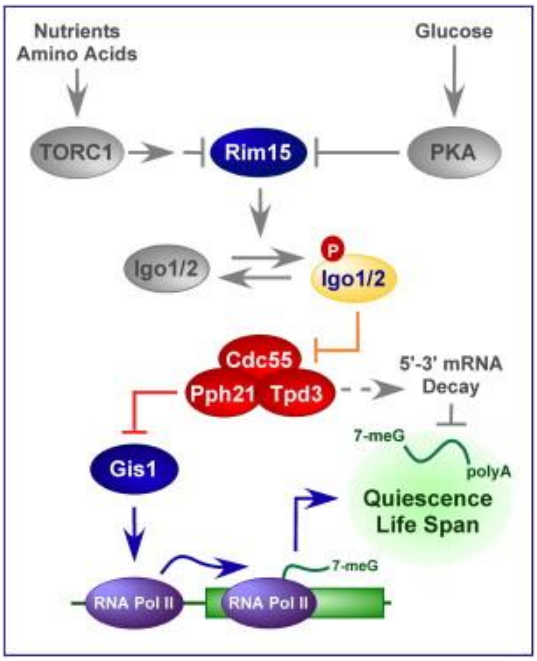

Figure 29 (from Bontron et al., 2013): **Scheme of the Rim15 pathway in quiescence entry of *S. cerevisiae***. *Rim 15 integrates TORC1 and PKA signals and controls a downstream signalling cascade that drastically inhibits the metabolic status of cells and inhibits growth related processes.*

2. Phase transition is a fast and reversible plastic behaviour in response to starvation

The entry into quiescence is accompanied by a massive reorganization of cellular structures that are thought to participate to the long-term viability of quiescence (Sagot and Laporte, 2019). We will thus first briefly describe some classical organelle remodelling that has been described in *S. cerevisiae* (see Fig 30 for the description of main structural changes observed in quiescence entry). Then, to generalize our description, we will introduce phase transition as a general concept thought to drive many (if not all) structural changes upon starvation.

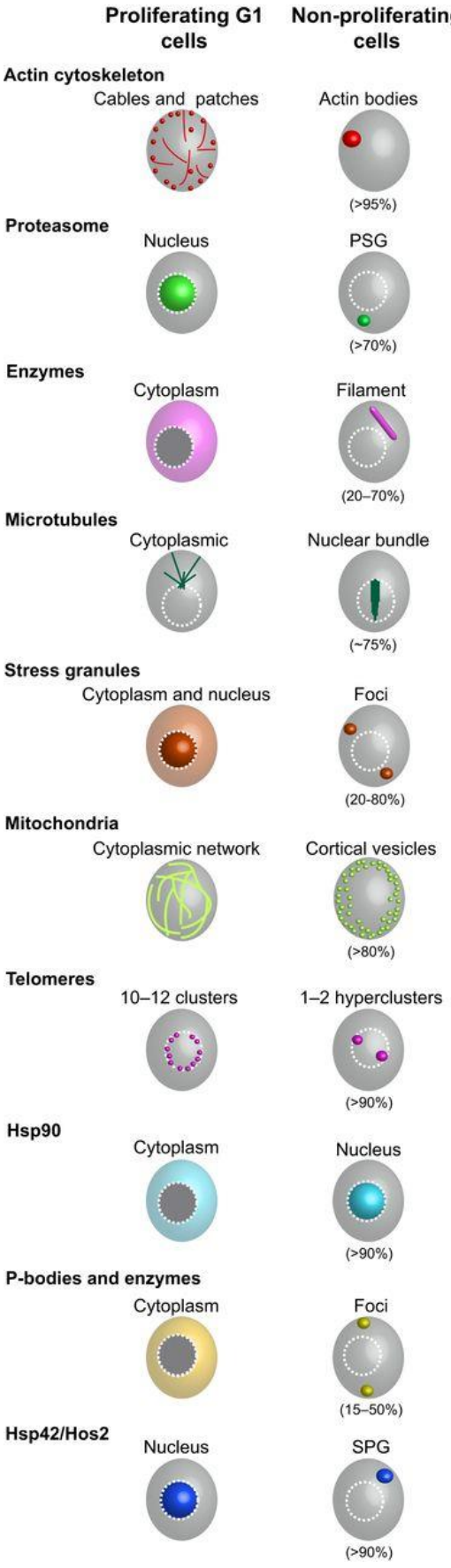

Figure 30 (from Laporte et al., 2019): **Scheme of the principle structure reorganizations observed in response to quiescence in the budding yeast S. cerevisiae.**

2.1. Cytoskeleton remodeling

The cytoskeleton is a major dynamical network that set the mechanical properties of cells (Fletcher and Mullins, 2010) and is required for a tremendous number of biological processes such as cell signalling (Moujaber and Stochaj, 2020). It is also involved in cell division (Heng and Koh, 2010; Meunier and Vernos, 2012). Upon quiescence entry and cell-cycle exit, the cytoskeleton is drastically remodelled (Fig. 20). In *S. cerevisiae*, actin transitions into a foci structure called 'Actin bodies' (Sagot et al., 2006) that contains an important pool of actin-binding proteins and F-actin. Microtubules are also reorganized into a tubular structure called nuclear bundles (Laporte et al., 2013). The presence of those structural reorganization has been found to coincide with the long-term viability of yeast cells into quiescence. However, their role in quiescence are not clear (Sagot and Laporte, 2019). It is however important to notice that both microtubules and actin cytoskeleton can reorganize into functional structures when cells exit quiescence from those quiescent structures. They are thus at least thought to represent storage compartments to rapidly re-enter proliferation (Laporte et al., 2013; Sagot et al., 2006).

2.2. Proteasome storage granules formation

Proteasomes are enzymatic complexes localized in both the endoplasmic reticulum and the nucleus of cells (Peters et al., 1994). Their principle functions include the control of proteostasis and the degradation of misfolded proteins by hydrolysis (Tanaka, 2009).

In *S. cerevisiae*, it has been observed that upon quiescence entry, 26S proteasomes were relocated from the nucleus into cytoplasmic foci structure called Proteasome Storage Granules (PSG) (see Fig 31) (Laporte et al., 2008). PSGs are also found in non-dividing mammalian cells and confer fitness under quiescence in *S. cerevisiae* cells (Enenkel, 2018). Recently, it has been shown that the PSG formation was protecting proteasomes from degradation by autophagy (Marshall and Vierstra, 2018). This demonstrates the functional role of the cytoplasmic reorganization upon quiescence. Similarly than for cytoskeleton remodelling's, PSG can be rapidly transformed back in functional proteasomes upon quiescence exit (Laporte et al., 2008).

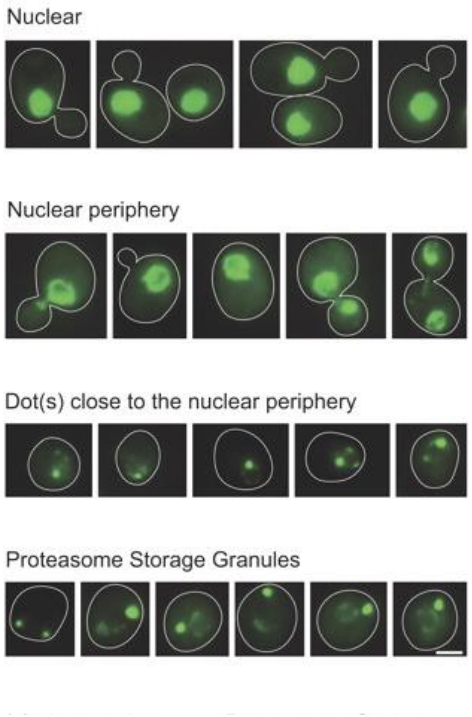

Figure 31 (from Laporte et al., 2008): **Proteasome localization during exponential growth and quiescence**. *The different localizations of the 26S proteasome in S. cerevisiae using Pre6-GFP, in exponential growth (Nuclear and Nuclear periphery localizations) and in quiescence (Dot structures/PSG).*

2.3. Mitochondrial network rearrangement and respiration sustain cells into quiescence

As we previously saw, the state of quiescence is intimately linked to the metabolic status of cells. Recently, it has been observed that the activation of respiration as well as autophagy was critically required to survive to starvation (Weber et al., 2020). Moreover, it had been previously observed that the mitochondrial network (that is directly depending on respiration activity) was drastically changed in quiescence and that the ability to respirate was linked to PSG formation under quiescence. On the contrary, cells that did not properly remodelled their mitochondrial network exhibited a very poor survival under starvation (Laporte et al., 2018a).

In budding yeast cells, especially in the S288c background, it has been reported that cells may spontaneously lose their mitochondrial potential, presumably because of the instability of their mitochondrial DNA (Dimitrov et al., 2009; Veatch et al., 2009). This phenotype is not caused by but accompanied by an incapacity to respirate (Veatch et al., 2009). The observation of a sub-population of cells not entering into quiescence has therefore been suggested to be associated to this mitochondrial instability (Laporte et al., 2018a) (see section 3. for more details about heterogeneities in quiescence).

Overall, those data suggest the important role of respiration in the establishment of both a long-term quiescence state and the related cellular reorganization observed in viable quiescent yeast cells.

2.4. Phase transition is a fast and reversible plastic behaviour in response to starvation

Indeed, the metabolic status of cells is thought to be the major determinant of the cellular reorganization into quiescence. It has been shown that upon starvation, cell's cytoplasm elicited a phase transition from a liquid-like state to a solid-like state (Heimlicher et al., 2019; Joyner et al., 2016; Munder et al., 2016a; Parry et al., 2014) associated with an increased molecular crowding and a decrease mobility of cytoplasmic aggregates (Heimlicher et al., 2019; Joyner et al., 2016; Munder et al., 2016a; Parry et al., 2014) (Fig 32a). On the contrary, it has been shown that the metabolic activity was fluidizing the cellular cytoplasm (Parry et al., 2014). Two biophysical parameters are thought to drive this starvation-dependent phase transition: the decrease of cell volume following starvation (Joyner et al., 2016) (thus increasing cellular crowding) but also by an indirect effect depending upon the cytosolic pH (Munder et al., 2016a; Riback et al., 2017).

Indeed, the cytosolic pH is mainly controlled by an ATP-dependent protein, Pma1, that pumps out proton from the cytoplasm (Orij et al., 2011). Upon starvation, the ATP concentration drops (Weber et al., 2020) and the cytoplasmic pH becomes acid (Munder et al., 2016a). The drop of pH has been shown to induce a widespread protein-aggregation that was participating to the phase transition and also to the resulting increased of molecular crowding observed in starvation (Munder et al., 2016a; Petrovska et al., 2014) (Fig 22b). Importantly, pH has been shown to trigger the aggregation of specific proteins and structures. In particular, the proteasome

storage granule formation has been shown to be dependent upon cytoplasm's acidification (Peters Lee Zeev et al., 2013).

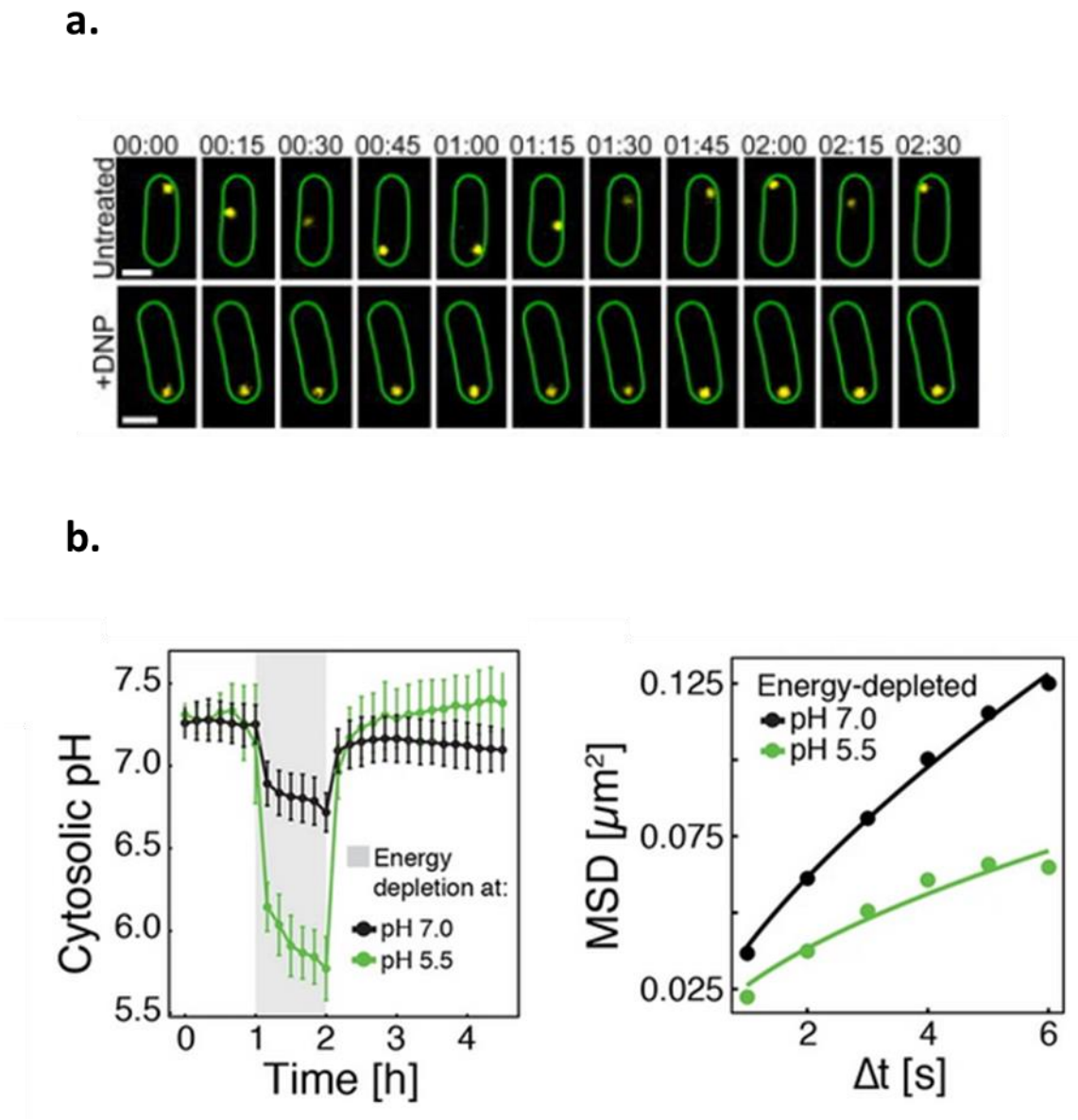

Figure 32 (adapted from Parry et al., 2014 and Munder et al., 2016): **Starvation induced phase transition and link with cytosolic pH** *(a) Mobility of a μNS-GFP particle within the cytoplasm of the bacterium* Caulobacter crescentus *(b) Internal pH following energy deprivation in different pH-buffer (5.5 or 7) and measure of the associated Mean Square Displacement (MSD) of μNS-GFP particles inside the cytoplasm of starved*

yeast cells at different pH (5.5 or 7). The reduced particle mobility observed in starvation required the acidification of the cytosolic pH.

Other structures observed in quiescence, such as P-bodies and stress granules (Mateju et al., 2017; Ramachandran et al., 2011; Riback et al., 2017), or metabolic enzymes such as the glutamine synthase Gln1 (Munder et al., 2016a; Petrovska et al., 2014) are also controlled by a pH-dependent phase transition.
Interestingly, those pH dependent protein aggregations have been shown to largely participate to cellular fitness upon starvation or quiescence (Marshall and Vierstra, 2018; Munder et al., 2016a; Ramachandran et al., 2011; Riback et al., 2017).

Overall, the drop of cytosolic pH and the associated phase transition are thought to play a critical role in the widespread reorganization of the cytoplasm upon quiescence entry.

3. The natural life cycle of the budding yeast: A dynamical and heterogeneous transition toward quiescence

In addition of introducing key concepts about the complexity of quiescence both in terms of inter-individuals' heterogeneities and dynamics, this section will also motivate and justify the critical methodological need in the field to study quiescence in a relevant manner.

3.1. A state of quiescence or quiescent states?

Until here, we described the main cellular reorganizations occurring in response to starvations and into quiescence entry. If this ensemble of processes may represent a 'typical' quiescent state, large heterogeneities are observed in the state of quiescence reached by clonal cells in a given population (Gray et al., 2004; Sagot and Laporte, 2019). Considering the diverse reorganizations described above, no one is thought to occur within 100% of cells (see the fractions Fig 20 for each structure). Any cell observed within the population will therefore exhibited a unique cocktails of quiescence hallmarks.

In particular, it has been reported that two distinct sub-populations were distinguishable in a clonal population of budding yeast cells based on very general features exhibited by those cells (Allen et al., 2006). Authors found that while a first population could be considered as quiescent based on its ability to re-enter the cell-cycle after several days, the other population was indeed in a 'non-quiescent state' since a large fraction this population could not re-enter the cell cycle after 21 days (Allen et al., 2006). Those 'non-quiescent cells' were less dense that quiescent cells and authors suggested that they were indeed young unbudded daughter cells. However, different studies strongly challenged this last idea recently (Laporte et al., 2018a, 2018b).

Instead of the mother/daughter status, the respirative capacity of cells has been suggested to determine those two populations (Laporte et al., 2018a). Indeed, another study had showed that while cells with a null respirative capacity rapidly died upon quiescence entry, a normal longevity into quiescence could be rescued by adding trehalose in the medium (Ocampo et al., 2012). This therefore strongly suggested the important metabolic role of respiration for quiescence establishment. However,

whether non respirative cells cannot enter quiescence or rather cannot remain viable for a long period is unclear. Moreover, whether those cells pre-exist in the population or rather emerge during quiescence establishment is also not known.

Finally, tremendous differences can sperate the states of quiescence reached under different nutrient deprivations (Klosinska et al., 2011). Authors showed that while some properties were conserved among those states, such as cell wall remodeling and stress tolerance, the metabolic status of cells (carbon or azote for example) could drastically change (Klosinska et al., 2011).

Overall, budding yeast cells can thus access various states upon nutrient starvation and quiescence cannot be considered as a unique state that may represent the response to starvation. In this context, the use of single-cell technologies appears of great interests to study quiescence establishment at the single cell level and the heterogeneities existing among cells.

3.2. Dynamic of quiescence entry and ecological relevance

In addition of varying among clonal individuals, quiescence have been reported as a highly dynamical process, that takes several days to establish and continuously evolves over time (Sagot and Laporte, 2019).

In *S. cerevisiae*, Mitchell et al. showed that cells may anticipate future predictable environmental changes to efficiently adapt. For example, they showed that the production of ethanol during fermentation was protecting against the production of ROS occurring during the next phase of the cycle, the respirative phase) (Mitchell et

al., 2009). Other works showed that bet-hedging strategies could diversify the response of cells in a given environment to better adapt to future environmental changes (Solopova et al., 2014; Venturelli et al., 2015). Indeed, it has been formalized that decision-making process driving cellular responses to environmental changes may be dependent upon probabilistic strategies inferring the probability of future changes to come and behave in consequences (Mitchell and Pilpel, 2011; Perkins and Swain, 2009).

However, despite the importance of environmental change dynamics and predictability for efficient cell responses, a large number of studies simplifies complex dynamics of natural environment changes by more simple synthetic changes, where individuals are abruptly and severely starved (Munder et al., 2016b; Parry et al., 2014; Petrovska et al., 2014). If such synthetic conditions enables a tight control of the environmental conditions and most importantly is compatible with single-cell observation (Cerulus et al., 2018), it is likely to miss important features of microorganisms' responses to naturally encountered environmental change dynamics.

Finally, it has been reported that response to environment could be shaped by the past history of microorganisms, mechanisms known as history dependent behaviours (Cerulus et al., 2018). In this view, the state of quiescence, considered as the 'final state' of the budding yeast's life cycle, may integrate and depend upon the whole history of individual budding yeast cells. It therefore appears crucial to study quiescence establishment in the light of the history of single individual cells.

Context and Objectives of the work

During its natural life cycle, the budding yeast *S. cerevisiae* undergo transitions between different metabolic phases: first, a rapid phase of sugar fermentation; then, a respiration phase during which the ethanol produced upon fermentation is consumed. In between these two phases, cells undergo a reversible proliferation arrest called the diauxic shift (DS). Those phases, in particular the respirative phase, are thought to largely influence the state of quiescence reached by cells upon complete nutrient exhaustion. This context therefore represents an idyl model to understand how the complex dynamics of nutrient exhaustion shapes the fate of cells during their life cycle. However, to our knowledge, it does not exist any methodology enabling to follow single microorganisms over time behaving as part of their colony in their natural environment.

a. Developing a microfluidic based method to track the whole life cycle of budding yeast cells

Here, we first aimed at developing such a single-cell ecology platform. The main objective of this work was to develop a microfluidic-based methodology enabling to follow and track the cell fate dynamic of single budding yeast cells along their whole natural life cycle (wine fermentation), from fermentation to quiescence entry. We envisioned that observing the plastic behaviours of cells resulting from colony-environment interactions both in time and at the single-cell level may represent a breakthrough methodology to tackle ecological questions with unprecedented resolutions (temporal and single-cell).

b. Exploring the timings of cell fate divergency and quiescence entry during the yeast life cycle as a proof-of-principle of our methodology

As a proof-of-principle of our methodology, we aimed at identifying whether and when cell fate divergencies are emerging during the life cycle of the budding yeast.

Indeed, as we described above, tremendous heterogeneities are observed within a clonal population of quiescent cells. We speculated that our longitudinal-tracking methodology must capture their origin and furnish cues about how environmental changes can induce brutal cell fate bifurcations among clonal individuals.

In particular, in our context, we asked whether we could capture the moment at which the bimodal population (the so called quiescent and non-quiescent populations) are emerging during the budding yeast life cycle.

RESULTS

Single-cell tracking of cell fate divergence and pH-driven phase transition during the budding yeast life cycle

Basile Jacquel[1234*], Théo Aspert[1234*], Damien Laporte[5], Isabelle Sagot[6], Gilles Charvin[1234]

* Equally contributed to the work

Affiliations:

1) Department of Developmental Biology and Stem Cells, Institut de Génétique et de Biologie Moléculaire et Cellulaire, Illkirch, France

2) Centre National de la Recherche Scientifique, UMR7104, Illkirch, France

3) Institut National de la Santé et de la Recherche Médicale, U964, Illkirch, France

4) Université de Strasbourg, Illkirch, France

5) University of Bordeaux

Introduction/Abstract

Microorganisms have evolved plastic growth control mechanisms that ensure adaptation to dynamical environmental changes, including those that arise from their own proliferation (such as nutrients limitations and cellular secretion in the medium). During its natural life cycle, budding yeast undergoes several metabolic transitions from fermentation to respiration, followed by entry into a reversible state of proliferation arrest known as quiescence (De Virgilio 2012; Gray et al. 2004). Despite quiescence being an essential part of the microorganism lifecycle that ensures cell survival over

prolonged periods of time (Fontana, Partridge, and Longo 2010), it has received little attention compared to the analysis of biological processes in proliferative contexts. Quiescent cells not only strongly differ from proliferating cells in terms of metabolic activity and signaling (Gray et al. 2004), they also display a large body of structural rearrangements in the cytoskeleton, mitochondria, nuclear organization, and the appearance of various protein aggregates (Sagot and Laporte 2019). So far, such complex and entangled cellular reorganizations precluded assessing whether and how a limited set of regulatory processes controls the establishment of this particular state. In particular, the detailed choreography of events describing how the dynamics of metabolic cues during the natural lifecycle drives the entry into quiescence is still missing.

In addition, an essential feature of microbial ecosystems in a stationary phase is the existence of phenotypic variability (Campbell, Vowinckel, and Ralser 2016; Avery 2006; Holland et al. 2014; Labhsetwar et al. 2013; Ackermann 2015) and history-dependent behaviours that lead to complex fate divergences (Balaban et al. 2004; Cerulus et al. 2018). In quiescent yeast cells, the coexistence of heterogeneous cell populations has been previously reported (Allen et al. 2006; Laporte et al. 2018). Yet, in this context, the scenario driving the emergence of heterogeneity in cell fate in a clonal population remains unknown (Fig. 1A). This is in part due to the difficulty to combine a population-based approach in which microorganisms collectively impact on their environment over a full life cycle, with single-cell longitudinal tracking to monitor the dynamics of individual cell behaviour over time.

Here, we have developed a microfluidic platform for single-cell ecology that allows us to continuously track the fate of individual cells that experience exhaustion of nutrients caused by population growth in a liquid culture over a full life cycle (up to 10 days).

Using a fluorescent reporter of internal pH (Mouton et al. 2020; Miesenböck, De Angelis, and Rothman 1998) that characterizes the metabolic status of the cells, we show that the onset of the diauxic shift induces a clear cell fate divergence, whereby a minority of cells experience a metabolic crash leading to the premature appearance of quiescence markers yet display limited survival. We then show that variations in internal pH drive the successive formation of distinct cellular reorganizations and ultimately controls the transition to a gel-like state of the cytoplasm. Altogether, our analysis reveals how environmental changes encountered by yeast cells during its natural life cycle lead to a temporal control of structural changes and elicits the emergence of heterogeneous cellular trajectories.

Results

In order to track the dynamics of individual cell behaviours during an entire life cycle, we set up a device composed of a 25mL liquid yeast culture (YPD medium) with constant stirring connected to a microfluidic device with a closed recirculation loop (Fig. 1B, Fig 1Supp A-D). Therefore, individual cells trapped in the microfluidic device could be imaged over time using time-lapse microscopy while experiencing the same environmental changes as the population in the liquid culture. In order to prevent the clogging of the microfluidic device due to the high cell concentration in the culture (up to 10^9 cells/ml, optical density (O.D600) ~ 20), we designed a filtration device based on inertial differential migration (Bhagat, Kuntaegowdanahalli, and Papautsky 2008) to reroute the cells back to the liquid culture before they could enter the microfluidic device. Using O.D. measurements, we observed a filtration efficiency of more than 99.15±0.35%, thus reducing the cellular concentration in the microfluidic device by ~2 orders of magnitude and allowing us to image the cells in the device over up to 10

days. We also checked that the same device could sort S. Pombe cells with 92% efficiency, thus highlighting the versatility of the methodology.

Based on this methodology, we recapitulated the successive transitions occurring during cell proliferation in a resources-limited environment ((Richards 1928), namely: a rapid exponential growth (doubling time = 84 min +/- 12 min) of microcolonies corresponding to glucose fermentation (referred to as the F phase in the following, from t=0 to t=5.5 h), followed by a sharp growth arrest, or diauxic shift (DS, from t = 5.5 h to t = 13.9 h); then, the resumption of a slow proliferative regime (doubling-time = 307 min +/- 52 min) which is associated with the use of ethanol as a carbon source for a respiratory metabolism (R, from t = 13.9 h to t = 31.6 h) and a final permanent arrest occurring upon resources exhaustion, leading to entry into quiescence (Q) (Fig 1C, D). The transition times between each metabolic phase were determined using piecewise exponential fits (Fig S1E). By reinjecting fresh YPD medium into the microfluidic device after 10 days, we observed that up to ~80% of cells re-entered the cell cycle within 5h (Fig S1F), confirming the reversibility of the cell proliferation in our growth conditions (Laporte et al. 2017).

A drop in medium pH has long been reported to coincide with the exhaustion of resources during microbial growth (Burtner et al. 2009). Yet, how internal pH evolves over an entire lifecycle has never been investigated. To address this, we used the ratiometric fluorescent probe of cytoplasmic pH pHluorin (Fig. 1E, (Miesenböck, De Angelis, and Rothman 1998; Mouton et al. 2020)), which can be calibrated to display the absolute internal pH (Fig. 1E-G and Fig. S1G). Using this readout, we observed that the pH, which was initially around 7.7, started to decline synchronously in all cells

during the F phase (Fig. 1F-G). At the onset of the DS, most cells abruptly reached a plateau (pH ~ 6.9, blue lines on Fig. 1G), which was followed by a slight pH increase (up to pH~7.2) that coincided with entry into a respiratory metabolism. In contrast, a minority of cells (Fig. 1F and red lines on Fig. 1G) experienced a further drop in pH down to about 5.8 during the DS. The fluorescence signal progressively disappeared in this subpopulation, precluding from monitoring the internal pH for more than 20h in a reliable manner.

In cells with high internal pH during the DS, the pH gradually declined after reaching a local maximum during the R phase. Then, these cells experienced a sharp pH drop down to about 5.8, which occurred at very heterogeneous times during the Q phase, unlike the cells with an early pH drop. Altogether, these observations revealed unprecedented dynamics of internal pH during the yeast life cycle. pH variations appeared to be in sync with the sequence of proliferation phases, hence suggesting that internal pH is a key marker of the metabolic status of the cells during its lifecycle.

These continuous pH measurements also unraveled an unexpected divergence in cell fate at the DS leading to the early emergence of heterogeneity within the population. Recently, it has been reported that the activation of respiration was a crucial metabolic response to survive glucose deprivation (Weber et al. 2020), that enabled the cells to store carbohydrate (Ocampo et al. 2012) and to later enter a prolonged quiescent state (Laporte et al. 2018). Interestingly, it was shown that a respiration defect was naturally observed in a fraction of cells undergoing entry into quiescence (Laporte et al. 2018).

To further characterize whether differences in metabolic status drove the emergence of divergent cell fates at the DS, first, we used single-cell volume measurements to quantify cellular proliferation over time. We found that cells with a late pH drop resumed growth and roughly doubled their biomass during the R phase (blue lines on Fig. 2A), in agreement with cell number measurements in Fig. 1. In contrast, cells that experienced an early pH drop (red lines on Fig. 2A) did not recover during the R phase, suggesting that they were unable to transition to respiratory metabolism. To investigate this hypothesis, we checked that these cells did not resume growth when adding lactate as a non-fermentable carbon source to the medium, (Fig. S2A). Yet, the vast majority of these cells were still viable after 3 days in quiescence - even though they displayed a greatly reduced lifespan compared to adapting cells (Fig. 2B).

In addition, we used the Ilv3-mCherry fusion as a marker of the mitochondrial network to reveal the respiratory status of the cells(Laporte et al. 2018). Whereas mitochondrial structure was similar (i.e. roughly tubular) in all cells before the DS, proliferating cells in the R phase displayed a fragmented phenotype that is typical of respiring cells (Fig. 2C). In contrast, non-proliferating cells underwent a globularization of their mitochondrial network (Fig. 2C). We further quantified the dynamics of the reorganization of the mitochondrial network by computing a custom aggregation index that discriminates globularized versus tubular and fragmented mitochondria (Fig. 2D, see Methods for details). Based on the clear distinction in the aggregation index between adapting and non-adapting cells, we measured that about ~10 % of the cells were unable to transition to respiratory metabolism (at t=12h post-DS, Fig. 2D), in agreement with previous findings (Laporte et al. 2018). Importantly, this quantification revealed that the mitochondrial globularization in non-adapting cells was temporally

closely associated with the DS, since it started as early as 1h20 ($p < 0.05$) after its onset (Fig. 2C). Altogether, these results demonstrated that adapting and non-adapting cells experienced divergent cell fates at the DS based on their ability to switch to respiration, hence were referred to in the following as respiration positive (R+) and negative (R-), respectively. In addition, these results suggested that the inability of R- cells to activate a respiratory metabolism was either triggered by this metabolic challenge or, alternatively, pre-existed the DS, knowing that respiratory deficient cells (i.e. ρ- cells) are common in the BY background due to the genetic instability of mitochondrial DNA (Dimitrov et al. 2009).

To discriminate among these two hypotheses, we used a strain carrying the pre-sequence of Cox4 fused to mCherry (Cox4 is a nuclear-encoded mitochondrial protein that is only imported in functional mitochondria (Veatch et al. 2009)) along with the mitochondrial localization marker Tom70-GFP (Tom70 is a protein of the outer mitochondrial membrane), as a proxy to assess the cells' ability to respire (Fehrmann et al. 2013). Using these markers, we first checked that all R+ cells, which are able to switch to respiration, maintained a functional preCox4-mCherry import from fermentation to respiration (i.e. they were ρ+ cells, Fig. 2E). Then, we observed that among the R- cells, only a minority (i.e. 19%) had a dysfunctional mitochondrial import before the DS, indicating that they had a pre-existing respiratory deficiency (see ρ- cells on Fig. 2E). In contrast, the vast majority of R- cells (81%) transitioned from ρ+ to ρ- during the DS. This demonstrated that, in contrast to a pre-existing condition, the respiration defect observed in R- cells appeared to be triggered by the environmental switch. Altogether, these observations supported a scenario in which a fate divergence

occurred early at the onset of the DS, whereby R+ cells quickly switched to a respiratory metabolism, while R- cells failed to do so.

Next, we sought to establish the links between successive changes in metabolism and the numerous structural cellular reorganizations that have been previously reported during entry into quiescence (Sagot and Laporte 2019). Indeed, since the metabolism controls internal cellular pH, which is known to induce major physicochemical changes in the proteome such as protein aggregation and phase transition (Munder et al. 2016; Dechant et al. 2010), we wondered how these reorganizations would be coordinated with internal pH dynamics in the context of quiescence. To do this, we monitored the dynamics of formation of supra-molecular bodies associated with various biological processes, such as P-bodies formation (using the Dhh1-GFP fusion), metabolic or regulatory enzymes prone to aggregation (Gln1-GFP and Ccd28-GFP), the formation of actin bodies (Abp1-GFP), and proteasome storage granules (PSG, using the Scl1-GFP fusion). Indeed, these proteins have been described to form such structures in quiescence or in response to starvation (Mugler et al. 2016; Balagopal and Parker 2009; Petrovska et al. 2014; Narayanaswamy et al. 2009; Shah et al. 2014; Sagot et al., n.d.; Laporte et al. 2008; Peters et al. 2013)

We found that the formation of fluorescence foci was highly coordinated with the sequence of metabolic phases and the cellular proliferation status (Fig. 3A): in R+ cells, Dhh1-GFP and Gln1-GFP foci appeared at the onset of the DS, then were partially dissolved during the R phase, and reappeared upon entry into quiescence. Other hallmarks of entry into quiescence, such as actin bodies, PSGs, as well as other markers of protein aggregation (Cdc28-GFP) showed up significantly later, i.e. at the end of the R phase. Importantly, we observed that R- cells also experienced a

consistent formation of fluorescent foci for the markers that were monitored, yet, unlike R+ cells, they all appeared during the DS. In addition, surprisingly, these foci ultimately disappeared, presumably as a consequence of the premature cell death observed in this subpopulation.

By overlapping the dynamics of fluorescence foci with that of internal pH (Fig 1G), we noticed that the formation of aggregation bodies overall coincided with variation in absolute pH level in both R+ and R- cells, although it appeared at different timescales. This finding supported the hypothesis that it is the drop in internal pH - which reflects low metabolic activity - that drives successive waves of protein aggregation and the appearance of quiescence hallmarks. To further check this hypothesis, since energy depletion was shown to induce a global modification of the cytoplasm to a gel-like state (Munder et al. 2016), we sought to observe this transition by monitoring the mobility of Gln1-GFP foci over time (Fig. 3B, (Munder et al. 2016)) - this marker was chosen because foci are already present at the DS. We found that the mobility of Gln1-GFP foci decreased sharply in R- cells during the DS and much later in R+ cells, consistently with the differences observed regarding the times of pH drops in both populations. To better establish the links between pH and mobility, we exploited the fact that lipid droplets (LD) could be conveniently observed using phase-contrast images (Heimlicher et al. 2019), and the freezing time of LDs correlated very well with that of Gln1-GFP foci (Fig S3A). By quantifying both the time of LD freezing and the dynamics of pH drop in single cells, we observed that both events were tightly correlated in all cells, despite the large cell-to-cell heterogeneity in the time of pH drop in R+ cells (Fig 3E and S3B). In addition, after synchronization of all single-cell trajectories from the time of LD freezing, we showed that the freezing of the cytoplasm occurred at a similar pH ~ 6 in both R+ and R- cells (Fig 3F). Altogether, these observations suggest that the internal pH, which displays very dynamic behaviour during the yeast life cycle, induces waves of

proteome structural remodeling that govern the establishment of quiescence markers and ultimately triggers a global transition of the cytoplasm to a gel-like state. Interestingly, the premature transition observed in respiratory deficient (R-) cells, which coincides with the early pH drop, further supports this model and suggests that this subpopulation undergoes a precocious transition to quiescence similar to the R+ cells. However, it is probable that the absence of the respiratory phase limits long-term viability in this subpopulation (Ocampo et al. 2012; Weber et al. 2020).

Discussion

In this study, we have developed a new microfluidic platform that allows us to monitor a full cell proliferation cycle in liquid culture with single-cell resolution. Individual cell tracking reveals how heterogeneous cell fates, which are triggered by successive metabolic switches, emerge in a clonal population.

Our analysis revealed a clear divergence in cell fate at the diauxic shift, whereby a minority of cells failed to establish a respiratory metabolism hence underwent a dramatic drop in internal pH. By and large, this phenomenon could not be explained by pre-existing phenotypic differences in the population during the fermentation phase, but rather appeared to be triggered by the metabolic challenge associated with the exhaustion of glucose.

Interestingly, both respiration-competent and respiration-deficient cells seem to undergo stereotypical cellular reorganizations previously observed in quiescent cells (Sagot and Laporte 2019) albeit at very different times. This suggests that the structural plasticity of the cells in response to the exhaustion of resources is controlled by a similar mechanism in both populations.

In particular, previous studies have demonstrated how cytoplasmic pH controls protein aggregation and the transition of the cytoplasm to a gel-like state (Munder et al. 2016),

but this had never been observed in an ecologically relevant context. Here, our results indicate that pH drops, which occur at very different times in respiration-competent cells, are systematically associated with the formation of protein super-assemblies and granules.

The drop in internal pH ultimately induces the transition of the cytoplasm to a gel-like state, which occurred either early or late in the lifecycle (as in R- and R+ cells, respectively). Remarkably, this transition occurs at very variable times in R+ cells, suggesting the existence of additional sources of heterogeneity in cellular metabolism. Overall, these data support a simple model in which changes in the cellular metabolic status during entry into quiescence modulate the internal pH level, which in turn drives a massive remodeling of the proteome.

We envision that this methodology could be further applied to other contexts in which collective cell behaviour impacts the environment, which in turn shapes individual cellular response (e.g. metabolic oscillations (Tu et al. 2005), cooperative behaviours (Dal Co et al. 2020; Campbell et al. 2015)).

Methods

Strains

Name	Mat	Background	Genotype	Origin
WT	a	S288C	his3Δ1; leu2Δ0; ura3Δ0; met15Δ0	Euroscarf
Abp1-GFP	a	S288C	his3Δ1; leu2Δ0; ura3Δ0; met15Δ0 Abp1-GFP	Invitrogen
Gln1-GFP	a	S288C	his3Δ1; leu2Δ0; ura3Δ0; met15Δ0 Gln1-GFP	Invitrogen
Dhh1-GFP	a	S288C	his3Δ1; leu2Δ0; ura3Δ0; met15Δ0 Dhh1-GFP	Invitrogen
Cdc28-GFP	a	S288C	his3Δ1; leu2Δ0; ura3Δ0; met15Δ0 Cdc28-GFP	Invitrogen
Scl1-GFP	a	S288C	his3Δ1; leu2Δ0; ura3Δ0; met15Δ0 Scl1-GFP	Invitrogen
Ilv3-mCherry	a	S288C	his3Δ1, leu2Δ0, met15Δ0, ura3Δ0 ILV3-tdimer-URA3, Scl1-GFP-HIS3	Sagot Lab

preCox4-mCherry Tom70-eGFP	a	S288C	*his3Δ1 leu2Δ0 lys2Δ0 trp1Δ63 ura3Δ0 TOM70-eGFP-CaURA3 PTDH3-preCOX4-Cherry-hphMX*	Fehrman et al.
SMY12, TEF1-pHluorin	a	S288C	leu2Δ0 met15Δ0, ura3Δ0 his3Δ1::PTEF1-pHluorin-HIS3	Veenhoff lab
Tdh3-GFP	a	S288C	his3Δ1; leu2Δ0; ura3Δ0; met15Δ0 Tdh3-GFP	Invitrogen

Cell filter

Briefly, particles above a certain size, in a spiral and rectangular microfluidic channel were submitted to several inertial forces, directed towards the center of the channel and towards the walls. The equilibrium position of these forces is set by the dimensions of the channel cross section and by the particle diameter. For a given and appropriate channel geometry, particles of similar diameter focus in a single line, allowing their separation from the rest of the fluid by splitting the channel in 2 parts. Here, we chose channel dimensions so that it should focus ~5um objects. The detailed dimensions are presented in Fig S1A. Any use with other microorganisms may only require adapting the dimensions of the filtration and observational microfluidics devices. We also added a particle filter before the spiral to avoid any clogging of the spiral because of dust particles or debris (Fig S1C).

To validate the filtration of the cell filter, the OD600 of the inlet and of the two outlets was measured at 4 different timepoints (0h, 24h, 48h and 120h) using a cell density meter (Fisherbrand) and the filtration efficiency was found independant of the inlet density (Data not shown) and equal to 99%.

Microfabrication

Microfluidic chips were generated using custom-made microfluidic master molds. The master molds were made using standard soft-photolithography processes using SU-8 2025 photoresist (Microchem, USA). The designs were made on AutoCAD (available

upon request) to produce chrome photomasks (jd-photodata, UK). The observation device was taken from a previous study (Goulev et al. 2017).

The mold of the dust filter chip was made by spin-coating a 25µm layer of SU-8 2025 photo-resist on a 3" wafer (Neyco, FRANCE) at 2700 rpm for 30sec. Then, we used a softbake of 7min at 95°C on heating plates (VWR) followed by an exposure to 365nm UVs at 160 mJ/cm² with a mask aligner (UV-KUB3 Kloé®, FRANCE). Finally, a post-exposure bake identical to the soft bake was performed before development using SU-8 developer (Microchem, USA).

The mold corresponding to the spiral device was obtained by spinning SU-8 2025 at a speed of 1750 rpm to achieve 50µm deposit. Bakes were 6 min long at 95°C and exposure to UV was done at 180 mJ/cm². Then, a hard bake at 150°C for 15min was performed to anneal potential cracks and to stabilize the resist.

Finally, the master molds were treated by chlorotrimethylsilane to passivate the surface.

Preparation of the cells

Freshly thawed cells were grown overnight. In the morning, 2mL of the culture was poured in 25mL of YPD was inoculated. After 5h, 2mL of the media was used to inject cells into the device (see next section) and the rest was used as circulating media for the experiment. This timing has been chosen so cells spend only 2 to 3 divisions in fermentation while in the microfluidic device, for imaging and tracking reasons.

Microfluidics

The microfluidic devices were fabricated by pouring polydimethylsiloxane (PDMS, Sylgard 184, Dow Chemical, USA) with its curing agent (10:1 mixing ratio) on the

different molds. The chips were punched with a 1mm biopsy tool (Kai medical, Japan) and covalently bound to a 24 × 50 mm coverslip using plasma surface activation (Diener, Germany). The assembled chips were then baked 1 hour at 60°C to consolidate covalent bonds between glass and PDMS. Then, the dust filter chip was connected to the spiral cell filter which was in turn connected to the observation chip. All the connections used 1mm (outside diameter) PTFE tubes (Adtech Polymer Engineering, UK).

All medium flows were driven using a peristaltic pump (Ismatec, Switzerland) at a 100µL/min rate. The system was connected to the tank of media and cells described in the previous section. The observation chip was loaded with the cells of interest using a 5mL syringe and a 23G needle. To complete the microfluidic setup, the cell-outlet of spiral as well as the outlet of the observation chip were plugged to the tank, so the system is closed and without loss of media nor cells.

Time-Lapse Microscopy

For all experiments except pH measurements, cells in the observation device were imaged using an inverted Zeiss Axio Observer Z1. Fluorescence illumination was achieved using LED light (precisExcite, CoolLed) and light was collected using a 63× N.A. 1.4 objective and an EM-CCD Luca-R camera (Andor; adaptation experiments). For experiments using the pHluorin cytosolic pH probe, a Nikon Ti-E microscope was used along with a LED light (Lumencor) fluorescence illumination system. Emitted light was collected using a 60x N.A. 1.4 objective and a CMOS camera Hamamatsu Orca Flash 4.0.

We used automated stages in order to follow up to 64 positions in parallel over the course of the experiment. Images were acquired every 15 min, 30min, 60min or

240min according to the phase of the culture (high frequency in fermentation VS lower frequencies in late quiescence) to avoid photodamage.

The temperature was controlled using a custom sample holder coupled with heating resistors, as well as with an objective heater. The control was achieved using a custom Arduino(r) based PID controller.

Image processing

The raw images were processed using custom software, called PhyloCell, based on MATLAB and the Image Processing Toolbox (Fehrmann et al. 2013; Paoletti et al. 2016). This software has a complete graphical interface for segmentation and tracking. The software can be downloaded online (charvin.igbmc.science/Resources). Here, the program was used to segment the cell contours using a watershed algorithm on phase-contrast images, to track the cells over time using the Hungarian method and to measure fluorescence inside the cells.

Quantification of growth rate

The growth rate was computed using the area of segmented cells over time.

Globularization score

The Ilv3-mCherry globularization score was measured in each cell by calculating, at each timepoint, the mean intensity of the 5 brightest pixels of the cell minus the rest of the other pixels.

Calibration of the cytosolic pH probe:

As described in (Mouton et al. 2020), 2 mL of exponentially growing culture with OD600 of 0.5 were centrifuged and resuspended in 200 µL calibration buffer (50 mM

MES, 50 mM HEPES, 50 mM KCl, 50 mM NaCl, 200 mM NH4CH3CO2) at pH 5, 5.5, 6, 6.5, 7, 7.5, and 8. To complete these buffers, drugs blocking the glycolysis were added: 75 µM monensin, 10 µM nigericin, 10 mM 2-deoxyglucose, and 10 mM NaN3 (final concentrations) to each buffer. The cells were then exposed 30min to the drug and their fluorescent was quantified in the microfluidic device (Fig S1G).

Fraction of cells with foci

The fraction of cells displaying a foci of GFP was manually scored at different timepoints.

Displacement of fluorescent foci

The fluorescent foci in each cell was detected using the centroid position of the 5 brightest pixels. Doing this for each frame then allows the computation of the frame-to-frame displacement of these foci.

Foci and lipid droplet freezing

The freezing of the Gln1-GFP foci as well as the lipid droplets was manually measured for each cell.

Piecewise linear fit and regime transition

To determine the limit between two regimes, a piecewise linear fit was done on the total number of cells (using the Shape Language Modeling Matlab addon). The point where the slope of the linear fit changes was defined as the time of transition (See Fig S1E).

(John D'Errico (2020). SLM - Shape Language Modeling (https://www.mathworks.com/matlabcentral/fileexchange/24443-slm-shape-language-modeling, MATLAB Central File Exchange), Retrieved November 2, 2020.)

Extend of pH drop

The beginning and end of the pH drops was determined using a piecewise linear fitting with a method similar than for regime transition.

Figures :

Figure1 :

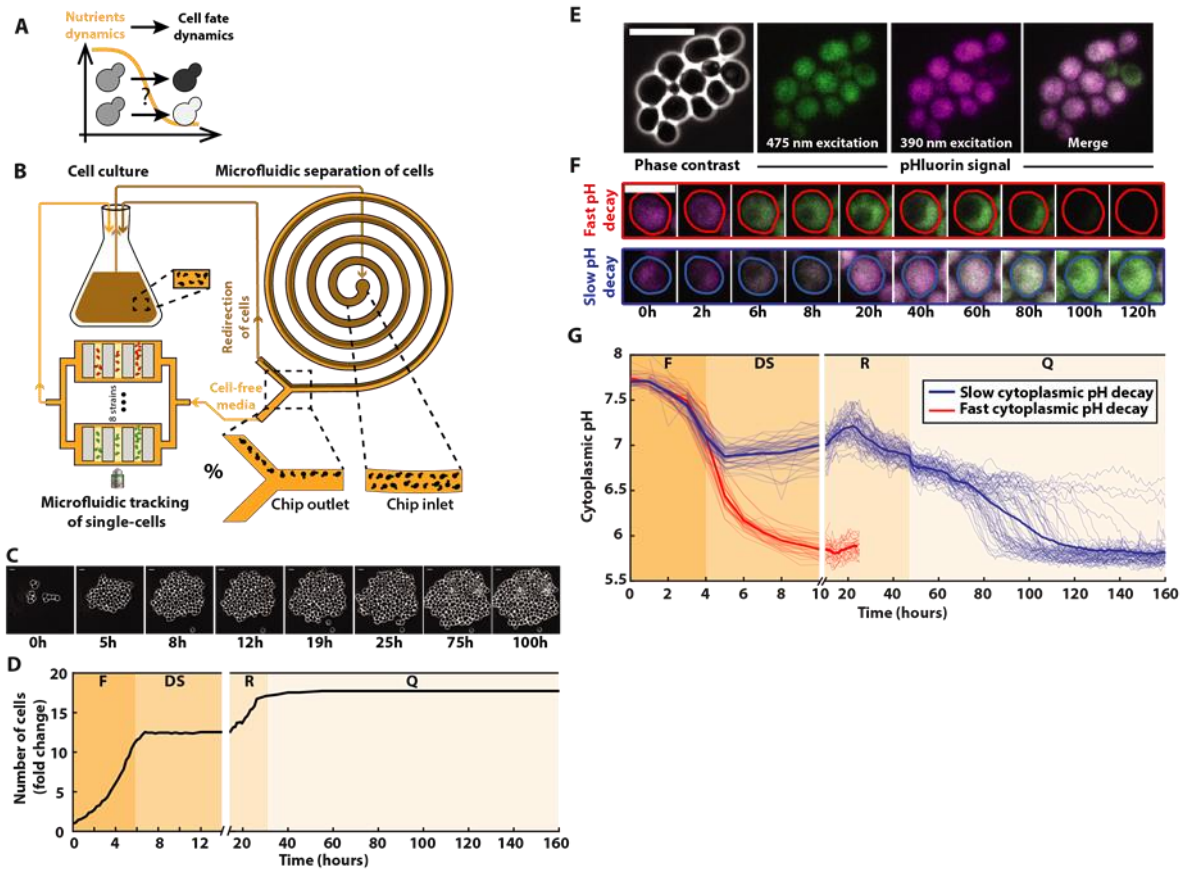

Figure 1 - A microfluidic platform for single cell tracking during the yeast proliferation cycle

(A) Schematics representing the main question addressed in this study, namely how the dynamics of environmental changes shapes non-uniform cellular responses and distinct cellular fates in a clonal population. **(B)** Schematics representing the liquid culture flask, the microfluidic device with trapped cells for optical imaging and the microfluidic device designed to redirect cells back to the liquid culture and to recirculate medium to the chamber filled with trapped cells. **(C)** Sequence of phase contrast images of cells growing in the microfluidic device; the scale bar represents 10.8 microns. **(D)** Fold increase in cell number over an entire life cycle; Each shaded area represents a distinct proliferation phase, which was determined using piecewise linear fitting to cell proliferation data (see Methods and S1E for details): fermentation (F), diauxic-shift (DS), respiration (R), Quiescence (Q); **(E)** Cluster of cells showing typical phase contrast, fluorescence and overlay images using the cytoplasmic pH sensor pHluorin. The scale bar represents 10.8 microns. **(F)** Typical sequences of overlaid fluorescence images obtained with the pHluorin sensor at indicated time points. Colored lines indicate cell contours. The scale bar represents 5.4 microns. **(G)** Quantification of absolute cytoplasmic pH as a function of time; Each line represents an individual cell, while the bold line indicates the average among cells with either an early decaying pH (red) or late decaying pH (blue).

Figure1 Supp :

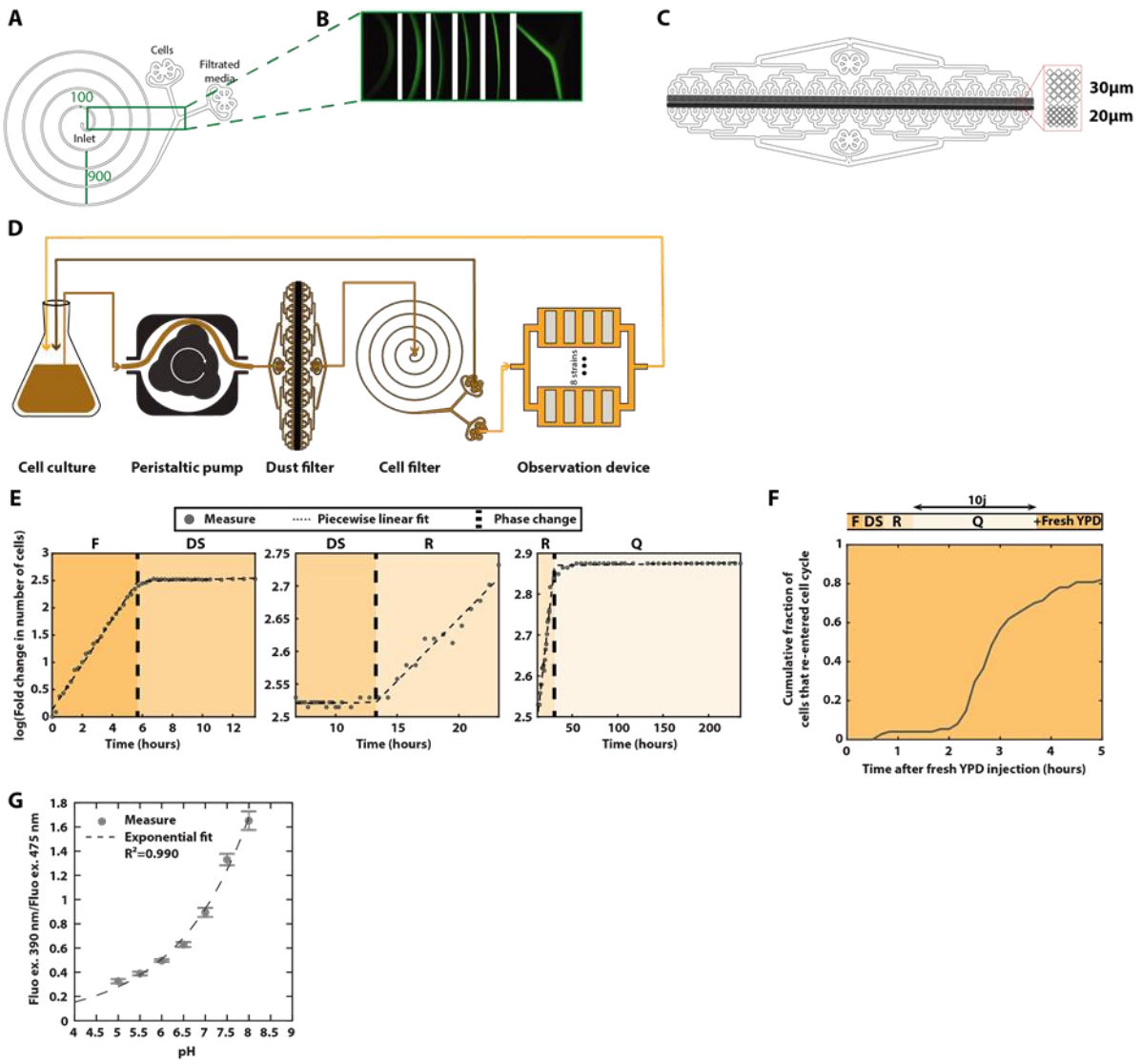

(A) Design of the cell filtering device; A spiral composed of 5 loops of 100µm width, separated by 900µm passively segregate ~5µm objects to the inside of the channel; The cells go from the center of the spiral to the outside and concentrate to the inside outlet while the outside one is almost cell free**.(B)** Images of TDH3-GFP cells being filtered; Each image represents a loop, from the inside to the outside**.(C)** Design of the dust filter device; It is composed of two subsequent arrays of squares with 30µm and 20µm size threshold. **(D)** Schematics of the whole closed-loop fluidic plateform; The flask is connected to a peristaltic pump, in turn connected to the dust filter. The dust-free media then flows in the inlet of the spiral. The cell outlet of the spiral is redirected into the flask while the cell-free outlet irrigates the observation device. To complete the closure of the loop, the outlet of the observation device is connected to the flask. **(E)** Determination of the metabolic transitions of the culture; A piecewise linear fit on the number of cells defines the limit between F and DS (left), DS and R (middle) or R and Q (right). Grey dots represent the measured number of cells, thin dashed lines

represent the fitting and thick dashed lines the transition time. Each shaded area represents a distinct proliferation phase **(F)** Cumulative fraction overtime of cells re-entering cell-cycle after 10 days in quiescence, when exposed to fresh YPD. **(G)** Calibration curve of the pHluorin probe; Grey dots represent the ratio of fluorescence collected while exciting at 390nm over the fluorescence collected while exciting at 475 nm, N=20; The dashed line correspond to an exponential fit f(x) = a*exp(b*x) of parameters (with 95% confidence bounds): a=0.01419 (0.005774, 0.0226) and b=0.5967 (0.5174, 0.6761)

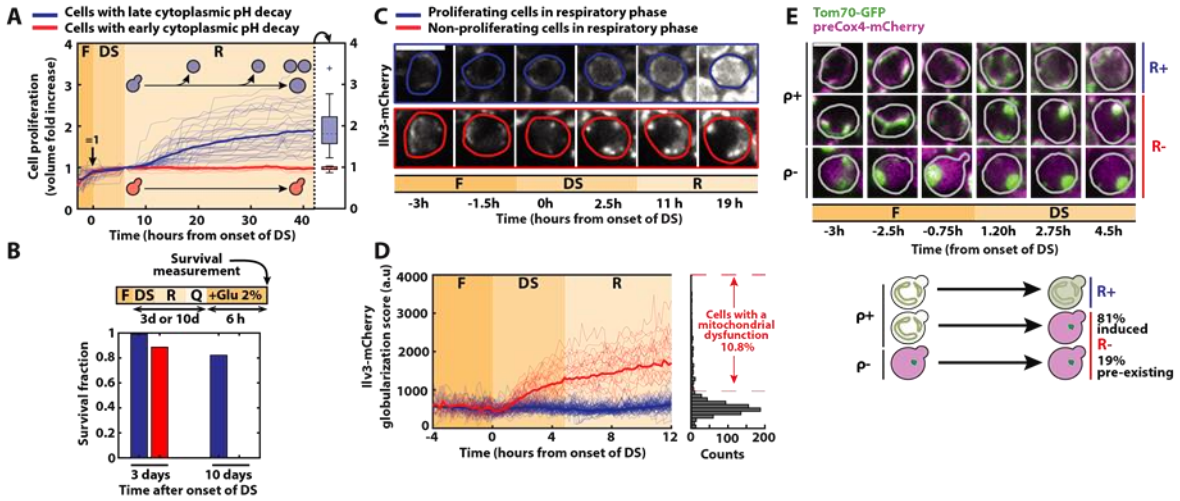

Figure 2 - Divergent cell fates induced by a metabolic challenge at the DS

(A) Quantification of single-cell growth during F, DS, and R phases, as defined in Fig. 1; Each line represents the volume increase of single-cell over time, normalized by cell volume at the end of the DS; The red and blue bold line represent the averages over all the cells that experience fast and slow pH decay, respectively; Right: box plot indicating the fold increase in cell volume in each subpopulation during the R phase; **(B)** Fraction of surviving cells among adapting (blue bars) and non-adapting (red bars) cells, measured by quantifying the cells' ability to resume growth 6h after feeding them with fresh medium (2% glucose) either 3 or 10 days after the DS; The scale bar represents 5 microns; **(C)** Typical sequence of fluorescence images obtained with the Ilv3-mCherry mitochondrial marker at indicated time points; Each strip represents a different field of view and the colored contours indicate a cell of interest. **(D)** Single-cell quantification of a globularization score from fluorescence images over time for both adapting (blue line) and non-adapting cells (red line); The bold lines represents averages within each subpopulation; Right: histogram of globularization score for each cell. **(F)** Pre-existing versus triggered respiratory defects in cells passing the DS; Sequence of fluorescence images (overlay of preCox4-mCherry and Tom70-GFP) obtained at indicated times. The scale bar represents 5 microns; Each strip represents a different type of cell fates (top : rho+ R+; middle: rho+ R-; bottom: rho- R-); Schematics: representation of the different cell fates based on the fluorescence patterns of preCox4-mCherry and Tom70-GFP; Right: quantification of the fraction of each subpopulation. **(G)** Heritability of the R+ and R- phenotype; Sample lineage of cells that pass the DS; Each horizontal bar represents a single cell using a specific color-code for R+ (blue), R- (red); The respiratory status is undetermined before the DS hence all the cells are displayed in grey before the DS;

Figure 2 Supp

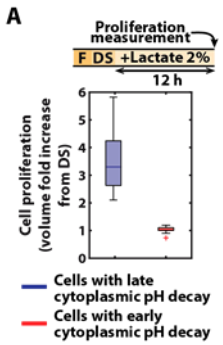

Supplementary Figure 2

(A) Proliferation capacity in a respirative media; Box plot indicating the fold increase in cell volume from DS, in each subpopulation (Blue for cells with a late cytoplasmic pH decay, red for cells with an early cytoplasmic pH decay), 12h after exposing cells to 2% Lactate respirative media after the DS.

Figure 3:

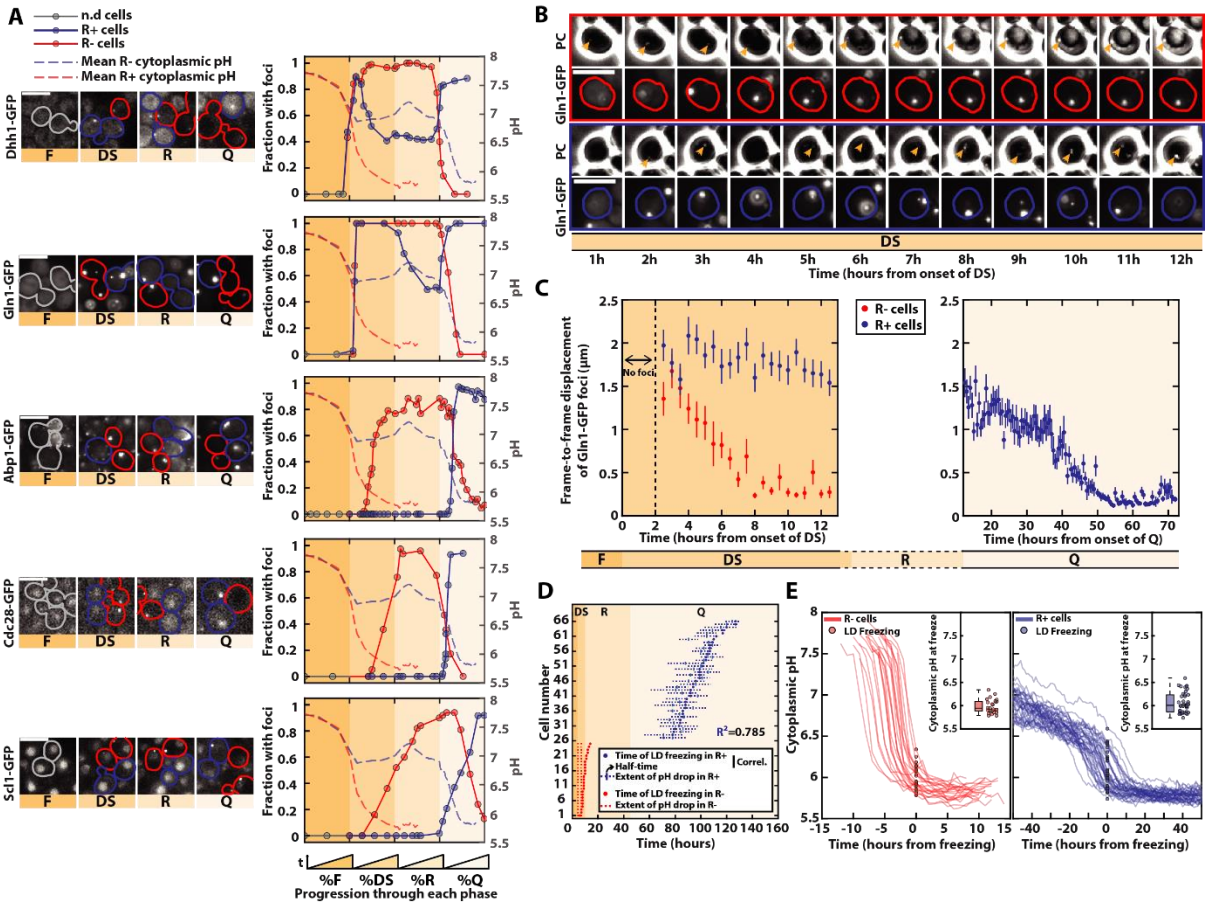

Figure 3 - pH-driven phase-transition to a gel-like state during entry into quiescence

A) Observation and quantification of fluorescence foci formation for indicated fluorescent fusion proteins (Dhh1-GFP, Gln1-GFP, Abp1-GFP, Cdc28-GFP, Scl1-GFP); Left: Each strip of fluorescence images displays unrelated cells at different phases during entry into quiescence; Colored contours indicate cells of interest (red for R- cells, blue for R+ cells, grey before the DS); Right: quantification of the fraction of cells with foci for each indicated fluorescent marker, as a function of the normalized time spent in each phase of entry into quiescence; Each solid colored line represents an indicated subpopulation of cells; The dashed colored lines represents an overlay the evolution of pH with time, based on data obtained in Figure 1; B) Mobility of Gln1-GFP fluorescent foci and observation of lipid droplets (LD); Sequence of phase contrast and Gln1-GFP fluorescence images at indicated timepoints; The colored contours indicate the cells of interest (red and blue for R- and R+ cells, respectively); The orange arrows on the phase contrast images indicate the lipid droplet; C) Mobility of Gln1-GFP fluorescent foci; Quantification of average frame-by-frame displacement of Gln1-GFP foci for R+ and R- cells (blue and red points, respectively); Quantification starts after appearance of foci (t > 2 hours after the onset of DS); Error bars represent the standard-error-on-mean; The right plot only features R+ cells, since Gln1-GFP foci are no longer present in the Q phase in R- cells; D) Temporal link between the drop in

internal pH and the time of freezing of LD; Each line corresponds to a single cells and represents the extent of pH drop (see Material and methods for details) and the time of LD freezing; F) Measurement of internal pH at the time of LD freezing; Overlay of internal pH in single cells obtained after synchronizing all traces with respect to the time of LD freezing, for R+ (left) and R- cells (right); Each dot represents the pH at the time of freezing in each cell; Inset: boxplot showing the distribution of pH values of each single cell at the time of LD freezing;

Figure 3 Supp

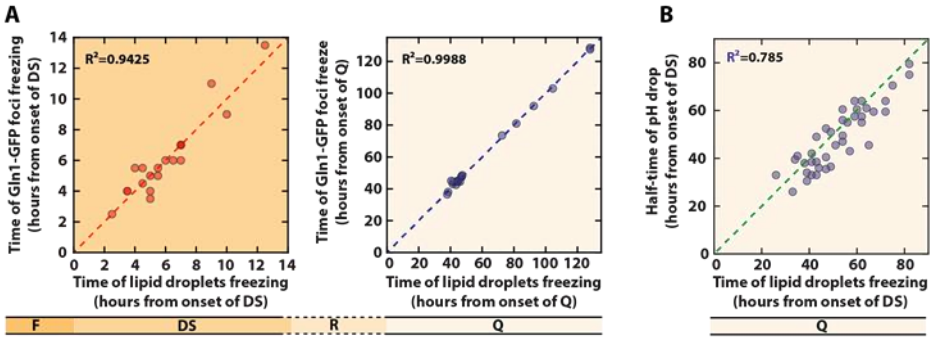

Supplementary Figure 3

(A) Correlation of Gln1-GFP foci freezing with the lipid droplet (LD) freezing in R- (left) or R+ (right) cells; The time origin is the proliferation arrest of these cells, respectively the onset of DS and the onset of Q; The dashed lines correspond to y=x. **(B)** Correlation of the half-time of the pH drop with the LD freezing, in R+ cells; The time origin is at the onset of Q; The dashed lines correspond to y=x.

DISCUSSION

a. Methodological validation: unraveling the early origin of the fate divergency between quiescent and non-quiescent cells in the budding yeast life cycle

In this work, we developed a microfluidic-based single-cell ecology platform that enables us to follow single individual yeast cells over up to 10 days, demonstrating the efficiency of our methodology.

Using the internal pH sensor pHluorin, we unraveled the complex metabolic routes followed by yeast cells during their life cycle, from fermentation to quiescence establishment. Most importantly, we unraveled that two cell populations diverged early in the life cycle. One of them exhibited a fast pH drop within ~90 min following glucose exhaustion, thus days before 'normal' entry into quiescence. While we confirmed that this population exhibited a very poor viability under starvation, we surprisingly observed that those cells exhibited several hallmarks of typical quiescent cells also right after glucose exhaustion. Indeed, after several days of quiescence, those cells had been considered as 'non-quiescent' based on the absence of quiescence hallmarks such as PSG (Laporte et al., 2018a) and poor viability (Allen et al., 2006). Our observation tends to suggest that their low viability results from their inability to sustain into quiescence rather than their inability to enter into quiescence. In agreement with this, Ocampo et al., showed that the low viability of mitochondrial deficient rho^0 cells could be fully rescued by adding trehalose in the medium. This tends to demonstrate that those R- cells have an important metabolic defect but

however conserve the ability to enter quiescence thanks to metabolic rescue (Ocampo et al., 2012).

Overall, our study therefore enables to unravel the onset of fate divergency (at DS) between the two populations previously described as ‘quiescent’ and ‘non-quiescent’ (Allen et al., 2006) in clonal budding yeast populations.

Altogether, this context enabled us to validate our methodology by showing its ability to capture transient and heterogeneous plastic behaviours previously undetected with the use of classical methodologies.

b. Role of respiration in phase transition

Taking advantage of those R- cells, we also investigated how respiration was affecting the biophysical properties of cells, in particular the liquid to solid phase transition commonly observed in response to starvation (Munder et al., 2016; Parry et al., 2014; Riback et al., 2017). Most importantly, our methodology enabled us to describe if and how cytoplasm gelification occurs in a naturally degrading environment. Both in R- and R+ cells, the pH drop was accompanied by a strong cytoplasmic gelification. If our data are correlative, we argue that the strong *in vitro* evidence that protein aggregation and cytoplasmic freezing are dependent upon pH acidification (Adame-Arana et al., 2020; Alberti et al., 2019; Franzmann et al., 2018; Riback et al., 2017). This suggests a link of causation in our data. Indeed, we strikingly observed that both in R- and R+

cells, the cytoplasm froze at pH ~6, thus in agreement with data obtained in synthetic conditions (Munder et al., 2016). Following on that, we can hypothesize that in response to a naturally evolving environment, while the pH at which phase transition occurs is not different than in synthetic conditions, it is rather the dynamics at which it occurs that is dramatically changed. Indeed, we observed that the pH dropped for some R+ cells more than 5 days after their complete growth cessation. On the contrary, in response to brutal synthetic starvation, cytoplasmic freezing occurs within seconds (Munder et al., 2016). It is quite likely that such a discrepancy between both dynamics dramatically influence the ability of cells to cope with stressors. Thus, we argue that our methodology may represent a breakthrough technology to approach at the single-cell level ecologically relevant microbial behaviours. We speculate that in other complex ecological environments our methodology could also have promising applications.

Bibliography

Adame-Arana, O., Weber, C.A., Zaburdaev, V., Prost, J., and Jülicher, F. (2020). Liquid Phase Separation Controlled by pH. Biophys. J. *119*, 1590–1605.
Alberti, S., Gladfelter, A., and Mittag, T. (2019). Considerations and Challenges in Studying Liquid-Liquid Phase Separation and Biomolecular Condensates. Cell *176*, 419–434.
Alepuz, P.M., Jovanovic, A., Reiser, V., and Ammerer, G. (2001). Stress-Induced MAP Kinase Hog1 Is Part of Transcription Activation Complexes pression of mammalian cells by the ets-related factor ERF (Le Gallic et al., 1999). In some cases, both negative and positive regulators are targeted by the activated butions can vary considerably with specific promoters.
Allen, C., Büttner, S., Aragon, A.D., Thomas, J.A., Meirelles, O., Jaetao, J.E., Benn, D., Ruby, S.W., Veenhuis, M., Madeo, F., et al. (2006). Isolation of quiescent and nonquiescent cells from yeast stationary-phase cultures. J. Cell Biol. *174*, 89–100.
Alon, U. (2007). Network motifs: Theory and experimental approaches. Nat. Rev. Genet. *8*, 450–461.
Amato, S.M., Orman, M.A., and Brynildsen, M.P. (2013). Metabolic Control of Persister Formation in Escherichia coli. Mol. Cell *50*, 475–487.
Ashe, M.P., De Long, S.K., and Sachs, A.B. (2000). Glucose depletion rapidly inhibits translation initiation in yeast. Mol. Biol. Cell *11*, 833–848.
Ayer, A., Tan, S.X., Grant, C.M., Meyer, A.J., Dawes, I.W., and Perrone, G.G. (2010). The critical role of glutathione in maintenance of the mitochondrial genome. Free Radic. Biol. Med. *49*, 1956–1968.
Balaban, N.Q., Merrin, J., Chait, R., Kowalik, L., and Leibler, S. (2004a). Bacterial persistence as a phenotypic switch. Science (80-.). *305*, 1622–1625.
Balaban, N.Q., Merrin, J., Chait, R., Kowalik, L., and Leibler, S. (2004b). Bacterial persistence as a phenotypic switch. Science (80-.). *305*, 1622–1625.
Balaban, N.Q., Helaine, S., Lewis, K., Ackermann, M., Aldridge, B., Andersson, D.I., Brynildsen, M.P., Bumann, D., Camilli, A., Collins, J.J., et al. (2019). Definitions and guidelines for research on antibiotic persistence. Nat. Rev. Microbiol. *17*, 441–448.
Belousov, V. V., Fradkov, A.F., Lukyanov, K.A., Staroverov, D.B., Shakhbazov, K.S., Terskikh, A. V., and Lukyanov, S. (2006). Genetically encoded fluorescent indicator

for intracellular hydrogen peroxide. Nat. Methods *3*, 281–286.
Berman, J., and Krysan, D.J. (2020). Drug resistance and tolerance in fungi. Nat. Rev. Microbiol. *18*, 319–331.
Bernard, C. INTRODUCTION À L'ÉTUDE DE LA MÉDECINE EXPÉRIMENTALE.
Berry, D.B., and Gasch, A.P. (2008). Stress-activated genomic expression changes serve a preparative role for impending stress in yeast. Mol. Biol. Cell *19*, 4580–4587.
Bigger, J.W. (1944). TREATMENT OF STAPHYLOCOCCAL INFECTIONS WITH PENICILLIN BY INTERMITTENT STERILISATION. Lancet *244*, 497–500.
Bilan, D.S., and Belousov, V. V. (2016). HyPer Family Probes: State of the Art. Antioxidants Redox Signal. *24*, 731–751.
Biteau, B., Labarre, J., and Toledano, M.B. (2003). ATP-dependent reduction of cysteine-sulphinic acid by S. cerevisiae sulphiredoxin. Nature *425*, 980–984.
Blair, J.M.A., Webber, M.A., Baylay, A.J., Ogbolu, D.O., and Piddock, L.J.V. (2015). Molecular mechanisms of antibiotic resistance. Nat. Rev. Microbiol. *13*, 42–51.
Bodvard, K., Peeters, K., Roger, F., Romanov, N., Igbaria, A., Welkenhuysen, N., Palais, G., Reiter, W., Toledano, M.B., Käll, M., et al. (2017). Light-sensing via hydrogen peroxide and a peroxiredoxin. Nat. Commun. *8*, 1–11.
Boisnard, S., Lagniel, G., Garmendia-Torres, C., Molin, M., Boy-Marcotte, E., Jacquet, M., Toledano, M.B., Labarre, J., and Chédin, S. (2009). H2O2 activates the nuclear localization of Msn2 and Maf1 through thioredoxins in Saccharomyces cerevisiae. Eukaryot. Cell *8*, 1429–1438.
Bontron, S., Jaquenoud, M., Vaga, S., Talarek, N., Bodenmiller, B., Aebersold, R., and De Virgilio, C. (2013). Yeast Endosulfines Control Entry into Quiescence and Chronological Life Span by Inhibiting Protein Phosphatase 2A. Cell Rep. *3*, 16–22.
Brauner, A., Fridman, O., Gefen, O., and Balaban, N.Q. (2016). Distinguishing between resistance, tolerance and persistence to antibiotic treatment. Nat. Rev. Microbiol. *14*, 320–330.
Bresson, S., Shchepachev, V., Spanos, C., Turowski, T.W., Rappsilber, J., and Tollervey, D. (2020). Stress-Induced Translation Inhibition through Rapid Displacement of Scanning Initiation Factors. Mol. Cell.
Broach, J.R. (2012). Nutritional control of growth and development in yeast. Genetics *192*, 73–105.
Broach, J.R., and Deschenes, R.J. (1990). The function of ras genes in: Saccharomyces cerevisiae. Adv. Cancer Res. *54*, 79–139.
Buchan, J.R., Muhlrad, D., and Parker, R. (2008). P bodies promote stress granule assembly in Saccharomyces cerevisiae. J. Cell Biol. *183*, 441–455.
Cameron, S., Levin, L., Zoller, M., and Wigler, M. (1988). cAMP-independent control of sporulation, glycogen metabolism, and heat shock resistance in S. cerevisiae. Cell *53*, 555–566.
Campbell, K., Vowinckel, J., Keller, M.A., and Ralser, M. (2016). Methionine Metabolism Alters Oxidative Stress Resistance via the Pentose Phosphate Pathway. Antioxidants Redox Signal. *24*, 543–547.
Cannon, W. (1932). The wisdom of the body, (New York: W.W. Norton & Company Inc.).
Cannon, J.F., and Tatchell, K. (1987). Characterization of Saccharomyces cerevisiae genes encoding subunits of cyclic AMP-dependent protein kinase. Mol. Cell. Biol. *7*, 2653–2663.
Cao, L., Tang, Y., Quan, Z., Zhang, Z., Oliver, S.G., and Zhang, N. (2016). Chronological Lifespan in Yeast Is Dependent on the Accumulation of Storage Carbohydrates Mediated by Yak1, Mck1 and Rim15 Kinases. PLOS Genet. *12*,

e1006458.
Capaldi, A.P., Kaplan, T., Liu, Y., Habib, N., Regev, A., Friedman, N., and O'shea, E.K. (2008). Structure and function of a transcriptional network activated by the MAPK Hog1. Nat. Genet. *40*, 1300–1306.
Casado, C., González, A., Platara, M., Ruiz, A., and Ariño, J. (2011). The role of the protein kinase A pathway in the response to alkaline pH stress in yeast. Biochem. J. *438*, 523–533.
Causton, H.C., Ren, B., Sang Seok Koh, Harbison, C.T., Kanin, E., Jennings, E.G., Tong Ihn Lee, True, H.L., Lander, E.S., and Young, R.A. (2001). Remodeling of yeast genome expression in response to environmental changes. Mol. Biol. Cell *12*, 323–337.
Cerulus, B., Jariani, A., Perez-Samper, G., Vermeersch, L., Pietsch, J.M.J., Crane, M.M., New, A.M., Gallone, B., Roncoroni, M., Dzialo, M.C., et al. (2018). Transition between fermentation and respiration determines history-dependent behavior in fluctuating carbon sources. Elife *7*.
Chandel, N.S. (2015). Navigating Metabolism.
Chang, Y.W., Howard, S.C., and Herman, P.K. (2004). The Ras/PKA signaling pathway directly targets the Srb9 protein, a component of the general RNA polymerase II transcription apparatus. Mol. Cell *15*, 107–116.
Chechik, G., Oh, E., Rando, O., Weissman, J., Regev, A., and Koller, D. (2008). Activity motifs reveal principles of timing in transcriptional control of the yeast metabolic network. Nat. Biotechnol. *26*, 1251–1259.
Chen, L., Zhang, Z., Hoshino, A., Zheng, H.D., Morley, M., Arany, Z., and Rabinowitz, J.D. (2019). NADPH production by the oxidative pentose-phosphate pathway supports folate metabolism. Nat. Metab. *1*, 404–415.
Christodoulou, D., Link, H., Fuhrer, T., Kochanowski, K., Gerosa, L., and Sauer, U. (2018). Reserve Flux Capacity in the Pentose Phosphate Pathway Enables Escherichia coli's Rapid Response to Oxidative Stress.
Cieśla, M., Towpik, J., Graczyk, D., Oficjalska-Pham, D., Harismendy, O., Suleau, A., Balicki, K., Conesa, C., Lefebvre, O., and Boguta, M. (2007). Maf1 Is Involved in Coupling Carbon Metabolism to RNA Polymerase III Transcription. Mol. Cell. Biol. *27*, 7693–7702.
Cohen, N.R., Lobritz, M.A., and Collins, J.J. (2013). Microbial persistence and the road to drug resistance. Cell Host Microbe *13*, 632–642.
Coller, J., and Parker, R. (2005). General translational repression by activators of mRNA decapping. Cell *122*, 875–886.
Conrad, M., Schothorst, J., Kankipati, H.N., Van Zeebroeck, G., Rubio-Texeira, M., and Thevelein, J.M. (2014). Nutrient sensing and signaling in the yeast *Saccharomyces cerevisiae*. FEMS Microbiol. Rev. *38*, 254–299.
Corvol, P., and Pierre (2013). Claude Bernard et la médecine expérimentale au Collège de France. Http://Journals.Openedition.Org/Lettre-Cdf 19–21.
D'Autréaux, B., and Toledano, M.B. (2007). ROS as signalling molecules: Mechanisms that generate specificity in ROS homeostasis. Nat. Rev. Mol. Cell Biol. *8*, 813–824.
Delaunay, A., Isnard, A.D., and Toledano, M.B. (2000a). H2O2 sensing through oxidation of the Yap1 transcription factor. EMBO J. *19*, 5157–5166.
Delaunay, A., Isnard, A.D., and Toledano, M.B. (2000b). H2O2 sensing through oxidation of the Yap1 transcription factor. EMBO J. *19*, 5157–5166.
Delaunay, A., Pflieger, D., Barrault, M.B., Vinh, J., and Toledano, M.B. (2002). A thiol peroxidase is an H2O2 receptor and redox-transducer in gene activation. Cell *111*,

471–481.
Dick, T.P., and Ralser, M. (2015a). Metabolic Remodeling in Times of Stress: Who Shoots Faster than His Shadow? Mol. Cell *59*, 519–521.
Dick, T.P., and Ralser, M. (2015b). Metabolic Remodeling in Times of Stress: Who Shoots Faster than His Shadow? Mol. Cell *59*, 519–521.
Dimitrov, L.N., Brem, R.B., Kruglyak, L., and Gottschling, D.E. (2009). Polymorphisms in multiple genes contribute to the spontaneous mitochondrial genome instability of Saccharomyces cerevisiae S288C strains. Genetics *183*, 365–383.
Domènech, A., Ayté, J., Antunes, F., and Hidalgo, E. (2018). Using in vivo oxidation status of one- and two-component redox relays to determine H2O2 levels linked to signaling and toxicity. BMC Biol. *16*, 1–15.
Enenkel, C. (2018). The paradox of proteasome granules. Curr. Genet. *64*, 137–140.
Fernandes, L., Rodrigues-Pousada, C., and Struhl, K. (1997). Yap, a novel family of eight bZIP proteins in Saccharomyces cerevisiae with distinct biological functions. Mol. Cell. Biol. *17*, 6982–6993.
Fisher, R.A., Gollan, B., and Helaine, S. (2017). Persistent bacterial infections and persister cells. Nat. Rev. Microbiol. *15*, 453–464.
Fletcher, D.A., and Mullins, R.D. (2010). Cell mechanics and the cytoskeleton. Nature *463*, 485–492.
Fomenko, D.E., Koc, A., Agisheva, N., Jacobsen, M., Kaya, A., Malinouski, M., Rutherford, J.C., Siu, K.L., Jin, D.Y., Winge, D.R., et al. (2011). Thiol peroxidases mediate specific genome-wide regulation of gene expression in response to hydrogen peroxide. Proc. Natl. Acad. Sci. U. S. A. *108*, 2729–2734.
Fourquet, S., Huang, M.E., D'Autreaux, B., and Toledano, M.B. (2008). The dual functions of thiol-based peroxidases in H2O2 scavenging and signaling. Antioxidants Redox Signal. *10*, 1565–1575.
Franzmann, T.M., Jahnel, M., Pozniakovsky, A., Mahamid, J., Holehouse, A.S., Nüske, E., Richter, D., Baumeister, W., Grill, S.W., Pappu, R. V., et al. (2018). Phase separation of a yeast prion protein promotes cellular fitness. Science (80-.). *359*.
Garrett, S., and Broach, J. (1989). Loss of Ras activity in Saccharomyces cerevisiae is suppressed by disruptions of a new kinase gene, YAKI, whose product may act downstream of the cAMP-dependent protein kinase. Genes Dev. *3*, 1336–1348.
Garrido, E.O., and Grant, C.M. (2002). Role of thioredoxins in the response of Saccharomyces cerevisiae to oxidative stress induced by hydroperoxides. Mol. Microbiol. *43*, 993–1003.
Gasch, A.P., Spellman, P.T., Kao, C.M., Carmel-Harel, O., Eisen, M.B., Storz, G., Botstein, D., and Brown, P.O. (2000). Genomic expression programs in the response of yeast cells to environmental changes. Mol. Biol. Cell *11*, 4241–4257.
Georgiou, G., and Masip, L. (2003). An overoxidation journey with a return ticket. Science (80-.). *300*, 592–594.
Giaever, G., Chu, A.M., Ni, L., Connelly, C., Riles, L., Véronneau, S., Dow, S., Lucau-Danila, A., Anderson, K., André, B., et al. (2002). Functional profiling of the Saccharomyces cerevisiae genome. Nature *418*, 387–391.
Gibney, P.A., Schieler, A., Chen, J.C., Rabinowitz, J.D., and Botstein, D. (2015). Characterizing the in vivo role of trehalose in Saccharomyces cerevisiae using the AGT1 transporter. Proc. Natl. Acad. Sci. U. S. A. *112*, 6116–6121.
Glasauer, A., and Chandel, N.S. (2014). Targeting antioxidants for cancer therapy. Biochem. Pharmacol. *92*, 90–101.
Godon, C., Lagniel, G., Lee, J., Buhler, J.M., Kieffer, S., Perrot, M., Boucherie, H.,

Toledano, M.B., and Labarre, J. (1998). The H2O2 stimulon in Saccharomyces cerevisiae. J. Biol. Chem. *273*, 22480–22489.
Gómez-Schiavon, M., and El-samad, H. (2020). CoRa – A general approach for quantifying biological feedback control. BioRxiv 1–7.
Gonskikh, Y., and Polacek, N. (2017). Alterations of the translation apparatus during aging and stress response. Mech. Ageing Dev. *168*, 30–36.
Görner, W., Durchschlag, E., Martinez-Pastor, M.T., Estruch, F., Ammerer, G., Hamilton, B., Ruis, H., and Schüller, C. (1998). Nuclear localization of the C2H2 zinc finger protein Msn2p is regulated by stress and protein kinase A activity. Genes Dev. *12*, 586–597.
Görner, W., Durchschlag, E., Wolf, J., Brown, E.L., Ammerer, G., Ruis, H., and Schüller, C. (2002). Acute glucose starvation activates the nuclear localization signal of a stress-specific yeast transcription factor. EMBO J. *21*, 135–144.
Goulev, Y., Morlot, S., Matifas, A., Huang, B., Molin, M., Toledano, M.B., and Charvin, G. (2017). Nonlinear feedback drives homeostatic plasticity in H2O2 stress response. Elife *6*.
Grably, M.R., Stanhill, A., Tell, O., and Engelberg, D. (2002). HSF and Msn2/4p can exclusively or cooperatively activate the yeast HSP104 gene. Mol. Microbiol. *44*, 21–35.
Grabowska, D., and Chelstowska, A. (2003). The ALD6 Gene Product is Indispensable for Providing NADPH in Yeast Cells Lacking Glucose-6-Phosphate Dehydrogenase Activity. Downloaded from 2 Downloaded from (JBC Papers in Press).
Granados, A.A., Crane, M.M., Montano-Gutierrez, L.F., Tanaka, R.J., Voliotis, M., and Swain, P.S. (2017). Distributing tasks via multiple input pathways increases cellular survival in stress. Elife *6*, 1–21.
Granados, A.A., Pietsch, J.M.J., Cepeda-Humerez, S.A., Farquhar, I.L., Tkačik, G., and Swain, P.S. (2018). Distributed and dynamic intracellular organization of extracellular information. Proc. Natl. Acad. Sci. U. S. A. *115*, 6088–6093.
Grant, C.M., MacIver, F.H., and Dawes, I.W. (1996). Glutathione is an essential metabolite required for resistance to oxidative stress in the yeast Saccharomyces cerevisiae. Curr. Genet. *29*, 511–515.
Grant, C.M., Perrone, G., and Dawes, I.W. (1998). Glutathione and catalase provide overlapping defenses for protection against hydrogen peroxide in the yeast Saccharomyces cerevisiae. Biochem. Biophys. Res. Commun. *253*, 893–898.
Gray, J. V., Petsko, G.A., Johnston, G.C., Ringe, D., Singer, R.A., and Werner-Washburne, M. (2004a). “Sleeping Beauty”: Quiescence in Saccharomyces cerevisiae. Microbiol. Mol. Biol. Rev. *68*, 187–206.
Gray, J. V., Petsko, G.A., Johnston, G.C., Ringe, D., Singer, R.A., and Werner-Washburne, M. (2004b). “Sleeping Beauty”: Quiescence in Saccharomyces cerevisiae. Microbiol. Mol. Biol. Rev. *68*, 187–206.
Grüning, N.M., Rinnerthaler, M., Bluemlein, K., Mülleder, M., Wamelink, M.M.C., Lehrach, H., Jakobs, C., Breitenbach, M., and Ralser, M. (2011). Pyruvate kinase triggers a metabolic feedback loop that controls redox metabolism in respiring cells. Cell Metab. *14*, 415–427.
Guan, Q., Haroon, S., Bravo, D.G., Will, J.L., and Gasch, A.P. (2012). Cellular memory of acquired stress resistance in Saccharomyces cerevisiae. Genetics *192*, 495–505.
Gutscher, M., Sobotta, M.C., Wabnitz, G.H., Ballikaya, S., Meyer, A.J., Samstag, Y., and Dick, T.P. (2009). Proximity-based protein thiol oxidation by H2O2-scavenging

peroxidases. J. Biol. Chem. *284*, 31532–31540.
Hall, A., Karplus, P.A., and Poole, L.B. (2009). Typical 2-Cys peroxiredoxins - Structures, mechanisms and functions. FEBS J. *276*, 2469–2477.
Hanzén, S., Vielfort, K., Yang, J., Roger, F., Andersson, V., Zamarbide-Forés, S., Andersson, R., Malm, L., Palais, G., Biteau, B., et al. (2016). Lifespan Control by Redox-Dependent Recruitment of Chaperones to Misfolded Proteins. Cell *166*, 140–151.
Harms, A., Maisonneuve, E., and Gerdes, K. (2016). Mechanisms of bacterial persistence during stress and antibiotic exposure. Science (80-.). *354*.
Hasan, R., Leroy, C., Isnard, A.D., Labarre, J., Boy-Marcotte, E., and Toledano, M.B. (2002). The control of the yeast H2O2 response by the Msn2/4 transcription factors. Mol. Microbiol. *45*, 233–241.
Hedbacker, K., and Carlson, M. (2008). SNF1/AMPK pathways in yeast. Front. Biosci. *13*, 2408–2420.
Heimlicher, M.B., Bächler, M., Liu, M., Ibeneche-Nnewihe, C., Florin, E.L., Hoenger, A., and Brunner, D. (2019). Reversible solidification of fission yeast cytoplasm after prolonged nutrient starvation. J. Cell Sci. *132*.
Heng, Y.W., and Koh, C.G. (2010). Actin cytoskeleton dynamics and the cell division cycle. Int. J. Biochem. Cell Biol. *42*, 1622–1633.
Hohmann, S. (2002). Osmotic Stress Signaling and Osmoadaptation in Yeasts. Microbiol. Mol. Biol. Rev. *66*, 300–372.
Howard, S.C., Hester, A., and Herman, P.K. (2003). The Ras/PKA Signaling Pathway May Control RNA Polymerase II Elongation via the Spt4p/Spt5p Complex in Saccharomyces cerevisiae. Genetics *165*, 1059–1070.
Hyslop, P.A., Hinshawz, D.B., Halsey, W.A., Schraufstatter, I.U., Sauerhebery, R.D., Spraggj, R.G., Jackson, J.H., and Cochrane, C.G. (1988). Mechanisms of oxidant-mediated cell injury. J. Biol. Chem. *263*.
Iraqui, I., Kienda, G., Soeur, J., Faye, G., Baldacci, G., Kolodner, R.D., and Huang, M.-E. (2009). Peroxiredoxin Tsa1 Is the Key Peroxidase Suppressing Genome Instability and Protecting against Cell Death in Saccharomyces cerevisiae. PLoS Genet. *5*, e1000524.
Izawa, S., Inoue, Y., and Kimura, A. (1996). Importance of catalase in the adaptive response to hydrogen peroxide: Analysis of acatalasaemic Saccharomyces cerevisiae. Biochem. J. *320*, 61–67.
Jamieson, D.J. (1998). Oxidative stress responses of the yeast Saccharomyces cerevisiae. Yeast *14*, 1511–1527.
Jang, H.H., Lee, K.O., Chi, Y.H., Jung, B.G., Park, S.K., Park, J.H., Lee, J.R., Lee, S.S., Moon, J.C., Yun, J.W., et al. (2004). Two enzymes in one: Two yeast peroxiredoxins display oxidative stress-dependent switching from a peroxidase to a molecular chaperone function. Cell *117*, 625–635.
Jeong, J.S., Kwon, S.J., Kang, S.W., Rhee, S.G., and Kim, K. (1999). Purification and characterization of a second type thioredoxin peroxidase (Type II TPx) from Saccharomyces cerevisiae. Biochemistry *38*, 776–783.
Jorgensen, P., Nishikawa, J.L., Breitkreutz, B.J., and Tyers, M. (2002). Systematic identification of pathways that couple cell growth and division in yeast. Science (80-.). *297*, 395–400.
Joyner, R.P., Tang, J.H., Helenius, J., Dultz, E., Brune, C., Holt, L.J., Huet, S., Müller, D.J., and Weis, K. (2016). A glucose-starvation response regulates the diffusion of macromolecules. Elife *5*.
Khademian, M., and Imlay, J.A. Escherichia coli cytochrome c peroxidase is a

respiratory oxidase that enables the use of hydrogen peroxide as a terminal electron acceptor.
Klosinska, M.M., Crutchfield, C.A., Bradley, P.H., Rabinowitz, J.D., and Broach, J.R. (2011). Yeast cells can access distinct quiescent states. Genes Dev. *25*, 336–349.
Kritsiligkou, P., Rand, J.D., Weids, A.J., Wang, X., Kershaw, C.J., and Grant, C.M. (2018). Endoplasmic reticulum (ER) stress–induced reactive oxygen species (ROS) are detrimental for the fitness of a thioredoxin reductase mutant. J. Biol. Chem. *293*, 11984–11995.
Kuehne, A., Emmert, H., Soehle, J., Winnefeld, M., Fischer, F., Wenck, H., Gallinat, S., Terstegen, L., Lucius, R., Hildebrand, J., et al. (2015). Acute Activation of Oxidative Pentose Phosphate Pathway as First-Line Response to Oxidative Stress in Human Skin Cells. Mol. Cell *59*, 359–371.
Kuge, S., and Jones, N. (1994). YAP1 dependent activation of TRX2 is essential for the response of Saccharomyces cerevisiae to oxidative stress by hydroperoxides. EMBO J. *13*, 655–664.
Kuge, S., Jones, N., and Nomoto, A. (1997). Regulation of yAP-1 nuclear localization in response to oxidative stress. EMBO J. *16*, 1710–1720.
Laporte, D., Salin, B., Daignan-Fornier, B., and Sagot, I. (2008). Reversible cytoplasmic localization of the proteasome in quiescent yeast cells. J. Cell Biol. *181*, 737–745.
Laporte, D., Lebaudy, A., Sahin, A., Pinson, B., Ceschin, J., Daignan-Fornier, B., and Sagot, I. (2011). Metabolic status rather than cell cycle signals control quiescence entry and exit. J. Cell Biol. *192*, 949–957.
Laporte, D., Courtout, F., Salin, B., Ceschin, J., and Sagot, I. (2013). An array of nuclear microtubules reorganizes the budding yeast nucleus during quiescence. J. Cell Biol. *203*, 585–594.
Laporte, D., Gouleme, L., Jimenez, L., Khemiri, I., and Sagot, I. (2018a). Mitochondria reorganization upon proliferation arrest predicts individual yeast cell fate. Elife *7*.
Laporte, D., Jimenez, L., Gouleme, L., and Sagot, I. (2018b). Yeast quiescence exit swiftness is influenced by cell volume and chronological age. Microb. Cell *5*, 104–111.
Lee, J.-C., Straffon, M.J., Jang, T.-Y., Higgins, V.J., Grant, C.M., and Dawes, I.W. (2001). The essential and ancillary role of glutathione in Saccharomyces cerevisiae analysed using a grande gsh1 disruptant strain . FEMS Yeast Res. *1*, 57–65.
Lee, J., Godon, C., Lagniel, G., Spector, D., Garin, J., Labarre, J., and Toledano, M.B. (1999a). Yap1 and Skn7 control two specialized oxidative stress response regulons in yeast. J. Biol. Chem. *274*, 16040–16046.
Lee, J., Spector, D., Godon, C., Labarre, J., and Toledano, M.B. (1999b). A new antioxidant with alkyl hydroperoxide defense properties in yeast. J. Biol. Chem. *274*, 4537–4544.
Lee, J., Spector, D., Godon, C., Labarre, J., and Toledano, M.B. (1999c). A New Antioxidant with Alkyl Hydroperoxide Defense Properties in Yeast*.
Leichert, L.I., Gehrke, F., Gudiseva, H. V., Blackwell, T., Ilbert, M., Walker, A.K., Strahler, J.R., Andrews, P.C., and Jakob, U. (2008). Quantifying changes in the thiol redox proteome upon oxidative stress in vivo. Proc. Natl. Acad. Sci. U. S. A. *105*, 8197–8202.
Levy, S.F., Ziv, N., and Siegal, M.L. (2012). Bet hedging in yeast by heterogeneous, age-correlated expression of a stress protectant. PLoS Biol. *10*.
Li, H., Tsang, C.K., Watkins, M., Bertram, P.G., and Zheng, X.F.S. (2006). Nutrient

regulates Tor1 nuclear localization and association with rDNA promoter. Nature *442*, 1058–1061.
Li, S., Giardina, D.M., and Siegal, M.L. (2018). Control of nongenetic heterogeneity in growth rate and stress tolerance of Saccharomyces cerevisiae by cyclic AMP-regulated transcription factors. PLoS Genet. *14*, e1007744.
Lippman, S.I., and Broach, J.R. (2009). Protein kinase A and TORC1 activate genes for ribosomal biogenesis by inactivating repressors encoded by Dot6 and its homolog Tod6. Proc. Natl. Acad. Sci. U. S. A. *106*, 19928–19933.
Magalhães, R.S.S., Popova, B., Braus, G.H., Outeiro, T.F., and Eleutherio, E.C.A. (2018). The trehalose protective mechanism during thermal stress in Saccharomyces cerevisiae: The roles of Ath1 and Agt1. FEMS Yeast Res. *18*, 66.
Maisonneuve, E., and Gerdes, K. (2014). Molecular mechanisms underlying bacterial persisters. Cell *157*, 539–548.
Mao, Y., and Chen, C. (2019). The Hap Complex in Yeasts: Structure, Assembly Mode, and Gene Regulation. Front. Microbiol. *10*, 1645.
Marchler, G., Schuller, C., Adam, G., and Ruis, H. (1993). A Saccharomyces cerevisiae UAS element controlled by protein kinase A activates transcription in response to a variety of stress conditions. EMBO J. *12*, 1997–2003.
Marion, R.M., Regev, A., Segal, E., Barash, Y., Koller, D., Friedman, N., and O'Shea, E.K. (2004). Sfp1 is a stress- and nutrient-sensitive regulator of ribosomal protein gene expression. Proc. Natl. Acad. Sci. U. S. A. *101*, 14315–14322.
Marshall, R.S., and Vierstra, R.D. (2018). Proteasome storage granules protect proteasomes from autophagic degradation upon carbon starvation. Elife *7*.
Martin, D.E., Soulard, A., and Hall, M.N. (2004). TOR regulates ribosomal protein gene expression via PKA and the Forkhead Transcription Factor FHL1. Cell *119*, 969–979.
Martínez-Pastor, M.T., Marchler, G., Schüller, C., Marchler-Bauer, A., Ruis, H., and Estruch, F. (1996). The Saccharomyces cerevisiae zinc finger proteins Msn2p and Msn4p are required for transcriptional induction through the stress-response element (STRE). EMBO J. *15*, 2227–2235.
Martins, D., and English, A.M. (2014). Catalase activity is stimulated by H 2 O 2 in rich culture medium and is required for H 2 O 2 resistance and adaptation in yeast $. Redox Biol. *2*, 308–313.
Mateju, D., Franzmann, T.M., Patel, A., Kopach, A., Boczek, E.E., Maharana, S., Lee, H.O., Carra, S., Hyman, A.A., and Alberti, S. (2017). An aberrant phase transition of stress granules triggered by misfolded protein and prevented by chaperone function. EMBO J. *36*, 1669–1687.
Mayer, C., Zhao, J., Yuan, X., and Grummt, I. (2004). mTOR-dependent activation of the transcription factor TIF-IA links rRNA synthesis to nutrient availability. Genes Dev. *18*, 423–434.
Mele, L., Paino, F., Papaccio, F., Regad, T., Boocock, D., Stiuso, P., Lombardi, A., Liccardo, D., Aquino, G., Barbieri, A., et al. (2018). A new inhibitor of glucose-6-phosphate dehydrogenase blocks pentose phosphate pathway and suppresses malignant proliferation and metastasis in vivo article. Cell Death Dis. *9*, 1–12.
Meunier, S., and Vernos, I. (2012). Microtubule assembly during mitosis - from distinct origins to distinct functions? J. Cell Sci. *125*, 2805–2814.
Minard, K.I., and McAlister-Henn, L. (2005). Sources of NADPH in yeast vary with carbon source. J. Biol. Chem. *280*, 39890–39896.
Mitchell, A., and Pilpel, Y. (2011a). A mathematical model for adaptive prediction of environmental changes by microorganisms. Proc. Natl. Acad. Sci. U. S. A. *108*,

7271–7276.
Mitchell, A., and Pilpel, Y. (2011b). A mathematical model for adaptive prediction of environmental changes by microorganisms. Proc. Natl. Acad. Sci. U. S. A. *108*, 7271–7276.
Mitchell, A., Romano, G.H., Groisman, B., Yona, A., Dekel, E., Kupiec, M., Dahan, O., and Pilpel, Y. (2009). Adaptive prediction of environmental changes by microorganisms. Nature *460*, 220–224.
Mitchell, A., Wei, P., and Lim, W.A. (2015). Oscillatory stress stimulation uncovers an Achilles' heel of the yeast MAPK signaling network. Science (80-.). *350*, 1379–1383.
Mitosch, K., Rieckh, G., and Bollenbach, T. (2017). Noisy Response to Antibiotic Stress Predicts Subsequent Single-Cell Survival in an Acidic Environment. Cell Syst. *4*, 393-403.e5.
Moir, R.D., Lee, J.H., Haeusler, R.A., Desai, N., Engelke, D.R., and Willis, I.M. (2006). Protein kinase A regulates RNA polymerase III transcription through the nuclear localization of Maf1. Proc. Natl. Acad. Sci. U. S. A. *103*, 15044–15049.
Molin, M., Yang, J., Hanzén, S., Toledano, M.B., Labarre, J., and Nyström, T. (2011). Life Span Extension and H2O2 Resistance Elicited by Caloric Restriction Require the Peroxiredoxin Tsa1 in Saccharomyces cerevisiae. Mol. Cell *43*, 823–833.
Moradas-Ferreira, P., and Costa, V. (2000). Adaptive response of the yeast Saccharomyces cerevisiae to reactive oxygen species: Defences, damage and death. Redox Rep. *5*, 277–285.
Morano, K.A., Grant, C.M., and Moye-Rowley, W.S. (2012). The response to heat shock and oxidative stress in saccharomyces cerevisiae. Genetics *190*, 1157–1195.
Morgan, B.A., and Veal, E.A. (2007). Functions of typical 2-Cys peroxiredoxins in yeast. Subcell. Biochem. *44*, 253–265.
Morgan, B., Van Laer, K., Owusu, T.N.E., Ezeriņa, D., Pastor-Flores, D., Amponsah, P.S., Tursch, A., and Dick, T.P. (2016). Real-time monitoring of basal H2O2 levels with peroxiredoxin-based probes. Nat. Chem. Biol. *12*, 437–443.
Morgan, B.A., Banks, G.R., Mark Toone, W., Raitt, D., Kuge, S., and Johnston, L.H. (1997). The Skn7 response regulator controls gene expression in the oxidative stress response of the budding yeast Saccharomyces cerevisiae. EMBO J. *16*, 1035–1044.
Moujaber, O., and Stochaj, U. (2020). The Cytoskeleton as Regulator of Cell Signaling Pathways. Trends Biochem. Sci. *45*, 96–107.
Munder, M.C., Midtvedt, D., Franzmann, T., Nüske, E., Otto, O., Herbig, M., Ulbricht, E., Müller, P., Taubenberger, A., Maharana, S., et al. (2016a). A pH-driven transition of the cytoplasm from a fluid- to a solid-like state promotes entry into dormancy. Elife *5*.
Munder, M.C., Midtvedt, D., Franzmann, T., Nüske, E., Otto, O., Herbig, M., Ulbricht, E., Müller, P., Taubenberger, A., Maharana, S., et al. (2016b). A pH-driven transition of the cytoplasm from a fluid- to a solid-like state promotes entry into dormancy. Elife *5*.
Muzzey, D., G??mez-Uribe, C.A., Mettetal, J.T., and van Oudenaarden, A. (2009). A Systems-Level Analysis of Perfect Adaptation in Yeast Osmoregulation. Cell *138*, 160–171.
Nikawa, J., Cameron, S., Toda, T., Ferguson, K.M., and Wigler, M. (1987). Rigorous feedback control of cAMP levels in Saccharomyces cerevisiae. Genes Dev. *1*, 931–937.
Nikel, P.I., Fuhrer, T., Chavarría, M., Sánchez-Pascuala, A., Sauer, U., and Lorenzo,

V. de (2020). Redox stress reshapes carbon fluxes of Pseudomonas putida for cytosolic glucose oxidation and NADPH generation. BioRxiv 2020.06.13.149542.
Nishimoto, T., Furuta, M., Kataoka, M., and Kishida, M. (2014). Important role of catalase in the cellular response of the budding yeast Saccharomyces cerevisiae exposed to ionizing radiation. Curr. Microbiol. *70*, 404–407.
Nishimoto, T., Watanabe, T., Furuta, M., Kataoka, M., and Kishida, M. (2016). Roles of catalase and trehalose in the protection from hydrogen peroxide toxicity in saccharomyces cerevisiae. Biocontrol Sci. *21*, 179–182.
Nogae, I., and Johnston, M. (1990). Isolation and characterization of the ZWF1 gene of Saccharomyces cerevisiae, encoding glucose-6-phosphate dehydrogenase. Gene *96*, 161–169.
Ocampo, A., Liu, J., Schroeder, E.A., Shadel, G.S., and Barrientos, A. (2012). Mitochondrial respiratory thresholds regulate yeast chronological life span and its extension by caloric restriction. Cell Metab. *16*, 55–67.
Okazaki, S., Tachibana, T., Naganuma, A., Mano, N., and Kuge, S. (2007). Multistep Disulfide Bond Formation in Yap1 Is Required for Sensing and Transduction of H2O2 Stress Signal. Mol. Cell *27*, 675–688.
Olin-Sandoval, V., Yu, J.S.L., Miller-Fleming, L., Alam, M.T., Kamrad, S., Correia-Melo, C., Haas, R., Segal, J., Peña Navarro, D.A., Herrera-Dominguez, L., et al. (2019). Lysine harvesting is an antioxidant strategy and triggers underground polyamine metabolism. Nature *572*, 249–253.
Orij, R., Brul, S., and Smits, G.J. (2011). Intracellular pH is a tightly controlled signal in yeast. Biochim. Biophys. Acta - Gen. Subj. *1810*, 933–944.
Pak, V. V., Ezerina, D., Lyublinskaya, O.G., Pedre, B., Tyurin-Kuzmin, P.A., Mishina, N.M., Thauvin, M., Young, D., Wahni, K., Martínez Gache, S.A., et al. (2020). Ultrasensitive Genetically Encoded Indicator for Hydrogen Peroxide Identifies Roles for the Oxidant in Cell Migration and Mitochondrial Function. Cell Metab. *31*, 642-653.e6.
Panieri, E., and Santoro, M.M. (2016). Ros homeostasis and metabolism: A dangerous liason in cancer cells. Cell Death Dis. *7*, e2253–e2253.
Parry, B.R., Surovtsev, I. V., Cabeen, M.T., O'Hern, C.S., Dufresne, E.R., and Jacobs-Wagner, C. (2014). The bacterial cytoplasm has glass-like properties and is fluidized by metabolic activity. Cell *156*, 183–194.
Pastor-Flores, D., Becker, K., and Dick, T.P. (2017). Monitoring yeast mitochondria with peroxiredoxin-based redox probes: the influence of oxygen and glucose availability. Interface Focus *7*, 20160143.
Pedruzzi, I., Dé Rique Dubouloz, F., Cameroni, E., Wanke, V., Roosen, J., Winderickx, J., De Virgilio, C., Sadeh, A., Movshovich, N., Volokh, M., et al. (2003). Fine-tuning of the Msn2/4-mediated yeast stress responses as revealed by systematic deletion of Msn2/4 partners. Mol. Cell *12*, 3127–3138.
Peeters, T., Louwet, W., Geladé, R., Nauwelaers, D., Thevelein, J.M., and Versele, M. (2006). Kelch-repeat proteins interacting with the Gα protein Gpa2 bypass adenylate cyclase for direct regulation of protein kinase A in yeast. Proc. Natl. Acad. Sci. U. S. A. *103*, 13034–13039.
PENNINCKX, M. (2002). An overview on glutathione in versus non-conventional yeasts. FEMS Yeast Res. *2*, 295–305.
Peralta, D., Bronowska, A.K., Morgan, B., Dóka, É., Van Laer, K., Nagy, P., Gräter, F., and Dick, T.P. (2015). A proton relay enhances H2O2 sensitivity of GAPDH to facilitate metabolic adaptation. Nat. Chem. Biol. *11*, 156–163.
Perkins, T.J., and Swain, P.S. (2009). Strategies for cellular decision-making. Mol.

Syst. Biol. *5*, 326.
Peters, J.M., Franke, W.W., and Kleinschmidt, J.A. (1994). Distinct 19 S and 20 S subcomplexes of the 26 S proteasome and their distribution in the nucleus and the cytoplasm. J. Biol. Chem. *269*, 7709–7718.
Peters Lee Zeev, Z., Hazan, R., Breker, M., Schuldiner, M., and Ben-Aroya, S. (2013). Formation and dissociation of proteasome storage granules are regulated by cytosolic pH. J. Cell Biol. *201*, 663–671.
Petrovska, I., Nüske, E., Munder, M.C., Kulasegaran, G., Malinovska, L., Kroschwald, S., Richter, D., Fahmy, K., Gibson, K., Verbavatz, J.M., et al. (2014). Filament formation by metabolic enzymes is a specific adaptation to an advanced state of cellular starvation. Elife *2014*.
Philippi, A., Steinbauer, R., Reiter, A., Fath, S., Leger-Silvestre, I., Milkereit, P., Griesenbeck, J., and Tschochner, H. (2010). TOR-dependent reduction in the expression level of Rrn3p lowers the activity of the yeast RNA Pol I machinery, but does not account for the strong inhibition of rRNA production. Nucleic Acids Res. *38*, 5315–5326.
PRINGLE, and R., J. (1981). The Saccharomyces cerevisiae cell cycle. Mol. Biol. Yeast Saccharomyces. 97–142.
Quan, Z., Cao, L., Tang, Y., Yan, Y., Oliver, S.G., and Zhang, N. (2015). The Yeast GSK-3 Homologue Mck1 Is a Key Controller of Quiescence Entry and Chronological Lifespan. PLoS Genet. *11*, e1005282.
Radzikowski, J.L., Vedelaar, S., Siegel, D., Ortega, Á.D., Schmidt, A., and Heinemann, M. (2016). Bacterial persistence is an active σ S stress response to metabolic flux limitation . Mol. Syst. Biol. *12*, 882.
Ralser, M., Wamelink, M.M., Kowald, A., Gerisch, B., Heeren, G., Struys, E.A., Klipp, E., Jakobs, C., Breitenbach, M., Lehrach, H., et al. (2007). Dynamic rerouting of the carbohydrate flux is key to counteracting oxidative stress. J. Biol. *6*, 10.
Ralser, M., Wamelink, M.M.C., Latkolik, S., Jansen, E.E.W., Lehrach, H., and Jakobs, C. (2009). Metabolic reconfiguration precedes transcriptional regulation in the antioxidant response. Nat. Biotechnol. *27*, 604–605.
Ramachandran, V., Shah, K.H., and Herman, P.K. (2011). The cAMP-Dependent Protein Kinase Signaling Pathway Is a Key Regulator of P Body Foci Formation. Mol. Cell *43*, 973–981.
Rand, J.D., and Grant, C.M. (2006a). The thioredoxin system protects ribosomes against stress-induced aggregation. Mol. Biol. Cell *17*, 387–401.
Rand, J.D., and Grant, C.M. (2006b). The thioredoxin system protects ribosomes against stress-induced aggregation. Mol. Biol. Cell *17*, 387–401.
Reczek, C.R., and Chandel, N.S. (2017). The Two Faces of Reactive Oxygen Species in Cancer. Annu. Rev. Cancer Biol. *1*, 79–98.
Reichmann, D., Voth, W., and Jakob, U. (2018). Maintaining a Healthy Proteome during Oxidative Stress. Mol. Cell *69*, 203–213.
Riback, J.A., Katanski, C.D., Kear-Scott, J.L., Pilipenko, E. V., Rojek, A.E., Sosnick, T.R., and Drummond, D.A. (2017). Stress-Triggered Phase Separation Is an Adaptive, Evolutionarily Tuned Response. Cell *168*, 1028-1040.e19.
Robertson, L.S., and Fink, G.R. (1998). The three yeast A kinases have specific signaling functions in pseudohyphal growth. Proc. Natl. Acad. Sci. U. S. A. *95*, 13783–13787.
Roger, F., Picazo, C., Reiter, W., Libiad, M., Asami, C., Hanzén, S., Gao, C., Lagniel, G., Welkenhuysen, N., Labarre, J., et al. (2020). Peroxiredoxin promotes longevity and h2o2-resistance in yeast through redox-modulation of protein kinase a.

Elife *9*, 1–32.
Sagot, I., and Laporte, D. (2019). The cell biology of quiescent yeast – a diversity of individual scenarios. J. Cell Sci. *132*.
Sagot, I., Pinson, B., Salin, B., and Daignan-Fornier, B. (2006). Actin bodies in yeast quiescent cells: An immediately available actin reserve? Mol. Biol. Cell *17*, 4645–4655.
Sanchez, Y., and Lindquist, S.L. (1990). HSP104 required for induced thermotolerance. Science (80-.). *248*, 1112–1115.
Schieber, M., and Chandel, N.S. (2014). ROS function in redox signaling and oxidative stress. Curr. Biol. *24*, R453–R462.
Schimel, J., Balser, T.C., and Wallenstein, M. (2007). Microbial stress-response physiology and its implications for ecosystem function. Ecology *88*, 1386–1394.
Schmitt, A.P., and Mcentee, K. (1996). Msn2p, a zinc finger DNA-binding protein, is the transcriptional activator of the multistress response in Saccharomyces cerevisiae. Proc. Natl. Acad. Sci. U. S. A. *93*, 5777–5782.
Schneider, E.D., and Kay, J.J. (1995). Order from disorder: the thermodynamics of complexity in biology. In What Is Life? The Next Fifty Years, (Cambridge University Press), pp. 161–174.
Schröder, E., Littlechild, J.A., Lebedev, A.A., Errington, N., Vagin, A.A., and Isupov, M.N. (2000). Crystal structure of decameric 2-Cys peroxiredoxin from human erythrocytes at 1.7 Å resolution. Structure *8*, 605–615.
Schrodinger, E. (1944). WHAT IS LIFE?
Schüller, C., Brewster, J.L., Alexander, M.R., Gustin, M.C., and Ruis, H. (1994). The HOG pathway controls osmotic regulation of transcription via the stress response element (STRE) of the Saccharomyces cerevisiae CTT1 gene. EMBO J. *13*, 4382–4389.
Seaver, L.C., and Imlay, J.A. (2001). Alkyl hydroperoxide reductase is the primary scavenger of endogenous hydrogen peroxide in Escherichia coli. J. Bacteriol. *183*, 7173–7181.
Selye, H. (1956). The stress of life. (New York: McGraw-Hill).
Selye, H. (1975). Homeostasis and Heterostasis. In Trauma, (Springer US), pp. 25–29.
Sha, W., Martins, A.M., Laubenbacher, R., Mendes, P., and Shulaev, V. (2013). The Genome-Wide Early Temporal Response of Saccharomyces cerevisiae to Oxidative Stress Induced by Cumene Hydroperoxide. PLoS One *8*, e74939.
Shcherbik, N., and Pestov, D.G. (2019). The Impact of Oxidative Stress on Ribosomes: From Injury to Regulation. Cells *8*.
Shenton, D., and Grant, C.M. (2003). Protein S-thiolation targets glycolysis and protein synthesis in response to oxidative stress in the yeast Saccharomyces cerevisiae. Biochem. J. *374*, 513–519.
Sies, H., and Jones, D.P. (2020). Reactive oxygen species (ROS) as pleiotropic physiological signalling agents. Nat. Rev. Mol. Cell Biol. *21*, 363–383.
Slekar, K.H., Kosman, D.J., and Culotta, V.C. (1996). The yeast copper/zinc superoxide dismutase and the pentose phosphate pathway play overlapping roles in oxidative stress protection. J. Biol. Chem. *271*, 28831–28836.
Smith, A., Ward, M.P., and Garrett, S. (1998a). Yeast PKA represses Msn2p/Msn4p-dependent gene expression to regulate growth, stress response and glycogen accumulation. EMBO J. *17*, 3556–3564.
Smith, A., Ward, M.P., and Garrett, S. (1998b). Yeast PKA represses Msn2p/Msn4p-dependent gene expression to regulate growth, stress response and glycogen

accumulation. EMBO J. *17*, 3556–3564.
Solopova, A., Van Gestel, J., Weissing, F.J., Bachmann, H., Teusink, B., Kok, J., and Kuipers, O.P. (2014). Bet-hedging during bacterial diauxic shift. Proc. Natl. Acad. Sci. U. S. A. *111*, 7427–7432.
Stewart, P.S., Franklin, M.J., Williamson, K.S., Folsom, J.P., Boegli, L., and James, G.A. (2015). Contribution of stress responses to antibiotic tolerance in Pseudomonas aeruginosa biofilms. Antimicrob. Agents Chemother. *59*, 3838–3847.
Stöcker, S., Maurer, M., Ruppert, T., and Dick, T.P. (2018). A role for 2-Cys peroxiredoxins in facilitating cytosolic protein thiol oxidation. Nat. Chem. Biol. *14*, 148–155.
Stone, J.R. (2004). An assessment of proposed mechanisms for sensing hydrogen peroxide in mammalian systems. Arch. Biochem. Biophys. *422*, 119–124.
Sullivan, L.B., and Chandel, N.S. (2014). Mitochondrial reactive oxygen species and cancer. Cancer Metab. *2*.
Tanaka, K. (2009). The proteasome: Overview of structure and functions. Proc. Japan Acad. Ser. B Phys. Biol. Sci. *85*, 12–36.
Tang, H.-M.V., Siu, K.-L., Wong, C.-M., and Jin, D.-Y. (2009). Loss of Yeast Peroxiredoxin Tsa1p Induces Genome Instability through Activation of the DNA Damage Checkpoint and Elevation of dNTP Levels. PLoS Genet. *5*, e1000697.
Tapia, H., Young, L., Fox, D., Bertozzi, C.R., and Koshland, D. (2015). Increasing intracellular trehalose is sufficient to confer desiccation tolerance to Saccharomyces cerevisiae. Proc. Natl. Acad. Sci. U. S. A. *112*, 6122–6127.
Tatchell, K. (1986). RAS genes and growth control in Saccharomyces cerevisiae. J. Bacteriol. *166*, 364–367.
Thevelein, J.M., and De Winde, J.H. (1999). Novel sensing mechanisms and targets for the cAMP-protein kinase A pathway in the yeast Saccharomyces cerevisiae. Mol. Microbiol. *33*, 904–918.
Thomas, R. (1990). Biological Feedback (CRC Press, Inc).
Thorpe, G.W., Fong, C.S., Alic, N., Higgins, V.J., and Dawes, I.W. (2004). Cells have distinct mechanisms to maintain protection against different reactive oxygen species: oxidative-stress-response genes. Proc. Natl. Acad. Sci. U. S. A. *101*, 6564–6569.
Toledano, M.B., Delaunay-Moisan, A., Outten, C.E., and Igbaria, A. (2013). Functions and cellular compartmentation of the thioredoxin and glutathione pathways in yeast. Antioxidants Redox Signal. *18*, 1699–1711.
Topf, U., Suppanz, I., Samluk, L., Wrobel, L., Böser, A., Sakowska, P., Knapp, B., Pietrzyk, M.K., Chacinska, A., and Warscheid, B. (2018). Quantitative proteomics identifies redox switches for global translation modulation by mitochondrially produced reactive oxygen species. Nat. Commun. *9*, 1–17.
Umbarger, H.E. (1956). Evidence for a negative-feedback mechanism in the biosynthesis of isoleucine. Science (80-.). *123*, 848.
Veatch, J.R., McMurray, M.A., Nelson, Z.W., and Gottschling, D.E. (2009). Mitochondrial Dysfunction Leads to Nuclear Genome Instability via an Iron-Sulfur Cluster Defect. Cell *137*, 1247–1258.
Venturelli, O.S., Zuleta, I., Murray, R.M., and El-Samad, H. (2015). Population Diversification in a Yeast Metabolic Program Promotes Anticipation of Environmental Shifts. PLoS Biol. *13*, 1–24.
de Virgilio, C. (2012). The essence of yeast quiescence. FEMS Microbiol. Rev. *36*, 306–339.
Weber, C.A., Sekar, K., Tang, J.H., Warmer, P., Sauer, U., and Weis, K. (2020). β-Oxidation and autophagy are critical energy providers during acute glucose depletion

in Saccharomyces cerevisiae. Proc. Natl. Acad. Sci. U. S. A. *117*, 12239–12248.
Weids, A.J., and Grant, C.M. (2014). The yeast peroxiredoxin Tsa1 protects against protein-aggregate-induced oxidative stress. J. Cell Sci. *127*, 1327–1335.
Winterbourn, C.C., and Metodiewa, D. (1999). Reactivity of biologically important thiol compounds with superoxide and hydrogen peroxide. Free Radic. Biol. Med. *27*, 322–328.
Woo, H.A., Chae, H.Z., Hwang, S.C., Yang, K.S., Kang, S.W., Kim, K., and Rhee, S.G. (2003). Reversing the inactivation of peroxiredoxins caused by cysteine sulfinic acid formation. Science (80-.). *300*, 653–656.
Wood, Z.A., Poole, L.B., and Karplus, P.A. (2003). Peroxiredoxin evolution and the regulation of hydrogen peroxide signaling. Science (80-.). *300*, 650–653.
Xiong, Y., Uys, J.D., Tew, K.D., and Townsend, D.M. (2011). S-Glutathionylation: From molecular mechanisms to health outcomes. Antioxidants Redox Signal. *15*, 233–270.
Yan, C., Lee, L.H., and Davis, L.I. (1998). Crm1p mediates regulated nuclear export of a yeast AP-1-like transcription factor. EMBO J. *17*, 7416–7429.
Young, J.W., Locke, J.C.W., and Elowitz, M.B. (2013). Rate of environmental change determines stress response specificity. Proc. Natl. Acad. Sci. U. S. A. *110*, 4140–4145.
Zaman, S., Lippman, S.I., Schneper, L., Slonim, N., and Broach, J.R. (2009). Glucose regulates transcription in yeast through a network of signaling pathways. Mol. Syst. Biol. *5*.
Zhang, J., Sonnenschein, N., Pihl, T.P.B., Pedersen, K.R., Jensen, M.K., and Keasling, J.D. (2016). Engineering an NADPH/NADP+ Redox Biosensor in Yeast. ACS Synth. Biol. *5*, 1546–1556.
Ziv, N., Siegal, M.L., and Gresham, D. (2013). Genetic and nongenetic determinants of cell growth variation assessed by high-throughput microscopy. Mol. Biol. Evol. *30*, 2568–2578.

ARTICLES EN FRANCAIS

La réponse adaptative au peroxyde d'hydrogène repose sur un compromis entre la résistance au stress et la tolérance

Basile Jacquel, Audrey Matifas, Gilles Charvin

Résumé
En réponse à un stress environnemental, les stratégies de défense cellulaire peuvent être divisées en deux catégories : celles qui, comme dans les systèmes homéostatiques, cherchent à maintenir la prolifération cellulaire en dégradant l'agent stressant (c'est la résistance) ; et celles qui assurent la survie cellulaire (la tolérance), même si cela se fait souvent au détriment de la prolifération cellulaire. Dans cette étude, nous avons exploré les bases génétiques de l'antagonisme entre résistance et tolérance dans la réponse au peroxyde d'hydrogène (H2O2) chez la levure bourgeonnante. Nous montrons que l'inactivation de la protéine kinase A (PKA) médiée par la signalisation du H2O2 induit une transition abrupte de la fonction homéostatique normale à un état de tolérance au stress en protégeant la machinerie de croissance, maximisant ainsi la capacité cellulaire dans un environnement changeant. Ce système modèle ouvre la voie au développement de stratégies antiprolifératives dans lesquelles les mécanismes de résistance et de tolérance pourraient être ciblés indépendamment pour prévenir les rechutes dans des contextes pathologiques.

Introduction

Les réponses cellulaires au stress sont basées sur des stratégies multiformes qui favorisent l'adaptation physiologique dans des environnements changeants. Une grande partie des mécanismes de défense contre les agressions environnementales et endogènes (par exemple, l'oxydation (Veal, Day et Morgan 2007 ; Toledano et al. 2004 ; Toledano, Planson et Delaunay-Moisan 2010), l'hyperosmolarité (Hohmann 2002)) utilisent des systèmes de régulation de type "détecter et répondre" qui fonctionnent selon le cadre homéostatique : les cellules tentent de restaurer un état cellulaire optimal préexistant en éliminant la cause du stress interne. Dans ce scénario, le rôle du système homéostatique est de restaurer ou de maintenir la prolifération sous stress, c'est-à-dire d'atteindre un état de "résistance au stress" (Brauner et al. 2016 ; Balaban et al. 2019). Alors que ces mécanismes de régulation peuvent conduire à d'excellentes propriétés adaptatives à l'état d'équilibre (Goulev et al. 2017 ; Muzzey et al. 2009 ; Milias-Argeitis et al. 2011), ils souffrent généralement d'un certain nombre de limitations, notamment une gamme homéostatique limitée et un temps de réponse lent (par exemple, une activation transcriptionnelle lente (Goulev

et al. 2017)), ce qui restreint la capacité de la cellule à faire face à des changements environnementaux abrupts et imprévisibles.
Un schéma de défense alternatif, appelé "tolérance au stress" (Brauner et al. 2016), a été décrit, selon lequel une population de cellules peut survivre à une menace physiologique transitoire sans nécessairement combattre la cause intrinsèque du stress interne. Dans ce cadre, la survie cellulaire est généralement associée à un arrêt de la prolifération et à une réduction du métabolisme, comme on l'observe couramment dans le contexte de la dormance cellulaire (Gray et al. 2004), ou dans des cas spécifiques de comportements cellulaires hétérogènes (par exemple, la persistance bactérienne (Bigger 1944 ; Balaban et al. 2004), la couverture de pari (Slatkin 1974 ; Levy, Ziv et Siegal 2012)). Les stratégies de réponse au stress peuvent donc être divisées en deux catégories : celles qui cherchent à maintenir la prolifération cellulaire sous l'effet du stress (résistance) et celles qui assurent la survie cellulaire (tolérance) (voir figure 1A). Les premières peuvent a priori maximiser l'aptitude cellulaire, mais leurs limites intrinsèques (par exemple l'échec homéostatique) exposent les cellules aux dommages et à la mort. Dans le second cas, la survie cellulaire se fait au prix d'une réduction de la prolifération cellulaire. Dans l'ensemble, les mécanismes de résistance et de tolérance au stress apparaissent donc comme des stratégies cellulaires antagonistes de maximisation de l'aptitude en réponse au stress, et, jusqu'à présent, la façon dont les cellules gèrent cet antagonisme n'a pas été étudiée.
L'homéostasie redox est une caractéristique essentielle qui assure une fonction cellulaire fiable dans les cellules soumises à des perturbations redox d'origine externe et interne (Veal, Day et Morgan 2007 ; Toledano et al. 2004). Chez la levure, le contrôle de la concentration en peroxyde d'hydrogène est assuré par un système homéostatique transcriptionnel de type sense-and-respond basé sur le facteur de transcription Yap1 (Lee et al. 1999 ; Delaunay, Isnard, and Toledano 2000 ; Kuge and Jones 1994). Le régulateur Yap1 commande l'expression d'une centaine de gènes (Godon et al. 1998 ; Gasch et al. 2000 ; Lee et al. 1999), y compris des enzymes antioxydantes dont les fonctions de détoxification du H_2O_2 se chevauchent quelque peu (Jiang et English 2006 ; Chae, Chung et Rhee 1994 ; Pedrajas et al. 2000 ; Wong et al. 2002 ; Iraqui et al. 2009). D'autres régulations participent à la restauration de l'équilibre redox interne : tout d'abord, le détournement de la glycolyse vers la voie des pentoses phosphates (PPP) conduit à une production accrue de NADPH (Ralser et al. 2007 ; Kuehne et al. 2015), qui est le donneur d'électrons ultime impliqué dans le tamponnement de H_2O_2 par le cycle peroxydatique (Hall, Karplus, et Poole 2009) ; ensuite, l'inhibition de la voie de la protéine kinase A (PKA), qui est une plaque tournante majeure pour le contrôle de la prolifération cellulaire (Broach 2012) et la réponse générale au stress (Gasch et al. 2000), contribue à l'adaptation au stress oxydatif (Hasan et al. 2002) et est reliée à la réponse de signalisation de H_2O_2 par divers mécanismes putatifs (Boisnard et al. 2009 ; Molin et al. 2011 ; Bodvard et al. 2017 ; Roger et al. 2020). Par conséquent, la réponse à l’H_2O_2 fournit un contexte idéal pour déchiffrer si et comment les mécanismes de résistance et de tolérance se coordonnent pour former une réponse adaptative intégrative au stress.

Pour répondre à cette question, nous avons utilisé l'imagerie des cellules vivantes et des approches microfluidiques qui permettent de distinguer les comportements cellulaires de résistance et de tolérance au H2O2. En utilisant un crible de gènes candidats, nous avons classé les principaux acteurs impliqués dans la réponse au stress H2O2 en catégories fonctionnelles qui mettent en évidence leurs rôles respectifs dans l'adaptation à ce facteur de stress. Plus précisément, notre étude a mis en évidence l'existence d'un fort antagonisme entre résistance et tolérance, exacerbé par les mutations qui affectent l'alimentation en NADPH dans le cycle peroxydatique (par exemple, les mutants zwf1 et trr1). D'autres résultats nous ont permis de déchiffrer les bases génétiques de la tolérance au H2O2 et son interaction avec la signalisation du H2O2. Au total, notre étude a donc révélé comment la réponse cellulaire intégrée à H2O2 résulte d'un compromis entre le système homéostatique qui assure la prolifération cellulaire et un mécanisme qui prévient la mort cellulaire en protégeant la machinerie de croissance. Ce système modèle ouvre la voie au développement de stratégies antiprolifératives dans lesquelles les mécanismes de résistance et de tolérance pourraient être ciblés indépendamment pour améliorer l'efficacité thérapeutique.

Résultats

La résistance et la tolérance sont des propriétés distinctes de la réponse au peroxyde d'hydrogène

Pour déterminer si la résistance au stress et la tolérance sont des propriétés physiologiques pertinentes et distinctes de la réponse au stress H2O2, nous devions établir si la levure pouvait tolérer (c'est-à-dire survivre) des doses de H2O2 supérieures à sa capacité de résistance (c'est-à-dire de prolifération). À cette fin, nous avons mesuré la résistance de la levure au H2O2 comme étant la concentration seuil au-delà de laquelle la prolifération cellulaire s'arrête, également appelée concentration minimale inhibitrice (ou CMI) (Brauner et al. 2016 ; Balaban et al. 2019). Il est important de noter que le H2O2 étant un composé assez instable, la mesure de la CMI du H2O2 a nécessité une chambre microfluidique avec un réapprovisionnement constant du milieu afin de maintenir une concentration constante de l'agent stressant, comme décrit précédemment (Goulev et al. 2017).
En utilisant la microscopie time-lapse, nous avons suivi la prolifération de cellules individuelles sous exposition continue au H2O2 (à partir de t=0). Nous avons constaté que, alors que les cellules étaient capables de reprendre leur prolifération après un délai lorsqu'elles étaient exposées à 0,5mM, une concentration de 1mM arrêtait complètement la croissance cellulaire, au moins pendant 16 heures (Fig. 1B). Cela indique que la CMI se situe entre 0,5mM et 1mM, en accord avec des mesures précédentes (Goulev et al. 2017). En revanche, la croissance cellulaire a repris après une impulsion de stress de 1h à 1mM, indiquant qu'une fraction des cellules a réussi à survivre au-dessus de la CMI, malgré l'absence de résistance (Fig. 1C). Il est intéressant de noter qu'en faisant varier la durée τ de l'exposition au stress (voir Fig.

1D avec τ = 4h), la fraction de survie (voir Matériel et Méthodes pour plus de détails) a affiché une décroissance similaire à la fois à 0,5mM et à 1mM pour $\tau \leq$ 2h, ce qui suggère que la survie cellulaire (c'est-à-dire la tolérance) était quelque peu indépendante de la résistance au stress (Fig. 1E). Pour $\tau >$ 3h, la survie cellulaire a atteint un plateau à 0,5mM mais a encore diminué à 1mM, en raison de la reprise de la croissance et de l'adaptation de la population à 0,5mM.

Dans l'ensemble, l'évaluation indépendante de la prolifération et de la survie, réalisée à l'aide de notre méthode de suivi des cellules individuelles, a révélé que la résistance et la tolérance sont deux aspects distincts du comportement cellulaire en réponse à H2O2.

Un criblage génétique identifie des mutants qui combinent un défaut de résistance sévère avec un phénotype d'hyper-tolérance.

Afin de déchiffrer les déterminants génétiques respectifs de la tolérance et de la résistance, nous avons conçu une approche par gènes candidats dans laquelle nous avons systématiquement mesuré la prolifération et la survie de mutants qui ont été précédemment signalés comme étant "sensibles" au H2O2. Il est important de noter que les essais de survie à 0,5 mM ont révélé que les cellules ont réagi au stress en deux étapes (Fig. 1) : une période aiguë, caractérisée par un arrêt de la croissance et un taux de mortalité élevé, suivie d'un état d'équilibre, dans lequel la prolifération cellulaire reprend et où aucune mortalité n'est observée. Par conséquent, afin de mieux distinguer le rôle des gènes individuels dans la réponse aiguë par rapport à l'état d'équilibre, nous avons utilisé une méthodologie dans laquelle la survie et la prolifération ont été comparées entre des schémas de stress en escalier (c'est-à-dire un régime de stress aigu) et en rampe (c'est-à-dire un régime d'état d'équilibre mais sans période aiguë, voir Fig. S2A) après une exposition de 4 heures à 0,5mM (voir Fig. 2A et Fig. S2B et (Goulev et al. 2017)). La prolifération cellulaire a été évaluée en mesurant la biomasse totale produite par les cellules survivantes uniquement pendant l'exposition au stress (Fig. 2B), et la tolérance a été calculée comme une fraction des cellules initiales qui ont repris ou maintenu leur croissance après le stress (Fig. 2C, voir Matériaux et méthodes pour plus de détails).

Nous avons criblé 14 gènes directement impliqués dans la défense contre H2O2 comme Yap1, des acteurs associés au cycle peroxydatique des peroxiredoxines 2-Cys (par exemple la peroxiredoxine Tsa1 (Wong et al. 2002), les thiorédoxines Trx1/2 (Boisnard et al. 2009), la thiorédoxine réductase Trr1 (Chae, Chung, and Rhee 1994)), d'autres gènes antioxydants (par ex. g la catalase Ctt1 (Guan et al. 2012) et la peroxydase mitochondriale Ccp1 (Jiang et English 2006)), des gènes qui pilotent la réponse générale au stress environnemental (ou ESR, par exemple Msn2/4 (Boisnard et al. 2009 ; Hasan et al. 2002)), ou des mutants spécifiques qui ont été observés comme étant sensibles au H202 (comme la phosphodiestérase Pde2 (Hasan et al. 2002)). (voir Fig. S2C). Les résultats ont été affichés en traçant la survie et la

résistance moyennes pour chaque mutant analysé dans des conditions de pas et de rampe, Fig. 2D et 2E.

Nous avons d'abord vérifié que le mutant yap1Δ présentait une faible prolifération et une faible survie dans ces conditions de stress, Fig. 2D et 2E, en accord avec des études précédentes (Delaunay, Isnard, et Toledano 2000). Ensuite, nous avons remarqué que les mutants pouvaient être classés en deux groupes différents (voir la zone ombrée sur les Fig. 2D et E) : le premier groupe (voir la zone ombrée jaune sur les Fig. 2D et 2E) comprenait des mutants présentant des défauts de prolifération et de survie légers (par exemple glr1Δ) à sévères (par exemple ctt1Δ) par rapport à WT. Il est important de noter que la prolifération et la survie ont augmenté de manière significative pour ce groupe de mutants lorsque l'on compare les essais paliers aux essais en rampe (voir la déviation de la diagonale dans les Fig. 2D et 2E). Cela indique que ces mutants, malgré leurs défauts variables en présence d'un stress aigu, présentaient tous un certain niveau d'adaptation à l'état d'équilibre, d'où leur appellation « d'adaptateurs ». Dans cette catégorie, la prolifération et la survie semblent être affectées de manière quelque peu proportionnelle, c'est-à-dire qu'aucun des gènes correspondants n'avait un rôle spécifiquement associé à la tolérance au stress ou à la résistance (à l'exception probable de pde2Δ, qui présentait une tolérance réduite mais une résistance similaire ou même supérieure à celle de WT).
Contrairement à la première catégorie, nous avons trouvé un deuxième groupe de mutants (appelés " non-adaptés ") qui s'étendaient le long de la diagonale sur les panneaux de survie et de prolifération (Fig. 2D et 2E). Cela indique que le fait de soumettre les cellules à une rampe (où la période de stress aigu est supprimée) n'améliore ni la prolifération ni la survie chez ces mutants, par rapport à un palier, ce qui indique que les gènes correspondants sont nécessaires pour atteindre un état stable adapté sous stress. Tous ces mutants ont également partagé une résistance fortement réduite par rapport à WT et au groupe d'adaptateurs (Fig. 2E). Il est intéressant de noter que les gènes de ce groupe de non-adaptateurs étaient tous associés à la voie biochimique des peroxydases dépendantes du NADPH : après leur réaction avec H_2O_2, les Tsa1 et Tsa2 oxydés sont réduits par les thiorédoxines Trx1 et Trx2, qui réagissent à leur tour avec la thiorédoxine réductase Trr1. Trr1 est réduit par le NADPH qui est principalement synthétisé lors du détournement du glucose dans la voie des pentoses phosphates (PPP) par la glucose-6-phosphate déshydrogénase (G6PD, ou Zwf1). Ces résultats suggèrent donc que cette voie biochimique est le principal effecteur de l'homéostasie du H_2O_2.

Pour tester davantage cette hypothèse, nous avons intégré un rapporteur transcriptionnel Srx1pr-GFP-degron dans chaque souche mutante testée ci-dessus (Srx1 encode une sulfiredoxine, dont l'expression est régulée par Yap1), comme proxy pour l'activation de la Yap1 et le déséquilibre H_2O_2. Les souches ont été soumises à une étape douce de 0,1mM H_2O_2 pour assurer la capacité de la cellule à conduire une réponse transcriptionnelle même chez les mutants à faible résistance. Dans ces conditions, la souche WT a présenté une explosion transitoire de la fluorescence de

la GFP, suivie d'une période de récupération menant à un niveau d'équilibre comparable au niveau pré-stress (Fig. 2F). Une telle décroissance de la fluorescence, qui implique la désactivation du régulateur Yap1, indique que l'équilibre interne de H2O2 a été rétabli. En quantifiant l'amplitude de la chute de fluorescence pendant la période allant de l'éclatement à l'état d'équilibre, nous avons défini un " indice d'adaptation à H2O2 " afin d'évaluer quantitativement la capacité de chaque mutant à rétablir l'équilibre H2O2 (voir les exemples de données obtenues avec des mutants spécifiques sur la Fig. 2F), et nous avons reporté ces mesures sur les données de résistance à la rampe de stress présentées ci-dessus (Fig. 2G). Cette analyse a révélé que la restauration de l'équilibre H2O2 était fortement altérée dans le groupe de non-adaptateurs défini ci-dessus, contrairement aux adaptateurs, qui étaient moins sévèrement affectés. De plus, la corrélation entre l'équilibre H2O2 et la résistance était assez bonne (Fig. 2G, r2=0.79). Cette analyse a donc démontré le rôle spécifique de la voie des peroxiredoxines dans la promotion de l'homéostasie de H2O2 et de la résistance au stress à l'état stable.

Cependant, malgré leur appartenance au même groupe, nous avons remarqué que les mutants non-adapteurs présentaient des phénotypes de tolérance très hétérogènes, qui ne pouvaient pas être expliqués par des différences dans l'homéostasie de H2O2 (Fig. 2G et Fig. S2D). En outre, deux d'entre eux (c'est-à-dire zwf1Δ, trr1Δ) présentaient une fraction de survie inattendue ~3-5 fois plus élevée que celle du WT (Fig. 2D). Une telle augmentation spectaculaire de la tolérance a été observée de manière cohérente avec une exposition à H2O2 allant jusqu'à 128mM (c'est-à-dire bien au-dessus de la CMI du WT, Fig. S2E, et Fig. S2F), c'est-à-dire dans des conditions dans lesquelles les cellules étaient peu susceptibles de déclencher une réponse active. Par conséquent, notre criblage a permis de découvrir des mutants dans lesquels un défaut prononcé de résistance à l'H2O2, associé à une perte de l'homéostasie de l'H2O2, était associé à un phénotype d'hyper-tolérance, validant ainsi davantage la nécessité de démêler les mécanismes de résistance et de tolérance au cours de la réponse au stress H2O2.

Un antagonisme dynamique et réversible entre le déséquilibre redox, la prolifération et la survie chez le mutant zwf1Δ

Comment des mutants peuvent-ils présenter à la fois un défaut de résistance sévère et une tolérance beaucoup plus forte que le WT ? En nous concentrant spécifiquement sur le mutant zwf1Δ, nous avons cherché à résoudre cette énigme en caractérisant davantage l'interaction entre le contrôle de la prolifération, le déséquilibre H2O2 et la tolérance dans ce contexte.

En mesurant la CMI du mutant zwf1Δ à l'aide de tests de croissance de colonies (Fig. 3A et 3B) et de la quantification de la fréquence de division d'une seule cellule (Fig. 3C), nous avons observé une réduction graduelle et dose-dépendante de la prolifération cellulaire avec l'augmentation des niveaux de H2O2, et la croissance et

la division cellulaires ont été complètement arrêtées au-dessus de 0,3 mM (i.e. MICzwf1Δ = 0,3 mM). Ce défaut de croissance sous H2O2 constant n'a pas pu être expliqué par une limitation potentielle du niveau de NADPH (qui pourrait être préjudiciable aux processus anaboliques), puisque le mutant trr1Δ, dans lequel les niveaux de NADPH ne sont pas altérés, a présenté le même phénotype que zwf1Δ (Fig S3A). De façon concomitante, nous avons observé une augmentation dose-dépendante de l'activation transcriptionnelle moyenne de Srx1 sous stress H2O2 (ainsi qu'une relocalisation nucléaire persistante de Yap1-GFP, voir Fig. S3B), dont l'upregulation était beaucoup plus importante que celle du WT (Fig. 3D). Il est intéressant de noter que les distributions de la prolifération cellulaire et de l'activation de Srx1pr obtenues en présence (0,1 mM) ou en l'absence de stress H2O2 présentaient une grande variabilité d'une cellule à l'autre (Fig. 3C et D). Dans ces conditions, le suivi de cellules uniques sur plusieurs divisions a révélé un modèle de division erratique avec une alternance de cycles cellulaires prolongés avec une forte expression de Srx1 suivie d'une période de récupération et de durées de cycle cellulaire proches de la normale (Fig. 3E). En appui à cette observation, nous avons observé une corrélation négative entre la fréquence de division et le niveau d'expression de Srx1 chez le mutant mais pas chez le WT (R^2 (zwf1Δ) = 0,73 et R^2(WT) = 0,02, respectivement, à 0 mM H2O2, voir Fig. 3F). Dans l'ensemble, ces résultats ont donc suggéré l'existence d'un antagonisme dynamique - et réversible - entre la croissance cellulaire et l'équilibre H2O2. Ils ont également soulevé l'hypothèse que les arrêts du cycle cellulaire observés chez le mutant zwf1Δ pourraient soit résulter d'un processus actif de régulation du contrôle de la croissance, soit, alternativement, de dysfonctionnements cellulaires dus à un déséquilibre H2O2 potentiellement toxique.

Pour tester ces hypothèses, nous nous sommes tournés vers des marqueurs fluorescents de l'oxydation des protéines afin de déterminer si les protéines du mutant zwf1Δ étaient plus oxydées que celles du WT et si cela pouvait compromettre la fonction cellulaire. À cette fin, nous avons d'abord suivi la formation de foyers de fluorescence à l'aide de la fusion Tsa1-GFP dans des cellules exposées à une concentration continue de 0,5mM de H2O2. En effet, il a été démontré que Tsa1 induit la formation d'assemblages supramoléculaires lorsqu'elle est super-oxydée en réponse à des niveaux modérés à élevés de H2O2 (Jang et al. 2004 ; Hanzén et al. 2016). Chez le WT, nous avons observé une formation progressive d'agrégats protéiques en réponse au stress, suivie d'une diminution qui était vraisemblablement due à l'adaptation au stress (Fig. 3G et H). Au contraire, chez le mutant zwf1Δ, l'agrégation était beaucoup plus rapide et s'est avérée irréversible sur une fenêtre de 8 heures. Nous avons obtenu des résultats similaires avec le marqueur Hsp104-GFP (Fig 3I et J), qui a été utilisé comme marqueur générique de l'agrégation des protéines (Hsp104 est une désagrégase qui se lie aux protéines agrégées mal repliées), et qui est connu pour former des foyers localisés en réponse à H2O2 (Erjavec et al. 2007). Ceci a suggéré qu'une partie du protéome est oxydée de manière irréversible dans le mutant zwf1Δ sous stress. Cependant, en libérant les cellules dans un milieu sans

stress, nous avons observé une désagrégation progressive de la Hsp104-GFP qui coïncidait avec (Fig. 3K et L) ou même précédait (Fig. S3C) la réentrée dans le cycle cellulaire, indiquant que l'oxydation cellulaire était réversible et que la restauration d'un équilibre interne de H2O2 provoquait la reprise de la prolifération cellulaire. Dans l'ensemble, ces résultats suggèrent que, dans le mutant zwf1Δ, la prolifération cellulaire est étroitement associée au déséquilibre interne de H2O2 par un mécanisme de régulation putatif.

Ensuite, nous avons demandé si les niveaux variables de déséquilibre H2O2 dans les cellules zwf1Δ, qui ont été signalés même en l'absence de stress (Fig. 3D), permettraient de prédire la tolérance au stress H2O2 aigu (1 heure à 64mM). En utilisant les fusions Srx1-GFP ou Tsa1-GFP comme indicateurs du déséquilibre interne de H2O2 (Fig. 3M), nous avons représenté la fraction de survie en fonction du niveau d'expression normalisé de chaque rapporteur (les données ont été regroupées puis classées en groupes de N=46 événements). Cette expérience a révélé que les cellules avec un plus grand déséquilibre H2O2 ont affiché une tolérance accrue, en accord avec le phénotype hyper-tolérant du mutant zwf1Δ par rapport au WT (Fig 3N). Dans l'ensemble, ces analyses unicellulaires ont confirmé le fort antagonisme entre la résistance, le déséquilibre H2O2 et la tolérance, et ont suggéré l'existence d'un mécanisme de régulation qui couple ces trois caractéristiques de la réponse au stress H2O2.

Une inhibition de la PKA dépendante de la thiorédoxine conduit à la tolérance au stress en partie en protégeant la machinerie de croissance sous le stress H2O2

La voie Ras - AMP cyclique (cAMP) - protéine kinase A (PKA) est une plaque tournante majeure du contrôle de la prolifération qui transmet des signaux nutritifs pour réguler l'activation transcriptionnelle des ribosomes et la synthèse des protéines (Broach 2012 ; Conrad et al. 2014 ; Tamaki 2007). De plus, l'inhibition de la PKA contrôle la réponse au stress en partie en induisant la relocalisation nucléaire du facteur de transcription Msn2/4 (Boisnard et al. 2009 ; Jacquet et al. 2003), qui conduit l'expression de centaines de gènes en réponse à divers facteurs de stress (Gasch et al. 2000). Dans le contexte spécifique du stress oxydatif, il a été observé depuis longtemps que le maintien d'une activité PKA élevée induit une sensibilité au H2O2 (Hasan et al. 2002), et des études récentes ont proposé un mécanisme par lequel la signalisation du H2O2 par l'intermédiaire des peroxiredoxines ou des thiorédoxines contrôle l'activation de la PKA et donc la réponse générale au stress en aval (Bodvard et al. 2017 ; Roger et al. 2020). Par conséquent, dans ce qui suit, nous avons cherché à déchiffrer le rôle de la PKA dans le contrôle de la résistance et de la tolérance au H2O2.

Nous avons pensé que, si la prolifération cellulaire est arrêtée dans le mutant zwf1Δ en raison de l'inhibition de la PKA, l'atténuation de cette inhibition pourrait sauver la

croissance dans des conditions de stress. Pour tester cette hypothèse, nous avons d'abord supprimé la phosphodiestérase Pde2, qui entraîne la linéarisation de l'AMPc et inactive donc la PKA. En quantifiant le déplacement nucléaire d'une fusion Msn2-GFP comme indicateur de l'activation de la PKA, nous avons d'abord vérifié que Msn2-GFP se relocalise transitoirement vers le noyau en réponse à une étape de 0,5mM H2O2 chez le WT (Fig. 4A), en accord avec l'arrêt de prolifération réversible observé dans la Fig.1. Dans le mutant zwf1Δ, au contraire, Msn2-GFP s'est avérée être au moins partiellement nucléaire à tout moment pendant l'exposition au stress, en accord avec l'inhibition prolongée de PKA (Fig. 4A). Il est frappant de constater que Msn2-GFP est restée presque entièrement cytoplasmique tout au long de l'expérience dans le double mutant zwf1Δ pde2Δ (Fig. 4A et S4B), de la même manière que dans le mutant simple pde2Δ (Fig. S4A et S4B), ce qui suggère que la suppression de Pde2 réactive PKA dans le mutant zwf1Δ.
Ensuite, pour vérifier directement si l'activation forcée de la PKA pouvait sauver la croissance cellulaire, nous avons comparé la croissance de ces mutants en réponse à une faible dose de H2O2 (0,1mM) (c'est-à-dire inférieure à la CMI du mutant zwf1Δ). Nous avons constaté que, contrairement à zwf1Δ, le double mutant zwf1Δ pde2Δ a retrouvé une prolifération similaire à celle de WT (Fig. 4B), démontrant ainsi clairement que l'arrêt de croissance dépendant de H2O2 chez le mutant zwf1Δ est contrôlé par l'inhibition de la PKA et ne peut être interprété comme la conséquence d'une toxicité associée à un déséquilibre de H2O2. De plus, en utilisant un rapporteur Srx1pr-GFP-deg intégré dans le double mutant zwf1Δ pde2Δ, nous avons observé un sauvetage du déséquilibre H2O2 dans ces conditions (Fig. 4C), indiquant que, de manière inattendue, la prévention de l'inhibition de la PKA induit le rétablissement de la fonction homéostatique H2O2 (Fig. S4C). Ce résultat suggère également que les sources de NADPH indépendantes de Zwf1 (Minard et al. 1998) pourraient alimenter avec succès la détoxification de H2O2 dans le fond zwf1Δ pde2Δ à de faibles doses de stress, et, inversement, que la restauration de l'équilibre de H2O2 dans le mutant zwf1Δ à faible dose était empêchée par l'inhibition de la PKA.

Ensuite, pour évaluer davantage le rôle de l'inhibition de la PKA dans la réponse au stress H2O2, nous avons demandé si la délétion de la Pde2 chez le mutant zwf1Δ permettrait également d'abolir son phénotype d'hyper-tolérance. En effet, nous avons constaté que la délétion de Pde2Δ était épistatique à zwf1Δ pour la survie à l'étape de 0,5mM H2O2 (Fig. 4D), ainsi qu'à des concentrations de stress beaucoup plus élevées (Fig. S4D). D'autres expériences utilisant un stress en rampe ont exacerbé les interactions génétiques entre pde2Δ et zwf1Δ (puisque le mutant pde2Δ n'a pas de défaut de tolérance en rampe) et ces deux gènes se sont révélés être des létaux synthétiques sous stress après l'ajout d'AMPc (qui entraîne une activation supplémentaire de la PKA) (Fig 4E). Dans l'ensemble, ces résultats ont démontré que l'hyper-tolérance au H2O2 chez le mutant zwf1Δ nécessite une inhibition de la PKA.

Comment le signal interne H2O2 est-il relayé pour médier l'inhibition de la PKA en réponse au stress ? Des études récentes ont proposé que les peroxiredoxines sous

leur forme oxydée (ou, alternativement, les thiorédoxines) puissent inactiver la PKA par un mécanisme redox-dépendant (Bodvard et al. 2017 ; Roger et al. 2020). Pour tester ce modèle dans le contexte de la tolérance au stress, nous avons cherché à savoir si la délétion des thiorédoxines ou des peroxiredoxines serait épistatique au mutant zwf1Δ dans les tests de survie. Lorsqu'ils sont soumis à un stress de pas, nous avons constaté que le phénotype hyper-tolérant des mutants zwf1Δ et trr1Δ sous stress de pas était aboli dans les mutants trx1/2Δ zwf1Δ et trx1/2Δ trr1Δ, respectivement (Fig. 4F), et des résultats similaires ont été obtenus avec des rampes (Fig. 4F). Fait important, la quantification de la localisation nucléaire de Msn2-GFP a confirmé que la PKA n'était plus inhibée dans le mutant trx1/2Δ zwf1Δ sous stress (Fig.S4E). En outre, le knocking des trois peroxiredoxines Tsa1, Tsa2 et Ahp1, mais pas Tsa1 seul, a aboli le phénotype hyper-tolérant du mutant zwf1Δ. La suppression de Tsa1 seul n'a pas non plus permis d'empêcher l'inhibition de la PKA dans le fond zwf1Δ (Fig.S4F), ce qui suggère que Tsa1 lui-même ne serait pas le relais médiant l'inactivation de la PKA. Dans ce scénario, la perte d'hyper-tolérance observée chez le mutant tsa1Δ tsa2Δ ahp1Δ zwf1Δ pourrait être interprétée comme le fait que les thiorédoxines ne peuvent plus être oxydées en l'absence de leur substrat principal (c'est-à-dire la peroxiredoxine). Par conséquent, ces résultats suggèrent que les thiorédoxines sont le principal acteur relayant les signaux H2O2 à la PKA et provoquant la tolérance au stress.

Enfin, nous nous sommes demandé par quel mécanisme l'inhibition de la PKA entraînerait des effets protecteurs cellulaires conduisant à la tolérance au stress. A cette fin, nous avons cherché à identifier les gènes en aval de la PKA dont la délétion abolirait le phénotype hyper-tolérant du mutant zwf1Δ (Fig. 4G). Nous avons constaté qu'un mutant msn2/4Δ était épistatique au mutant zwf1Δ pour la tolérance (Fig. 4H), vraisemblablement en raison des rôles pléiotropiques de Msn2/4 dans la réponse générale au stress (Gasch et al. 2000). Il est intéressant de noter que la tolérance était également abolie dans le triple mutant pat1Δ dhh1Δ zwf1Δ (Fig. 4H). Ceci suggère que Pat1 et Dhh1, qui sont impliqués dans la formation des P-bodies et des granules de stress (Nissan et al. 2010 ; Decker et Parker 2012), peuvent contribuer à protéger la machinerie de traduction en présence de H2O2 - même si aucune épistasie de ce type n'a été observée en mutant Gcn2, qui contrôle l'initiation de la traduction (Garcia-Barrio et al. 2000), voir Fig. 4H). Pour vérifier davantage cette hypothèse, en utilisant une fusion Pat1-GFP comme rapporteur de la formation des P-bodies, nous avons observé une plus forte agrégation de ce marqueur chez le mutant zwf1Δ par rapport au WT sous stress, en accord avec son phénotype de haute tolérance (Fig. 4I et S4G). Inversement, toute mutation empêchant l'inhibition de la PKA a diminué le niveau d'agrégation de Pat1-GFP pour le ramener au niveau WT ou plus bas (Fig. 4I). Ce résultat suggère que la formation de P-bodies et de granules de stress contribue à l'établissement de la tolérance en protégeant la machinerie de croissance sous le stress H2O2.

Au total, l'analyse du déterminisme génétique du phénotype d'hyper-tolérance chez le mutant zwf1Δ a ainsi permis de démêler les rôles antagonistes de la PKA dans l'orchestration de la réponse au stress H2O2 : alors que l'inhibition de la croissance médiée par la PKA conduit à la survie cellulaire en partie en protégeant la machinerie de traduction, elle se fait au détriment du système homéostatique H2O2, qui nécessite la croissance cellulaire pour fonctionner (Fig. 4B).

Un compromis de fitness dépendant de l'activité de PKA contrôlé par la résistance et la tolérance au stress oxydant

Puisque la tolérance au stress exige l'arrêt de la prolifération alors que la résistance au stress vise à la maximiser, les cellules doivent décider laquelle des deux stratégies possibles est la plus appropriée en fonction du niveau de stress. Pour explorer davantage ce processus de décision, nous avons cherché à comparer l'aptitude cellulaire entre deux souches qui ont été modifiées pour afficher une stratégie de défense unique (c'est-à-dire soit la résistance, soit la tolérance) en contrôlant le statut d'activation de la PKA. Pour cela, nous avons mesuré l'aptitude cellulaire globale, définie comme la biomasse totale produite pendant un intervalle donné, dans le mutant zwf1Δ (c'est-à-dire PKA inhibée) par rapport au mutant pde2Δ zwf1Δ (c'est-à-dire PKA activée), pendant et après une exposition à H2O2 à différents niveaux.
En dessous de la MIC, zwf1Δ / pde2Δ zwf1Δ (c.-à-d. < 0,3 mM, Fig. 3B et Fig. 5A), il n'y avait pas de différence de survie entre les deux mutants (Fig. 5A et C), mais la prolifération cellulaire était plus importante, de sorte que l'aptitude globale était plus élevée pour la souche pde2Δ zwf1Δ que pour le seul mutant, en raison du sauvetage de l'activation de la PKA (Fig. 5B) et du rétablissement de la fonction homéostatique de l'H2O2 (Fig. 4B).
À des concentrations de stress plus élevées, la croissance cellulaire a été inhibée dans les deux mutants dans la même mesure, de sorte que la forme physique pendant l'exposition au stress était identique (Fig. 5B et S5B). Cependant, dans ces conditions, la survie cellulaire a été considérablement réduite dans le fond pde2Δ zwf1Δ, mais pas dans le mutant zwf1Δ, en raison de l'activation de la PKA (en accord avec les résultats de la Fig. 4D). En conséquence, la fitness cellulaire mesurée après l'exposition au stress a tourné à l'avantage du mutant zwf1Δ pour des concentrations de stress supérieures à 0,4mM (Fig 5B). Globalement, transposés au contexte WT, ces résultats suggèrent que le passage abrupt de la résistance (activité PKA élevée, système homéostatique H2O2 fonctionnel) à la tolérance (activité PKA faible, système homéostatique arrêté) au niveau du MIC maximise la fitness cellulaire, en empêchant la diminution massive de la survie qui se produirait si les cellules essayaient de maintenir la prolifération (Fig 5D et S5C).

Discussion

Dans cette étude, nous avons utilisé une méthodologie de time-lapse unicellulaire pour étudier les mécanismes qui sous-tendent l'adaptation au stress oxydatif chez la

levure bourgeonnante. Notre analyse révèle que la capacité des cellules à croître sous stress (résistance) est distincte de leur capacité à survivre à l'agent stressant (tolérance), et nous montrons que chacun de ces aspects est déterminé par des mécanismes différents. Il est important de noter que cette distinction ne pourrait pas être opérée sans l'utilisation d'analyses longitudinales, qui sont essentielles pour déterminer le destin des cellules individuelles en réponse au stress. En revanche, les tests de "sensibilité" à l'H2O2 basés sur la mesure sur plaque, même s'ils peuvent être très quantitatifs, ne permettent pas de faire la distinction entre résistance et tolérance, puisque les deux contrôlent la forme cellulaire et la production de biomasse. Par conséquent, les analyses classiques n'ont pas pu évaluer correctement le comportement de mutants, tels que l'hyper tolérant zwf1Δ, qui ont été précédemment caractérisés comme sensibles à H2O2.

L'absence de distinction entre tolérance et résistance pourrait expliquer en partie pourquoi le rôle détaillé des acteurs classiques de l'oxydoréduction dans l'adaptation au stress oxydatif est resté insaisissable, malgré une caractérisation approfondie de leurs fonctions biochimiques spécifiques. Ici, notre crible génétique de gènes candidats nous permet de classer les mutants en fonction de leurs rôles fonctionnels respectifs. Il révèle que des mutations spécifiques peuvent altérer le noyau homéostatique de H2O2 et donc diminuer la résistance cellulaire, tout en contribuant à améliorer la tolérance cellulaire à H2O2. L'élucidation de ce rôle antagoniste a priori est essentielle pour parvenir à une compréhension intégrée des mécanismes de défense contre l'H2O2.
Notre étude met clairement en évidence l'existence de mécanismes distincts de réponse au stress qui entraînent des comportements cellulaires différents : la résistance, qui marque la capacité de se développer sous stress, semble être directement liée à la capacité de restaurer un équilibre interne de H2O2 ; la tolérance, qui peut être définie comme la capacité de survivre sous stress, est une propriété distincte qui repose sur l'inhibition de la PKA. Connaissant les limites intrinsèques associées au système homéostatique H2O2, la résistance cellulaire est maximisée soit à de faibles niveaux d'H2O2, soit lorsque les niveaux d'H2O2 sont progressivement augmentés (c'est-à-dire un stress progressif). En revanche, en réponse à des étapes aiguës de H2O2 supérieures à 0,6mM, la tolérance est le principal mécanisme de défense. C'est la coordination de ces deux processus qui détermine la réponse globale à l'H2O2.

Le rôle de la PKA dans la réponse au stress oxydatif a été signalé depuis longtemps et a été récemment affiné en fournissant des preuves génétiques et biochimiques que son inhibition est médiée soit par des peroxiredoxines, soit par des thiorédoxines, qui relaient les signaux H2O2. Le modèle généralement admis dans la littérature est que la fonction de l'inhibition de la PKA était principalement de déclencher la réponse au stress environnemental par l'activation de Msn2/4. Ici, nous proposons en outre qu'elle est nécessaire pour protéger la machinerie de croissance par la formation de P-bodies

et de granules de stress, qui seraient autrement exposés à H2O2 et généreraient donc des dommages qui compromettraient la survie cellulaire.

Les diverses fonctions des peroxiredoxines (ainsi que des partenaires impliqués dans cette voie biochimique) ont été soigneusement documentées. Parmi elles, le rôle de Tsa1 en tant que molécule de signalisation de l'H2O2 (en particulier pour l'inhibition de la PKA) a reçu une attention considérable. Cela a contribué à minimiser son importance en tant qu'enzyme de piégeage de H2O2. Ici, nos résultats soulignent que les deux fonctions sont également importantes : la fonction peroxydase est essentielle (contrairement à la catalase Ctt1) pour la fonction homéostatique du système et donc la résistance, tandis que la signalisation Tsa1/Trx à la PKA est le mécanisme clé qui conduit la tolérance.

La tolérance et la résistance présentent un certain chevauchement fonctionnel à des niveaux de stress intermédiaires, car l'activation transitoire du régulon Yap1 (qui est une marque du système homéostatique) est concomitante avec l'inhibition de la croissance cellulaire, comme le montrent l'arrêt du cycle cellulaire et l'activation de Msn2-GFP. Or, ces deux mécanismes sont antagonistes puisque la résistance vise à maximiser la fitness cellulaire en limitant les dommages cellulaires et donc en assurant la croissance cellulaire, alors que la tolérance est basée sur la régulation négative de la croissance cellulaire. Par conséquent, cette étude fournit un exemple intéressant d'une stratégie de réponse au stress qui est basée sur un compromis entre la croissance et la survie.

De manière intéressante, alors que les mécanismes de réponse au stress sont souvent associés à la tolérance dans la recherche sur les antibiotiques, les études qui se concentrent sur les systèmes homéostatiques physiologiques tentent plutôt de comprendre les déterminants de la résistance. Notre analyse de la réponse au stress H2O2 montre que la résistance et la tolérance sont des éléments entrelacés dont les bases moléculaires se chevauchent, et qui contribuent tous deux à la fitness cellulaire. Il est important de noter que les mutations qui altèrent la résistance (par exemple, zwf1) n'affectent pas nécessairement la tolérance et peuvent même l'améliorer. Inversement, limiter la tolérance en empêchant l'inhibition de la PKA (par exemple, pde2) n'altère pas nécessairement la résistance cellulaire (le mutant pde2 ne présente pas de défaut de croissance dans les rampes H2O2). Cependant, modifier à la fois la résistance et la tolérance conduit à un fort défaut de fitness, quel que soit le profil temporel du stress. De nombreuses thérapies contre le cancer sont basées sur des médicaments qui altèrent la fonction cellulaire, entraînant ainsi des défauts de résistance. Pourtant, les mécanismes de tolérance peuvent être responsables des rechutes après le traitement. Cibler les deux aspects de la réponse au stress pourrait fournir un cadre intéressant pour prévenir les rechutes dans les stratégies thérapeutiques contre le cancer.

Suivi unicellulaire de la divergence du destin cellulaire et de la transition de phase pilotée par le pH au cours du cycle de vie de la levure bourgeonnante

Basile Jacquel, Théo Aspert, Damien Laporte, Isabelle Sagot, Gilles Charvin

Introduction/Abstrait

Les micro-organismes ont évolué vers des mécanismes plastiques de contrôle de la croissance qui assurent l'adaptation aux changements dynamiques de l'environnement, y compris ceux qui découlent de leur propre prolifération (comme les limitations de nutriments et la sécrétion cellulaire dans le milieu). Au cours de son cycle de vie naturel, la levure bourgeonnante subit plusieurs transitions métaboliques, de la fermentation à la respiration, suivies de l'entrée dans un état réversible d'arrêt de prolifération connu sous le nom de quiescence (De Virgilio 2012 ; Gray et al. 2004). Bien que la quiescence soit une partie essentielle du cycle de vie des microorganismes qui assure la survie des cellules sur des périodes prolongées (Fontana, Partridge et Longo 2010), elle a reçu peu d'attention par rapport à l'analyse des processus biologiques dans des contextes prolifératifs.

Non seulement les cellules quiescentes diffèrent fortement des cellules en prolifération en termes d'activité métabolique et de signalisation (Gray et al. 2004), mais elles présentent également un grand nombre de réarrangements structurels dans le cytosquelette, les mitochondries, l'organisation nucléaire et l'apparition de divers agrégats de protéines (Sagot et Laporte 2019). Jusqu'à présent, des réorganisations cellulaires aussi complexes et enchevêtrées empêchaient d'évaluer si et comment un ensemble limité de processus de régulation contrôle l'établissement de cet état particulier. En particulier, la chorégraphie détaillée des événements décrivant comment la dynamique des signaux métaboliques au cours du cycle de vie naturel conduit à l'entrée en quiescence est toujours manquante.

En outre, une caractéristique essentielle des écosystèmes microbiens en phase stationnaire est l'existence d'une variabilité phénotypique (Campbell, Vowinckel et Ralser 2016 ; Avery 2006 ; Holland et al. 2014 ; Labhsetwar et al. 2013 ; Ackermann 2015) et de comportements dépendant de l'histoire qui conduisent à des divergences de destin complexes (Balaban et al. 2004 ; Cerulus et al. 2018). Dans les cellules de levure quiescentes, la coexistence de populations cellulaires hétérogènes a été précédemment rapportée (Allen et al. 2006 ; Laporte et al. 2018). Pourtant, dans ce contexte, le scénario conduisant à l'émergence de l'hétérogénéité du destin cellulaire dans une population clonale reste inconnu (Fig. 1A). Cela est en partie dû à la difficulté de combiner une approche populationnelle dans laquelle les micro-organismes ont un impact collectif sur leur environnement au cours d'un cycle de vie complet, avec un

suivi longitudinal unicellulaire pour surveiller la dynamique du comportement des cellules individuelles au fil du temps.
Ici, nous avons développé une plateforme microfluidique pour l'écologie unicellulaire qui nous permet de suivre en continu le destin de cellules individuelles qui subissent un épuisement des nutriments causé par la croissance de la population dans une culture liquide sur un cycle de vie complet (jusqu'à 10 jours). En utilisant un rapporteur fluorescent du pH interne (Mouton et al. 2020 ; Miesenböck, De Angelis, and Rothman 1998) qui caractérise le statut métabolique des cellules, nous montrons que le début du changement diauxique induit une divergence claire du destin cellulaire, où une minorité de cellules subit un crash métabolique menant à l'apparition prématurée de marqueurs de quiescence tout en affichant une survie limitée. Nous montrons ensuite que les variations du pH interne entraînent la formation successive de réorganisations cellulaires distinctes et contrôlent finalement la transition vers un état de gel du cytoplasme. Dans l'ensemble, notre analyse révèle comment les changements environnementaux rencontrés par les cellules de levure au cours de leur cycle de vie naturel conduisent à un contrôle temporel des changements structurels et suscitent l'émergence de trajectoires cellulaires hétérogènes.

Résultats

Afin de suivre la dynamique des comportements cellulaires individuels au cours d'un cycle de vie complet, nous avons mis en place un dispositif composé d'une culture de levure liquide de 25mL (milieu YPD) avec une agitation constante connectée à un dispositif microfluidique avec une boucle de recirculation fermée (Fig. 1B, Fig 1Supp A-D). Ainsi, les cellules individuelles piégées dans le dispositif microfluidique peuvent être observées au fil du temps à l'aide de la microscopie time-lapse tout en subissant les mêmes changements environnementaux que la population dans la culture liquide. Afin d'éviter le colmatage du dispositif microfluidique dû à la forte concentration de cellules dans la culture (jusqu'à 109 cellules/ml, densité optique (D.O.600) ~ 20), nous avons conçu un dispositif de filtration basé sur la migration différentielle inertielle (Bhagat, Kuntaegowdanahalli et Papautsky 2008) pour réacheminer les cellules vers la culture liquide avant qu'elles ne puissent entrer dans le dispositif microfluidique. En utilisant des mesures de D.O., nous avons observé une efficacité de filtration de plus de 99,15±0,35%, réduisant ainsi la concentration cellulaire dans le dispositif microfluidique de ~2 ordres de grandeur et nous permettant d'imager les cellules dans le dispositif jusqu'à 10 jours. Nous avons également vérifié que le même dispositif pouvait trier les cellules de S. Pombe avec une efficacité de 92%, soulignant ainsi la polyvalence de la méthodologie.

Sur la base de cette méthodologie, nous avons récapitulé les transitions successives survenant lors de la prolifération cellulaire dans un environnement à ressources limitées ((Richards 1928), à savoir : une croissance exponentielle rapide (temps de doublement = 84 min +/- 12 min) des microcolonies correspondant à la fermentation du glucose (appelée phase F dans la suite, de t=0 à t=5,5 h), suivie d'un arrêt brutal

de la croissance, ou shift diauxique (DS, de t = 5. 5 h à t = 13,9 h) ; puis, la reprise d'un régime de prolifération lente (temps de doublement = 307 min +/- 52 min) qui est associé à l'utilisation de l'éthanol comme source de carbone pour un métabolisme respiratoire (R, de t = 13,9 h à t = 31,6 h) et un arrêt définitif se produisant lors de l'épuisement des ressources, conduisant à l'entrée en quiescence (Q) (Fig 1C, D). Les temps de transition entre chaque phase métabolique ont été déterminés en utilisant des ajustements exponentiels par morceaux (Fig S1E). En réinjectant du milieu YPD frais dans le dispositif microfluidique après 10 jours, nous avons observé que jusqu'à ~80% des cellules réintègrent le cycle cellulaire en 5h (Fig S1F), confirmant la réversibilité de la prolifération cellulaire dans nos conditions de croissance (Laporte et al. 2017).

Une baisse du pH du milieu a longtemps été rapportée comme coïncidant avec l'épuisement des ressources pendant la croissance microbienne (Burtner et al. 2009). Pourtant, la façon dont le pH interne évolue tout au long d'un cycle de vie n'a jamais été étudiée. Pour y remédier, nous avons utilisé la sonde fluorescente ratiométrique du pH cytoplasmique pHluorin (Fig. 1E, (Miesenböck, De Angelis, et Rothman 1998 ; Mouton et al. 2020)), qui peut être calibrée pour afficher le pH interne absolu (Fig. 1E-G et Fig. S1G). En utilisant cette lecture, nous avons observé que le pH, qui était initialement autour de 7,7, a commencé à diminuer de manière synchrone dans toutes les cellules pendant la phase F (Fig. 1F-G). Au début de la DS, la plupart des cellules ont brusquement atteint un plateau (pH ~ 6,9, lignes bleues sur la Fig. 1G), qui a été suivi d'une légère augmentation du pH (jusqu'à pH~7,2) qui a coïncidé avec l'entrée dans un métabolisme respiratoire. En revanche, une minorité de cellules (Fig. 1F et lignes rouges sur la Fig. 1G) ont connu une nouvelle baisse du pH jusqu'à environ 5,8 pendant le DS. Le signal de fluorescence a progressivement disparu dans cette sous-population, empêchant de suivre le pH interne au-delà de 20h de manière fiable.

Dans les cellules ayant un pH interne élevé pendant la DS, le pH a progressivement diminué après avoir atteint un maximum local pendant la phase R. Ensuite, ces cellules ont connu une forte baisse du pH. Ensuite, ces cellules ont connu une chute brutale du pH jusqu'à environ 5,8, qui s'est produite à des moments très hétérogènes pendant la phase Q, contrairement aux cellules présentant une chute précoce du pH. Dans l'ensemble, ces observations ont révélé une dynamique sans précédent du pH interne au cours du cycle de vie de la levure. Les variations de pH semblent être synchronisées avec la séquence des phases de prolifération, ce qui suggère que le pH interne est un marqueur clé de l'état métabolique des cellules au cours de leur cycle de vie.

Ces mesures continues du pH ont également mis en évidence une divergence inattendue dans le destin des cellules au niveau du DS, ce qui a conduit à l'émergence précoce de l'hétérogénéité au sein de la population. Récemment, il a été signalé que l'activation de la respiration était une réponse métabolique cruciale pour survivre à la privation de glucose (Weber et al. 2020), qui permettait aux cellules de stocker des

glucides (Ocampo et al. 2012) et d'entrer ensuite dans un état de quiescence prolongé (Laporte et al. 2018). De manière intéressante, il a été montré qu'un défaut de respiration était naturellement observé dans une fraction des cellules subissant l'entrée en quiescence (Laporte et al. 2018).

Pour caractériser davantage si les différences de statut métabolique ont conduit à l'émergence de destins cellulaires divergents au DS, nous avons d'abord utilisé des mesures de volumes unicellulaires pour quantifier la prolifération cellulaire au fil du temps. Nous avons constaté que les cellules ayant subi une chute tardive du pH ont repris leur croissance et ont à peu près doublé leur biomasse pendant la phase R (lignes bleues sur la figure 2A), ce qui correspond aux mesures du nombre de cellules de la figure 1. En revanche, les cellules qui ont subi une baisse de pH précoce (lignes rouges sur la Fig. 2A) n'ont pas récupéré pendant la phase R, ce qui suggère qu'elles n'ont pas pu passer au métabolisme respiratoire. Pour étudier cette hypothèse, nous avons vérifié que ces cellules ne reprenaient pas leur croissance lors de l'ajout de lactate comme source de carbone non fermentescible dans le milieu (Fig. S2A). Pourtant, la grande majorité de ces cellules étaient encore viables après 3 jours de quiescence - même si elles présentaient une durée de vie fortement réduite par rapport aux cellules en adaptation (Fig. 2B).

En outre, nous avons utilisé la fusion Ilv3-mCherry comme marqueur du réseau mitochondrial pour révéler le statut respiratoire des cellules (Laporte et al. 2018). Alors que la structure mitochondriale était similaire (c'est-à-dire grossièrement tubulaire) dans toutes les cellules avant le DS, les cellules en prolifération dans la phase R ont présenté un phénotype fragmenté typique des cellules respirantes (figure 2C). En revanche, les cellules non proliférantes ont subi une globalisation de leur réseau mitochondrial (Fig. 2C). Nous avons quantifié plus précisément la dynamique de la réorganisation du réseau mitochondrial en calculant un indice d'agrégation personnalisé qui distingue les mitochondries globularisées des mitochondries tubulaires et fragmentées (Fig. 2D, voir Méthodes pour plus de détails). Sur la base de la distinction claire de l'indice d'agrégation entre les cellules qui s'adaptent et celles qui ne s'adaptent pas, nous avons mesuré qu'environ ~10 % des cellules étaient incapables d'effectuer la transition vers le métabolisme respiratoire (à t=12h post-DS, Fig. 2D), en accord avec les résultats précédents (Laporte et al. 2018). Fait important, cette quantification a révélé que la globularisation mitochondriale dans les cellules non adaptatives était temporellement étroitement associée au DS, puisqu'elle a commencé dès 1h20 ($p < 0,05$) après son déclenchement (Fig. 2C). Dans l'ensemble, ces résultats ont démontré que les cellules qui s'adaptent et celles qui ne s'adaptent pas ont connu des destins cellulaires divergents au moment

de la DS, en fonction de leur capacité à passer à la respiration, et ont donc été appelées dans la suite du document respiration positive (R+) et négative (R-), respectivement. En outre, ces résultats suggèrent que l'incapacité des cellules R- à activer un métabolisme respiratoire a été déclenchée par ce défi métabolique ou,

alternativement, préexistait au DS, sachant que les cellules déficientes sur le plan respiratoire (c'est-à-dire les cellules ρ-) sont courantes dans le fond BY en raison de l'instabilité génétique de l'ADN mitochondrial (Dimitrov et al. 2009).

Pour distinguer ces deux hypothèses, nous avons utilisé une souche portant la pré-séquence de Cox4 fusionnée au mCherry (Cox4 est une protéine mitochondriale codée par le noyau qui n'est importée que dans les mitochondries fonctionnelles (Veatch et al. 2009)) ainsi que le marqueur de localisation mitochondriale Tom70-GFP (Tom70 est une protéine de la membrane mitochondriale externe), afin d'évaluer la capacité des cellules à respirer (Fehrmann et al. 2013). En utilisant ces marqueurs, nous avons d'abord vérifié que toutes les cellules R+, qui sont capables de passer à la respiration, ont maintenu une importation fonctionnelle de preCox4-mCherry de la fermentation à la respiration (c'est-à-dire qu'il s'agissait de cellules ρ+, Fig. 2E). Ensuite, nous avons observé que parmi les cellules R-, seule une minorité (i.e. 19%) présentait une importation mitochondriale dysfonctionnelle avant le DS, indiquant qu'elles avaient une déficience respiratoire préexistante (voir les cellules ρ- sur la Fig. 2E). En revanche, la grande majorité des cellules R- (81 %) sont passées de ρ+ à ρ- pendant le SD. Cela démontre que, contrairement à une condition préexistante, le défaut de respiration observé dans les cellules R- semble être déclenché par le changement environnemental. Dans l'ensemble, ces observations soutiennent un scénario dans lequel une divergence de destin s'est produite tôt au début du DS, les cellules R+ passant rapidement à un métabolisme respiratoire, alors que les cellules R- n'y sont pas parvenues.

Ensuite, nous avons cherché à établir les liens entre les changements successifs du métabolisme et les nombreuses réorganisations cellulaires structurelles qui ont été précédemment rapportées lors de l'entrée en quiescence (Sagot et Laporte 2019). En effet, le métabolisme contrôlant le pH cellulaire interne, connu pour induire des modifications physico-chimiques majeures du protéome telles que l'agrégation des protéines et la transition de phase (Munder et al. 2016 ; Dechant et al. 2010), nous nous sommes demandé comment ces réorganisations seraient coordonnées avec la dynamique du pH interne dans le contexte de la quiescence. Pour ce faire, nous avons suivi la dynamique de formation de corps supra-moléculaires associés à divers processus biologiques, tels que la formation de P-bodies (en utilisant la fusion Dhh1-GFP), d'enzymes métaboliques ou régulatrices sujettes à l'agrégation (Gln1-GFP et Ccd28-GFP), la formation de corps d'actine (Abp1-GFP), et de granules de stockage du protéasome (PSG, en utilisant la fusion Scl1-GFP). En effet, ces protéines ont été décrites comme formant de telles structures en quiescence ou en réponse à la famine (Mugler et al. 2016 ; Balagopal et Parker 2009 ; Petrovska et al. 2014 ; Narayanaswamy et al. 2009 ; Shah et al. 2014 ; Sagot et al., n.d. ; Laporte et al. 2008 ; Peters et al. 2013).

Nous avons constaté que la formation des foyers de fluorescence était hautement coordonnée avec la séquence des phases métaboliques et le statut de prolifération

cellulaire (Fig. 3A) : dans les cellules R+, les foyers Dhh1-GFP et Gln1-GFP sont apparus au début de la DS, puis ont été partiellement dissous pendant la phase R, et sont réapparus à l'entrée en quiescence. D'autres signes de l'entrée en quiescence, tels que les corps d'actine, les PSG, ainsi que d'autres marqueurs d'agrégation de protéines (Cdc28-GFP) sont apparus significativement plus tard, c'est-à-dire à la fin de la phase R. Il est important de noter que les cellules R- ont également connu une formation cohérente de foyers fluorescents pour les marqueurs qui ont été suivis, mais, contrairement aux cellules R+, ils sont tous apparus pendant la DS. En outre, de manière surprenante, ces foyers ont fini par disparaître, vraisemblablement en raison de la mort cellulaire prématurée observée dans cette sous-population.

En superposant la dynamique des foyers de fluorescence avec celle du pH interne (Fig 1G), nous avons remarqué que la formation des corps d'agrégation coïncidait globalement avec la variation du niveau de pH absolu dans les cellules R+ et R-, bien qu'elle apparaisse à des échelles de temps différentes. Cette constatation confirme l'hypothèse selon laquelle c'est la baisse du pH interne - qui reflète une faible activité métabolique - qui entraîne des vagues successives d'agrégation de protéines et l'apparition des signes de quiescence. Pour vérifier davantage cette hypothèse, puisqu'il a été démontré que l'épuisement énergétique induit une modification globale du cytoplasme vers un état de gel (Munder et al. 2016), nous avons cherché à observer cette transition en surveillant la mobilité des foyers Gln1-GFP au cours du temps (Fig. 3B, (Munder et al. 2016)) - ce marqueur a été choisi car les foyers sont déjà présents au DS. Nous avons constaté que la mobilité des foyers Gln1-GFP diminuait fortement dans les cellules R- pendant le DS et beaucoup plus tard dans les cellules R+, de manière cohérente avec les différences observées concernant les moments de chute du pH dans les deux populations. Pour mieux établir les liens entre le pH et la mobilité, nous avons exploité le fait que les gouttelettes lipidiques (LD) pouvaient être observées de manière pratique à l'aide d'images en contraste de phase (Heimlicher et al. 2019), et que le temps de congélation des LD était très bien corrélé avec celui des foyers Gln1-GFP (Fig S3A). En quantifiant à la fois le temps de congélation des LD et la dynamique de la chute du pH dans des cellules uniques, nous avons observé que les deux événements étaient étroitement corrélés dans toutes les cellules, malgré la grande hétérogénéité de cellule à cellule dans le temps de chute du pH dans les cellules R+ (Fig 3E et S3B). De plus, après synchronisation de toutes les trajectoires unicellulaires à partir du moment de la congélation du LD, nous avons montré que la congélation du cytoplasme se produisait à un pH ~ 6 similaire dans les cellules R+ et R- (Fig 3F). Dans l'ensemble, ces observations suggèrent que le pH interne, qui présente un comportement très dynamique au cours du cycle de vie de la levure, induit des vagues de remodelage structurel du protéome qui régissent l'établissement de marqueurs de quiescence et déclenchent finalement une transition globale du cytoplasme vers un état de gel. Il est intéressant de noter que la transition prématurée observée dans les cellules déficientes sur le plan respiratoire (R-), qui coïncide avec la chute précoce du pH, confirme ce modèle et suggère que cette sous-population subit une transition précoce vers la quiescence similaire à celle des cellules

R+. Cependant, il est probable que l'absence de la phase respiratoire limite la viabilité à long terme de cette sous-population (Ocampo et al. 2012 ; Weber et al. 2020).

Discussion

Dans cette étude, nous avons développé une nouvelle plateforme microfluidique qui nous permet de suivre un cycle complet de prolifération cellulaire en culture liquide avec une résolution unicellulaire. Le suivi de cellules individuelles révèle comment des destins cellulaires hétérogènes, qui sont déclenchés par des commutations métaboliques successives, émergent dans une population clonale.

Notre analyse a révélé une nette divergence dans le destin cellulaire lors du changement diauxique, où une minorité de cellules n'a pas réussi à établir un métabolisme respiratoire et a donc subi une chute spectaculaire du pH interne. Dans l'ensemble, ce phénomène ne pouvait pas être expliqué par des différences phénotypiques préexistantes dans la population pendant la phase de fermentation, mais semblait plutôt être déclenché par le défi métabolique associé à l'épuisement du glucose.

Il est intéressant de noter que les cellules compétentes et déficientes en matière de respiration semblent subir des réorganisations cellulaires stéréotypées précédemment observées dans les cellules quiescentes (Sagot et Laporte, 2019), mais à des moments très différents. Cela suggère que la plasticité structurelle des cellules en réponse à l'épuisement des ressources est contrôlée par un mécanisme similaire dans les deux populations.

En particulier, des études antérieures ont démontré comment le pH cytoplasmique contrôle l'agrégation des protéines et la transition du cytoplasme vers un état de gel (Munder et al. 2016), mais cela n'avait jamais été observé dans un contexte écologiquement pertinent. Ici, nos résultats indiquent que les chutes de pH, qui se produisent à des moments très différents dans les cellules compétentes en matière de respiration, sont systématiquement associées à la formation de super-assemblages de protéines et de granules.

La chute du pH interne induit finalement la transition du cytoplasme vers un état de gel, qui se produit soit au début, soit à la fin du cycle de vie (comme dans les cellules R- et R+, respectivement). De façon remarquable, cette transition se produit à des moments très variables dans les cellules R+, ce qui suggère l'existence de sources supplémentaires d'hétérogénéité dans le métabolisme cellulaire. Dans l'ensemble, ces données soutiennent un modèle simple dans lequel les changements du statut métabolique cellulaire pendant l'entrée en quiescence modulent le niveau de pH interne, ce qui entraîne un remodelage massif du protéome.

Nous envisageons que cette méthodologie puisse être appliquée à d'autres contextes dans lesquels le comportement collectif des cellules a un impact sur l'environnement, qui à son tour façonne la réponse cellulaire individuelle (par exemple, les oscillations métaboliques (Tu et al. 2005), les comportements coopératifs (Dal Co et al. 2020 ; Campbell et al. 2015)).

Université de Strasbourg

École doctorale Sciences de la vie et de la santé | ED 414
Université de Strasbourg

Résumé

En réponse au stress environnemental, les stratégies de défense cellulaire peuvent être divisées en deux catégories : celles qui, comme dans les systèmes homéostatiques, cherchent à maintenir la prolifération cellulaire en dégradant le facteur de stress (c'est-à-dire la résistance) ; et celles qui assurent la survie des cellules (c'est-à-dire la tolérance), même si cela se fait souvent au détriment de la prolifération cellulaire. Dans cette étude, nous avons exploré les bases génétiques de l'antagonisme entre résistance et tolérance dans la réponse au peroxyde d'hydrogène (H2O2) chez la levure bourgeonnante. Nous montrons que l'inactivation de la protéine kinase A (PKA) médiée par la signalisation H2O2 induit une transition abrupte de la fonction homéostatique normale à un état de tolérance au stress en protégeant le mécanisme de croissance, maximisant ainsi la forme cellulaire dans un environnement changeant. Ce système modèle ouvre la voie au développement de stratégies antiprolifératives dans lesquelles les mécanismes de résistance et de tolérance pourraient être ciblés indépendamment pour prévenir les rechutes.

Mots clés : adaptation au stress, H2O2, Peroxiredoxines, PKA, tolérance et résistance au stress, microfluidique, analyse cellule unique

Résumé en anglais

In response to environmental stress, cellular defense strategies may be divided into two categories: those, as in homeostatic systems, that seek to maintain cell proliferation by degrading the stressor (i.e., resistance); and those that ensure cell survival (i.e. tolerance), even if this is often at the expense of cell proliferation. In this study, we have explored the genetic bases of the antagonism between resistance and tolerance during the response to hydrogen peroxide (H2O2) in budding yeast. We show that inactivation of protein kinase A (PKA) by H2O2 signaling induces an abrupt transition from normal homeostatic function to a stress-tolerant state by protecting the growth machinery, hence maximizing cellular fitness in a changing environment. This model system paves the way for developing antiproliferative strategies that target both resistance and tolerance mechanisms to prevent relapse.

Keywords: stress adaptation, H2O2, Peroxiredoxins, PKA, stress tolerance and resistance, microfluidics, single-cell analysis